INDUCTION AND PATTERNING OF NEURAL CREST CELLS IN THE DEVELOPING MOUSE EMBRYO: ROLES FOR *GCNF* AND *HHAT*

BY

Jennifer F. Dennis

M.S., Neuroscience, University of Arizona, 2004
B.A., Biology & Chemistry, University of Missouri-Kansas City, 2002

Submitted to the graduate degree program in Neuroscience and the Graduate Faculty of the University of Kansas in partial fulfillment of the requirements for the degree of Doctor of Philosophy

Committee:

_____
Paul Trainor, Ph.D. (Chair)

_____
Juan Bruses, Ph.D.

_____
Paul Cheney, Ph.D.

_____
Robb Krumlauf, Ph.D.

_____
Greg Vanden Heuvel, Ph.D.

_____
Douglas Wright, Ph.D.

Defense Date: December 12th, 2008

The Dissertation Committee for Jennifer F. Dennis certifies that this is the approved version of the following dissertation:

INDUCTION AND PATTERNING OF NEURAL CREST CELLS IN THE DEVELOPING MOUSE EMBRYO: ROLES FOR *GCNF* AND *HHAT*

_____
Paul Trainor, Ph.D. (Chair)

Date approved: _____

Table of Contents

I. Acknowledgments……..……..…….6

II. Dedication…….…….7

III. List of Figures…….……. 8

IV. Goals of the Study…….....13

V. Introduction…….....17

A.) Significance of the Neural Crest……..…….....17

B.) Neural Crest Cell Induction: an Intersection of Multiple Signaling Pathways…….....18

C.) Migration, and Derivatives of the Neural Crest……..…….28

D.) Neural Crest Cell Contribution to the Developing Face…….....33

E.) Neural Crest Cell Patterning is mediated by Extrinsic Signaling.....44

F.) Ectodermal & Endodermal Hedgehog Signaling regulates Craniofacial Development……...……....45

G.) *Fgf8* & the Facial Ectoderm…….....52

H.) *Bmp4* in Mandibular Development…….....56

I.) Cartilage & Bone Development……...61

VI. Chapter One: *Germ cell nuclear factor* (*Gcnf /Nr6a1*) plays a novel role in the induction of neural crest cells in the developing mouse embryo. Dennis, J.F., Cooney, A.J., and Trainor, P.A.

A.) Abstract……..…….....79

B.) Introduction……..……....80

C.) Results……..…….....83

D.) Discussion……..……....116

E.) Experimental Methods……...125

VII. Chapter Two: Conditional Inactivation of FGF8 Signaling in the Frontonasal Prominence using the *AP-2cre* Transgene does not result in Craniofacial Defects.

A.) Abstract……..…….....129

B.) Introduction……..……..130

C.) Results……..…….....137

D.) Discussion……..……....152

E.) Experimental Methods……..…….....156

VIII. Chapter Three: Insertional Mutation of *Skinny Hedgehog (Skn/Hhat)* results in disrupted Hedgehog Signaling and Severe Craniofacial Defects. Dennis, J.F., Williams, T., and Trainor, P.A.

A.) Abstract……..……158

B.) Introduction……..……..159

C.) Results……..…….....161

D.) Discussion……..……....195

E.) Experimental Methods……...210

IX. Conclusions…….....217

X. Materials & Methods…….....231

XI. References…….....239

I. Acknowledgements

First, I want to acknowledge and thank my parents and the B.R.E.W. crew for all of the support throughout my graduate studies and I am so grateful for what you all have done for me. I owe you all many thanks and I promise this is it!

Additionally, I would like to acknowledge my committee members, Drs. Juan Bruses, Paul Cheney, Robb Krumlauf, Greg Vanden Heuvel, and Doug Wright for their suggestions and comments that have enhanced my projects and the support staff in the Department of Anatomy and Cell Biology and the Neuroscience Program at KUMC. I would also like to thank the members of the core facilities at the Stowers Institute for all of their efforts. Last but not least, I owe many thanks to the members of the Trainor lab, past and present, for all of their suggestions on my projects; you all have taught me so much and made the lab a wonderful place to be, laugh, and work.

Most importantly, I am indebted to my mentor, Paul Trainor, for making all of the scientific genius that you are unconditionally available, while at the same time, letting me develop as an independent scientist. I was given space, freedom, and the opportunity to make hundreds of mistakes, even though you were always in your office, if I ever needed help. As your first student I hope that you will look at this body of work and see it as a positive reflection of all that you have taught me. Thank you so very much for being a wonderful mentor and advisor; I could never have learned as much from anyone else, although, I am sure they would have eaten significantly less chocolate.

II. Dedication

To my husband Grant,

more than yesterday, less than tomorrow.

III. List of Figures

Figure 1. Genetic Regulation of Neural Crest Cell Induction.....20

Figure 2. Derivatives of the Neural Crest……...30

Figure 3. Neural Crest Cells populate the Branchial Arches via Migratory Streams.....34

Figure 4. Contribution of Cranial Neural Crest Cells to the developing Frontonasal Region and Branchial Arches…….....36

Figure 5. Development of the Craniofacial Primordia.....37

Figure 6. *Distal-less* Genes regulate Intra-BA Identity……..41

Figure 7. Contribution of Neural Crest Cells and the Paraxial Mesoderm to the Cranial Vault……64

Figure 8. Schematic of Endochondral Ossification……68

Figure 9. An IHH and PTHrP Negative Feedback Loop regulates Endochondral Ossification……..73

Chapter One: *Germ cell nuclear factor* (*Gcnf /Nr6a1*) plays a novel role in the induction of neural crest cells in the developing mouse embryo

Figure 10. Notch Signaling is not required for Neural Crest Cell Induction….....84

Figure 11. *Pax3* and *Pax7* are not required for Neural Crest Cell Formation in Murine Embryos ……88

Figure 12. Neural Crest Cells populate the developing Facial Region in *Pax3*$^{-/-}$;*Pax7*$^{-/-}$ Double Mutants …….....89

Figure 13. Development of the Cranial Explant Culture System…..…….92

Figure 14. Cranial Explants lack Neural Crest Cell Identity at the Time of Harvest……..…….....93

Figure 15. Antagonist Treatment does not inhibit Neural Crest Cell Induction in Cranial Explants…….…….....95

Figure 16. SU5402 Treatment for Twenty-Four Hours inhibits the Neural Plate in Cranial Explant Cultures...…….....97

Figure 17. SU5402 Treatment for Eight Hours inhibits the Formation of Neural Crest Cells…….....99

Figure 18. SU5402 Treatment for Twelve Hours inhibits Neural Crest Cell Formation ……..100

Figure 19. FGF8 Signaling is not required for Neural Crest Cell Induction in the Mouse…….....102

Figure 20. *Gcnf* is downregulated in *Tcof1*$^{+/-}$ Embryos…….…….....106

Figure 21. *Gcnf* is dynamically expressed during Mid-Embryonic Development...107

Figure 22. *Gcnf* Mutants have Neural Crest Cell Formation Defects.....109

Figure 23. Neural Plate Identity is unaltered in *Gcnf* Mutants….....111

Figure 24. *Gcnf*$^{-/-}$ Embryos exhibit prolonged Neural Plate Maintenance…….112

Figure 25. Identification of Putative *Gcnf* Binding Sites in Genes required for Neural Crest Cell Development…….115

Figure 26. Model for *Gcnf* in regulating Neural Crest Cell Formation and Differentiation……..…… 124

Chapter Two: Conditional inactivation of FGF8 signaling in the frontonasal prominence using the *AP-2cre* transgene does not result in craniofacial defects

Figure 27. Breeding Scheme of *Fgf8* Conditional Mutants…….....138

Figure 28. Skeletogenesis is unaffected in *AP-2cre;Fgf8*$^{fx/fx}$ Mutants…..…….....140

Figure 29**.** *AP-2cre;Fgf8*$^{fx/fx}$ Mutants do not exhibit Defects in Chondrogenesis….141

Figure 30. *Fgf8* Expression in *AP-2cre;Fgf8*$^{fx/fx}$ Embryos…….…….....142

Figure 31. Conditional *AP-2cre;Fgf8*$^{\Delta 2,3/fx}$ Mutants do not have Cranial Bone Defects…….....145

Figure 32. Cartilage and Bone Staining of *AP-2cre;Fgf8*$^{\Delta 2,3/fx}$ Embryos…….....146

Figure 33. *Fgf8* is expressed in *AP-2cre;Fgf8*$^{\Delta 2,3/fx}$ Embryos……..…….....147

Figure 34**.** Comparison of *AP-2cre*^{2}*;Fgf8*$^{\Delta 2,3/fx}$ and *AP-2cre*$^{T/T}$ Mutant Embryos at 14.5dpc…….……..149

Figure 35. Expression Pattern of the *AP-2cre* Transgene using the *Rosa26 Reporter* Mice.....151

Chapter Three: Insertional Mutation of *Skinny hedgehog (Skn/Hhat)* results in disrupted Hedgehog signaling and severe craniofacial defects

Figure 36. *Hhat* is disrupted by the Insertion of the *Cre-face* Transgene…….163

Figure 37. *Hhat*$^{Cre\text{-}face}$ Mutants exhibit Holoprosencephaly & Craniofacial Defects…….....165

Figure 38. *Hhat*$^{Cre\text{-}face}$ Embryos have defects in Organogenesis at 14.5dpc.....166

Figure 39. Section Histology of *Hhat*$^{Cre\text{-}face}$ Mutants at 14.5dpc…….....168

Figure 40. *Shh* is downregulated in *Hhat*$^{Cre\text{-}face}$ Mutants throughout Development.....170

Figure 41. SHH Signaling is disrupted in *Hhat*$^{Cre\text{-}face}$ Mutants 172

Figure 42. *Patched (Ptc)* Activation is diminished in *Hhat*$^{Cre\text{-}face}$ Mutants …….....174

Figure 43. *Hhat*$^{Cre\text{-}face}$ Mutants exhibit increased Apoptosis in the Developing Head.....177

Figure 44. Branchial Arch Patterning is disrupted in *Hhat*$^{Cre\text{-}face}$ Mutants.....179

Figure 45. *Hhat*$^{Cre\text{-}face}$ Mutants have defects in Neural Crest Cell Lineage Segregation…….....182

Figure 46. Lineage Tracing using *Wnt1-cre* in *Hhat*$^{Cre\text{-}face}$ Mutants does not reveal Neural Crest Cell Formation Defects…….....184

Figure 47. *Hhat*$^{Cre\text{-}face}$ Mutants exhibit Cranial Nerve Fusion Defects….....187

Figure 48. *Hhat*$^{Cre\text{-}face}$ Mutants have Cartilage and Bone Defects.…….....190

Figure 49. *Hhat*$^{Cre\text{-}face}$ Mutants have defects in Endochondral Bone Formation resulting from defective Hh Signaling.……..193

Goals of the Study

Cranial neural crest cells are a multipotent, migratory cell population which forms the majority of the bone, cartilage, nerves, and connective tissue of the head and face. Craniofacial malformations account for one-third of all congenital birth defects, and are mainly attributed to defects in cranial neural crest cell induction, patterning, or differentiation. Because of their importance in craniofacial development, it is essential to understand the mechanisms underlying the formation and patterning of this unique cell population. Therefore, the main goal of these studies was to examine the signaling pathways regulating neural crest cell formation and patterning.

The first study detailed herein examines the molecular morphogens required for neural crest cell induction in the mouse embryo. Multiple signaling pathways, including BMP, FGF, NOTCH, PAX, and WNT signaling have shown to be involved in the induction of neural crest cells. Despite evidence indicating the requirement of these morphogens in other model systems, a specific role for these pathways has not been addressed in the mouse. Therefore, we took an *in vivo* and *in vitro* approach to determine which of these signaling pathways, if any, were required for neural crest cell induction. Analysis of *Pax3*$^{-/-}$*;Pax7*$^{-/-}$, *Fgf8*$^{\Delta 2,3/\Delta 2,3}$, and *RBP-Jκ*$^{-/-}$ mutants failed to reveal the requirement of any of these pathways in crest cell formation. Additionally, antagonist treatment of embryo explants *in vitro* did not prevent the expression of *Sox10*, a marker of migratory neural crest cells, indicating that BMP, FGF, NOTCH, and WNT signaling are not regulating the induction process.

Our data demonstrates that BMP, FGF, NOTCH, PAX, and WNT signaling are not required for neural crest cell induction in the mouse, indicating that novel regulators of this process have yet to be elucidated. Indeed, we have identified *Germ cell nuclear factor* (*Gcnf/Nr6a1*) as a novel regulator of neural crest cell induction. *Gcnf* is transiently expressed in neural crest cells in the cranial region and analysis of $Gcnf^{-/-}$ embryos revealed a complete absence of the neural crest cell markers C*rabp1, Sox9, Sox10,* and *Snail*. In contrast, the neural plate markers *Sox2, Pax3*, and *Wnt1* were expanded in mutant embryos, suggesting a failure in the transition from a neuroepithelial to neural crest cell. Indeed, *Gcnf* may govern initial formation of neural crest cells via activation of *Snail,* the gene required for their epithelial-to-mesenchymal transition. Additionally, we have identified putative *Gcnf* binding sites within neural crest cell specific genes that regulate viability, migration, and lineage selection. Therefore, *Gcnf* appears to act as a bi-modal regulator of neural crest cell induction acting at the onset of crest cell formation and in the subsequent activation of crest cell differentiation paradigms.

The second study addresses the roles for *Fgf8* in the patterning of the frontonasal prominence (FNP), the craniofacial primordium that gives rise to mid-facial structures, such as the nose, forehead, and philtrum of the upper lip (Tapadia et al. 2005). We set out to conditionally inactivate *Fgf8* in the surface ectoderm of the FNP using the Cre-loxP system via an *AP-2cre* driver, which is expressed in the ectoderm and mesenchyme of the frontonasal region (Zhang and Williams 2003). Despite examining both *AP-2cre;*$Fgf8^{fx/fx}$ and *AP-2cre;*$Fgf8^{\Delta 2,3/fx}$ embryos, excision

of *Fgf8* in the surface ectoderm did not occur. Further examination of the *AP-2cre* mice revealed that *AP-2cre* expression was present in the mesenchyme of the FNP, but not in the surface ectoderm of this region as had originally been reported (Zhang and Williams 2003), most likely due to background strain differences. The lack of overlap between *Fgf8* and the *AP-2cre* in the surface ectoderm of the FNP results in a lack of *Fgf8* excision from this region and does not contribute to obvious craniofacial phenotypes in conditional *Fgf8* mutants.

Finally, we have identified an insertional mouse mutant of *Hedgehog acyltransferase (Hhat)*, a gene required for the palmitoylation of Hedgehog proteins. $Hhat^{Cre\text{-}face}$ embryos exhibit holoprosencephaly (HPE), a midline craniofacial anomaly characterized by the failure of the cerebral cortex to divide into left and right hemispheres (Belloni et al. 1996a; Roessler et al. 1996). Additionally, $Hhat^{Cre\text{-}face}$ mutants exhibit neural crest cell and branchial arch patterning defects as well as defects in skeletogenesis. Underpinning the HPE phenotype in $Hhat^{Cre\text{-}face}$ embryos is disrupted SHH signaling, as evidenced by the lack of Shh transcript and protein at 9.5dpc; loss of SHH in the pharyngeal endoderm results in altered branchial arch development and disrupted patterning of the lower jaw, ultimately leading to cartilage and bone defects. Disrupted Hh signaling impacts on neural crest cell lineage selection as the expression of *Sox9* and *Sox10* is decreased. Additionally, peripheral nerve development is impaired in $Hhat^{Cre\text{-}face}$ mutants. At later developmental stages, $Hhat^{Cre\text{-}face}$ mutants exhibit delayed chondrogenesis, tooth agenesis, and an absence of cranial vault bones. Interestingly, Chromosome 1, where *Hhat* is positioned, has been

identified as a HPE locus in human cases of HPE, indicating that *Hhat*$^{Cre\text{-}face}$ embryos provide a model for understanding the role of hedgehog signaling during craniofacial development and the etiology of HPE.

V. Introduction

Significance of the Neural Crest

Neural crest cells are a transient population of multipotent cells that arise along the dorsal neural folds and migrate throughout the embryo to give rise to numerous derivatives (LaBonne and Bronner-Fraser 1999; Le Douarin and Kalcheim 1999). Derivatives include, but are not limited to, the peripheral nervous system, the dermis, connective tissue, muscle, bone, and pigment cells (Le Douarin and Kalcheim 1999). Indeed, there is not a single organ or tissue in the vertebrate body that is not comprised of neural crest cells, even if the contribution is minor (Le Douarin 2004). Therefore, neural crest cells are a classic model used by developmental biologists for studying cell induction, migration, and differentiation.

One such structure that is highly dependent on neural crest cells for proper development is the craniofacial complex, which is the most anatomically sophisticated part of the body. The craniofacial complex is composed of neural crest cells and paraxial mesoderm (Noden 1988; Couly et al. 1992), with additional contribution from the endoderm and surface ectoderm (Couly and Le Douarin 1990). Normal craniofacial development requires the orchestrated differentiation of these germ layers for functional integration of the facial and skull bones, muscle, connective tissue, skin, and the central and peripheral nervous systems (Trainor 2005). Therefore, it is not surprising that without the proper integration of these tissues during development craniofacial defects arise, accounting for one-third of all congenital malformations within human populations. Craniofacial malformations

primarily arise from defects in the formation, migration and/or differentiation of cranial neural crest cells and understanding the mechanisms which regulate these processes is crucial for the prevention or repair of congenital craniofacial defects. Of central importance, is a more thorough understanding of the specific tissue interactions that occur between the neural crest cells and surrounding tissues in regulating craniofacial morphogenesis.

Collectively, neural crest cells provide an intriguing model for studying a wide range of developmental processes. Additionally, they provide a unique paradigm for studying how changes in the craniofacial architecture affect the evolutionary adaptation of the face (Helms et al. 2005). Although neural crest cells have a number of roles along the anterior-posterior axis of the embryo, this work focuses on the neural crest cells and their role in the development of the craniofacial complex; experiments addressing the induction and patterning of the neural crest are presented herein.

Neural Crest Cell Induction: an Intersection of Multiple Signaling Pathways

Neural crest cells arise along the dorsal aspect of the neural plate border: the junction of the non-neural ectoderm (presumptive epidermis) and the neural plate (presumptive central nervous system). Neural crest cells flank the neural plate bilaterally and are induced along the entire region caudal to the prospective diencephalon (LaBonne and Bronner-Fraser 1999; Yanfeng et al. 2003; Basch et al. 2004; Huang and Saint-Jeannet 2004). The induction and formation of the neural

crest is tightly linked to the neurulation process, in which the neural plate and surrounding epidermal cells undergo changes in cell shape that result in the formation of the neural tube, and ultimately the central nervous system (Colas and Schoenwolf 2001). Previous experiments have demonstrated that the neural crest forms as a result of inductive interactions between the border of the neural plate and surrounding surface ectoderm (Selleck and Bronner-Fraser 1995; LaBonne and Bronner-Fraser 1999; Christiansen et al. 2000). Multiple signaling molecules have been shown to play a role in the induction of neural crest cells including BMP, FGF, NOTCH , PAX and WNT signaling (Figure One), although specifies-specific differences exist in the induction process.

Although inductive interactions between the surface ectoderm and neural plate are necessary for inducing neural crest cells, the molecular signals underlying this process are less understood and multiple morphogens have been indicated in regulating this process. Experiments in *Xenopus* have suggested that a gradient of BMP signaling is necessary to induce neural crest cells (Mayor et al. 1995; Morgan and Sargent 1997; Marchant et al. 1998), with the highest concentrations of BMP molecules present in the surface ectoderm. In avian embryos, BMP4/7 have also been implicated neural crest cell induction (Liem et al. 1995; Selleck et al. 1998); *Bmp4/7* are expressed in the epidermal ectoderm adjacent to the neural plate in cranial regions. Contact-mediated interactions between the surface ectoderm and neural plate explants are required for the induction of *Slug*$^{+}$ and HNK-1^{+} neural crest

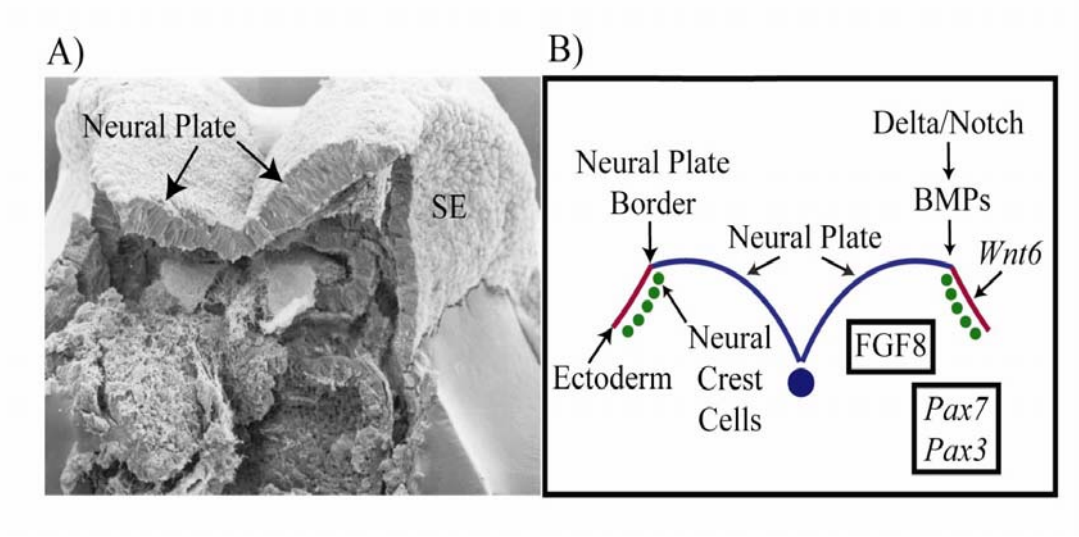

Figure One. Genetic Regulation of Neural Crest Cell Induction. A) Scanning electron micrograph of an 8.5dpc mouse embryo. Neural crest cells (NCC) are induced along the neural plate border, the junction of the neural plate (NP) and the surface ectoderm (SE); experiments have indicated that both the NP and SE give can rise to NCC. B) Schematic of the tissue interactions and morphogens required for NCC induction. A gradient of BMP signaling is required at the neural plate border to specify NCC identity; the effects of BMP signaling are partially modulated by NOTCH signaling. In the SE, *Wnt6* is sufficient to induce NCC in avian embryos. Additionally, *Pax3* and *Pax7* play a role in the induction process; the domain of *Pax7* expression in the early epiblast-staged avian embryo has been shown to specify NCC, while mouse mutants of *Pax3* and *Pax7* have decreased numbers of NCC. Finally, FGF8 signaling from the paraxial mesoderm converges on *Pax3* to regulate NCC formation in *Xenopus*. Adapted from Trainor et al. 2003.

cells *in vitro* (Liem et al. 1995). BMP4- or BMP7-conditioned media enhances the expression of *Slug*$^+$ and HNK-1$^+$ migratory cells, mimicking the epidermis and its ability to induce neural crest cells in neural plate explants (Liem et al. 1995). In contrast, grafts of Noggin-expressing cells into the neural tube results in the downregulation of *Bmp4* and subsequent absence of *Slug*$^+$ migratory neural crest cells

(Selleck et al. 1998). BMP4 appears to be a downstream target of NOTCH signaling (Endo et al. 2002); electroporation of dominant-negative constructs to *Delta1* (a Notch ligand) results in a marked reduction of *Slug* and *Bmp4*, thereby indicating an indirect requirement for NOTCH signaling in neural crest cell induction. Transient exposure to NOTCH signaling is required for the induction of *Bmp4* in the surface ectoderm, which in turn, regulates neural crest cell formation (Endo et al. 2002).

Interestingly, *Bmp4* mouse mutants are embryonic lethal at approximately 9.5dpc but exhibit normal branchial arch development (Winnier et al. 1995), suggesting that *Bmp4* is not a key regulator of neural crest cell induction as has been indicated in avian and *Xenopus* embryos. In contrast, $Bmp2^{-/-}$ embryos exhibit little evidence for the existence of migrating $Crabp1^{+}$ neural crest cells (Kanzler et al. 2000), although embryonic lethality has precluded further examination of additional neural crest cell markers. Furthermore, although the phenotype of *Bmp2* null embryos was suggestive of a role for BMP signaling in neural crest cell induction (Kanzler et al. 2000), a more recent conditional allele of *Bmp2* has shown it is only required for neural crest cell migration (Correia et al. 2007). Conditional ablation of *BMPr1a* (*Alk3*) signaling in neural crest cells using *Wnt1-cre* results in cardiac outflow tract defects, such as a lack of septation and shortened conotruncal length (Stottmann et al. 2004). Despite the cardiac defects, the induction of neural crest cells is normal, suggesting that signaling through the *BMPr1a* is not a requirement during the initial specification of neural crest cells at early somite stages (Stottmann et al. 2004). Interestingly, this data suggests that contact mediated BMP induction of

neural crest cells is highly conserved in avian and *Xenopus* embryos, but that this pathway may not be the key regulator in the mouse.

In addition to BMP signals from the epidermis, there is considerable evidence for a role of the underlying mesoderm in the induction of the neural crest. Paraxial mesoderm, which is a source of FGF signaling, has been shown to be a potent inducer of the neural plate border (Bang et al. 1997) and neural crest cell markers (Monsoro-Burq et al. 2003). Co-culture of presumptive paraxial mesoderm with animal cap explants induces *Slug* and *Twist* in *Xenopus*; conversely, removal of presumptive paraxial mesoderm results in decreased expression of *Slug* (Bonstein et al. 1998; Marchant et al. 1998). In particular, *Fgf8* has been shown to regulate this process (Monsoro-Burq et al. 2003), injection of *Fgf8* in *Xenopus* embryos or animal caps results in the upregulation of *Slug*, as well as the additional crest cell markers *Zic5* and *FoxD3* (Monsoro-Burq et al. 2003). Induction of neural crest cells by *Fgf8* is mediated through *Pax3* (Monsoro-Burq et al. 2005), indicating that integration of multiple signaling pathways is required for proper neural crest cell induction in *Xenopus*.

A role for WNT signaling in neural crest cell induction comes from experiments performed in *Xenopus* and avian embryos. In *Xenopus,* analysis of the *Slug* promoter region identified a Lef/β-catenin binding site necessary for expression of *Slug*, indicating the direct activation of neural crest cell induction via WNT signaling (Vallin et al. 2001). Multiple *Wnt* family members have been identified as inducers of neural crest cells; *Wnt7b* in conjunction with BMP inhibition induces *Slug*

and *Twist* in ectodermal explants (Saint-Jeannet et al. 1997; Chang and Hemmati-Brivanlou 1998; LaBonne and Bronner-Fraser 1998) and overexpression of *Wnt1* or *Wnt3a* results in an increased *Slug* expression at the expense of the ectoderm (Saint-Jeannet et al. 1997; Chang and Hemmati-Brivanlou 1998; LaBonne and Bronner-Fraser 1998). Additionally, overexpression of downstream members of the Wnt canonical pathway, such as *β-catenin* (LaBonne and Bronner-Fraser 1998; Wu et al. 2005) or *dishevelled* (Yanfeng et al. 2003) results in ectopic expression of neural crest cell markers. In contrast, overexpression of dominant-negative *Wnt* ligands or the Wnt antagonist *glycogen synthase kinase-3* blocks neural crest cell production (Saint-Jeannet et al. 1997; Chang and Hemmati-Brivanlou 1998; LaBonne and Bronner-Fraser 1998). In avian embryos, *Wnt6a* is expressed in the epidermis during the induction process and *in vivo* treatment with a dominant negative *Wnt1* construct blocks *Slug* expression with embryos exhibiting altered crest cell migration as indicated by HNK-1 staining (Garcia-Castro et al. 2002). *Wnt6* appears to be acting through the canonical signaling pathway as β-catenin was located within the nuclei of the neural folds, consistent with reports highlighting the importance of canonical WNT signaling in *Xenopus*. Wingless-conditioned media (*Wg*, *Drosophila* homologue of *Wnt1*) induces neural crest cells from naïve neural plate tissue *in vitro*, an effect that was inhibited with the addition of functional antibodies to Wg (Garcia-Castro et al. 2002). Interestingly, treatment with BMP4-conditioned media did not induce neural crest cells without additional additives (Garcia-Castro et al. 2002), suggesting that early reports demonstrating the induction of crest cells *in vitro* by

BMP4 were most likely a result of serum additives present within the culture media as opposed to a specific role for BMP4 in the induction process.

Genetic analysis of *Wnt* pathway mutants in the mouse has revealed roles for WNT signaling in the maintenance of neural crest cell progenitors but not as regulators of the induction process. *Wnt1*$^{-/-}$*;Wnt3a*$^{-/-}$ embryos have decreased expression of *Mash1* and *Pax3*, markers of dorsolateral progenitor cells of the neural tube (Ikeya et al. 1997). Further, analysis of *Wnt1*$^{-/-}$*;Wnt3a*$^{-/-}$ double mutants revealed migratory *Crabp1*$^{+}$ and *Ap2*α^{+} neural crest cells, although the cells were reduced in number compared to wild-type littermates. Decreased neural crest cell production is a result of the requirement of WNT signaling in the maintenance and/or expansion of neural crest cell progenitors. This is reflected by the hypoplastic dorsal root ganglia at 11.5dpc and the lack of the stapes and hyoid bone at 18.5dpc in *Wnt1*$^{-/-}$*;Wnt3a*$^{-/-}$ embryos (Ikeya et al. 1997).

Subsequent analysis of conditional inactivation of β-catenin in neural crest cells using *Wnt1-cre* has revealed a role for WNT signaling in the maintenance of neural crest cells as well as lineage selection of sensory neurons (Brault et al. 2001; Hari et al. 2002). Conditional β-catenin mutants exhibit severe craniofacial defects at late developmental stages and lack all neural crest derived bone, including the maxillary and mandibular bones (Brault et al. 2001). Underlying these late stage craniofacial defects is increased apoptosis at mid-gestational stages. Indeed, analysis of mutant embryos at 9.5dpc revealed migratory *Ap2*α^{+}, *Crabp1*$^{+}$, and *Hoxa2*$^{+}$ neural crest cells that were comparable in number to wild-type littermates; cells which are

subsequently lost due to increased apoptosis at 10.5dpc (Brault et al. 2001). Although neural crest cell induction proceeds normally in conditional β-catenin mutants, mutant analysis at 12.5dpc revealed an absence of sensory neurons, indicating WNT signaling in neural crest cell lineage selection (Hari et al. 2002). Indeed, *Sox10*$^{+}$ neural crest cells in wildtype littermates differentiate into sensory neuronal precursors as indicated by the transcription factors *Ngn2* and *Brn-3A*. In contrast, mutant *Sox10*$^{+}$ neural crest cells fail to express *Ngn2* and do not differentiate into *Brn-3A*$^{+}$ precursors (Hari et al. 2002). As a result, conditional β-catenin mutants lack dorsal root ganglia, but exhibit normal formation of the enteric and sympathetic chain ganglia.

Furthermore, overexpression of a constitutively active β-catenin in mouse embryos results in ectopic sensory neurogenesis at the expense of other neuronal cell fates (Lee et al. 2004). Mutant embryos have decreased migratory neural crest cells populating the cranial nerve ganglia as evidenced by *Sox10*; in contrast, expression of the sensory neuron marker *Cadherin-6 (Cad6)* was significantly upregulated in regions normally devoid of *Cad6*, including the mesenchyme surrounding the cranial nerve ganglia, indicating that the neural crest cells in these regions had adopted a sensory neuron fate (Lee et al. 2004). Consistent with the loss of *Ngn2* in conditional β-catenin mutants, *Ngn2* was dramatically increased in mutants with sustained activation of β-catenin; *Ngn2*$^{+}$ cells were increased in the trunk as were the sensory neuron markers *Neurogenin 1 (Ngn1)* and *NeuroD*. In contrast, the autonomic markers *Mash1* and *eHand* were absent in the mutants in comparison to wildtype

littermates (Lee et al. 2004). Overall these data indicate that WNT signaling through β-catenin is promotes the differentiation of neural crest-derived sensory neurons.

Two members of the *Pax* family of genes, *Pax3* and *Pax7*, have been implicated in neural crest cell formation. In *Xenopus*, *Pax3* has been shown to regulate neural crest cell formation as knockdown of *Pax3* function using antisense morpholinos results in decreased neural crest cell markers (Sato et al. 2005; Hong and Saint-Jeannet 2007). More recently, *Pax7* has been shown to regulate neural crest cell formation in the avian embryo, acting during early gastrulation stages to specify neural crest cell precursors; treatment of chick embryos with *Pax7* morpholinos resulted in decreased expression of the neural crest cell markers *Slug, Sox9,* and HNK-1 (Basch et al. 2006). In zebrafish, both *Pax3* and *Pax7* are expressed in neural crest cells (Lacosta et al. 2007), but do not appear to be required for the formation of the population as a whole. Morpholinos directed to either *Pax3* or *Pax7* do not prevent neural crest cell induction, but rather reduce specific populations of crest cells that contribute to xanthophores (pigment cells) (Lacosta et al. 2007; Minchin and Hughes 2008) and enteric neuron development (Minchin and Hughes 2008).

In the mouse, *Pax3* and *Pax7* have similar domains of expression within the neural tube and both genes are expressed in neural crest cells (Mansouri et al. 1996). *Pax3*$^{-/-}$ embryos, or *Splotch* mutants, exhibit defects in neural crest cells migrating into the developing heart, cranial and dorsal root ganglia, and pigmentation defects (Conway et al. 1997; Epstein et al. 2000). *Splotch* mutants survive until late gestational stages and exhibit trunk specific defects. Indeed, examination of neural

crest cell migration in *Splotch* mutants has revealed that mutant embryos exhibit normal crest cell migration in anterior regions of the embryo, with the most caudal tail regions lacking any identifiable migration (Serbedzija and McMahon 1997). Interestingly, *Pax7*$^{-/-}$ embryos survive until postnatal stages and exhibit minor defects in the overall size of the maxilla (Mansouri et al. 1996). Neural crest cell defects have been described in both *Pax3*$^{-/-}$ and *Pax7*$^{-/-}$ embryos but the overall lack of severity in phenotype has been attributed to functional redundancy between the two genes (Mansouri et al. 1996). To date, *Pax3*$^{-/-}$;*Pax7*$^{-/-}$ double mutant embryos have not been assayed for defects in neural crest cell formation, examination of double mutant embryos would ultimately clarify the direct role, if any, for *Pax3* and *Pax7* in neural crest cell induction in the mouse.

Evidence in avian, frog, and fish embryos indicate that *Bmp Fgf, Notch, Pax* and *Wnt* play significant species specific roles in neural crest cell induction (Figure One). In contrast, in the mouse, none of the *Bmp Fgf, Notch, Pax* or *Wnt* pathway mutants that have been generated, exhibit a complete absence of neural crest cell formation. Instead, these pathways appear only to effect the migration and/or differentiation of mammalian neural crest cells. One reason for the discrepancy may be that in frogs, fish, and chicks it is very difficult to temporally separate the process of neurulation from neural crest cell induction and those key signaling pathways are used reiteratively. In mice, the slower pace of embryogenesis combined with conditional mutagenesis provides for a better, more specific assessment of the neural crest cell induction process, separately from neurulation.

Migration and Derivatives of the Neural Crest

During the induction process, neural crest cells are formed via an epithelial to mesenchymal transition, after which they delaminate from the neural tube, and migrate throughout the embryo (Le Douarin and Kalcheim 1999; Christiansen et al. 2000; Yanfeng et al. 2003; Basch et al. 2004; Huang and Saint-Jeannet 2004). This epithelial to mesenchymal transition is marked by specific transcription factors, such as *Snail (Snail1* & *Snail2)*, which are some of the earliest known markers of neural crest induction. The *Snail* family of genes act as transcriptional repressors which downregulate cell adhesion molecules, in particular, *E-cadherin,* allowing individual crest cells to delaminate from the neural tube and migrate to appropriate destinations in the developing embryo (Cano et al. 2000). The first evidence of the involvement of the *Snail* family of genes in neural crest cell EMT was reported in avian embryos; treatment with antisense oligonucleotides to *Slug* (the avian homologue of *Snail*) resulted in the inhibition of neural crest cell delamination (Nieto et al. 1994). Treatment with an antisense or dominant negative constructs in *Xenopus* embryos lead to defects in crest cell migration (Carl et al. 1999; LaBonne and Bronner-Fraser 2000; Mayor et al. 2000); conversely, overexpression of *Snail* results in increased neural crest cell production (del Barrio and Nieto 2002). Although *Snail/Slug* is required for the delamination of neural crest cells in avian and *Xenopus* embryos, genetic analyses in mouse have indicated that *Snail1* and *Snail2* are not required for crest cell delamination, suggesting that additional pathways may regulate this process

(Murray and Gridley 2006). Indeed, recent reports have indicated non-canonical WNT-signaling as a regulator of neural crest cell formation as injection of dominant-negative *Dishevelled* results in complete inhibition of neural crest cell migration (De Calisto et al. 2005; Matthews et al. 2008).

The migration patterns of neural crest cells are highly conserved across vertebrate species, but the onset of migration differs. For example, neural crest cells in mice and opossums begin to migrate prior to the closure of the neural tube (Le Douarin and Kalcheim 1999; Kulesa et al. 2004), while crest cells in avian embryos do not migrate until neural tube closure is complete (Le Douarin and Kalcheim 1999; Kulesa et al. 2004), suggesting that neural tube closure is not required for neural crest cell induction and migration.

Neural crest cells can be divided into four major domains along the anterior-posterior axis; the cranial, cardiac, trunk and vagal populations (Le Douarin 2004) and fate maps have elegantly demonstrated the specific derivatives that arise from each axial population of neural crest cells (Le Douarin and Kalcheim 1999; Le Douarin 2004) (Figure Two). Cranial neural crest cells arise from the mid-diencephalon caudally to rhombomere 7 of the hindbrain (Osumi-Yamashita et al. 1994; Osumi-Yamashita et al. 1996) and migrate in highly conserved migratory streams (see *Neural Crest Cell Contribution to the Developing Face*). Cranial neural crest cells give rise to the connective tissue, teeth, melanocytes, and sensory and parasympathetic ganglia of the head (Larson 1993). In addition, the cranial neural

crest forms the majority of bone and cartilage of the head and face; two endogenous derivatives unique to this domain of crest cells.

Cardiac neural crest cells migrate ventrally from a region spanning the rhombomere 6 of the hindbrain to somites 3, with each somitic level contributing to the septation of the aorta and pulmonary artery as well as the aortic arch smooth muscle (Kirby et al. 1983; Kirby and Stewart 1983). Additional contribution to the heart includes the semilunar and atrioventricular valves as well as the parasympathetic innervation of the heart (Hutson and Kirby 2007). Cardiac neural

Cell Types	Tissue/Organs
Sensory Neurons	Craniofacial skeleton
Cholinergic neurons	Cornea
Adrenergic neurons	Teeth & Dentine
Glial cells	Thymus
Schwann cells	Thyroid gland
Chromaffin cells	Parathyroid gland
Parafollicular cells	Adrenal gland
Calcitonin-producing cells	Spinal ganglia
Melanocytes	Parasympathetic nervous system
Chondroblasts	Sympathetic nervous system
Chondrocytes	Connective tissue
Osteoblasts	Adipose tissue
Osteocytes	Cardiac septa
Odontoblasts	Smooth muscles
Fibroblasts	Meninges
Striated myoblasts	Dermis
Smooth myoblasts	Blood vessels
Adipocytes	Endothelia
Mesenchymal cells	Heart

Figure Two. Derivatives of the Neural Crest. Neural crest cells are a multipotent cell population which give rise to a diverse array of cell types. Neural crest cells contribute to the majority of the tissues and organs in the body extending the length of the anterior-posterior body axis. From Crane & Trainor, 2006.

crest cells give rise to the connective tissue of the thymus, thyroid, and parathyroid glands. Cardiac neural crest cells were first identified in chick ablation experiments (Kirby et al. 1983) and were so named due to the resulting cardiac phenotypes identified in ablated-embryos. Interestingly, ablation of premigratory cardiac neural

crest cells results in cardio- and non-cardiovascular defects, including persistent truncus arteriosus, an incomplete septation of the aortic and pulmonary outflow tracts; non-cardiovascular phenotypes include defects in thymic, parathyroid, and often thyroid gland development (Hutson and Kirby 2007).

Trunk neural crest cells arise at the axial level of somite 5 to the caudal tip of the neural tube and follow two migratory routes that dictate the types of derivatives formed. Neural crest cells that migrate along the dorsolateral pathway travel between the ectoderm and somites and give rise to melanocytes (Krull 2001); cells that travel along the ventromedial pathway generate the dorsal root and sympathetic ganglia, adrenomedullary cells and Schwann cells (Krull 2001). In avian and murine embryos, cells migrate ventrally through the anterior portion of each somite, a process mediated by repulsive Eph/ephrin signaling. Posterior portions of each somite express *ephrin-B1*, while neural crest cells express *EphB3*; Eph/ephrin signaling restricts neural crest cells to the anterior somitic regions (Krull et al. 1997). In addition to the restrictive signaling mediated by Eph/ephrin signaling, neural crest cell migration through the somites is regulated by neuropilin/semaphorin signaling. *Neuropilin2* (*Npn2*) is expressed in migratory neural crest cells in avian and murine embryos that normally only cross the anterior half of each somite. Loss of *Npn2* results in aberrant migration through anterior and posterior halves of the somites, with cells migrating as a uniform sheet instead of in characteristic streams (Gammill et al. 2006). *Semaphorin 3f* (*Sema3f*), a ligand for *Npn2*, is expressed in the posterior region of the somites, in a complimentary pattern to *Npn2*, indicating that reciprocal

signaling may restrict neural crest cell migration to the anterior half of each somite; indeed, analysis of *Sema3f*$^{-/-}$ embryos mimics the phenotype of *Npn2*$^{-/-}$ mutants (Gammill et al. 2006). Two additional domains of neural crest cells, the vagal and sacral neural crest contribute to the parasympathetic ganglia of the gut (Burns and Douarin 1998; Le Douarin and Kalcheim 1999). Vagal neural crest cells (somites 1-7) colonize the entire length of the gut, while the sacral neural crest cells (caudal to somite 28) only contribute to the caudal portions of the bowel (Le Douarin and Kalcheim 1999).

Because of the multipotent nature and numerous derivatives produced by neural crest cells, the neural crest has been suggested to be a stem cell or stem cell-like population (Bronner-Fraser and Fraser 1989). Although extensive evidence demonstrates the multipotent nature of neural crest cells *in vivo* and *in vitro*, the actual numbers of bona fide neural crest stem cells is extremely small, accounting for approximately 1-3% of the entire crest cell population (Bronner-Fraser and Fraser 1989; Crane and Trainor 2006). However, while this suggests that the neural crest population does contain a small percentage of cells with stem cell characteristics, the neural crest is a transient population generated during a limited time window at each axial level. Therefore, the neural crest population, as a whole, consists of both multipotent and more developmentally restricted progenitor cells (Crane and Trainor 2006).

Neural Crest Cell Contribution to the Developing Face

Neural crest cells stereotypically migrate into the developing face in patterns highly conserved across vertebrate species. Populations of neural crest cells contributing to the posterior facial structures migrate out from the hindbrain (Figure Three) (Lumsden et al. 1991; Osumi-Yamashita et al. 1994). Rhombomeres are structurally distinct segments of the hindbrain and are critically important for specifying the crest cell contribution to each particular migratory stream (Trainor and Krumlauf 2000a). Indeed, the contribution of crest cells to a branchial arch is highly conserved across multiple vertebrate species (Kiecker and Lumsden 2005).

Cells migrate laterally into the first branchial arch (BA1) from rhombomeres one and two and rostrally from rhombomere 3 (Lumsden et al. 1991; Serbedzija et al. 1992; Sechrist et al. 1994), to form the maxilla and mandible, trigeminal ganglia, and the incus and malleus bones of the middle ear (Le Douarin and Kalcheim 1999). The second branchial arch (BA2) is populated by cells arising from rhombomeres three, four, and five (Lumsden et al. 1991; Sechrist et al. 1994; Trainor and Tam 1995; Trainor and Krumlauf 2000b). Interestingly, this second stream receives laterally migrating cells from rhombomere four (R4) as well as caudal and rostrally migrating cells from R3 and R5, respectively (Sechrist et al. 1993). Indeed, very little to no neural crest cells are found in regions lateral to the odd-numbered rhombomeres, the underlying mechanism of which remains poorly understood. Repulsive signaling

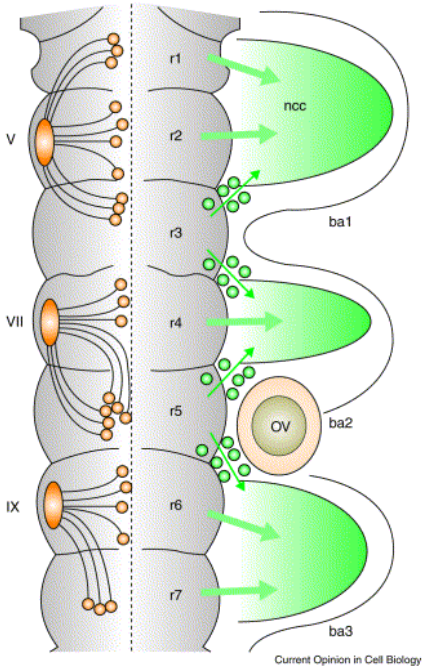

Figure Three. Neural Crest Cells migrate from the Hindbrain in Three Streams conserved across Vertebrates. Neural crest cells (NCC) (green) migrating from rhombomere (r) 1, r2, and r3 form the first stream of migratory NCCs that will populate branchial arch (ba) 1. The second stream is composed of NCCs migrating from r3, r4, and r5 to populate ba2. The third stream is composed of NCCs from r5, r6, and r7. This pattern of migration correlates to the position of cranial nerve ganglia (orange), including the trigeminal (V), facial (VII), and glossopharyngeal (IX), seen at later developmental stages. From Trainor and Krumlauf, 2001.

may play a role as intermingling between segments is restricted by interactions between the *ephrin/Eph* receptors and *Neuropilin2/semaphorin3f*, further defining segmental identity (Becker et al. 1994; Mellitzer et al. 1999; Xu et al. 1999; Gammill et al. 2006). Derivatives of the second branchial arch include the hyoid bone, styloid processes of the temporal bone, the stapes bone (middle ear), as well as the facial nerve ganglia (Le Douarin and Kalcheim 1999). BA3 is populated by cells from the sixth and seventh rhombomeres and contributes to the hyoid bone and the glossopharyngeal ganglia (Kontges and Lumsden 1996; Le Douarin and Kalcheim 1999).

The mid- to upper facial region is populated by neural crest arising from the developing dien- and mesencephalon (Figure Four & Five) (Osumi-Yamashita et al. 1994). In total, seven prominences comprise the vertebrate face: the frontonasal prominence (FNP), and the paired lateral nasal, maxillary and mandibular prominences (Helms et al. 2005; Tapadia et al. 2005). The FNP is derived from a midline primordium that forms on top of the forebrain and is populated by neural crest cells that migrate ventrally from the mid-diencephalon, integrating with rhombomeric neural crest cells (Osumi-Yamashita et al. 1994; Tapadia et al. 2005). Neural crest cells begin to migrate into the FNP as early as 8.25dpc (5-somite stage) and will continue to populate this region until late 8.5 to early 9.0dpc (9-10 somite stage) (Osumi-Yamashita et al. 1994). At 9.0dpc, the FNP is distinguishable as a smooth outgrowth in the developing facial region and by 10.5dpc the FNP is divided into the median (frontal) and lateral nasal prominences. The median nasal prominence is a bi-partite structure that, in conjunction with the lateral nasal prominences, form the nasal pits. The median nasal prominence will give rise to the forehead, middle of the nose, philtrum of the upper lip, and primary palate. The lateral nasal prominence contributes to the nasal pits, and forms the sides of the nose (Tapadia et al. 2005). Additionally, the lateral nasal prominence is required for components of the upper jaw in avian embryos, including the lateral edges of the premaxillary bone (Szabo-Rogers et al. 2008).

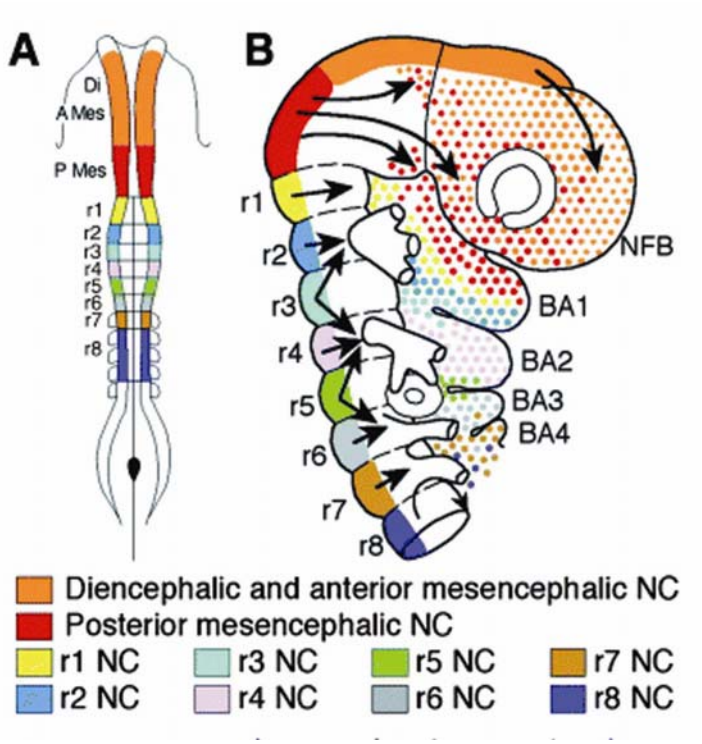

Figure Four. Contribution of Cranial Neural Crest Cells to the Developing Frontonasal Region and Branchial Arches. A) Neural crest cell (NCC) territories prior to migration from the diencephalon (orange) to the posterior hindbrain (dark blue). B) Schematic of NCC and the craniofacial regions they populate. The frontonasal region (orange/red) is populated by diencephalic & mesencephalic NCC. BA1 (red/yellow/light blue) is populated by NCC from the posterior mesencephalon and r1-r3, while BA2 (light blue/pink/green) is populated by NCC from r3-r5. BA3 and BA4 are populated by cells from r5-r7 and r7-r8, respectively. From Creuzet et al. 2005.

The two remaining prominences, the mandibular and maxillary prominences, are components of the first branchial arch that contribute to lower facial structures. The mandibular prominences are a bilateral outgrowth of BA1, identifiable as early as 8.5dpc and continue to extend distally until they begin to fuse maybe as early as 9.5dpc. The mandibular prominences give rise to the components of the lower jaw, including Meckel's cartilage. The maxillary prominence is first identifiable at

approximately 8.75dpc as a proximal bulge of tissue positioned just anterior to the mandibular prominence. As it is populated by neural crest cells, the maxillary prominence extends antero-ventrally and forms the zygomatic complex (cheekbones), upper jaw components, lips, and the secondary palate (Tapadia et al. 2005).

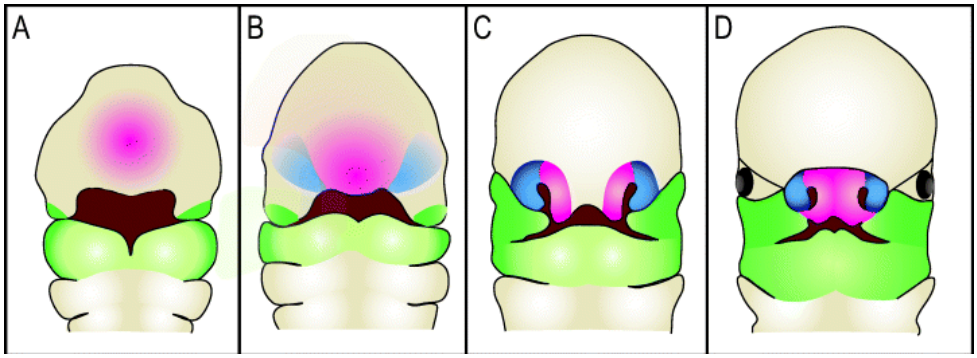

Figure Five. Development of the Craniofacial Primordia. A) At 9.5dpc, the frontonasal prominence (pink) is medially positioned; the maxillary and mandibular prominences (green) are also identifiable. B) By 10.5dpc, the medial nasal prominence (pink) and lateral nasal prominence (blue) are identifiable and will give rise to the middle and lateral sides of the nose. C) At 11.5dpc, the maxillary and mandibular prominences (green) have fully formed and will give rise to upper and lower jaw components, including the mandible and secondary palate. D) View of an embryo indicating the final position of each facial primordium. Adapted from Tapadia et al. 2005.

The positional identity of the branchial arches is mediated in part by two families of homeodomain transcription factors, the *Homeobox* (*Hox)* and *Distal-less (Dlx)* genes. *Hox* genes were first identified in *Drosophila* for their ability to cause homeotic transformations of the body plan (Akam et al. 1988). While flies have eight *Hox*, (*HomC)* genes located in a single cluster, mammals have 39 *Hox* genes, resulting

from duplications of the ancestral *Hox* cluster. Mammalian *Hox* genes are arranged in four clusters, *Hoxa-Hoxd*, of 13 paralogous groups; paralogous *Hox* genes have been established based on sequence similarity and position within the cluster. The identification of conserved *Hox* genes throughout vertebrate evolution has indicated their importance in patterning the vertebrate body plan (Santagati and Rijli 2003).

The expression of *Hox* genes in the hindbrain mediates the antero-posterior identity of the rhombomeres as well as neural crest cells migrating from this region (Trainor and Krumlauf 2000a). Rhombomeric segments and neural crest cells share a unique pattern of *Hox* gene expression, although each tissue is independently regulated (Trainor and Krumlauf 2000a). For example, rhombomere 1 (r1) does not express any *Hox* genes, nor do neural crest cells migrating from this segment to populate BA1 (Trainor and Krumlauf 2000a). In contrast, rhombomere 2 (r2) expresses *Hoxa2* up to the posterior r1 boundary, as well as in the more posterior hindbrain segments. Despite Hoxa2 expression in r2, neural crest cells migrating from this segment do not express *Hoxa2*, leaving BA1 devoid of any *Hox* gene expression as it is populated by cells from r1 and r2. Instead, $Hoxa2^{+}$ neural crest cells populate the second branchial arch from rhombomeres 3/4 (Hunt et al. 1991). This *Hox* code, present in neural crest cells, results in the regulation of inter-BA identity (Depew et al. 2002). Indeed, specific deletion of *Hoxa2* results in the transformation of second branchial arch derivatives to those of the first branchial arch (Gendron-Maguire et al. 1993; Rijli et al. 1993). Conversely, overexpression of *Hoxa2* in the first branchial arch (normally devoid of *Hox* expression) results in the

transformation of first arch derivatives, such as Meckel's cartilage, to those of the second arch (Grammatopoulos et al. 2000; Pasqualetti et al. 2000). These transformations indicate a role for *Hoxa2* in the specification of second branchial arch identity and that an absence of *Hox* gene expression in r1/r2 is responsible for the patterning of the first branchial arch and its derivatives.

Despite the evidence supporting a patterning role for *Hox* genes in neural crest cell and branchial arch development, the surrounding environment in which neural crest cells migrate also influences crest cell patterning and plasticity. Elegant experiments involving intra-species grafts have highlighted the degree of plasticity exhibited by neural crest cells (Trainor and Krumlauf 2000b). Intra-species transplantation of small numbers of *Hox*-expressing neural crest cells into a non-*Hox* environment, results in neural crest cells reprogramming the *Hox* genes expressed to match the surrounding environment (Trainor and Krumlauf 2000b). In contrast, when large numbers of Hox^{+} neural crest cells are grafted into a *Hox*-negative environment, the original *Hox* code is maintained, indicating that migratory neural crest cells are subject to community as well as environmental cross-talk; plasticity is ultimately dependent on the size of the population affected as well as timing. Collectively, these results indicate a unique role for *Hox* genes in the patterning of neural crest cells and their facial derivatives that is dependent on the numbers of neural crest cells present within a cohort.

While *Hox* genes regulated the antero-posterior identity of the caudal BAs, the antero-posterior and proximo-distal identity of BA1 is mediated by *Distal-less (Dlx)*

genes. *Dlx* genes were first identified in *Drosophila* as regulators of proximodistal patterning of the limbs (Cohen 1990). In vertebrates, *Dlx* genes are expressed at various sites of outgrowth, including the limbs and branchial arches (Depew et al. 2005). Mice have six *Dlx* genes, *Dlx1-Dlx6,* which are clustered as first-order paralogues adjacent to the *Hox* genes (Panganiban and Rubenstein 2002) and can further subdivided into second-order paralogues based on sequence similarity (Depew et al. 2005). The genomic clustering of *Dlx* genes results in set of genes being tightly regulated, which directly impacts their expression patterns within the BAs. Indeed, *Dlx* genes exhibit a nested pattern of expression within the ectomesenchyme of BA1 (Figure Six). BA1 has two proximodistal subdivisions, the maxillary (MxBA1, proximal) and mandibular (MdBA1, distal) arches, which contribute to the upper and lower jaws, respectively. First-order paralogues *Dlx1* and *Dlx2* are expressed throughout the mesenchyme of BA1, including the proximal MxBA and distal MnBA (Depew et al. 2002; Depew et al. 2005). In contrast, *Dlx5*/*Dlx6* and *Dlx3*/*Dlx4* share more restrictive domains within the distal MnBA (Depew et al. 2002; Depew et al. 2005). Overall, this results in a unique array of *Dlx* gene expression within BA1 along the proximodistal axis.

The nested pattern of *Dlx* expression in the branchial arches indicates that a *Dlx* code is responsible for establishing intra-BA identity. Indeed, mutant analysis of single or compound *Dlx* embryos supports the specific role of *Dlx* family members in specifying BA identity along the proximodistal axis. Indeed, single mutants of *Dlx1* and *Dlx2* exhibit varying degrees of skeletal defects in maxillary derived structures.

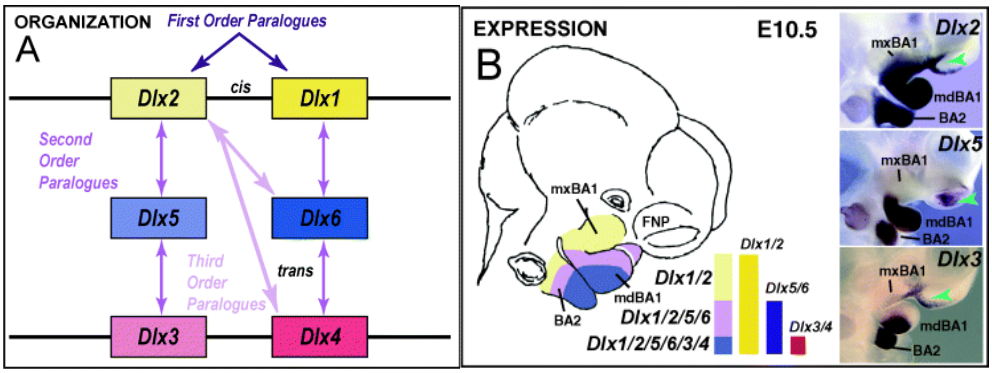

Figure Six. *Distal-less* Genes regulate Intra-BA Identity. A) Mice have six *Dlx* genes that are tightly clusted and arranged in bigene pairs of first-order (*cis*) paralogues, *Dlx1/2*, *Dlx5/6*, and *Dlx3/4* (dark blue arrows). Similarity of genomic sequence outside of the homeodomain further identifies two groups of second-order (*trans*) paralogues, *Dlx1, 6,* and *4* and *Dlx2, 3*, and *5* (purple arrows). Third-order paralogues (light purple arrows) are those that are not linked as first-order or are not part of a second-order paralogous group. B) First-order *Dlx* paralogues exhibit a nested pattern of expression in the ectomesenchyme of the BAs; *Dlx1/2* (yellow/purple/blue) are expressed throughout the proximodistal axis of BA1/BA2. *Dlx5/6* (purple/blue) and *Dlx3/4* (red/blue) are expressed in more distally restricted patterns in the distal portion of BA1/BA2; only *Dlx1/2* are expressed in the maxillary prominence, the proximal region of BA1. Images to the right of panel B are *in situ* hybridizations of *Dlx2*, *Dlx5*, and *Dlx3*, demonstrating the progressive restriction of *Dlx5* and *Dlx3* to more distal portions of BA1/2. From Depew et al. 2005.

Dlx1$^{-/-}$ embryos lack the ala temporalis (proximal component of the sphenoid bone, a MxBA derivative) and the incus has an altered morphology in comparison to wildtype embryos (Qiu et al. 1997), while *Dlx2*$^{-/-}$ mutants have defects in the ali- and basisphenoid bones (Qiu et al. 1995). *Dlx1/2*$^{-/-}$ compound mutants are embryonic lethal and exhibit more severe defects of proximal MxBA-derived bones than single

Dlx1/2 mutants, indicating that *Dlx1/2* are particularly important for proximal MxBA derivatives (Qiu et al. 1997).

The distal component of BA1, the mandible, is patterned by more distally restricted *Dlx* genes, in particular *Dlx5* and *Dlx6*. *Dlx5*$^{-/-}$ mutants exhibit a shortening of Meckel's cartilage which is split proximally and exhibits ectopic intramembranous bone; the ectopic bone associated with Meckel's cartilage is abnormally jointed to the tympanic ring (Depew et al. 1999). Mutant embryos exhibit a thickening of the tympanic ring and the malleus and dentary bones (Depew et al. 1999). Compound *Dlx5/6*$^{-/-}$ embryos exhibit a homeotic transformation of MnBA into MxBA derivatives, highlighting the importance of *Dlx5/6* in the specification of antero-posterior identity of the mandible. Additionally, the proximo-distal patterning of MnBA is altered in *Dlx5/6*$^{-/-}$ embryos; heterozygous embryos exhibit *Dlx*3, *Alx4*, and *Bmp7* at the distal edge of the developing mandible, domains of expression that were lost or altered in *Dlx5/6*$^{-/-}$ mutants. In contrast, markers of more proximal maxillary regions, such as *Dlx2*, *Wnt5a*, and *Prx2*, are upregulated in the mandible of mutant but not heterozygous embryos (Depew et al. 2002).

At later developmental stages, mutant embryos exhibit a duplication of upper jaw structures; where the mandible would normally be positioned, mutant embryos have ectopic maxillary and palatine bones and Meckel's cartilage was transformed into a duplicate ala temporalis. Additionally, soft tissue structures normally associated with the upper jaw were duplicated in *Dlx5/6*$^{-/-}$ embryos; whisker vibrissae

and a second set of rugae (roof of the mouth) were present in the duplicated jaw structure (Depew et al. 2002).

Studies from *Dlx1/2*$^{-/-}$ and *Dlx5/6*$^{-/-}$ mutants demonstrate the importance of first-order *Dlx* paralogues in the patterning of proximal and distal skeletal elements. Recent analysis of compound *Dlx2/5*$^{-/-}$ mutants has indicated cross-talk between first- and second-order *Dlx* paralogues. As expected, *Dlx2/5*$^{-/-}$ embryos exhibit defects similar to those originally characterized in single *Dlx2* (Qiu et al. 1995) or *Dlx5* mutant embryos (Depew et al. 1999). Additionally, *Dlx2/5*$^{-/-}$ mutants exhibit more severe defects in distal regions of BA1, where *Dlx2/5* have overlapping domains of expression. *Dlx2/5*$^{-/-}$ mutants lack all but the rostral region of Meckel's cartilage and exhibit cleft mandibles; the soft tissues are also abnormal with vibrissae and rugae present on the mandible (Depew et al. 2005), similar to *Dlx5/6*$^{-/-}$ embryos (Depew et al. 2002). Collectively, analysis of *Dlx1/2*$^{-/-}$ (Qiu et al. 1997), *Dlx5/6*$^{-/-}$ (Depew et al. 2002), and *Dlx2/5*$^{-/-}$ (Depew et al. 2005) compound mutants highlights the requirement of a *Dlx*-code in establishing intra-BA1 identity through the antero-posterior and proximodistal patterning of maxillary and mandibular derivatives. Furthermore, the alterations in BA morphology and patterning in compound *Dlx* mutant embryos demonstrate the importance of first-order and second-order *Dlx* paralogues in regulating BA identity.

Neural Crest Cell Patterning is mediated by Extrinsic Signaling

The vertebrate face is an integration of multiple craniofacial primordia: the frontonasal (FNP), maxillary, and mandibular prominences, and requires the proper assimilation of tissue layers and cell types for craniofacial development to occur. Indeed, the outgrowth and patterning of the developing face is partially a result of extrinsic signaling between multiple tissue layers, including the ectoderm, mesoderm, endoderm, and neural crest-derived mesenchyme. For example, within the FNP, the mesenchyme receives signals from the underlying forebrain and overlying facial ectoderm which are required for proper outgrowth and patterning of the FNP and its derivatives (Hu et al. 2003; Marcucio et al. 2005; Tapadia et al. 2005). Additionally, the pharyngeal endoderm (PE) mediates tissue interactions that regulate the development of the mandibular prominence. The mandibular prominence is comprised of multiple tissues, including the ectoderm, mesoderm and neural crest cell-derived mesenchyme; extrinsic signaling from the PE acts on the mandibular ectoderm (Moore-Scott and Manley 2005; Haworth et al. 2007) and neural crest cells (Brito et al. 2006) to regulate the proper development of the lower jaw. Collectively, tissue interactions between neural crest cells and the ectoderm and endoderm play a key role in the development of the craniofacial complex and involve multiple signaling pathways, such as SHH, FGF, and BMP signaling; the key roles of each of these pathways in craniofacial development are discussed below.

Ectodermal & Endodermal Hedgehog Signaling regulates Craniofacial Development

Hedgehog (Hh) proteins are a family of secreted proteins, first characterized in *Drosophila*, that are essential for the patterning of multiple regions of the developing embryo. Mammals have three Hh orthologues, *Sonic hedgehog (Shh), Indian hedgehog (Ihh),* and *Desert hedgehog (Dhh)*, each regulating various aspects of embryonic development. *Dhh* is required for spermatogenesis (Bitgood et al. 1996) and the formation of peripheral nerve sheaths (Parmantier et al. 1999); *Ihh* regulates endothelial cell development in the yolk sac (Byrd et al. 2002), hematopoiesis (Dyer et al. 2001), and endochondral bone development (St-Jacques et al. 1999) see *Cartilage and Bone Development* below). Roles for *Shh* in the patterning of the embryonic axis (Mohler and Vani 1992), craniofacial complex (Jeong et al. 2004; Brito et al. 2006), spinal cord (Echelard et al. 1993), and limb bud (Riddle et al. 1993; Chang et al. 1994) have been extensively studied.

Disruptions of SHH in humans results in a range of craniofacial birth defects, the hallmark being holoprosencephaly (HPE), a failure of the forebrain to divide into the left and right hemispheres (Belloni et al. 1996a; Roessler et al. 1996). Classic knockouts of *Shh* result in HPE and a complete absence of the anterior craniofacial skeleton (Chiang et al. 1996). *Shh*$^{-/-}$ embryos have a single optic vesicle along the midline and a reduction in the overall size of the brain and dorsalization of the spinal cord. At later developmental stages, a single nasal proboscis extends from the rostral midline and no external eye structures are seen (Chiang et al. 1996).

In the mouse, *Shh* is expressed in the prechordal plate, zone of polarizing activity (ZPA), floorplate, notochord, pharyngeal endoderm, and in the surface ectoderm of the maxillary and mandibular prominences (Echelard et al. 1993; Chang et al. 1994). *Shh* expression in the notochord and floorplate is required for proper development of ventral cell fates in the brain and spinal cord (Echelard et al. 1993; Riddle et al. 1993); while expression in the ZPA is required for antero-posterior patterning of the developing limb (Riddle et al. 1993).

SHH is a secreted glycoprotein that undergoes cholesterol modification via autocatalytic cleavage of its carboxyl (C)-terminus (Porter et al. 1996a; Porter et al. 1996b), which is required for determining the range of SHH diffusion to Hh-responsive cells. In *Drosophila*, lack of C-terminal modification results in an extended range of SHH signaling in the imaginal discs (Porter et al. 1996a), while in the mouse, the cholesterol modification is required in restricting the spread of SHH from its sites of synthesis (Huang et al. 2007). The role of cholesterol modification differs in various model organisms but overall plays a role in establishing the SHH signaling gradient via regulation of SHH diffusion.

Shh undergoes an additional modification at its amino (N)-terminus via the addition of a palmitic acid moiety (Pepinsky et al. 1998), which has been suggested to increase SHH potency (Taylor et al. 2001). In *Drosophila*, *skinny hedgehog* (*ski*) (Chamoun et al. 2001), *sightless* (*sit*) (Lee and Treisman 2001), *central missing (cmn)* (Amanai and Jiang 2001) and *rasp* (Micchelli et al. 2002) correspond to the same gene which encodes a Hedgehog acyltransferase responsible for the palmitoylation of

Hh proteins (Pepinsky et al. 1998; Chamberlain et al. 2008). *Drosophila* mutants that lack *ski/sit/cmn/rasp* resemble other mutants of Hh signaling and exhibit aberrant patterning defects, indicating that palmitoylation is required in Hh-producing cells to establish a normal Hh-signaling gradient (Amanai and Jiang 2001; Chamoun et al. 2001; Lee and Treisman 2001; Micchelli et al. 2002).

More recently, the murine homologue of *ski*, *Skinny hedgehog* (*Skn*) or *Hedgehog acyltransferase* (*Hhat*) has been characterized. *Skn* mutants lack N-terminal palmitoylation of SHH and exhibit HPE as well as neural tube and limb patterning defects (Chen et al. 2004). Classical knockouts of *Skn* indicate a direct role for palmitoylation in establishing the long-range SHH signaling gradient in the neural tube due to the lack of formation of SHH multimeric complexes (Chen et al. 2004). Additionally, palmitoylation of SHH is required for the formation of SHH multimeric complexes *in vitro* (Goetz et al. 2006) and enhances the ability of SHH to induce neuronal differentiation paradigms in forebrain explants (Kohtz et al. 2001).

Ski/Skn/Hhat are all members of a large family of multipass transmembrane proteins termed MBOAT (membrane-bound *O*-acyltransferase) (Hoffman 2000). MBOAT family members include a diverse group of enzymes responsible for the transfer of fatty acid residues and other lipids onto hydroxyl groups of membrane-embedded lipids (Hoffman 2000). *Skn/Hhat* are palmitoylacyltransferases (PAT) that add a palmitic acid moiety to an N-terminal cysteine via an amide bond linkage (Pepinsky et al. 1998; Buglino and Resh 2008). Studies have indicated that *Skn/Hhat* functions to specifically palmitoylate SHH and IHH. The direct palmitoylation of

DHH has not been demonstrated, although the amino acid consensus site where *Skn/Hhat* acts on SHH and IHH is conserved in DHH, indicating that DHH is most likely palmitoylated in a manner similar to other Hh proteins (Buglino and Resh 2008). *Porcupine (Porc)* is a PAT required for the acylation of Wnt/Wg proteins (Kadowaki et al. 1996; Tanaka et al. 2002) and is responsible for the palmitoylation of WNT1 and WNT3a at N-terminal cysteine residues (Galli et al. 2007). Although the palmitoylation of Wnt and Hh proteins occurs at similarly positioned cysteine residues, cross-talk between *Porc/Hhat* and Hh/Wnt proteins does not occur; Hhat shows specificity for SHH palmitoylation and does not modify WNT3a or WNT7a. Similarly, *Porc* does not palmitoylate SHH, indicating that there is no cross talk between the two PATs despite similar sites of activity within their respective family of proteins.

In contrast, *rasp*, the *Drosophila* homologue of *Hhat*, has been shown to palimtoylate SPITZ, the ligand for the epidermal growth factor receptor (Miura et al. 2006). RASP palmityolates SPITZ at an N-terminal cysteine residue which is required for restricting SPITZ secretion and enhancing its association with the plasma membrane; overexpression of an unpalmitoylated SPITZ *in vitro* results in an increased range of secretion but the protein exhibits decreased activity (Miura et al. 2006). Interestingly, *rasp/Hhat* is required in Hh-producing cells for the spread of the Hh protein, thereby establishing the Hh signaling gradient (Amanai and Jiang 2001; Chamoun et al. 2001; Lee and Treisman 2001; Micchelli et al. 2002; Chen et al. 2004). Evidence of *rasp* restricting the spread of SPITZ protein (Miura et al. 2006)

suggests that *rasp/Hhat* may have dual functions in protein modification, although the determinant of whether palmitoylation at N-terminal cysteine residues restricts or enhances protein distribution remains to be addressed. Collectively, palmitoylation of Hh proteins by *Skn/Hhat* is required for establishing the Hh signaling gradient during development in a manner conserved in other signaling pathways, such as WNT signaling, highlighting the importance of palmitoylation in embryonic development.

During craniofacial development, SHH signaling arises from two sources: the ectoderm and pharyngeal endoderm. *Shh* expression in the cranial region is restricted to the epithelia of the frontonasal and BA ectoderm; each domain of *Shh* has distinct roles in the patterning of the facial prominences and neural crest cells that migrate into these regions. *Shh* in the frontonasal ectoderm defines a region of tissue known as the frontonasal ectoderm zone (FEZ), which is responsible for the outgrowth and patterning of the FNP (Hu et al. 2003). In avian embryos, the FEZ is comprised of adjacent domains of *Shh* and *Fgf8* that correspond to the tip of the upper beak (Hu et al. 2003). Ectopic transplantation of the FEZ results in the reactivation of signaling events in the neural crest-derived mesenchyme resulting in duplicated upper- and lower-beak structures (Hu et al. 2003), indicating that *Shh* in the FEZ is not only required for the outgrowth but also the patterning of FNP derivatives. In contrast, inhibition of FEZ formation through SHH blockades results in truncations of the upper jaw structures (Cordero et al. 2004; Marcucio et al. 2005). SHH signaling from the ventral telencephalon induces *Shh* in the FEZ and is required for FEZ formation and subsequent facial outgrowth (Cordero et al. 2004; Marcucio et al. 2005).

The second domain of *Shh* is located in the maxillary ectoderm and is required for tooth germ initiation (Hardcastle et al. 1998). Mammalian teeth form in the maxillary and mandibular processes of the head via reciprocal interactions between the oral ectoderm and the underlying neural crest-derived mesenchyme (Tucker and Sharpe 1999). In the mouse, individual thickenings within the BA ectoderm at 11.5dpc mark the first morphological signs of tooth development. These thickenings proliferate to form an epithelial bud that, together with BA mesenchyme, forms a tooth germ (Tucker and Sharpe 2004). As development proceeds, the mesenchyme will give rise to the tooth pulp and dentine, while the ectoderm gives rise to the tooth enamel (Tucker and Sharpe 2004).

During the tooth bud initiation, expression of *Shh* is localized to the ectodermal thickenings of future teeth and has been shown to positively regulate tooth development (Bitgood and McMahon 1995; Hardcastle et al. 1998). *In vitro,* SHH acts as a mitogen, inducing proliferation as the thickenings form a tooth bud (Hardcastle et al. 1998; Sarkar et al. 2000; Cobourne et al. 2001). Overexpression of *Shh* results in the activation of target genes in the mandibular mesenchyme (Hardcastle et al. 1998), while inhibition of SHH signaling in mandibular explants results in a failure of bud formation and an arrest of tooth development (Sarkar et al. 2000; Cobourne et al. 2001). Furthermore, conditional knockouts of *Shh* in the developing tooth germ leads to a reduction in overall size of the developing tooth bud (Dassule et al. 2000). Collectively, the localized sites of *Shh* in the oral ectoderm are important for specifying the sites of tooth bud initiation and development.

In addition to the requirement of *Shh* in the facial and oral ectoderm, SHH signaling from the pharyngeal endoderm (PE) is required for the development of the lower jaw structures. Removal of the pharyngeal endoderm in avian embryos results an absence of lower jaw structures, including Meckel's cartilage; a phenotype that is rescued by exogenous SHH (Brito et al. 2006). Additionally, injection of *Shh*-expressing cells into the PE results in the duplication of the lower jaw (Brito et al. 2008). SHH emanating from the PE is necessary for the maintenance of *Bmp4* and *Fgf8* in the mandibular ectoderm (Moore-Scott and Manley 2005; Brito et al. 2006; Haworth et al. 2007; Brito et al. 2008), genes with well characterized roles in the proximo-distal patterning of this region (Moore-Scott and Manley 2005; Brito et al. 2006; Yamagishi et al. 2006; Haworth et al. 2007). Collectively, SHH signaling in the PE is responsible for the maintenance of genes in the BA1 ectoderm and is a source of an organizing center required for the development of the lower jaw.

Neural crest cells populating the facial and mandibular mesenchyme are directly impacted by SHH signaling. Treatment with SHH antibodies, tissue ablation, or conditional activation of *Shh* in neural crest cells results in a range of craniofacial dysmorphologies. In avian embryos, treatment with SHH-antibodies results in embryos that exhibit reduced growth of the facial prominences, increased cell death, and decreased proliferation (Ahlgren and Bronner-Fraser 1999). Ablation of the pharyngeal endoderm, a potent source of SHH, results in markedly increased apoptosis in the mandible (Brito et al. 2006; Brito et al. 2008). $Shh^{-/-}$ embryos exhibit a reduction in the outgrowth of the maxillary and mandibular prominences and have

increased apoptosis in these regions (Yamagishi et al. 2006), while conditional inactivation of *Shh* in neural crest cells using *Wnt1-cre* results in reduced facial outgrowth, increased cell death, and bone formation defects (Jeong et al. 2004). Collectively, SHH signaling, whether emanating from the ectoderm or endoderm, plays multiple roles in the development of the craniofacial complex and is critically important in the integration of other signaling pathways during craniofacial development.

Fgf8 and the Facial Ectoderm

Fibroblast growth factors (*Fgfs*) are a large family of signaling polypeptides with diverse functions during embryogenesis; in mammals, twenty-two *Fgfs* have been identified, arising from two phases of genome duplication. FGFs vary in size from 17 to 34 kDa and share a conserved 120 amino acid sequence (Ornitz and Itoh 2001). FGFs signal to surrounding tissues, often mediating epithelia-mesenchymal interactions, which is achieved through the binding and activation of the FGF-receptors. *FGF-receptors* are a family of receptor tyrosine kinases and include four family members, *Fgfr1–Fgfr4*. Additionally, FGFs bind heparan sulfate proteoglycans (HSPG), which function as an accessory molecule that regulates FGF-binding and the activation of FGFRs (Eswarakumar et al. 2005; Itoh and Ornitz 2008). Upon binding to FGFRs, receptor/ligand complexes dimerize and phosphorylation of cytoplasmic tyrosine residues results in the activation of multiple intracellular signaling cascades, including the MAP kinase, PI-3 kinase, and PLCγ

pathways (Eswarakumar et al. 2005; Itoh and Ornitz 2008). *Fgfs* are expressed in many, if not all, mammalian tissues in distinct yet overlapping patterns. A number of *Fgfs* (*Fgf3, 4, 8, 15, 17,* and *19*) are expressed only during embryogenesis, highlighting the importance of FGF-mediated tissue-specific interactions required during development (Ornitz and Itoh 2001).

In particular, *Fgf8* has well characterized roles in the patterning of the embryo during development (Itoh and Ornitz 2004). Indeed, roles for *Fgf8* in neural patterning (Delaune et al. 2004; Fletcher et al. 2006), limb development (Lewandowski et al. 2000), and cardiovascular development (Abu-Issa et al. 2002) have been reported. *Fgf8* is expressed in the primitive streak and newly formed mesoderm at early developmental stages (Crossley and Martin 1995). At mid-gestational stages, *Fgf8* is present in the frontonasal ectoderm of the medial and lateral nasal prominences and the proximal surface ectoderm of the first branchial arch; *Fgf8* is also heavily expressed in the apical ectodermal ridge (AER) of the developing limb (Crossley and Martin 1995). *Fgf8* null embryos ($Fgf8^{\Delta 2,3/\Delta 2,3}$) are gastrulation defective and are embryonic lethal by 9.5dpc (Meyers et al. 1998). *Fgf8* hypomorphs ($Fgf8^{neo}$) also exhibit multiple developmental defects including perturbed brain development and an absence of posterior midbrain and anterior hindbrain tissues as well as the olfactory bulbs (Meyers et al. 1998). At both early and mid-gestational stages, FGF8 signaling is required for the patterning of multiple regions of the developing embryo.

Fgf8 is expressed in the developing head in the ectoderm of the nasal prominences and the mandible. FGF signaling is well characterized in mediating tissue-tissue interactions, such as in the limb (Niswander et al. 1993; Fallon et al. 1994; Sun et al. 2002); FGF8 signaling from the AER signals to the underlying mesenchyme to promote outgrowth of the limb buds (Lewandoski et al. 2000; Moon and Capecchi 2000). In the head, nasal ectoderm serves a similar role in promoting outgrowth. As cranial neural crest cell populate the frontonasal prominence (FNP), interactions between FGF8 and migrating crest cells regulate various aspects of craniofacial development. Indeed, *Fgf8* in the frontonasal ectoderm is a critical component of the frontonasal ectoderm zone (FEZ), a region of tissue comprised of adjacent domains of *Fgf8* and *Shh*. The FEZ is responsible for the outgrowth and patterning of the upper beak (Hu et al. 2003); transplantation of the FEZ results in the duplication of upper or lower jaw derivatives (Hu et al. 2003). Furthermore, recent data indicates regionalized FGF signaling from the surface ectoderm coordinates the growth and contact of the facial prominences and their derivatives (Szabo-Rogers et al. 2008). Conditional inactivation of *Fgf8* in the forebrain using *Foxg1-cre* results in reduced forebrain and frontonasal structures (Kawauchi et al. 2005). Mutants at late developmental stages have a small, shortened snout, and the lower jaw and ears are reduced in size or absent (Kawauchi et al. 2005). Additionally, *Foxg1-cre;Fgf8* conditional mutants exhibit an absence or reduction of the nasal cavity/olfactory epithelium and accompanying nasal bone (Kawauchi et al. 2005).

Conditional inactivation of *Fgf8* in the branchial arch ectoderm using *Nestin-cre (Nes-cre)* (Trumpp et al. 1999) or *AP2α-IREScre* (Macatee et al. 2003) results in craniofacial defects. *Fgf8;Nes-cre* conditional mutants exhibit a marked reduction of the maxillary and mandibular prominences due to increased cell death in the branchial arch mesenchyme, indicating a role for FGF8 in the survival of cells populating BA1 (Trumpp et al. 1999). Additionally, patterning of the maxillary and mandibular prominences is disrupted in mutant embryos, as assayed by the expression of *Fgf8*-target genes, *Lhx6, Gsc, Barx1*, and *Et1* (Trumpp et al. 1999). Analysis of cartilage and bone development in *Fgf8;Nes-cre* conditional mutants at 14.5dpc revealed an absence of the cartilaginous elements derived from BA1, including the ala temporalis and incus as well as Meckel's cartilage (Trumpp et al. 1999). At birth, most of the neural crest-derived bones of BA1 are absent, such as the mandible, palantine, pterygoid, and tympanic bones; additionally, the squamosal, maxillary, and alisphenoid bones are significantly reduced. The removal of *Fgf8* from the *Nestin-cre* domain of BA1 results in severe craniofacial defects caused by increased cell death, BA1 patterning defects, and a lack of neural crest-derived bone (Trumpp et al. 1999).

Conditional inactivation of *Fgf8* from the BA ectoderm using *AP2α-IREScre* results craniofacial defects similar to those in *Fgf8;Nes-cre* mutants. *Fgf8;AP2α-IREScre* mutants exhibit severe hypoplasia of BA1 as early as 9.5dpc and lack derivatives of the lower jaw at 18.5dpc (Macatee et al. 2003). Cell death is increased in *Fgf8;AP2α-IREScre* mutants, although increased TUNEL staining specifically in BA1 was not addressed; neural crest cells in more posterior BAs (BA2-6) were

TUNEL-positive, indicating that the increased cell death the pharyngeal region directly affects neural crest cell survival (Macatee et al. 2003). Overall, these studies demonstrate the requirement of FGF8 signaling within two craniofacial primordia, the FNP and BA1, in the development of upper and lower jaw structures.

Bmp4 in Mandibular Development

Bone morphogenetic proteins (Bmps) are members of the *Transforming growth factor-β* (*TGF-β*) family of paracrine factors which share similar sequence alignment with *decapentaplegic (ddp)* in *Drosophila* (Hogan 1996). To date, more than twenty *Bmp* family members have been characterized, many of which are required for normal embryonic development (Hogan 1996). *Bmps* are expressed in regions of the developing embryo where reciprocal interactions between epithelia and mesenchymal cells are required for cellular differentiation and tissue morphogenesis, including the amnion (Zhang and Bradley 1996), kidney (Dudley et al. 1995), cartilage (Kingsley et al. 1992), and skin (Wilson and Hemmati-Brivanlou 1995). Knockout analysis has revealed critical roles for *Bmp2* and *Bmp4* in heart (Zhang and Bradley 1996) and mesoderm formation (Winnier et al. 1995). Finally, BMP signaling through *BMP receptor I* (*BMPR1a*) is required for gastrulation (Mishina et al. 1995).

BMPs are synthesized as large precursor proteins which are cleaved so that the C-terminal active domain is released (Rosen 2006); mature BMP molecules homodimerize and are secreted from the cell. BMPs elicit their cellular responses

through activation of the SMAD pathway via binding of type I and type II serine/threonine kinase receptors (Rosen 2006). Three type I receptors have been shown to bind BMP ligands: BMPr1a (Alk3), BMPr1b (Alk6), and the type IA activin receptor (ActRIA or Alk2). BMPs activate the type II receptors BMPR-II and the activin receptors type II and IIb (ActR-II, ActR-IIb) (Rosen 2006).

Ligand binding of type I receptors results in the intracellular association of type I and type II receptors, resulting in the phosphorylation of type I receptors (Li and Cao 2006). Once activated, type I receptors recognize and phosphorylate the Smad proteins 1, 5, and 8, present in the cytoplasm; phosphorylated Smads1, 5, and 8 dissociate and form complexes with the common Smad partner, Smad4 (Li and Cao 2006). Once complexed, the Smad dimer translocates to the nucleus to regulate gene transcription, either in a positive or negative manner (Li and Cao 2006; Rosen 2006).

Multiple *Bmp* family members are expressed during craniofacial development, including *Bmp2, -4, -5*, and *-7*. *Bmp2* is transiently expressed in the early-staged embryo in the surface ectoderm adjacent to the neural folds (Kanzler et al. 2000), while *Bmp4, -5*, and *-7* are expressed in the developing branchial arches (Winnier et al. 1995; Solloway and Robertson 1999). Additionally, *Bmp4* is expressed in the frontonasal prominences at mid-embryonic stages (Winnier et al. 1995). *Bmp5* and *Bmp7* mutants exhibit minor craniofacial defects, including reduced ears (Kingsley et al. 1992) and anophthalmia (Dudley et al. 1995). Analysis of *Bmp2* and *Bmp4* mutants has precluded any examination of cranioskeletal development due to embryonic lethality (Winnier et al. 1995; Kanzler et al. 2000).

Of the *Bmp* family members expressed in the craniofacial primordia, *Bmp4* is particularly important for the development and outgrowth of the lower jaw (Barlow and Francis-West 1997). At 10.5dpc, *Bmp4* is expressed in the distal branchial arch ectoderm and at later stages in the branchial arch mesenchyme (Bennett et al. 1995). During development, the mandible is patterned in a proximo-distal gradient and reports have demonstrated that *Bmp4* is required for the specification of lower jaw derivatives, including teeth, cartilage, and bone (Tucker et al. 1999; Liu et al. 2005a).

Conditional inactivation of *Bmp4* in the ectoderm of the mandible using *Nestin-cre* results in cleft lip due to the lack of fusion between the median nasal and maxillary prominences (Liu et al. 2005b); lack of analyses at late developmental stages has precluded any characterization of cartilage and bone defects. Analysis of *Bmp4* conditional mutants using $Nkx2.5^{cre}$, also expressed in the mandibular ectoderm, results in the absence of the lower jaw and its derivatives; only a rudimentary mandible is present in the conditional mutants by 17.5dpc (Liu et al. 2005a). *Bmp4* is also required for the development of the jaw joint; *Bmp4* regulates *Bapx1*, a gene expressed in the mandibular arch in two distinct domains and is required for the positioning of the jaw joint (Wilson and Tucker 2004). *Bmp4* is required for restricting *Bapx1* to the proximal part of the mandible, thereby regulating the final position of the jaw joint; indeed, ectopic application of BMP4 downregulates *Bapx1*, resulting in jaw fusion defects (Wilson and Tucker 2004).

Finally, *Bmp4* from the mandibular ectoderm is required for the maintenance of odontogenic precursors and positively regulates target genes, such as *Msx1*, that

specify the development of the incisors (Tucker et al. 1998). In contrast, BMP4 signaling from the ectoderm negatively regulates *Barx1*, which is required for the specification of molar teeth (Tucker et al. 1998). In mandibular explants, application of Noggin resulted in a marked upregulation of *Barx1* and an absence of *Msx1*; culturing of molar or incisor explants treated with Noggin resulted in the expected numbers of teeth forming from the molar explants, but multi-cuspid molars developed from incisor explants (Tucker et al. 1998). Collectively, these data indicate an important role for *Bmp4* in regulating multiple aspects of lower jaw development, including cartilage and bone formation and the development and patterning of the teeth.

Bmp4 expression in the mandible is regulated by *Shh*; *Shh*$^{-/-}$ embryos lack *Bmp4* in the distal ectoderm of the mandible (Moore-Scott and Manley 2005; Washington Smoak et al. 2005; Yamagishi et al. 2006). More specifically, the pharyngeal endoderm, a source of SHH signaling, is required for *Bmp4* activation; conditional inactivation of *Shh* from the pharyngeal endoderm results in the loss of *Bmp4* in the mandible (Goddeeris et al. 2007) as does surgical ablation of the pharyngeal endoderm in avian embryos (Brito et al. 2006). Collectively, these data indicate that SHH signaling from the pharyngeal endoderm is required for the maintenance *Bmp4* and the subsequent development of the lower jaw.

Finally, *Bmp4* has been shown to be critical for the evolutionary changes associated with beak morphology in Darwin's finches. Darwin's finches are a group of 14 related songbirds on the Galapogos Islands analyzed by Charles Darwin during

the Beagle expedition in 1835 (Abzhanov et al. 2004). Although closely related, the birds exhibit morphological diversity in the size and shape of their beaks; ground finches have broad and deep beaks used for crushing seeds and cactus finches have long, pointed beaks for reaching into flowers. The differences in beak morphology are suggested to reflect differences in the respective craniofacial skeletons, which are apparent at hatching, and therefore genetically determined (Abzhanov et al. 2004).

In a series of elegant experiments embryos from six species of Darwin's finches belonging to the genus *Geospiza* were analyzed for species-specific differences in beak morphology. Three species of ground finches, *G. fuliginosa, G. fortis,* and *G. magnirostris* (small, medium, and large ground finches) and two species of cactus finches (cactus and large cactus finches), *G. scandens* and *G. conirostris* were analyzed. The most basal species of the genus, *G. difficilis*, was analyzed as well (Abzhanov et al. 2004). Species-specific differences in the frontonasal prominence, which gives rise to the upper beak, were identifiable by embryonic stage 26 (Stage 26 of 35), indicating that genetic factors responsible for variations in beak morphology should also be present at this time. Indeed, analysis of *Bmp4* in St. 26 embryos revealed *Bmp4* in the mesenchyme of *G. magnirostris, G. fortis,* and *G. conirostris*, which was absent in *G. difficilis*, *G. fuliginosa*, and *G. scandens* (Abzhanov et al. 2004).

By St. 29, increased levels of *Bmp4* were present in *G. magnirostris, G. fortis*, and *G. fuliginosa*, coinciding with the appearance of species-specific differences in beak morphology (Abzhanov et al. 2004). Additionally, functional

analysis of *Bmp4* overexpression in chick embryos using retroviral constructs results in beaks with increased width and depth; conversely, overexpression of *Noggin*, a *Bmp* antagonist, results in a dramatic decrease in beak size (Abzhanov et al. 2004). Overexpression of *Bmp4* or *Noggin* resulted in increased and decreased *type II collagen*, which is required for the development of beak skeletal elements. In contrast, other genes known for regulating beak outgrowth, such as *Shh* and *Fgf8*, did not show any differences between species (Abzhanov et al. 2004). Collectively, these data indicate that increased *Bmp4* in the FNP mesenchyme regulates the width and depth of developing beak and highlights the evolutionary importance of *Bmp4* in species diversification.

Cartilage and Bone Development

The skeletal system is comprised of specialized forms of supportive and connective tissue, cartilage and bone. While both cell types are derived from mesenchymal precursors during development, each has unique functions within the vertebrate skeleton. Cartilage provides semi-rigid support in the ear, lungs, and joints. Additionally, cartilage is often an intermediate during development in bone formation. Bone, which forms through two main modes of osteogenesis, provides rigid structural skeleton for the soft tissues of the body.

The vertebrate skeleton can be divided into three lineages; cranial neural crest cells give rise to the majority of the skull, although a few bones are derived from mesodermal precursors (Noden 1978a; Couly et al. 1993; Jiang et al. 2002;

McBratney-Owen et al. 2008). The two remaining lineages, the axial and limb skeletons are derived from somitic tissue from the paraxial mesoderm and the lateral plate mesoderm, respectively (Olsen et al. 2000). In general, osteogenesis occurs through intramembranous or endochondral ossification, each giving rise to bone from preexisting mesenchymal tissue. Intramembranous ossification involves the differentiation of mesenchymal cells directly into osteoblasts and is mainly restricted to the facial skeleton and anterior skull (Opperman 2000; Franz-Odendaal et al. 2006; McBratney-Owen et al. 2008). In contrast, endochondral ossification involves the condensation of mesenchymal cells into a cartilaginous matrix that is eventually replaced by bone (Olsen et al. 2000; Kronenberg 2003); the long bones of the axial skeleton and bones of the limbs are formed via endochondral ossification (Olsen et al. 2000).

Intramembranous ossification involves the direct formation of bone without a cartilage intermediate (Opperman 2000; Franz-Odendaal et al. 2006); this process governs the ossification of the developing skull. The skull is divided into two compartments; the viscerocranium, which comprises the facial skeleton and the neurocranium, which comprises the cranial vault and the cranial base. The viscerocranium is derived entirely from neural crest cells (Jiang et al. 2002; McBratney-Owen et al. 2008). In contrast, the developing neurocranium arises from two distinct cell populations, the neural crest and the paraxial mesoderm (Noden 1978a; Couly et al. 1993; Jiang et al. 2002; Yoshida et al. 2008), the contribution of which appears to be species dependent. In avian embryos, reports have indicated that

the cranial vault is derived from both neural crest cells and paraxial mesoderm (Noden 1978b; Couly et al. 1993), although some discrepancies exist regarding the frontal and parietal bones. Reports from Couly and colleagues (Couly et al. 1993) have indicated that the cranial vault, including the frontal and parietal bones, is derived from entirely from neural crest cells, with the exception of the occipital bone and the otic capsule, which are derived from the paraxial mesoderm. Lineage tracing experiments performed by Noden indicate that the frontal bone is a derivative of both neural crest cells and paraxial mesoderm (Noden 1978b), a result that is supported in recent lineage tracing of neural crest cells and the mesoderm using retroviral constructs (Evans and Noden 2006). Additionally, the parietal bone has been shown to be entirely of mesodermal origin (Evans and Noden 2006).

In murine embryos, the contribution of neural crest cells and paraxial mesoderm to the developing skull has been elucidated through the use of genetic labeling experiments. The frontal and nasal bones are derived entirely from neural crest cells, which also contribute to a small portion of the interparietal bone (Jiang et al. 2002). The remaining bones of the cranial vault, the parietal, ex- and supraoccipital, and occipital bones, are derived from the paraxial mesoderm (Yoshida et al. 2008). Similarly, the cranial base is also derived from neural crest cells and the paraxial mesoderm (Yoshida et al. 2008). The cranial base includes the ethmoid, presphenoid, basisphenoid, and basioccipital bones as well as auditory capsule (a region of the temporal bone) (Yoshida et al. 2008). Neural crest cells contribute to the anterior cranial base, the ethmoid, presphenoid and basisphenoid bones; the

paraxial mesoderm contributes to the posterior basioccipital bone and the auditory capsule (Yoshida et al. 2008) (Figure Seven).

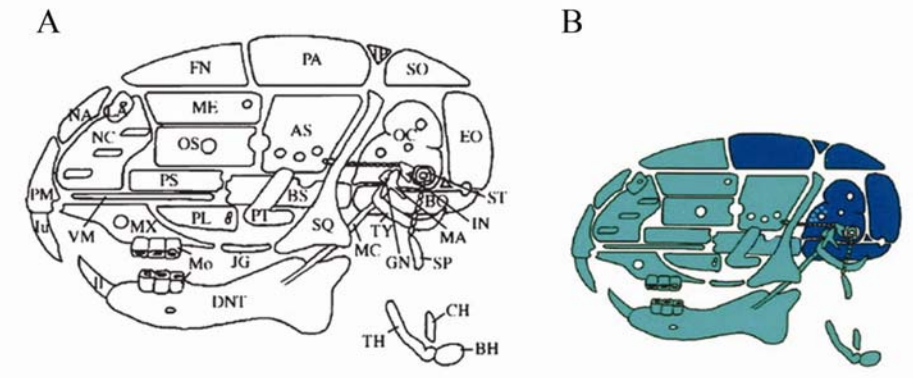

Figure Seven. Contribution of Neural Crest Cells and the Paraxial Mesoderm to the Developing Skull. A) Schematic of a portion of the bones of the skull. B) Contributions of neural crest cells (light blue) and paraxial mesoderm (dark blue) to the facial skeleton, cranial vault, and cranial base. Neural crest cells contribute to the frontal (FN), interparietal (IP), and nasal (NA) bones of the cranial vault as well as the facial skeleton (light blue). The parietal (PA), occipital (OC), and supraoccipital (SO) bones of the cranial vault are derived from the paraxial mesoderm. The cranial base is derived from neural crest cells (basisphenoid, BS) and paraxial mesoderm (basioccipital, BO). (AS) alisphenoid; (BH) basihyoid; (BO) basioccipital; (BS) basisphenoid; (CH) ceratohyoid; (DNT) dentary; (EO) exoccipital; (FN) frontal; (GN) gonial; (Il) lower incisor; (IN) incus; (IP) interparietal; (Iu) upper incisor; (JG) jugal; (MA) malleus; (MC) Meckel's cartilage; (ME) mesethmoid; (Mo) molar; (MX) maxilla; (NA) nasal bone; (NC) nasal cartilage; (OC) otic capsule; (OS) orbitosphenoid; (PA) parietal; (PL) palatine; (PM) premaxilla; (PS) presphenoid; (PT) pterygoid; (SO) supraoccipital; (SQ) squamosal; (ST) stapes; (TH) thyrohyoid; (TY) tympanic ring; (VM) vomer. From Jeong et al. 2004, McBratney-Owen et al. 2008, and Yoshida et al. 2008.

Initiation of intramembranous ossification occurs through the development of condensations (Franz-Odendaal et al. 2006) and consists of neural crest-derived mesenchymal cells; osteoblasts differentiate directly from the mesenchyme without the formation of a cartilage intermediate and begin to secrete an osteoid matrix rich in collagen types I, II, and III. Collagen fibers are laid down in a polarized fashion and osteoblasts orient themselves along the edge of the nodules, the osteogenic front (Franz-Odendaal et al. 2006).

Early bone condensations/nodules ultimately transition into ossification centers as the deposition of osteoid matrix continues, osteoblasts become embedded within the osteoid matrix and transform into osteocytes (Franz-Odendaal et al. 2006). Differentiation of osteoblasts into osteocytes is regulated by *Runx2 (Cbfa1)*. *Runx2* is a member of the *Runx* family of transcription factors which contain a Runt DNA-binding domain (Adams et al. 2007). *Runx2* is required for the activation of multiple osteoblast-specific genes, including osteopontin, bone sialoprotein (BSP) and osteocalcin (Ducy et al. 1997). *Runx2*$^{-/-}$ embryos lack all osteoblasts and do not form any bones of the cranial vault (Komori et al. 1997; Otto et al. 1997). The activation of bone matrix proteins such as osteocalcin by *Runx2* results in the calcification of the osteoid matrix along the osteogenic fronts (Ducy et al. 1999). Osteoblasts embedded in the calcified matrix transform into osteocytes, or bone cells, and mesenchymal cells encase these fronts, forming the periosteum. Matrix secretion and osteoblast differentiation proceed in a repetitive fashion as the calvarial bones enlarge and calcify (Franz-Odendaal et al. 2006).

As the brain enlarges during development the ossification centers continue to enlarge but never fuse with adjacent bones. Instead, the cranial bones abut at the junction sites known as sutures (Opperman 2000; Ornitz and Marie 2002). Comprised of fibrous tissue, sutures are required for the separation of the cranial bones and regulate expansive growth of the skull. In humans, five sutures are present in the developing cranial vault: the metopic (between the frontal bones), the sagittal (between the parietal bones), the paired coronal (between each set of frontal and parietal bones), the paired lamboid (between each set of parietal and supraoccipital bones), and the squamosal (located between the parietal, temporal, and sphenoid bones) (Opperman 2000).

As the skull continues to develop, sutures act as major sites of intramembranous bone growth and continue to add bone throughout development. Osteogenic mesenchymal cells located along sutures edges differentiate into osteoblasts and express type I collagen, BSP, and osteocalcin (Ornitz and Marie 2002). Growth and differentiation at the sutures is regulated by interactions between the mesenchyme, osteogenic front, and the dura mater, the fibrous tissue that surrounds the brain (Opperman 2000); signaling from these tissues directs the secretion of bone matrix from osteoblasts along the bone margins (Ornitz and Marie 2002). The majority of sutures remain patent, allowing for continued growth of the brain and calvaria, although they fuse late in adulthood (Opperman 2000).

In the axial and limb skeleton, bone development occurs via endochondral ossification (Figure Eight) which requires the formation of a cartilage intermediate

before ossification takes place (Olsen et al. 2000; Kronenberg 2003). Endochondral ossification commences as mesenchymal cells become adherent and form condensations, ultimately giving rise to chondrocytes (cartilage precursors). Chondrocytes within a developing skeletal element extensively proliferate and secrete a matrix rich in type II collagen (Olsen et al. 2000); the developing cartilage enlarges as chondrocytes proliferate, secreting matrix at the most distal regions of the skeletal element. Chondrocytes positioned along the exterior-most regions of the mesenchymal condensations form the perichondrium, which will give rise to the bone collar once ossified (Kronenberg 2003).

Centrally located chondrocytes become hypertrophic: they increase in size, cease proliferating, and become post-mitotic (Kronenberg 2003). Hypertrophy of chondrocytes occurs once the cells are a significant distance from the end of an elongating skeletal element, a process that appears to be regulated by *Indian hedgehog and Parathyroid hormone-related protein (PTHrP)* (discussed below) (Vortkamp et al. 1996; Olsen et al. 2000; Kronenberg 2003). Once the cells undergo hypertrophy, they secrete type X collagen, a protein unique to these cells. Additionally, hypertrophic chondrocytes adjacent to the perichondrium secrete angiogenic factors, such as vascular endothelial growth factor (VEGF), and initiate the vascular remodeling of the skeletal element (Olsen et al. 2000; Kronenberg 2003).

Simultaneously, hypertrophic chondrocytes direct the differentiation of the perichondrium into osteoblasts, giving rise to the bone collar (Kronenberg 2003). The invasion of blood vessels and the ossification of the perichondrium identify this

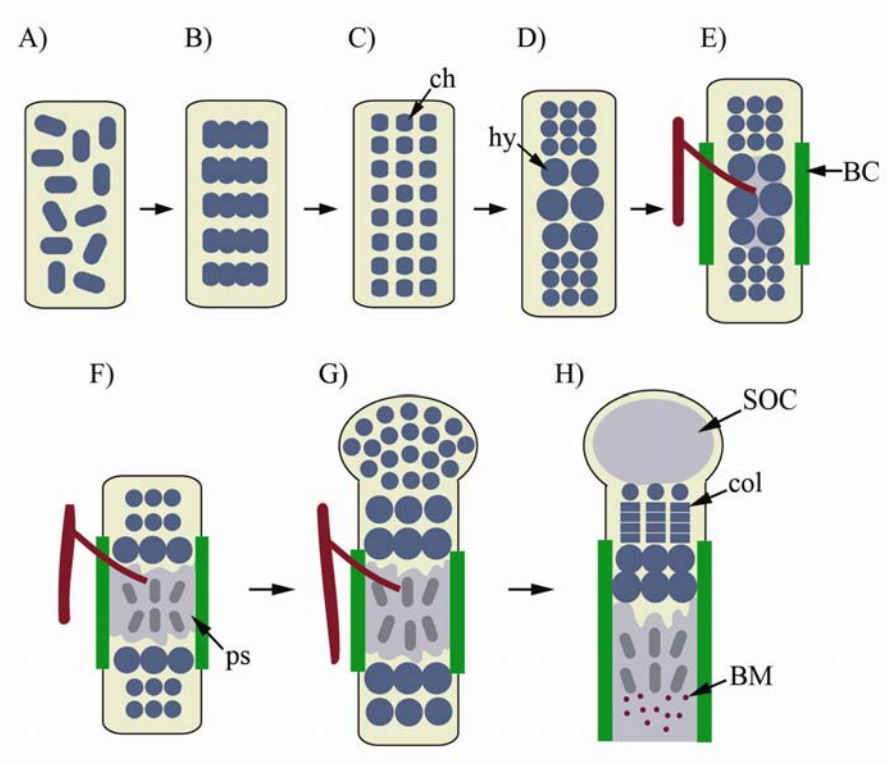

Figure Eight. Schematic of Endochondral Ossification. Mesenchymal cells (A) coalesce to form organized condensations (B) and cells subsequently differentiate into chondrocytes (ch) (C). D) Centrally located chondrocytes cease proliferating and become hypertrophic chondrocytes (hy). E) Perichondrial cells at the outermost regions ossify, forming the bone collar (BC, green). Hypertrophic chondrocytes secrete a matrix containing VEGF that attracts blood vessels (red) and then undergo apoptosis. F) Osteoblasts (dark gray), the precursors of bone, invade the remaining scaffold left behind by apoptotic chondrocytes to form the primary spongiosa (ps, light gray); this region is also known as the primary ossification center. G) Chondrocytes continue to proliferate and lengthen the distal ends of the element. H) At the end of the developing bone a secondary ossification center (SOC) forms. SOCs form through cycles of chondrocytes undergoing hypertrophy and apoptosis, and is accompanied by vascular invasion and osteoblasts. Bone growth continues as chondrocytes (col) between the primary and secondary ossification sites proliferate; these regions are referred to as the growth plates. In humans, growth plates eventually disappear after puberty. Recreated from Kronenberg, 2003.

region as the primary ossification center, thereby forming the diaphysis (Olsen et al. 2000). Within the primary ossification center, hypertrophic chondrocytes undergo apoptosis and osteoblasts replace the cartilage with trabecular bone. At this point in development, bone marrow is formed and hemataepoesis begins. At the epiphyses, the ends of the skeletal element, secondary ossification centers form, leaving a plate of cartilage known as the growth plate between the epiphyses and diaphysis (Olsen et al. 2000). Coordinated regulation of chondrocyte proliferation, hypertrophy, and apoptosis results in the longitudinal growth of the developing bone. Remarkably, proliferating and hypertrophic chondrocytes move towards the epiphyses as elongation proceeds (Olsen et al. 2000); this is accompanied by simultaneous elongation of bone collar (Kronenberg 2003).

Numerous transcription factors are required during endochondral ossification to regulate cellular differentiation and growth (Olsen et al. 2000; Kronenberg 2003). During the initial stages of chondrocyte development, *Sox9,* a member of the SRY-related (sex-determining region Y gene) HMG (high-mobility-group) family of transcription factors (Pevny and Lovell-Badge 1997), is expressed by proliferating chondrocytes. *Sox9* is required for the differentiation, proliferation, and survival of chondrocytes from mesenchymal precursors and is essential for preventing the premature conversion of proliferative chondrocytes into hypertrophic (non-proliferating) chondrocytes (Wright et al. 1995). *Sox9* stimulates the production of collagens type II, IX, and XI and aggregan, a proteoglycan involved in the structural support of mature cartilage (Bell et al. 1997; Lefebvre et al. 1997; Bi et al. 1999). In

humans, haploinsufficiency of *SOX9* results in camplomelic dysplasia, a rare form of congenital short-limb dwarfism, where patients exhibit bowing of the long bones, pelvic hypoplasia, decreased number of ribs, and a reduced cranial vault (Foster et al. 1994; Wagner et al. 1994; Akiyama et al. 2002). Heterozygous $Sox9^{+/-}$ mice mimic these malformations, indicating a role for *Sox9* in determining bone length (Bi et al. 2001). Additionally, *Sox5* and *Sox6*, two other *Sox* family members, are involved in the expression of *type II collagen* and complex with SOX9 to regulate chondrocyte development (Zhou et al. 1998; Smits et al. 2001; Akiyama et al. 2002). Collectively, multiple *Sox* family members, particularly *Sox9*, are required for chondrocyte development, including the initial differentiation of chondrocytes from mesenchymal precursors to regulating cartilage matrix secretion and outgrowth.

For bone development to proceed, proliferating chondrocytes are required to elongate the growth plate but must also undergo hypertrophy and apoptosis for osteoblasts to invade the bone collar. This balance is regulated by two signaling pathways, Indian hedgehog and parathyroid hormone-related protein signaling, which regulate a feedback loop necessary for the maintenance of proliferative chondrocytes and bone growth (Vortkamp et al. 1996). *Indian Hedgehog (Ihh)* coordinates chondrocyte proliferation and differentiation as well as osteoblast differentiation (Vortkamp et al. 1996; St-Jacques et al. 1999). *Ihh* is synthesized by prehypertrophic chondrocytes (those leaving the proliferative pool) and by early hypertrophic chondrocytes (Vortkamp et al. 1996). $Ihh^{-/-}$ embryos have normal bones at the initial stages of mesenchymal condensation but develop pronounced defects at later stages

of bone development; all cartilage elements are reduced due to decreased chondrocyte proliferation, ultimately resulting in dwarfism (St-Jacques et al. 1999). Additionally, *Ihh*$^{-/-}$ embryos exhibit increased numbers of hypertrophic chondrocytes due to premature maturation. At late developmental stages, mutant embryos lack any signs of osteoblast formation and do not show any signs of endochondral bone formation (St-Jacques et al. 1999).

Parathyroid hormone-related protein (PTHrP) is a protein secreted by early proliferative chondrocytes and functions to negatively regulate chondrocyte hypertrophy within the growth plate (Karaplis et al. 1994). PTHrP also maintains a proliferative pool of chondrocytes just distal to the hypertrophic zone (Lee et al. 1996). PTHrP effects are mediated through the parathyroid hormone receptor (PPR), present in proliferative and prehypertrophic chondrocytes (Lanske et al. 1996). *PTHrP* (Karaplis et al. 1994) or *PPR* (Lanske et al. 1996) mutants exhibit decreased proliferating chondrocytes at the growth plate and increased numbers of hypertrophic chondrocytes. Conversely, overexpression of *PTHrP* results in the delayed appearance of hypertrophic cells but increased proliferative cells (Schipani et al. 1997). Both loss of function or gain of function mutations in *PTHrP* results in dwarfism; loss of function mutations cause a decrease in the pool of proliferative chondrocytes thereby decreasing the number of chondrocytes undergoing hypertrophy (Olsen et al. 2000; Kronenberg 2003). Gain of function mutations also result in decreased chondrocyte hypertrophy due to impaired chondrocyte maturation. Hence,

PTHrP signaling is crucial for maintaining chondrocytes in the proliferative pool, thereby allowing for proper elongation at the growth plate.

Interestingly, *Ihh* and *PTHrP* are partners in a feedback loop (Figure Nine) that negatively regulates the differentiation of hypertrophic chondrocytes (Vortkamp et al. 1996; Kronenberg 2003; Ehlen et al. 2006). IHH^{+} prehypertrophic chondrocytes activate *PTHrP* in distal proliferative chondrocytes (Karaplis et al. 1994; Lanske et al. 1996). In turn, PTHrP prevents the differentiation of proliferating chondrocytes in distal regions into Ihh^{+} prehypertrophic cells (Vortkamp et al. 1996). As a result, IHH and PTHrP act as paracrine factors, controlling the decision of chondrocytes to leave the proliferative pool (Kronenberg 2003; Ehlen et al. 2006). As the distance within the growth plate increases, more centrally located chondrocytes are no longer stimulated by distal PTHrP signaling; at this point, the cells cease proliferating and activate *Ihh* (St-Jacques et al. 1999). Because IHH directly stimulates PTHrP production at the distal ends of the developing bone, distal chondrocytes remain in a proliferative state and the elements continue to elongate (St-Jacques et al. 1999). Although interactions between IHH and PTHrP are crucial for the proper regulation of chondrocyte proliferation and bone elongation (Kronenberg 2003; Ehlen et al. 2006), *Ihh* acts as a master regulator of endochondral bone development by directly stimulating chondrocyte proliferation through its regulation of PTHrP synthesis. In addition, *Ihh* determines the region in which chondrocytes undergo hypertrophy. Finally, *Ihh* is required for the differentiation of perichondrial

cells into osteoblasts and the subsequent formation of the bone collar (Vortkamp et al. 1996).

Chondrocyte proliferation and differentiation is also regulated by FGF and BMP signaling. Numerous members of the *Fgf* gene family and their receptors (*Fgfrs*) are expressed during bone development (Ornitz and Marie 2002), which has made studying their direct roles in endochondral ossification particularly difficult.

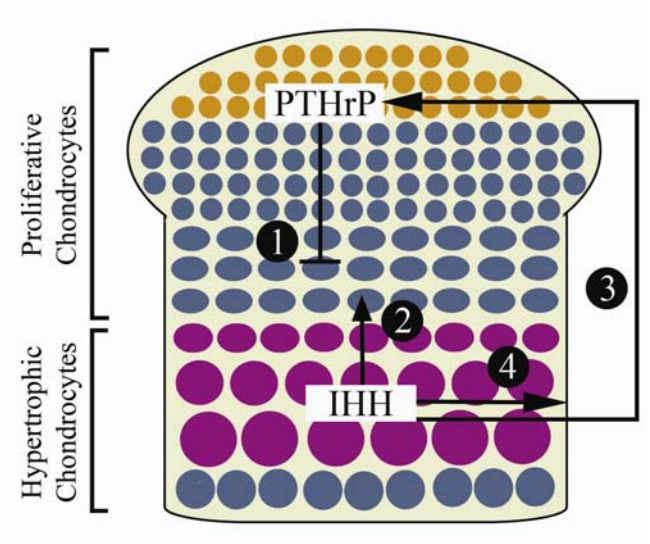

Figure Nine. An IHH and PTHrP Negative Feedback Loop regulates Endochondral Ossification. Parathyroid hormone-related protein (PTHrP) is secresed from chondrocytes at the distal ends of skeletal elements. 1) PTHrP acts on proliferating chondrocytes (blue) to delay activation of *Indian hedgehog (Ihh)*. When chondrocytes are are sufficiently distant from the PTHrP source, they activate *Ihh*. IHH acts on chondrocytes to increase proliferation (2) and directly stimulates PTHrP at the ends of the developing bone (3). 4) IHH also directs the differentiation of the perichondrium into osteoblasts, forming the bone collar. Recreated from Kronenberg, 2003.

Indeed, *Fgfr2* is expressed in condensing mesenchyme and perichondrial cells, *Fgfr3* is present in proliferating chondrocytes, and *Fgfr1* is expressed in prehypertrophic/hypertrophic chondrocytes. Of each of these receptors expressed during development, the role for *Fgfr3* is best understood. *Fgfr3* knockouts results in increased rates of proliferation of chondrocytes and increased length of the skeletal elements (Colvin et al. 1996; Deng et al. 1996). Transgenic mice with activating point mutations of *Fgfr3* result in decreased rate of chondrocyte proliferation, which mimic human chondrodysplasias, and lead to shortened disorganized chondrocyte elements (Naski et al. 1998). Overall these studies indicate an anti-proliferative role for FGF signaling in bone development, although the activating ligand(s) responsible are not fully defined. One *Fgf* ligand that appears to regulate this process is *Fgf18*; mutant embryos exhibit delayed ossification along the anterior-posterior body axis (Liu et al. 2002). *Fgf18*$^{-/-}$ embryos are more severe than *Fgfr3*$^{-/-}$ embryos, indicating that *Fgf18* may also be signaling through *Fgfr1* in hypertrophic chondrocytes and *Fgfr2* in early condensing mesenchyme and the perichondrium.

In contrast, activation of BMP signaling induces ectopic bone formation, so remarkably that it is from this process that the gene family name is derived. Similar to *Fgf* family members, numerous *Bmps* and their receptors, (*BMPrs*), are expressed throughout cartilage and bone formation. *BMPr1b* is expressed in cartilage condensations (Kawakami et al. 1996; Zou et al. 1997), while *BMPr1a* is expressed within the mesenchyme (Zou et al. 1997). *Bmp2, -4, -5*, and -*7* are expressed in the

perichondrium, *Bmp2* and *-6* are present in hypertrophic chondrocytes, and *Bmp7* is expressed in proliferating chondrocytes (reviewed in (Li and Cao 2006)).

As indicated by the expression pattern of numerous *Bmp* genes, BMP signaling is required for the initial formation of cartilage condensations. Exposure to Noggin, a BMP signaling antagonist in the developing avian limb results in the suppression of condensation formation (Pizette and Niswander 2000); in contrast, *Noggin*$^{-/-}$ mice exhibit enlarged cartilage primordia (Brunet et al. 1998). Numerous mutations in *Bmp5* ("short ear mice") results in abnormal or absent ear cartilage (Kingsley et al. 1992); *BMPr1b* mutants have abnormal digit formation resulting from the failure of chondrocyte condensations to extend into digits (Baur et al. 2000; Yi et al. 2000). Collectively, these results highlight the importance of BMP signaling in positively regulating chondrocyte development, although individual roles for *Bmp* family members need additional characterization.

Interestingly, it appears that both FGF and BMP signaling directly impact on IHH/PTHrP signaling to regulating growth and differentiation of the skeletal elements. *Fgfr3* knockouts results in increased *Ihh* expression (Ornitz and Marie 2002), while activation of *Fgfr3* results in decreased *Ihh* (Naski et al. 1998). These data suggests that part of the effects of FGF signaling is mediated through suppression of *Ihh*, thereby decreasing chondrocyte proliferation in an indirect (via *Ihh*) and direct manner (*Fgfr3*). Data indicating a positive role for BMP signaling impacting *Ihh* comes from *in vitro* limb explant assays; BMP signaling increases *Ihh* in prehypertrophic chondrocytes (Minina et al. 2001; Minina et al. 2002), resulting in

increased proliferation and lengthening of skeletal elements. Overall, BMP and FGF signaling have opposite effects on the differentiation of hypertrophic chondrocytes, indicating that these two pathways antagonize each other during bone development, the mechanisms of which remain unknown.

Finally, in addition to its role in intramembranous ossification, *Runx2* is important for osteoblast differentiation in endochondral ossification. As previously discussed, *Runx2*$^{-/-}$ embryos lack all bone due to the absence of osteoblast formation but mutant embryos do develop a cartilaginous skeleton (Komori et al. 1997; Otto et al. 1997). Although *Runx2* is not required for chondrocyte formation, it does appear to have a role in chondrocyte maturation. *Runx2*$^{-/-}$ embryos have decreased numbers of hypertrophic chondrocytes and the few that are present fail to mineralize their matrix (Komori et al. 1997; Otto et al. 1997). Interestingly, transgenic expression of *Runx2* in wildtype mice accelerates the transition of chondrocytes to hypertrophic chondrocytes and can even induce ectopic bone formation in cells that would normally never ossify, such as the tracheal rings; conversely, overexpression of a dominant-negative form of *Runx2* blocks the hypertrophy of all chondrocytes (Ueta et al. 2001). These data indicate a dual role for *Runx2* in endochondral ossification; *Runx2* is initially required for the maturation of proliferating chondrocytes, driving their differentiation into hypertrophic chondrocytes. Furthermore, *Runx2* is required for the subsequent differentiation of osteoblasts through the activation of multiple osteoblast-specific genes, including osteopontin, BSP, and osteocalcin (Ducy et al. 1997). Additionally, *Runx2* is required for the deposition of bone matrix by

osteoblasts (Ducy et al. 1999). Indeed, haploinsufficiency of *RUNX2* in humans (Zhang et al. 1997) and mice (Otto et al. 1997) results in cleidocranial dysplasia which is characterized by a delayed skeletal development, alterations in the closure of cranial sutures, hypoplastic or aplastic clavicles, and dental anomalies (Mundlos et al. 1997). Collectively, *Runx2* is an important mediator of endochondral ossification at multiple stages of cartilage and bone development.

Concluding Remarks

This body of work examines both early and late aspects of neural crest cell development, from their initial formation to the final stages of patterning during late embryogenesis. The studies herein have made important contributions in understanding how a neural crest cell forms and the key steps required in regulating migration and differentiation paradigms under normal developmental circumstances. Additionally, this work addresses the signaling required for neural crest cell patterning in order to result in the proper development of the craniofacial complex. The prevalence of congenital craniofacial birth defects in human populations also requires the examination of how neural crest cell patterning is disrupted, resulting in the array of craniofacial malformations. Classically, cranial neural crest cells have been thought to function cell autonomously and that intrinsic defects resulted in the majority of craniofacial malformations. However, cranial neural crest cells have recently been shown to be influenced by extrinsic cues able to govern patterning and differentiation. As a consequence, craniofacial anomalies can arise due to primary

defects in the tissues with which the neural crest cells interact; Holoprosencephaly (HPE) is one such anomaly resulting from impaired survival and improper patterning of neural crest cells, which affects the forebrain and facial structures. Analysis of mouse models of HPE, contributes to the understanding of the etiology of this syndrome with the aim of future preventative measures.

VI. Chapter One: *Germ cell nuclear factor* (*Gcnf /Nr6a1*) plays a novel role in the induction of neural crest cells in the developing mouse embryo. Dennis, J.F., Cooney, A.J., and Trainor P.A.

A) Abstract

Neural crest cells (NCC) are a multipotent migratory cell population that generates the majority of the bone, cartilage, nerves, connective tissue, and pigment cells in the vertebrate head and face. During embryonic development, NCCs are generated along the neural plate border, the junction between the dorsal neuroepithelium and the surface ectoderm, although, the mechanisms regulating their induction are poorly understood. We recently identified *Germ cell nuclear factor (Gcnf /Nr6a1),* an orphan nuclear receptor, as an important regulator of mammalian NCC formation. In $Gcnf^{-/-}$ loss of function analyses, mutant embryos lack migrating NCCs as evidenced by the absence or downregulation of the NCC markers *Crabp1, Snail, Sox9,* and *Sox10*. Interestingly, *Sox2, Wnt1,* and *Pax3* expression in the neuroepithelial population from which NCCs are derived was expanded in mutant embryos, coinciding with an enlarged neural plate and increased numbers of mitotic cells. This is indicative of a disruption in the balance between neuroepithelial proliferation and differentiation, implying that *Gcnf* plays important roles in regulating the epithelial to mesenchymal transition (EMT) of neuroepithelial cells into NCCs. The transcriptional repressor *Snail* is a key global regulator of EMT and importantly we have identified a putative *Gcnf* binding domain within the *Snail*

promoter. Therefore, we propose that *Gcnf* regulates EMT and the formation of NCCs via the direct activation of *Snail*. Additionally, putative binding sites for *Gcnf* have been identified in *Sox9, Sox10, Sip1,* and *Crabp1*, indicating a role for *Gcnf* in the activation of neural crest specific genes once the cells have undergone EMT. Collectively, these data suggest a role for *Gcnf* in regulating EMT and the formation of NCCs as well as the activation of NCC specific genes. Our work has important implications for understanding NCC evolution together with the origins and pathogenesis of congenital craniofacial birth defects since they arise primarily through abnormalities in NCC patterning and development.

B) Introduction

Neural crest cells (NCC) are a multipotent, migratory cell population induced at the neural plate border, the junction of the surface ectoderm and the neuroepithelium; each of these tissue layers gives rise to NCCs (Selleck and Bronner-Fraser 1995) and interactions between the ectoderm and neuroepithelium are required for NCC formation (Rollhauser-ter Horst 1977; Moury and Jacobson 1990). Upon their induction, NCCs undergo an epithelial to mesenchymal transition regulated by the transcriptional repressor *Snail* (Nieto et al. 1994). *Snail*, expressed in NCCs, is required for the downregulation of cell adhesion molecules, such as *E-Cadherin* (Cano et al. 2000), allowing for NCCs to delaminate from the neuroepithelium. Cells migrate in a stereotypic manner along the entire neuraxis of the developing embryo (reviewed in (Kulesa et al. 2004)), contributing to derivatives unique to each axial

level. Cranial neural crest cells, which give rise to the cartilage and bone of the head, are a vertebrate invention and are fundamental to vertebrate craniofacial evolution (Trainor et al. 2003).

Because of their importance in craniofacial development, numerous efforts have focused on the key events required for the commencement of NCC formation. Indeed, multiple signaling pathways have been implicated in this process including, BMP, FGF, NOTCH, PAX, and WNT signaling. At the neural plate border in *Xenopus* and zebrafish embryos, a gradient of BMP signaling within the ectoderm is required for NCC formation to occur (Mayor et al. 1995; Morgan and Sargent 1997); intermediate levels of BMP are required to induce *Slug* and are established by the secretion of BMP antagonists from the underlying mesoderm (Marchant et al. 1998). In the mouse, *Bmp2* mutants lack migratory neural cells (Kanzler et al. 2000). Finally, *Bmp4/7* have been shown to induced NCC markers in avian embryos (Liem et al. 1995; Selleck et al. 1998) and are mediated in part through NOTCH signaling (Endo et al. 2002).

In addition to roles for BMP and NOTCH signaling, reports have argued the importance of WNT and FGF signaling in NCC induction. In avian and zebrafish embryos, dominant negative constructs of *Wnt1* (Garcia-Castro et al. 2002) and morpholinos to *Wnt8* (Lewis et al. 2004) result in the loss of crest cell markers. In *Xenopus*, FGF signaling, particularly FGF8, from the underlying mesoderm has also been shown to induce NCC formation (Monsoro-Burq et al. 2003), through mediation of *Pax3* and *Msx1* (Monsoro-Burq et al. 2005). Additionally, *Pax3* and *Pax7* have

long been suggested as NCC regulators in the mouse, but analyses of *Pax3*$^{-/-}$ (Conway et al. 1997; Epstein et al. 2000) and *Pax7*$^{-/-}$ (Mansouri et al. 1996) embryos has revealed that NCCs are decreased, albeit present, in mutant embryos. More recently, *Pax7* reemerged as a mediator of crest cell induction in avian embryos, acting during early gastrulation stages to specify NCCs (Basch et al. 2006).

Collectively, multiple signaling pathways have been indicated as having a role in NCC induction in an array of model systems. From these analyses, one caveat to note is the fact that embryonic development in model aquatic species, where much of the data has been generated, proceeds quite rapidly, making it very difficult to distinguish the signaling required for NCC induction independent of neural patterning. Furthermore, the same signaling pathways suggested to regulate crest cell formation are also involved in neural patterning, making it difficult to ascertain which pathway directly activates NCC formation, if any. In the mouse, a longer developmental window separates neural versus NCC induction; indeed, genetic analysis of *Bmp, Fgf, Notch, Pax,* and *Wnt* pathway mutants has not indicated these genes as regulators of crest cell development. Furthermore, the roles for these signaling molecules have not been extensively addressed *in vitro*. Therefore, we set out to identify the key regulator of NCC induction in the mouse embryo using both *in vivo* and *in vitro* approaches. Analyses of *Fgf8*$^{\Delta 2,3/\Delta 2,3}$, *Pax3*$^{-/-}$;*Pax7*$^{-/-}$, and NOTCH signaling mutants has revealed that none of these pathways are required for NCC induction in the mouse embryo. Additionally, we developed an explant culture system for assaying the known regulators of NCC development *in vitro*; our data

support our *in vivo* analyses and do not indicate any of the current pathways suggested to be involved in crest cell formation as being required. Finally, we have identified *Germ cell nuclear factor, Gcnf (Nr6a1)*, as a novel regulator of NCC induction in the mouse.

C) Results

Notch Signaling is not required for Neural Crest Cell Induction

One signaling pathway shown to regulate NCC induction is the Delta/Notch signaling pathway; alterations in NOTCH signaling results in an expansion or reduction of *Slug* in avian embryos (Endo et al. 2002; Endo et al. 2003). Furthermore, activation of NOTCH signaling in *Xenopus* embryos results in expanded neural crest cell territories (Glavic et al. 2004). Activation of NOTCH signaling occurs when Notch, a transmembrane receptor, binds to its transmembrane ligand, Delta, on neighboring cells. Upon binding of Delta, the Notch Intracellular Domain (NICD) is cleaved by the enzyme γ-secretase (reviewed in (Selkoe and Kopan 2003)) and translocates to the nucleus to activate recombinant binding protein J-κ (*RBP-Jκ*), the nuclear effector of NOTCH signaling (Oka et al. 1995; de la Pompa et al. 1997).

To address the role of NOTCH signaling in NCC induction, we analyzed *RBP-Jκ* mutants for defects in NCC formation. *RBP-Jκ* mutants were harvested at 8.5-9.5dpc and processed for *in situ* hybridization for *Snail*, *Crabp1*, *Sox9*, and *Sox10*

Figure Ten. Notch Signaling is not required for Neural Crest Cell Induction. *RBP-Jκ* heterozygote (left columns) and mutant embryos (right colums) were processed for *in situ* hybridization with neural plate and neural crest cell markers. The neural plate marker *Sox2* (C, D) is not affected in *RBP-Jκ*$^{-/-}$ embryos. Mutant embryos express *Snail* (G, H) and *Crabp1* (K, L), indicating neural crest cell formation in the mouse does not require NOTCH signaling. In contrast, *Sox9* (O,P) and *Sox10* (S, T) are present but decreased in the mutants, indicating that NOTCH signaling is required for lineage selection of *Sox9*$^{+}$ and *Sox10*$^{+}$ neural crest cells.

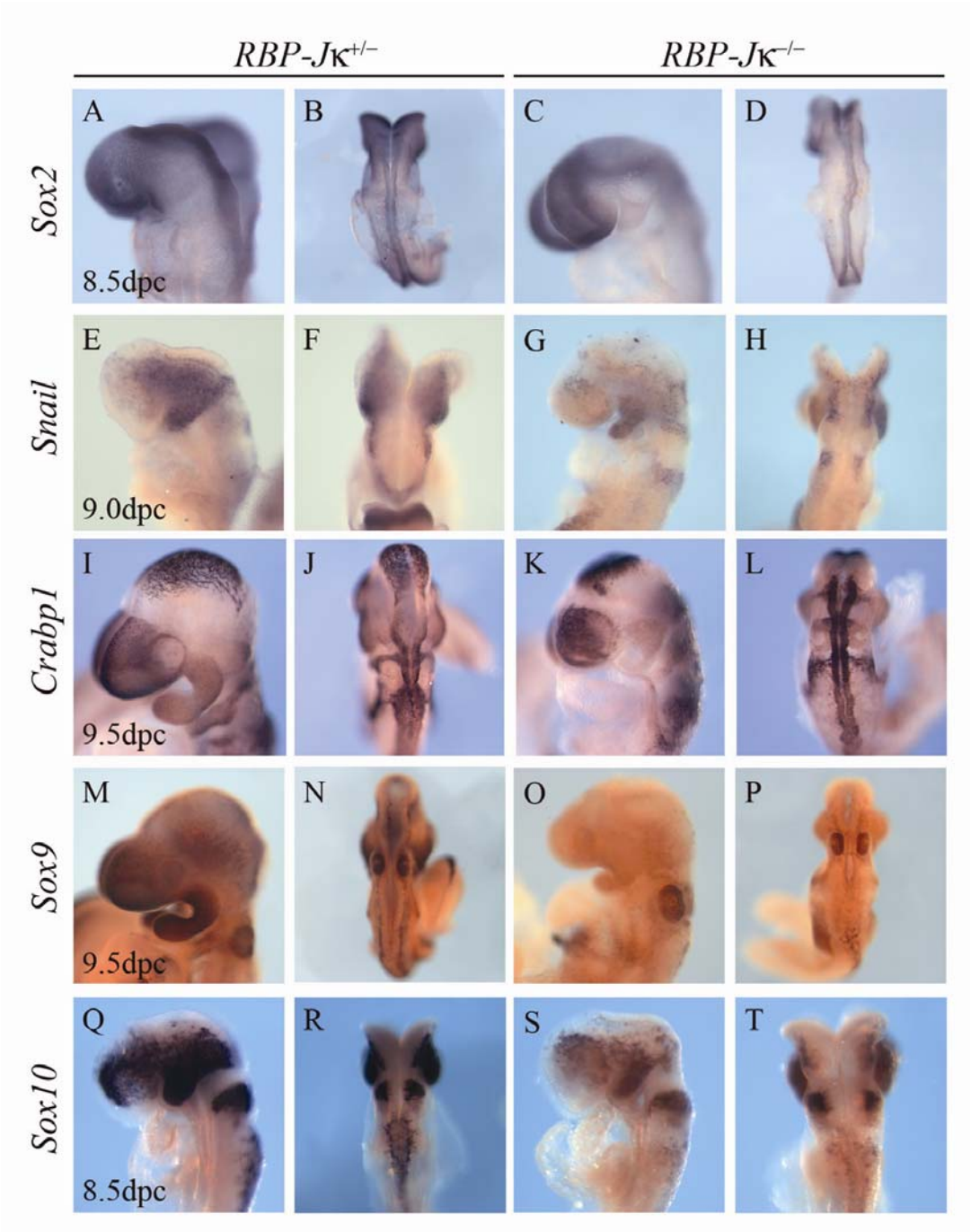
RBP-Jκ+/–
RBP-Jκ–/–
Sox2
Snail
Crabp1
Sox9
Sox10
A
B
C
D
8.5dpc
E
F
G
H
9.0dpc
I
J
K
L
9.5dpc
M
N
O
P
9.5dpc
Q
R
S
T
8.5dpc

(Fig. 10). Although *Snail* (Fig. 10G, H) and *Crabp1* (Fig. 10K, L) were similarly expressed in mutant embryos in comparison to heterozygous littermates, the neural crest cell lineage markers *Sox10* and *Sox9* were affected. *Sox10* (Fig. 10S, T) was slightly reduced, while *Sox9* was absent in the cranial region of *RBP-Jκ*$^{-/-}$ embryos (Fig. 10O, P). *Sox9* was present in the otic vesicle and in cells along the neural tube at mid-axial levels, indicating that *Sox9* was not completely downregulated in mutant embryos, but is more affected in anterior regions. *RBP-Jκ*$^{-/-}$ embryos were also processed for *Sox2* to determine if the neural plate was intact; *Sox2* expression in mutant embryos was comparable to that seen in heterozygote littermates, indicating that the precursor population from which NCCs arise was present (Fig. 10 compare A, B with C, D). Overall, analysis of *RBP-Jκ*$^{-/-}$ mutants indicates that NOTCH signaling is not required for NCC formation as a whole in the mouse but rather appears to be required for lineage selection of *Sox10*$^{+}$ and *Sox9*$^{+}$ cells.

Migratory Neural Crest Cells are present in Pax3$^{-/-}$*;Pax7*$^{-/-}$ *Mutants*

Pax3 and *Pax7* are expressed in the dorsal neural tube and have been implicated in the induction of NCCs in *Xenopus* (Sato et al. 2005; Hong and Saint-Jeannet 2007) and avian (Basch et al. 2006) embryos. In the mouse, *Pax7*$^{-/-}$ mutants are perinatal lethal and have malformations of the maxilla and nose (Mansouri et al. 1996); *Pax3*$^{-/-}$ embryos exhibit decreased NCCs (Conway et al. 1997; Epstein et al. 2000). The presence of NCC in single *Pax3* and *Pax7* mutants has been attributed to functional redundancy of the two genes, thereby underlying the failure to prevent

NCC induction as a whole (Mansouri et al. 1996). To directly address the role of *Pax3* and *Pax7* in NCC induction in the mouse embryos, we analyzed *Pax3*$^{-/-}$;*Pax7*$^{-/-}$ double mutants for defects in NCC formation using the migratory markers *Sox10* (Fig. 11) and *Crabp1* (Fig. 12). At 9.0dpc, *Sox10* was present in the first two migratory streams of neural crest cells that will populate branchial arches one (BA1) and two in *Pax3*$^{+/-}$;*Pax7*$^{+/-}$ (Fig. 11A, E) and *Pax3*$^{+/-}$;*Pax7*$^{-/-}$ embryos (Fig. 11B, F). Additionally, *Sox10* was present in the otic vesicle and in the dorsal neural tube. In *Pax3*$^{-/-}$;*Pax7*$^{+/-}$ embryos, *Sox10*$^{+}$ cells populating the developing frontonasal region and along the dorsal neural tube were present (Fig. 11C, G), although there was clearly a decrease in the number of *Sox10*$^{+}$ cells, which could be developmental delay or decreased proliferation in the neural tube and neural crest cells. Finally, in *Pax3*$^{-/-}$;*Pax7*$^{-/-}$ double mutants, *Sox10*$^{+}$ cells were present along the dorsal neural folds and had migrated ventrally into the developing facial region (Fig. 11D, H).

In addition to the analysis of *Sox10* in *Pax3*$^{-/-}$;*Pax7*$^{-/-}$ double mutants, we analyzed the expression of *Crabp1* at 10.5dpc. *Pax3*$^{-/-}$;*Pax7*$^{-/-}$ double mutants had *Crabp1*$^{+}$ cells along the anterior dorsal neural folds and in the frontonasal region, indicating that migratory NCCs were present (Fig. 12M, N), although the medial (MNP) and lateral (LNP) nasal prominences were difficult to distinguish. Sections at the level of the frontonasal prominences in *Pax3*$^{-/-}$;*Pax7*$^{-/-}$ double mutants revealed the specific location of *Crabp1*$^{+}$ NCCs in the frontonasal region (Fig. 12O), although the numbers in mutant embryos are reduced in comparison to littermates (Fig. 12).

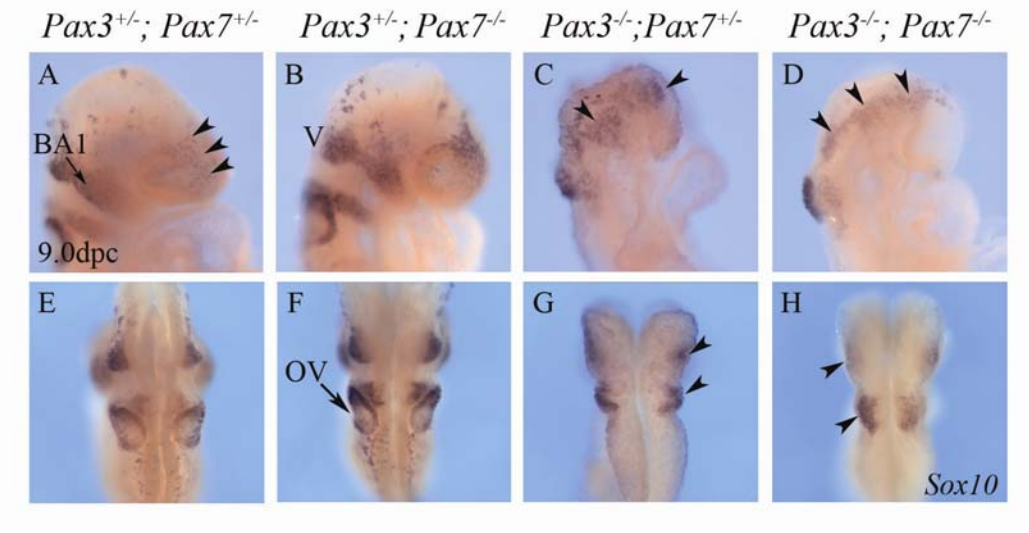

Figure Eleven. *Pax3* and *Pax7* are not required for Neural Crest Cell Formation in Murine Embryos. Embryos were harvested at 9.0dpc and processed for *Sox10 in situ* hybridization. A, E) *Pax3*$^{+/-}$*;Pax7*$^{+/-}$ compound heterozygous embryos have *Sox10* expression in migratory neural crest cells populating BA1 (arrow). Additional *Sox10*$^{+}$ cells (arrowheads) are located in the frontonasal region. B, F) *Pax3*$^{+/-}$*;Pax7*$^{-/-}$ embryos exhibit *Sox10* expression in the developing head (B) and dorsal neural tube (F) as seen in *Pax3*$^{+/-}$*;Pax7*$^{+/-}$ embryos; *Sox10*$^{+}$ cells present in the trigeminal (V) ganglia and the otic vesicle (OV). C, G) *Pax3*$^{-/-}$*;Pax7*$^{+/-}$ embryos are slightly delayed in comparison to compound heterozygotes but still exhibit *Sox10*$^{+}$ neural crest cells (arrowheads) in the developing head (C) and along the dorsal neural plate (G, arrowheads). In *Pax3*$^{-/-}$*;Pax7*$^{-/-}$ double mutants (D, H), *Sox10*$^{+}$ migratory neural crest cells (arrowheads) are present in the anterior head and the dorsal neural plate, albeit reduced in number, indicating that *Pax3* and *Pax7* are not required for neural crest cell induction in the mouse embryo.

Figure Twelve. Neural Crest Cells populate the developing Facial Region in *Pax3$^{-/-}$;Pax7$^{-/-}$* Double Mutants. *Pax3;Pax7* litters were harvested at 10.5dpc and processed for *Crabp1 in situ* hybridization. *Pax3$^{+/-}$;Pax7$^{+/+}$ and Pax3$^{+/-}$;Pax7$^{+/-}$* embryos express *Crabp1* in neural crest cells populating the medial (MNP, arrowhead) and lateral (LNP, arrow) nasal prominences (B, F) as well as the maxillary (Mx, arrow) and mandibular (Mn, arrow) prominences (A, E). Sections of *Pax3$^{+/-}$;Pax7$^{+/+}$* (C, D) and *Pax3$^{+/-}$;Pax7$^{+/-}$* (G, H) embryos revealed *Crabp1^{+}* neural crest cells throughout the MNP and LNP (arrowheads) and the dorsal neural tube (NT, arrow). *Pax3$^{+/-}$;Pax7$^{-/-}$* mutants (I, J) exhibit altered morphology of LNP (arrow) but still have *Crabp1^{+}* neural crest cells in the MNP (J,K arrowheads). L) *Crabp1* is also present in the neural tube (arrowheads). M, N) *Pax3$^{-/-}$;Pax7$^{-/-}$* double mutants have *Crabp1^{+}* neural crest cells (NC, arrows) in the frontonasal region (O, arrowheads), but the overall distribution of cells is reduced. P) *Crabp1^{+}* cells are present in the dorsal NT (arrowheads) of *Pax3$^{-/-}$;Pax7$^{-/-}$* double mutants. The overall reduction of the neuroepithelium in comparison to wildtype littermates may be indicative of a role for *Pax* genes in neuroepithelial proliferation and maintenance.

A
Mx
Mn
10.5dpc
B
LNP
MNP
C
LNP
MNP
D
NT
E
F
G
H
I
J
MNP
LNP
K
MNP
L
M
N
NC
NC
O
NC
NC
P
50μM
Pax3+/-;Pax7+/+
Pax3+/-;Pax7+/-
Pax3+/-;Pax7-/-
Pax3-/-;Pax7-/-

Analysis of neural tube sections revealed *Crabp1*$^{+}$ cells at the dorsal-most aspect of the neural tube in both heterozygous (Fig. 12H) and mutant (Fig. 12P) embryos, despite the neural tube closure defect in mutant embryos. Overall, migratory NCCs were present in *Pax3*$^{-/-}$;*Pax7*$^{-/-}$ embryos but were slightly decreased in number, indicating that these genes are not conserved in the mouse in the specification of NCCs but probably play a more important role in maintaining neural plate proliferation.

Development of the Cranial Explant Culture System

In conjunction with the *in vivo* analyses of genes required for NCC induction, we analyzed this process *in vitro*, taking advantage of the longer developmental period separating neural versus NCC induction in the mouse embryo. In the mouse, NCCs migrate from the dorsal neural folds prior to the closure of the neural tube in a rostral-caudal manner with cranial NCCs commencing this process at the 4-5ss stage (Nichols 1986), well after neural plate identity is established. Therefore, we developed a cranial explant culture assay to block NCC formation before their initial induction *in vitro*, using antagonists to known signaling pathways involved in the induction process. To test for proper NCC formation in the culture system, we isolated 7.5dpc cranial explants, cultured them for 24hours, and processed the explants for the expression of *Sox10* to determine the presence of migratory NCCs (Fig. 13A, B). Indeed, *Sox10* was present in all control explants (Fig. 13C, D), in a pattern similar to that seen in the cranial region of whole-mount 8.5dpc embryos. The

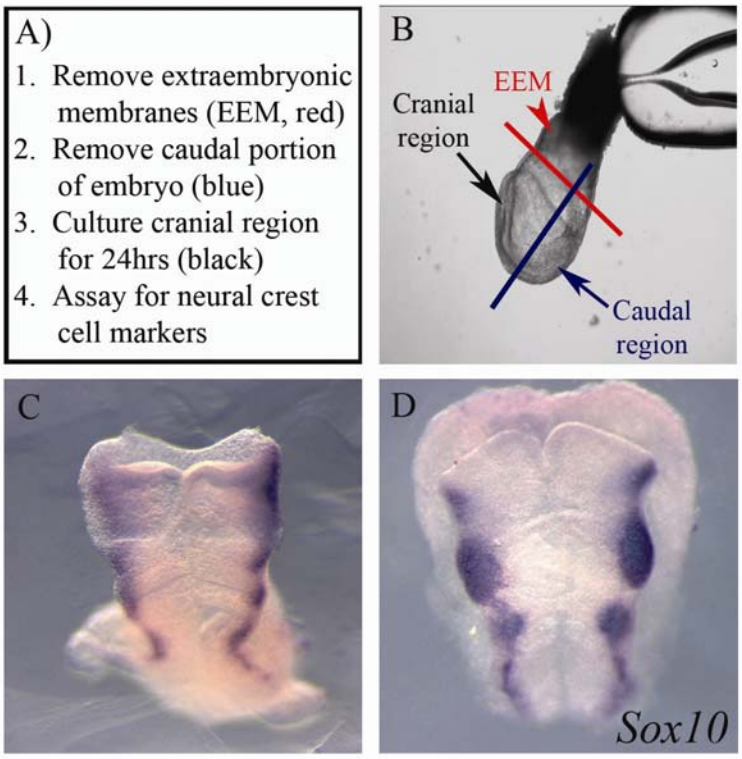

Figure Thirteen. Development of the Cranial Explant Culture System. A) Embryos were harvested at 7.5dpc and dissected as indicated. B) Embryos were removed from the extraembryonic membranes (EEM, red). The embryos were bisected using insect pins and the caudal region (blue, arrow) containing the primitive streak was discarded. The cranial region (black, arrow) was positioned on a cell culture membrane in standard DMEM/F12 media containing glutamax; explants were cultured for 24hrs at 37°C in 5% CO_2. Explants were assayed for beating heart tissue prior to fixation to ensure optimum culture conditions. C, D) Explants were processed for *Sox10 in situ* hybridization to mark migratory neural crest cells; neural crest cells were present in all control explants examined. *Sox10* expression in the explants is reminiscent of the *Sox10* staining pattern in whole-mount embryos at 8.5dpc.

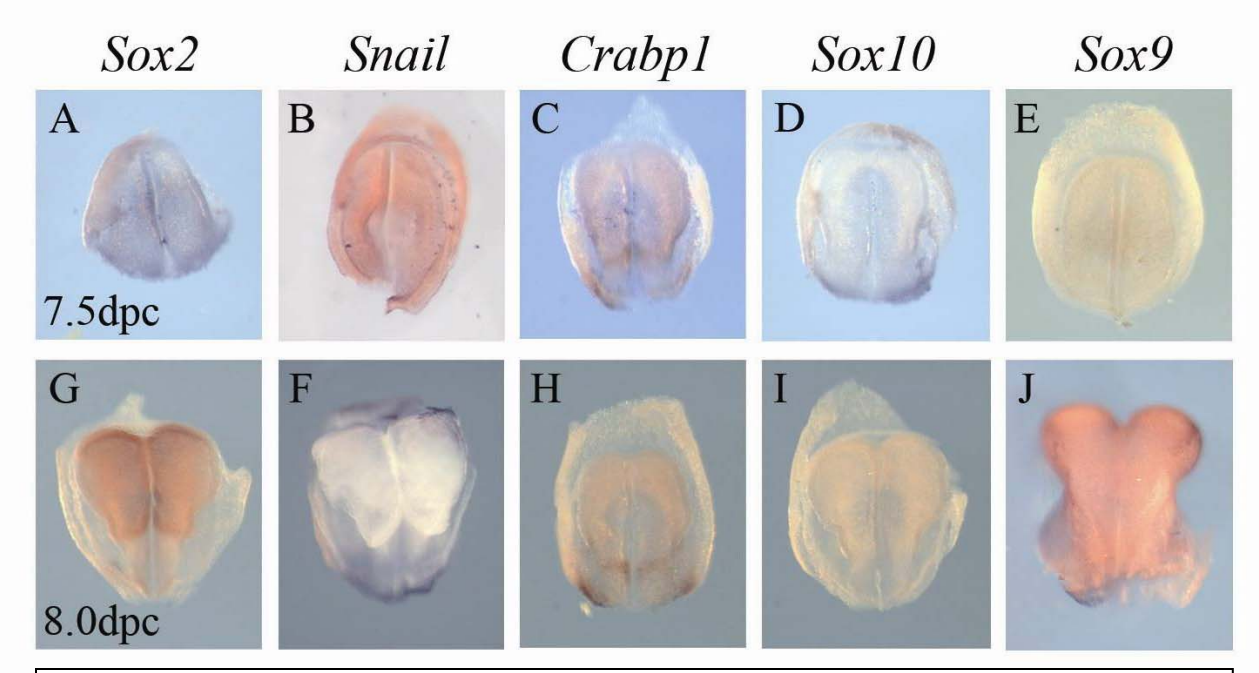

Figure Fourteen. Cranial Explants lack Neural Crest Cell Identity at the Time of Harvest. Cranial explants were harvested at 7.5 (A-E) and 8.0dpc (G-J) and immediately fixed and processed for *in situ* hybridization. Explants at both 7.5 and 8.0dpc were harvested prior to the onset of neural crest cell induction and lack the neural crest cell markers *Snail* (B, F), *Crabp1* (C, H), *Sox10* (D, I) and *Sox9* (E, J). In contrast, explants express *Sox2* (A, G) indicating that neural plate identity is already specified when explants are harvested.

presence of *Sox10*$^{+}$ NCCs in our cranial explants indicated that the culture system was appropriate for assaying the morphogens required for NCC induction in the mouse embryo.

As control experiments, we analyzed 7.5 and 8.0dpc cranial explants for the expression of neural plate and NCC markers to ensure that we were harvesting the explants prior to NCC induction. Cranial explants at both stages diffusely expressed *Sox2* throughout the neuroepithelium (Fig. 14A, G), indicating the presence of the progenitor neuroepithelial population, from which NCCs arise. In contrast to the expression of *Sox2*, NCC specific markers *Crabp1*, *Snail*, *Sox9*, and *Sox10* were not present in the cranial explants at 7.5 (Fig. 14B-E) or 8.0dpc (Fig. 14F-J), demonstrating that the tissue was harvested prior to the formation of NCCs.

BMP, NOTCH, and WNT Signaling are not required for Neural Crest Cell Induction In Vitro

To determine the key regulator for the induction of NCCs in the mouse, we introduced antagonists in our explant cultures to known pathways involved in NCC formation. Explants were treated with recombinant Noggin/Fc, SU5402, DAPT, or Frizzled-8/Fc proteins to inhibit the BMP, FGFR, NOTCH, and WNT signaling pathways and the effect of neural crest cell induction was subsequently analyzed via examination for migrating NCC with *Sox10*. The presence of *Sox10*$^{+}$ cells indicated that treatments as high as 100μg/μL (Noggin/Fc and Frizzled-8/Fc) or 100μM (DAPT) did not affect the induction of NCCs in the explant cultures (Fig. 15B-D).

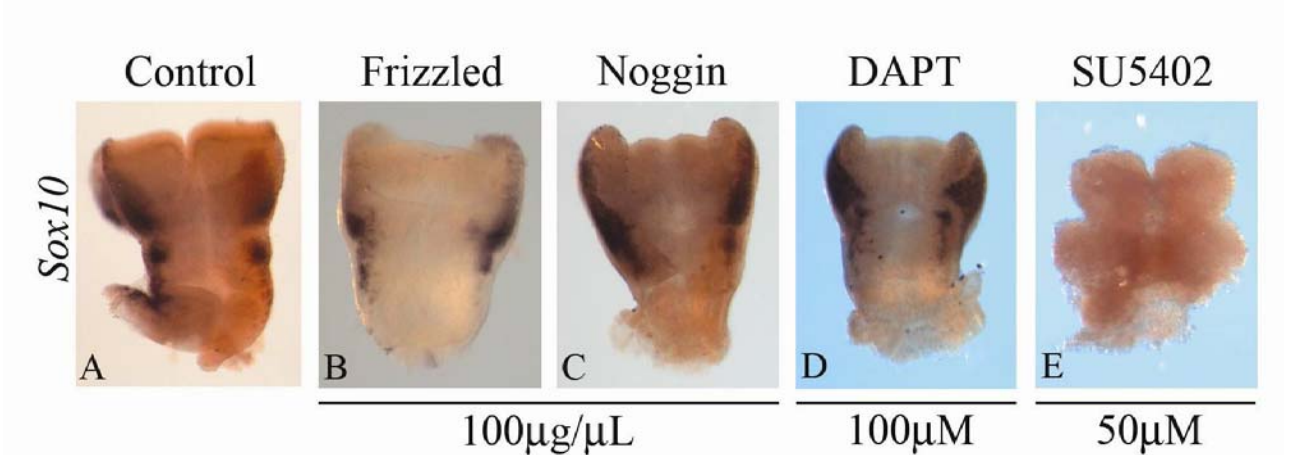

Figure Fifteen. Antagonist Treatment does not inhibit Neural Crest Cell Induction in Cranial Explants. A) Control explants cultured for 24hrs exhibit a normal pattern of *Sox10* expression, indicating the formation of neural crest cells. B-D) Antagonist treatment in 24hr cultures does not inhibit *Sox10* expression. Treatment with 100µg/µL of Frizzled (B) or Noggin (C) to block WNT and BMP signaling does not inhibit *Sox10* expression. D) 100µM treatment with DAPT to block NOTCH signaling does not inhibit *Sox10*. E) Treatment with 50µM SU5402 to inhibit FGFR signaling prevents neural crest cell induction as indicated by the loss of *Sox10* expression.

Collectively, this data in conjunction with knockout analyses, suggests that BMP, NOTCH, and WNT signaling pathways do not regulate NCC induction in the mouse embryo.

In contrast, treatment with SU5402 at 50μM resulted in an absence of *Sox10* (Fig. 15E; 16L-O) as well as *Crabp1* (Fig. 16G-J), but the explants exhibited an altered morphology in comparison to controls; cranial explants had a tufted appearance and were reduced in size, indicating problems regarding viability. Additionally, the lack of *Sox10* and *Crabp1* in cranial explants could be a secondary defect due to failure of neural plate maintenance. We examined *Sox2* expression in cranial explants to determine if there were alterations in the maintenance of the neural plate with SU5402 treatment; indeed, there was a progressive loss of *Sox2* throughout the neural plate with increasing concentrations of SU5402 when cultured for 24hrs (Fig. 16B-E). Therefore, the loss of *Sox10* and *Crabp1* in SU5402-treated cranial explants is most likely a secondary defect from the inhibition of FGF signaling and failure to maintain the neural plate.

Neural Crest Cells are present after 8- and 12-Hour SU5402-Treated Explant Cultures

Treatment with SU5402 in cranial explant cultures resulted in the absence of *Sox10* and *Crabp1* possibly as a secondary defect due to failure of neural plate maintenance. Despite the lack of NCC markers, FGF signaling may still be important for NCC induction independent of neural plate maintenance.

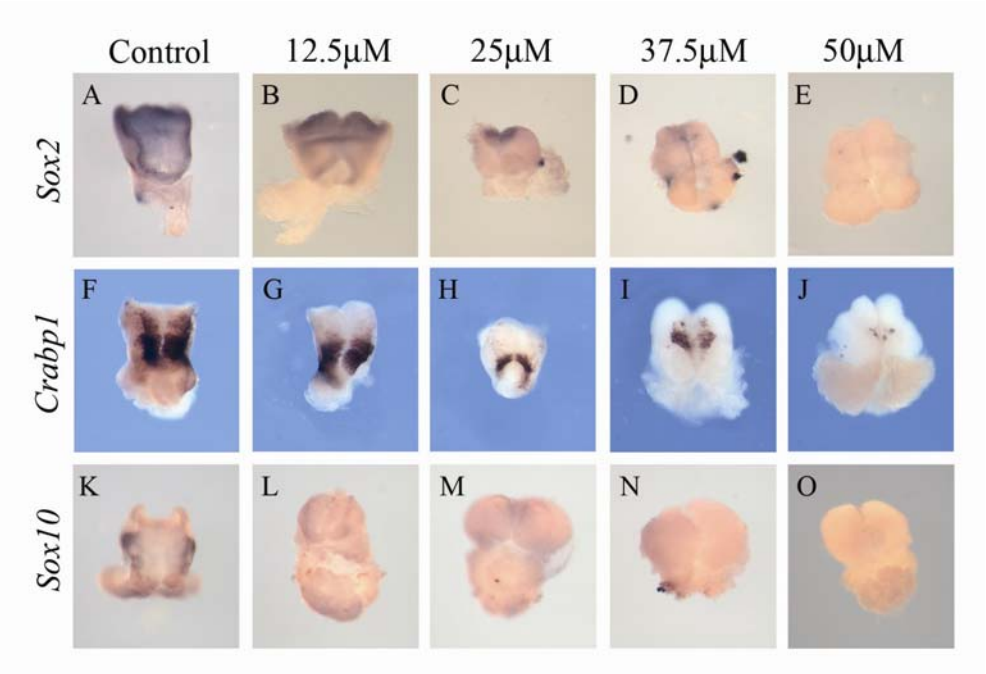

Figure Sixteen. SU5402 Treatment for Twenty-Four Hours inhibits the Neural Plate in Cranial Explant Cultures. A-E) Treatment with SU5402 results in the downregulation of the neural plate marker, *Sox2*, concomitant with increasing SU5402 concentration. Decreased *Sox2* expression indicates the lack of neural plate maintenance and inhibition of the progenitor population from which neural crest cells arise. Additionally, explants exhibit altered morphology at 50µM SU5402, indicating poor culture conditions at high concentrations of SU5402. Neural crest cell markers *Crabp1* (F-J) and *Sox10* (K-O) were inhibited with increasing SU5402 concentration, indicating the loss of neural crest cells with prolonged SU5402 exposure.

To further dissect the specific role for FGF signaling in NCC induction, we attempted to rescue the defects in the neural plate while blocking crest cell formation by varying the exposure time and concentration of SU5402. Additionally, we harvested embryos at 8.0dpc, prior to the appearance of somites and cultured the whole embryo as an explant; embryo explants were directly attached to the cell culture insert membranes via the surrounding extraembryonic tissues and cultured in 37.5μM SU5402 for 8- or 12-hours, fixed, and processed for *in situ* hybridization.

In all cultures harvested at 8.0dpc, beating heart tissue was present and the cultures did not exhibit significant alterations in morphology. As previously shown, 8.0dpc explants lacked NCC markers (Fig. 14F-J) indicating that the explants were harvested prior to crest cell induction. Embryo explants cultured for 8- (Fig. 17G-J) and 12hrs (Fig. 18G-J) exhibited a decrease in the NCC markers *Snail*, *Crabp1*, *Sox10*, and *Sox9* indicating that NCCs were reduced in number but still present. Additionally, analysis of *Sox2* (Fig. 17,18 compare F with A) indicated that neural plate identity was somewhat compromised, as the marker was decreased despite the reduced culture period and SU5402 concentration. Therefore, the specific role for FGF signaling in NCC induction remains unclear as reduced numbers of NCCs were present in both treatment groups, which in conjunction with the decreased *Sox2*, suggests that FGF signaling may not directly regulate NCC induction in the mouse but rather is responsible for maintenance of the neural plate.

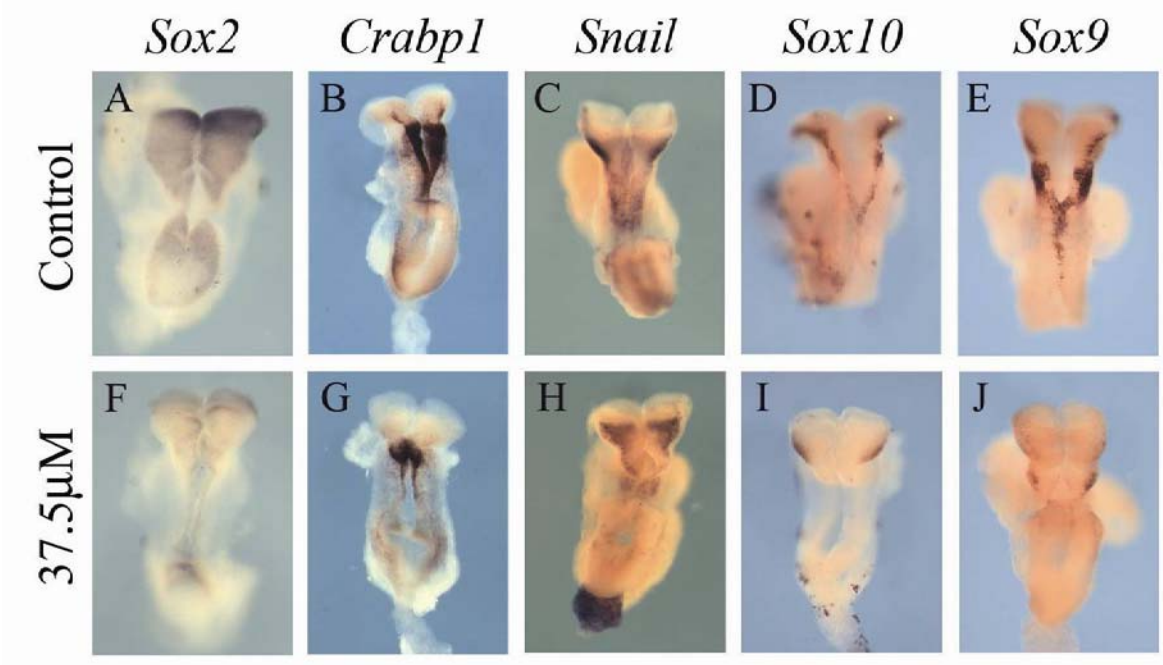

Figure Seventeen. SU5402 Treatment for Eight Hours inhibits Neural Crest Cell Formation. Explants were harvested at 8.0dpc and cultured for 8hrs in 37.5μM SU5402; explants were processed for *in situ* hybridization. Neural crest cell markers *Crabp1* (G), *Snail* (H), *Sox10* (I), and *Sox9* (J) were all decreased in comparison to non-treated controls (B-E). The loss of crest cell identity is accompanied by the inhibition of the neural plate as indicated by the decreased expression of *Sox2* (compare F with A).

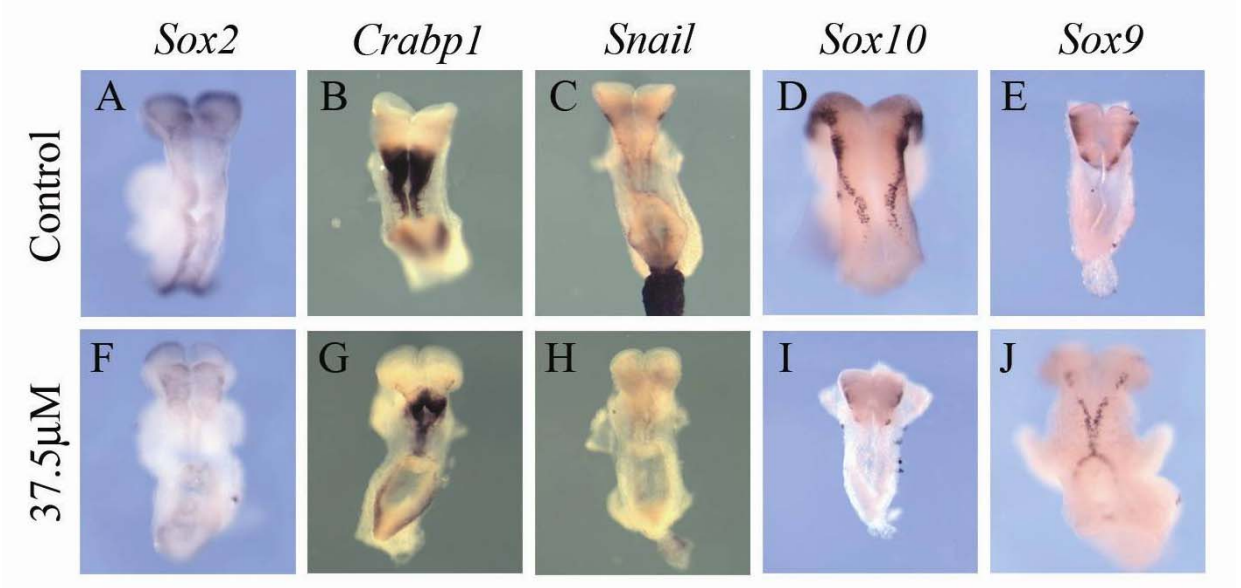

Figure Eighteen. SU5402 Treatment for Twelve Hours inhibits Neural Crest Cell Formation. Explants were harvested at 8.0dpc and cultured for 12hrs in 37.5μM SU5402; explants were processed for *in situ* hybridization. Neural crest cell markers *Crabp1* (G), *Snail* (H), *Sox10* (I), and *Sox9* (J) were all decreased in comparison to non-treated controls (B-E). The loss of crest cell identity is concomitant with the decreased *Sox2* in the neural plate (compare F with A).

Fgf8 is not required for Neural Crest Cell Induction in the Mouse

Reports in *Xenopus* have demonstrated the role for FGF8 signaling from the paraxial mesoderm in regulating NCC induction through mediation of *Pax3* (Monsoro-Burq et al. 2005). Indeed, overexpression of *Fgf8 in vivo* or animal cap assays results in an expanded domain NCC markers (Monsoro-Burq et al. 2003; Monsoro-Burq et al. 2005). Therefore we analyzed the *Fgf8* null mouse mutant, $Fgf8^{\Delta 2,3/\Delta 2,3}$ (Meyers et al. 1998), for defects in NCC formation to ascertain whether this signaling pathway was conserved in the mouse and to gain further insight from our *in vitro* studies using SU5402. Because the identity of the neural plate was compromised in our explant cultures, we first analyzed *Sox2* in $Fgf8^{\Delta 2,3/\Delta 2,3}$ embryos at 9.5dpc. Despite the altered morphology of the neural tube, which was often kinked or failed to close in mutant embryos, *Sox2* was present throughout the neural plate (Fig. 19C, D). Analysis of the NCC markers *Snail*, *Crabp1*, *Sox10* and *Sox9* revealed a normal pattern of expression for each of these genes (Fig. 19I-X), indicating that *Fgf8* is not involved in NCC induction in the mouse.

Interestingly, the expression of *Pax3* is downregulated in $Fgf8^{\Delta 2,3/\Delta 2,3}$ mutants (Fig. 19G, H), suggesting that while FGF8 signaling may be acting upstream of *Pax3* within the neural plate, neither pathway is required for crest cell induction. This is consistent with our data obtained in $Pax3^{-/-};Pax7^{-/-}$ double mutants and *Pax3* and *Pax7* knockout mice. Collectively, these data demonstrate that the requirement for FGF8 signaling in NCC induction in *Xenopus* is not conserved in the developing mouse embryo. Additionally, our data implicate a direct role for FGF signaling in the

Figure Nineteen. FGF8 Signaling is not required for Neural Crest Cell Induction in the Mouse. Embryos were harvested at 9.5dpc and processed for *in situ* hybridization. A, B) Lateral (A) and dorsal (B) views of $Fgf8^{+/\Delta 2,3}$ embryos stained for *Sox2* to label the neural plate. C, D) $Fgf8^{\Delta 2,3/\Delta 2,3}$ mutants also exhibit a normal pattern of *Sox2* expression, indicating proper maintenance of the neural plate in *Fgf8* mutants. Analysis of the neural crest cell markers *Snail* (K, L), *Crabp1* (O, P), *Sox10* (S, T), and *Sox9* (W, X) in $Fgf8^{\Delta 2,3/\Delta 2,3}$ mutants revealed a lack of crest cell formation defects, indicating that FGF8 signaling is not required in the mouse for neural crest cell induction. Additionally, analysis of *Pax3* (E-H) revealed a slight decrease in expression in mutant embryos (G, H) indicating that *Fgf8* acts upstream of *Pax3*.

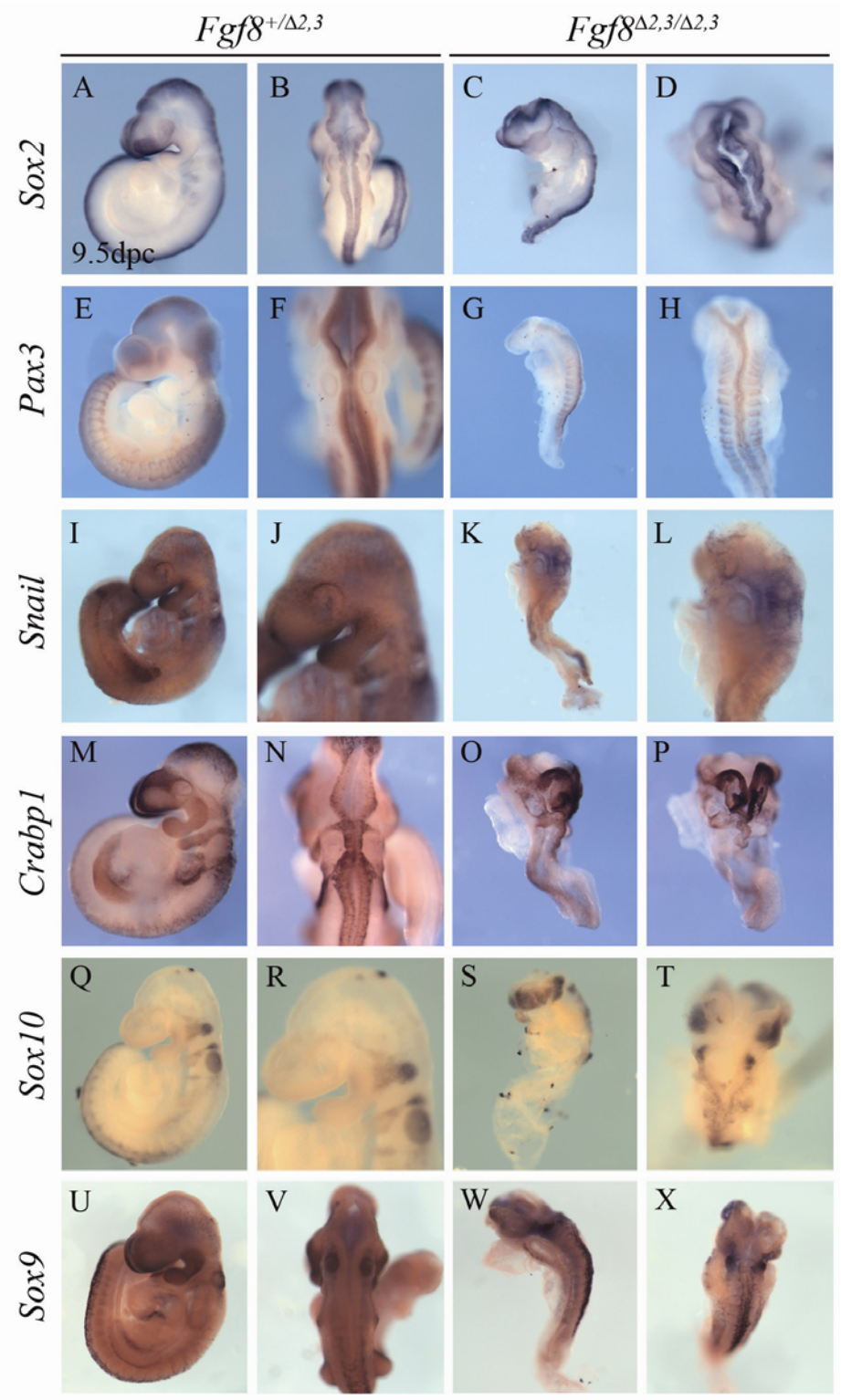
Fgf8+/Δ2,3
Fgf8Δ2,3/Δ2,3
Sox2
Pax3
Snail
Crabp1
Sox10
Sox9
A
B
C
D
9.5dpc
E
F
G
H
I
J
K
L
M
N
O
P
Q
R
S
T
U
V
W
X

maintenance of the neural plate rather than a direct requirement for FGF signaling in NCC induction which is supported by conditional knockouts of *FgfR1* (Trokovic et al. 2003) or full knockouts of *FgfR2* (Xu et al. 1998) which still generate NCCs.

Germ cell nuclear factor (Gcnf) is required for Neural Crest Cell Formation

In vivo and *in vitro* experiments aimed at identifying the key morphogens regulating NCC induction in the mouse failed to identify any known signaling pathways as a requirement to produce crest cells. To identify new regulators in NCC induction, we used data from a microarray screen performed in *Tcof1*$^{+/-}$ embryos (Jones et al. 2008), searching for genes that were significantly downregulated in an attempt to identify novel regulators of NCC development. *Tcof1*$^{+/-}$ embryos have defects in neural crest cell formation due apoptosis of neural crest cells as well as in the neuroepithelial progenitors from which they arise (Dixon et al. 2006). Hence, any genes associated with neural crest cell development, in theory, would be downregulated in *Tcof1*$^{+/-}$ embryos due to decreased numbers within the neural crest population. We identified *Germ cell nuclear factor* (*Gcnf*/*Nr6a1*) as significantly downregulated in *Tcof1*$^{+/-}$ embryos compared to wildtype. *Gcnf* is an orphan nuclear receptor required during embryogenesis in the regulation of pluripotency genes (Fuhrmann et al. 2001; Gu et al. 2005), neural development (Chung et al. 2006), and somitogenesis (Chung et al. 2001).

In the microarray screen performed in *Tcof1*$^{+/-}$ embryos, *Gcnf* was downregulated almost two-fold (N. Jones and P. Trainor, unpublished) in comparison

to *Tcof1*$^{+/+}$ littermates. To validate these data, we performed *in situ* hybridization for *Gcnf* in *Tcof1*$^{+/-}$ embryos at 8.5dpc. Indeed, *Tcof1*$^{+/-}$ mutants express *Gcnf* throughout the neuroepithelium but at levels decreased in comparison to wildtype littermates (Fig. 20, compare A,B). Faint staining of migratory neural crest cells in the stream originating from rhombomere 2 (r2) is present in *Tcof1*$^{+/+}$ embryos, which are absent in the heterozygous littermates (Fig. 20 compare C, D).

Analysis of *Gcnf* beginning at 7.5dpc revealed a regionally restricted pattern of expression; at 7.5dpc *Gcnf* was specifically expressed in the primitive streak, but was absent in more anterior regions of the embryo (Fig. 21A-C). By 8.5dpc, *Gcnf* was present throughout the neuroepithelium (Fig. 21D), with heaviest expression along the dorsal neural folds (Fig. 21E), the region from which neural crest cells arise; sections of 8.75dpc embryos revealed *Gcnf* expression in migratory NCCs (Fig. 21J, K). *Gcnf* was restricted to the neural tube at 9.5dpc (Fig. 21F), subsequently downregulated at 10.5dpc (Fig. 21G), and was completely absent by 11.5 and 12.5dpc (Fig. 21H, I). Overall, these data validate that *Gcnf* is downregulated in *Tcof1*$^{+/-}$ embryos and identifies *Gcnf* expression along the dorsal-most regions of the neural folds and in migratory neural crest cells.

Gcnf expression in migratory NCCs and the confirmation that *Gcnf* was downregulated in *Tcof1*$^{+/-}$ embryos with decreased NCCs suggested that this gene may be regulating NCC development. Therefore, we examined *Gcnf*$^{-/-}$ embryos for defects in NCC formation. Indeed, *Gcnf* mutants exhibited an absence or

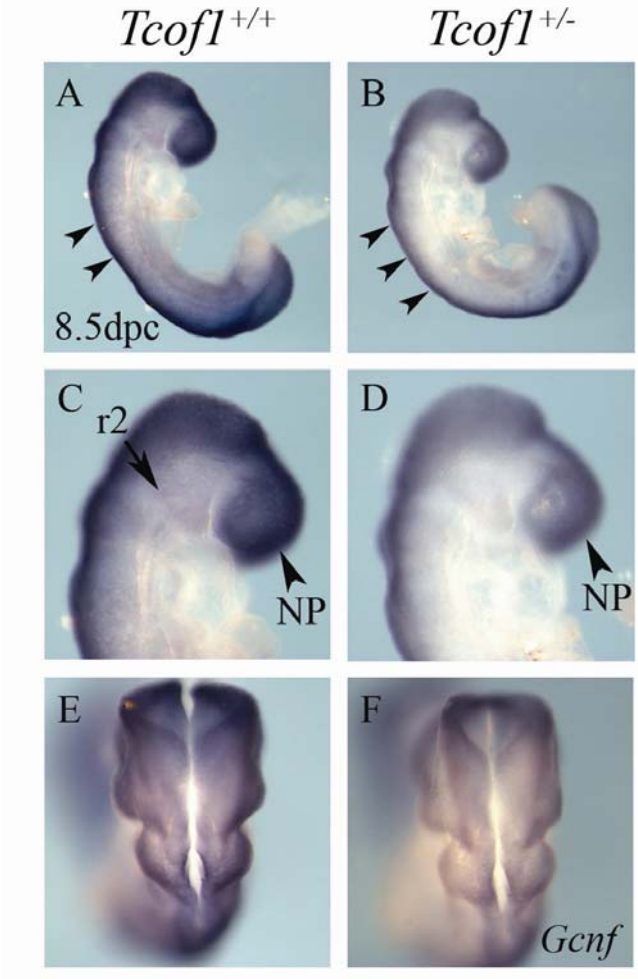

Figure Twenty. *Gcnf* is downregulated in *Tcof1*$^{+/-}$ Embryos. *Tcof1*$^{+/-}$ embryos were harvested at 8.5dpc and processed for *Gcnf in situ* hybridization to validate microarray results (Jones and Trainor, unpublished). A) In *Tcof1*$^{+/+}$ embryos *Gcnf* is expressed throughout the neuroepithelium (arrowheads). B) *Gcnf* is present in *Tcof1*$^{+/-}$ embryos throughout the neuroepithelium (arrowheads) although its expression is not as intense as in wildtype littermates (A). C) Faint *Gcnf* expression is identifiable in migratory neural crest cells arising from rhombomere 2 (r2) to populate the first branchial arch. *Gcnf* is also present in the developing nasal prominence (NP). In contrast, *Gcnf* expression is barely detectable in migratory neural crest cells; *Gcnf* is reduced in cells populating the NP (arrowhead). E, F) Dorsal view of *Tcof1*$^{+/+}$ and *Tcof1*$^{+/-}$ embryos reveals decreased *Gcnf* expression within the hindbrain.

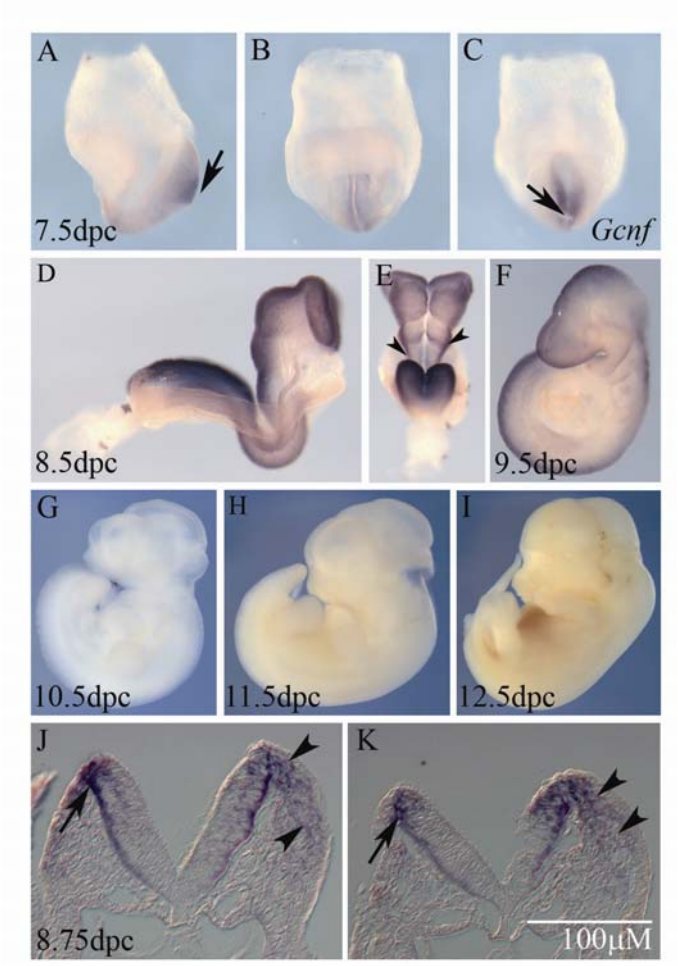

Figure Twenty-One. *Gcnf* is dynamically expressed during Mid-Embryonic Development. A-C) Embryos collected at 7.5dpc have *Gcnf* expression in the posterior region of the embryo within the primitive streak (arrow). D, E) By 8.5dpc, *Gcnf* is expressed throughout the neuroepithelium, with heaviest expression along the dorsal neural folds (arrowheads). F) At 9.5dpc, *Gcnf* remains in the neural tube along the anterior-posterior axis. G-I) By 10.5dpc, *Gcnf* is downregulated and is no longer expressed in the embryo. J, K) Sections at the level of the first branchial arch of 8.75dpc embryos demonstrates that *Gcnf* is transiently expressed in emigrating neural crest cells (arrowheads) and is present along the dorsal neuroepithelium (arrows).

significant downregulation of *Crabp1*, *Snail*, *Sox10*, and *Sox9* expression at 9.5dpc (Fig. 22E-H) indicating a role for *Gcnf* in regulating NCC induction. *Crabp1* expression was absent in mutants (Fig. 22H), while *Crabp1*$^{+}$ cells were present along the dorsal neural folds in *Gcnf*$^{+/-}$ littermates (Fig. 22D). *Snail* and *Sox9* were present in the developing frontonasal region and along the dorsal neural folds in *Gcnf*$^{+/-}$ embryos, respectively (Fig. 22A, C); while each of these genes was absent in mutant embryos (Fig. 22E, G). Additionally, *Sox10* was significantly downregulated in *Gcnf* $^{/-}$ embryos and exhibited an altered pattern of expression (Fig. 22F); *Sox10*$^{+}$ cells (arrowheads) were present along the anterior half of the embryo and were positioned as abnormal groups of cells. In contrast, *Gcnf*$^{+/-}$ embryos had *Sox10*$^{+}$ NCC in the cranial nerve ganglia (Fig. 22B). Interestingly, throughout our analysis an occasional embryo was processed that exhibited very few *Sox10*$^{+}$, *Sox9*$^{+}$, or *Crabp1*$^{+}$ NCC, although these embryos were not representative of the total numbers of embryos processed. *Gcnf* expression in migratory NCCs and the absence of multiple NCC markers in *Gcnf*$^{/-}$ embryos clearly indicate a direct role for *Gcnf* in regulating NCC induction in the mouse.

Gcnf$^{/-}$ *Embryos have an Enlarged Neural Plate due to Proliferation Defects*

To ensure that the defects in NCC formation were not due to inhibition of the neural plate, we analyzed the expression of *Sox2*, *Wnt1*, and *Pax3* in *Gcnf*$^{/-}$ embryos. *Gcnf*$^{/-}$ mutants exhibit an enlarged neural plate, coinciding with increased expression of *Sox2* (Fig. 23D). Dorsal neural tube markers, such as *Wnt1* (Fig. 23E) and *Pax3*

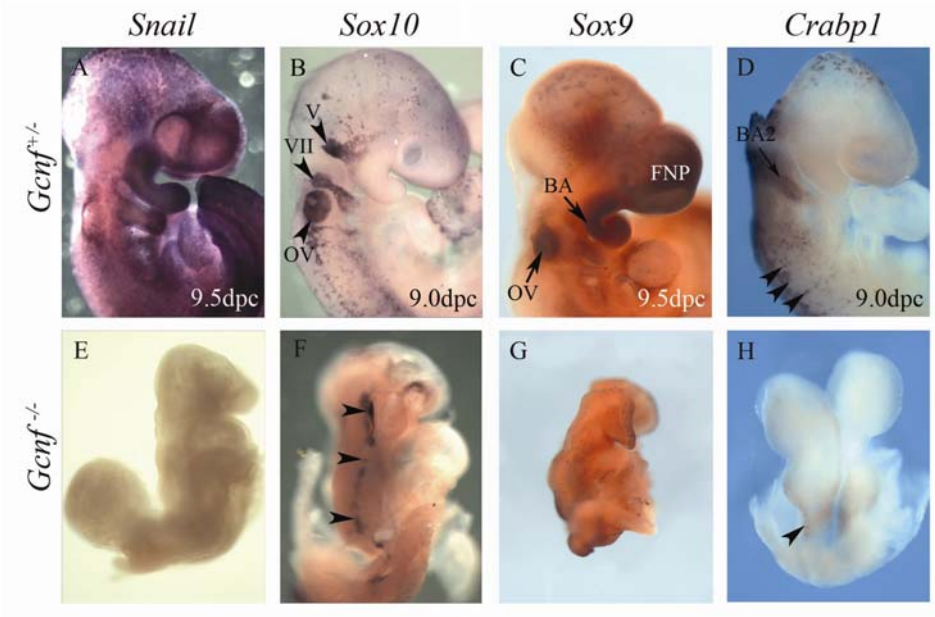

Figure Twenty-Two. *Gcnf* Mutants have Neural Crest Cell Formation Defects. A) At 9.5dpc, *Gcnf*$^{+/-}$ embryos have normal expression of *Snail*, a marker of migratory neural crest cells undergoing an epithelial-to-mesenchymal transition. In contrast, *Gcnf*$^{-/-}$ embryos (E) lack any expression of *Snail*, indicating that the mutant embryos have decreased neural crest cell production. B) Migratory *Sox10*$^{+}$ neural crest cells are present in *Gcnf*$^{+/-}$ embryos in the trigeminal (V) and facial (VII) ganglia as well as the otic vesicle (OV). F) *Gcnf*$^{-/-}$ embryos have an abnormal pattern of *Sox10* expression; punctuate regions of *Sox10*$^{+}$ cells are present along the anterior half of the embryos (arrowheads) but do not exhibit the classic migratory streams seen in the heterozygous littermates. C) *Sox9* is present in the frontonasal prominence (FNP), branchial arch (BA), and OV in *Gcnf*$^{+/-}$ embryos; *Gcnf* mutants (G) have a complete absence of *Sox9* expression. D) *Crabp1*$^{+}$ neural crest cells are present along the dorsal neural tube (arrowheads) and cells can be seen in the migratory stream populating BA2 (arrow). H) In *Gcnf*$^{-/-}$ embryos, no *Crabp1*$^{+}$ cells are present in anterior regions, although decreased *Crabp1* expression is present in the posterior neural plate (arrowhead).

(Fig. 23F) were also expanded in *Gcnf*$^{-/-}$ embryos in comparison to wildtype littermates (Fig. 23A-C). Furthermore, we examined the distribution of the neural plate markers SOX2 (Fig. 24A-B) and PAX3 (Fig. 24E-F) in *Gcnf*$^{-/-}$ embryos as well as the mitotic marker phospho Histone H3 (pH3) (Fig. 24C-D). SOX2 was upregulated throughout the neural plate of *Gcnf*$^{-/-}$ embryos while in contrast was only present along the medial neural plate in *Gcnf*$^{+/+}$ embryos (Fig. 24A-B), indicating that cells within the neuroepithelium of mutant embryos are maintained in a progenitor-like state. Additionally, pH3^{+} mitotic cells were increased in number in *Gcnf*$^{-/-}$ embryos indicating enhanced proliferation in the mutants which ultimately results in an enlarged neuroepithelium (Fig. 24C-D). Consistent with *in situ* hybridization analysis of *Pax3*, PAX3^{+} cells were present at the dorsal-most aspect of the neural plate in *Gcnf*$^{+/+}$ and *Gcnf*$^{-/-}$ embryos, indicating that dorsal neural plate identity remains intact in *Gcnf*$^{-/-}$ embryos. Interestingly, PAX3^{+} neural crest cells (arrowheads) were present in *Gcnf*$^{+/+}$ embryos (Fig. 24E, E') but were absent in *Gcnf*$^{-/-}$ embryos (Fig. 24F, F') indicating a failure of PAX3^{+} neural crest cells to migrate. Collectively, the expanded SOX2 and increased number of mitotic cells within the neural plate of *Gcnf*$^{-/-}$ embryos demonstrate that neural plate identity is intact and the precursor population from which NCCs arise is present, which in conjunction with the absence of NCC markers and PAX3^{+} neural crest cells, suggests that *Gcnf* mutants have specific defects in the transition from a neuroepithelial to neural crest cell.

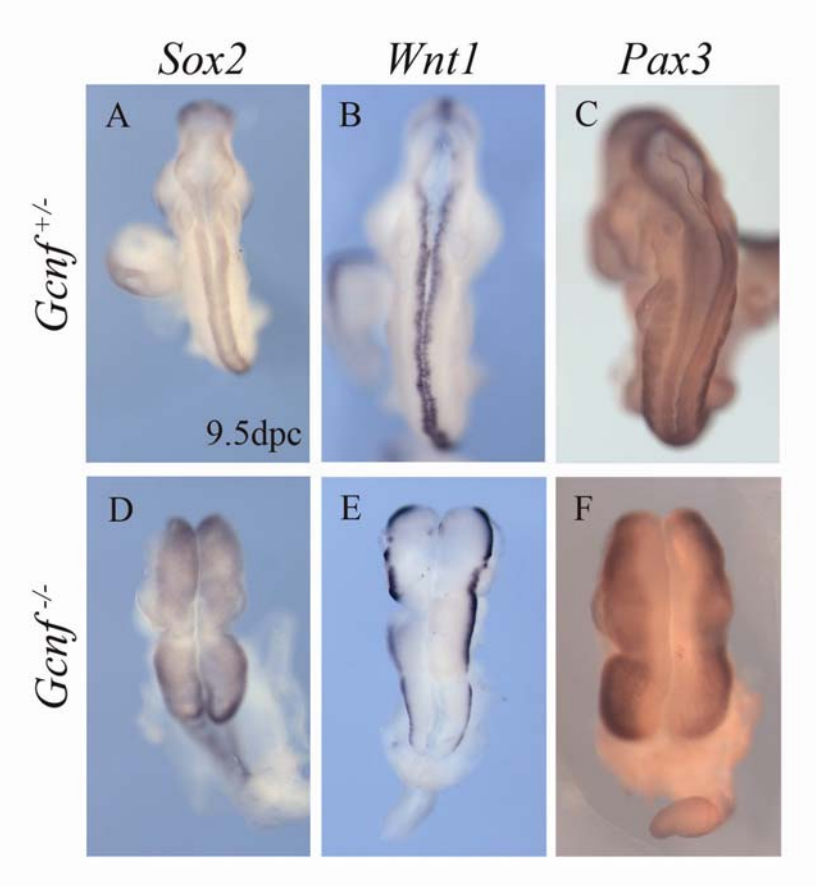

Figure Twenty-Three. Neural Plate Identity is unaltered in *Gcnf* Mutants. A) *Sox2* is expressed throughout the neural plate in *Gcnf*$^{+/-}$ embryos. D) *Gcnf* mutants have increased *Sox2* expression in the neural plate; mutants also exhibit open neural tube defects. B, E) *Wnt1* is expressed in the dorsal lip of the neural tube in heterozygous (B) and mutant (C) *Gcnf* embryos, but appears to be more intensely stained in *Gcnf*$^{-/-}$ embryos. C) *Pax3* is expressed in the dorsal neural tube of *Gcnf*$^{+/-}$ embryos. F) In *Gcnf*$^{-/-}$ embryos *Pax3* expression remains but appears expanded in comparison to heterozygous littermates.

Figure Twenty-Four. *Gcnf*$^{-/-}$ Embryos exhibit prolonged maintenance of the Neural Plate. SOX2 is present in the medial (arrows) regions of the neural plate in *Gcnf*$^{+/+}$ embryos (A, A'). Similarly, *Gcnf*$^{-/-}$ embryos have SOX2 present in the medial neural plate but was expanded to the lateral tips (arrows) of the neural plate (B, B'). C-D) Analysis of mitotic cells using phospho Histone H3 (pH3) in *Gcnf*$^{-/-}$ embryos (D, D') revealed a dramatic increase in the number of mitotic cells (arrowheads) in comparison to *Gcnf*$^{+/+}$ embryos (C, C'). E-F) PAX3 staining in the dorsal neural tube is comparible between *Gcnf*$^{+/+}$ (E, E') and *Gcnf*$^{-/-}$ (F, F') embryos; in contrast, PAX3^{+} neural crest cells (NCC) are only identifiable in *Gcnf*$^{+/+}$ embryos (E, arrowheads) indicating an absence of migratory PAX3^{+} NCC in mutant embryos (F, F'). Green, SOX2; Red, pH3 (C, D) or PAX3 (E, F). Blue, DAPI. Scale bar, 50μM.

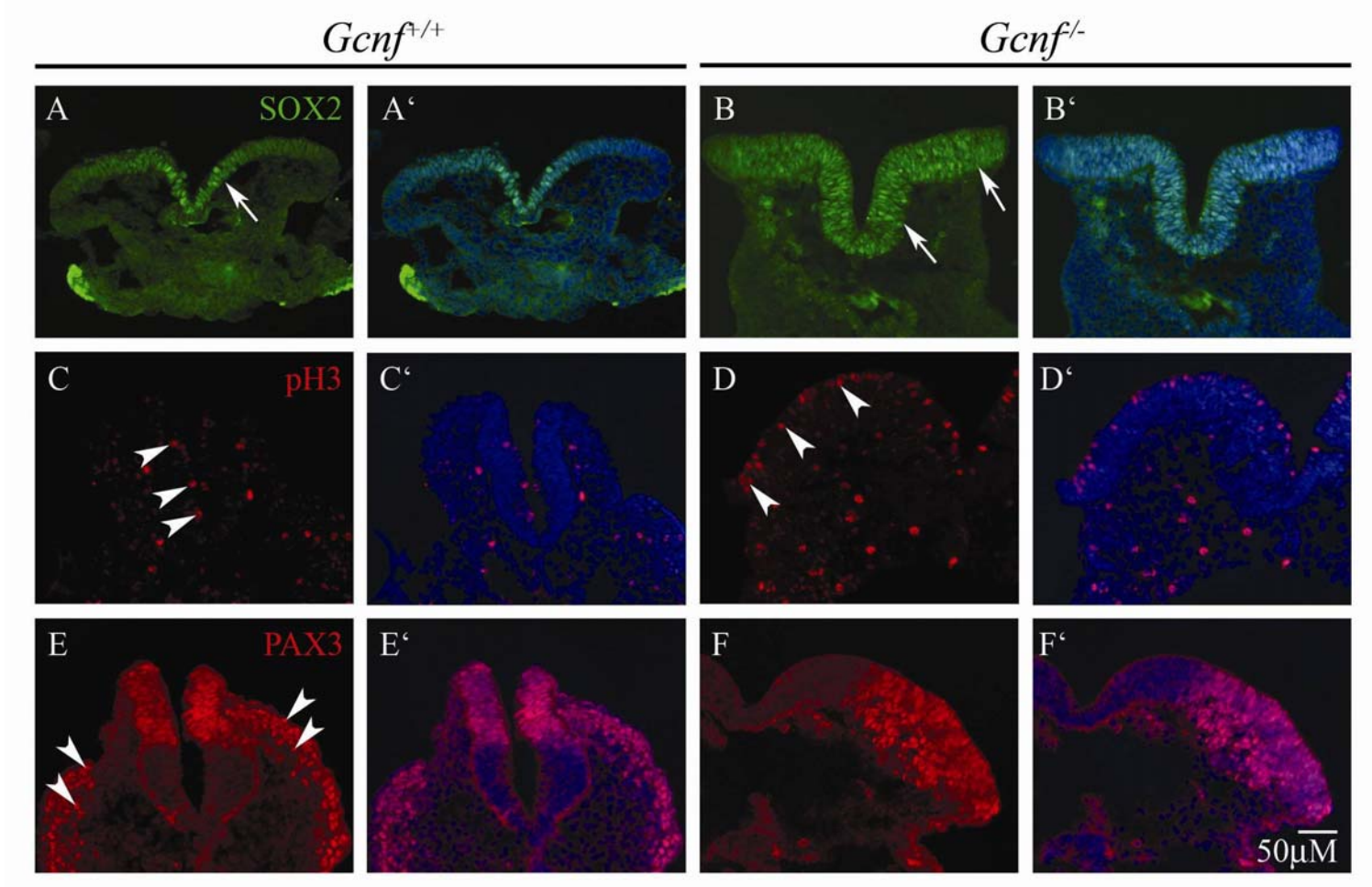
Gcnf+/+
Gcnf-/-
A
SOX2
A‘
B
B‘
C
pH3
C‘
D
D‘
E
PAX3
E‘
F
F‘
50µM

Gcnf is required for the activation of Neural Crest Cell Specific Genes

Gcnf has been previously shown to specifically downregulate the pluripotency genes *Oct4* and *Nanog* in embryonic stem cells (Fuhrmann et al. 2001; Gu et al. 2005), allowing for the activation of differentiation paradigms. The upregulation of the pluripotency marker SOX2 and increased numbers of mitotic cells in *Gcnf*$^{-/-}$ embryos suggests that the absence of NCC may result from defects in the transition of a neuroepithelial to NCC and the subsequent activation of NCC specific differentiation paradigms. Therefore, we hypothesized that *Gcnf* might directly regulate NCC formation through the activation of NCC specific genes. Indeed, a putative *Gcnf* binding site (AGGTCA) was identified in the promoter region of *Snail1* and *Snail2* (Fig. 25), genes responsible for the epithelial-to-mesenchymal transition in NCCs from the neural plate border (Nieto et al. 1994). Additionally, putative *Gcnf* binding sites were also identified in *Sox9, Sox10, Sip1,* and *Crabp1* (Fig. 25) indicating that *Gcnf* may be responsible for the activation of neural crest cell specific gene paradigms. Chromatin immunoprecipitation (ChIP) assays are currently underway to determine the extent of GCNF binding to these putative consensus sequences and the role of *Gcnf* in the activation of neural crest cell specific gene paradigms.

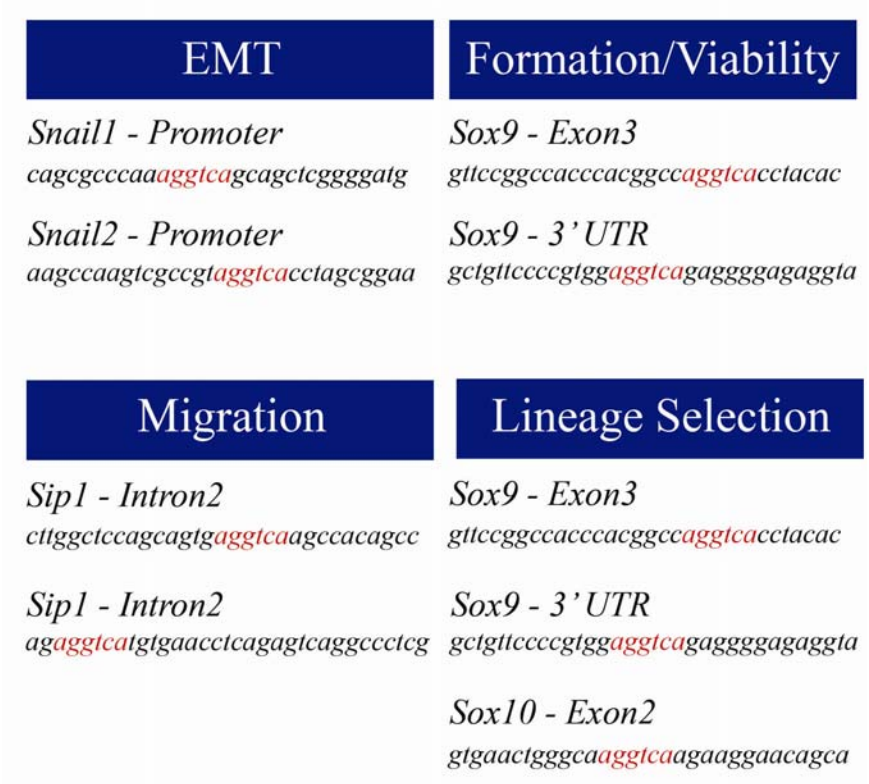

Figure Twenty-Five. Identification of Putative *Gcnf* Binding Sites in Genes required for Neural Crest Cell Development. Putative *Gcnf* binding sites (red) were identified in multiple neural crest cell specific genes. A *Gcnf* binding site was identified in the promoter regions of *Snail1* (nt315-320) and *Snai2* (nt336-341), genes required for the epithelial to mesenchymal transition (EMT) of neural crest cells. Two *Gcnf* binding sites were also identified in Intron 2 of *Sip1* (nt6035-540, top; 12603-608, bottom), a gene important for crest cell migration. Binding sites for the neural crest cell lineage specific genes, *Sox9* (nt3298-3303; 6450-6455) and *Sox10* (nt2282-2287), were identified, suggesting a role for *Gcnf* in neural crest cell formation and viability (*Sox9*) and lineage pathway selection (*Sox9* and *Sox10*).

D) Discussion

Analyses of a variety of model organisms has resulted in the identification of multiple signaling pathways potentially regulating neural crest cell induction, including BMP, FGF, NOTCH, PAX and WNT signaling. Interestingly, while these signaling pathways are a consistent theme across multiple species, analysis of the current literature suggests that crest cell formation is regulated in a species dependent manner and that a single pathway may not be conserved across multiple model systems. Interestingly, each of these pathways is also required for neural induction, which in species such as *Xenopus* and avian embryos, occurs just before neural crest cell induction, indicating that the identification of the key signaling pathway required for neural crest cell induction may be difficult due to temporal overlap of these two processes. In contrast, murine embryos have a much larger window separating neural and neural crest cell induction, suggesting that this model system may be ideal for determining the key regulator of crest cell induction, thereby allowing one to decipher the role, if any, of known signaling pathways, such as BMP or FGF signaling, in neural and/or neural crest cell induction.

BMP, FGF, NOTCH, PAX and WNT Signaling are not required for Neural Crest Cell Induction

Previous reports in avian embryos have demonstrated that NOTCH signaling is required for the induction of neural crest cells (Endo et al. 2002), although our analyses in the mouse have indicated that NOTCH signaling is not required for this

process *in vivo* and *in vitro*. Treatment of cranial explants with DAPT *in vitro* at concentrations up to 100μM failed to prevent the expression of *Sox10*, indicating that neural crest cells were induced in the explant cultures (Fig. 15). These data are consistent with our *in vivo* analyses of *RBP-Jκ* mutants (Fig. 10); we failed to detect any differences in the expression of *Crabp1* and *Snail*, general markers of migratory neural crest cells. *RBP-Jκ* is the nuclear effector of NOTCH signaling and is required for the activation of target genes through all of the Notch receptors (*Notch1-4*) (Kato et al. 1996). Hence, our analyses provide a functional knockout of all NOTCH signaling, thereby preventing examination of individual or compound Notch receptor mutants.

Although *RBP-Jκ* mutants did not exhibit alterations in *Crabp1* or *Snail,* the expression of neural crest cell lineage specific markers, *Sox9* and *Sox10* were reduced (Fig. 10), indicating a role for NOTCH signaling in neural crest cell lineage selection. *Sox9* (Cheung and Briscoe 2003) and *Sox10* (Britsch et al. 2001) are both required for the development of glial cells in the peripheral nervous system; additionally, *Sox10* is important in the development neurons of the dorsal root ganglia (Carney et al. 2006) and the enteric nervous system (Herbarth et al. 1998; Southard-Smith et al. 1998). Interestingly, it has been only recently that the role of NOTCH in regulating *Sox9* or *Sox10* expression has been addressed. NOTCH promotes the expression of *Sox9* in the central and peripheral nervous systems, as conditional removal of *RBP-Jκ* in the *Wnt1-cre* or *Nestin-cre* domains results in the absence of *Sox9* during gliogenesis

(Taylor et al. 2007). Additionally, NOTCH signaling is an important mediator of *Sox10* expression; particularly in the maintenance of *Sox10*$^{+}$ neural crest cells that will give rise to the enteric nervous system (Okamura and Saga 2008). Conditional inactivation of a core component of the NOTCH signaling pathway, *Pofut1*, in neural crest cells results in the absence of *Sox10*, leading to a lack of enteric ganglia development. Hence, NOTCH signaling is required for the maintenance of *Sox10* in neural crest cells prior to their differentiation into enteric neurons (Okamura and Saga 2008). Collectively, the decreased expression of *Sox9* and *Sox10* in *RBP-Jκ*$^{-/-}$ embryos does not reflect defects in neural crest cell induction but rather role for NOTCH signaling in the maintenance of neuronal and glial progenitors.

Our analyses of *Pax3*$^{-/-}$;*Pax7*$^{-/-}$ double mutants did not reveal a role for either of these genes in neural crest cell formation as has been previously reported (Mansouri et al. 1996; Conway et al. 1997; Epstein et al. 2000; Monsoro-Burq et al. 2005; Basch et al. 2006). Indeed, double mutant embryos form migratory *Sox10*$^{+}$ and *Crabp1*$^{+}$ neural crest cells (Fig. 11, 12), although the cells were reduced in number. *Pax3*$^{-/-}$;*Pax7*$^{-/-}$ double mutants exhibited a decrease in the thickness of the neural plate, which was significantly thinner in double mutant embryos in comparison to single- and compound heterozygous littermates. Overall, the presence of migratory neural crest cells and the decreased thickness of the neural plate indicate a potential role for *Pax3*/*Pax7* in the maintenance of neural plate progenitors; hence, loss of both of these genes in double mutants may result in decreased numbers of cells in the neural plate and therefore decreased NCCs.

Pax3 and *Pax7* have been suggested as serving functionally redundant roles in the neural tube. Interestingly, *Pax3* heterozygous embryos exhibit increased thinning of the neural tube with progressive loss of *Pax7* alleles; $Pax3^{+/-}$;$Pax7^{+/-}$ and $Pax3^{+/-}$;$Pax7^{-/-}$ embryos have decreased thickness of the neural plate in comparison to $Pax3^{+/-}$;$Pax7^{+/+}$ embryos (Fig. 12), indicating a redundant role for *Pax7* and *Pax3* in neural plate maintenance. Indeed, it is not until the loss of both *Pax3/7* alleles occurs that the neural plate is severely affected. Previous data has demonstrated the dramatic upregulation of *Pax7* in $Pax3^{-/-}$ embryos (Borycki et al. 1999), indicating that *Pax3* normally functions to negatively regulate *Pax7* in the neural tube. In the absence of *Pax3*, the upregulation of *Pax7* results in PAX7 mediating PAX3 signaling (Borycki et al. 1999). Hence, the specific role of *Pax3/7* in neural plate maintenance cannot be fully characterized unless both genes are absent. Subsequent analysis of neural plate identity, proliferation, and apoptosis in $Pax3^{-/-}$;$Pax7^{-/-}$ double mutants would serve to further characterize the specific roles of these genes in the development of the neural plate. Collectively, *Pax3* and *Pax7* are not conserved in mouse NCC induction as in *Xenopus* and avian embryos, but instead appear to be required for maintenance and proliferation.

Furthermore, analysis of *Fgf8* null embryos, $Fgf8^{\Delta 2,3/\Delta 2,3}$, revealed no defects in the induction of neural crest cells in the absence of FGF8 signaling (Fig. 19). FGF8 signaling from the paraxial mesoderm is required for neural crest cell induction in *Xenopus* and mediates its affects in part through *Pax3*. $Fgf8^{\Delta 2,3/\Delta 2,3}$ embryos do exhibit reduced *Pax3*, indicating that *Fgf8* does act upstream of *Pax3* in the mouse,

but that this signaling pathway is not conserved in crest cell induction. Although our *in vivo* analyses did not support a role for *Fgf8* in neural crest cell formation, our *in vitro* data using the FGF receptor antagonist, SU5402 (Fig. 16-18), did result in defects in crest cell production. *Sox10* was decreased in SU5402-treated cultures even with decreased concentration and exposure to SU5402, preventing us from precisely dissecting the specific role of FGF signaling in neural plate maintenance versus neural crest cell induction. Concomitant with the deceased *Sox10* expression was a decrease in *Sox2*, indicating that the neural plate maintenance was inhibited with the FGF signaling blockade. FGF signaling is necessary for the maintenance of *Sox2* (Takemoto et al. 2006; Stavridis et al. 2007; Rogers et al. 2008), indicating that SU5402 results in the failure of neural plate maintenance and the loss of the precursor population from which neural crest cells arise. Although there is considerable evidence supporting the role of FGF signaling in the maintenance and viability of the neural plate, we cannot rule any loss of *Sox2* due to cell death. Finally, our *in vivo* and/or *in vitro* analyses of BMP, FGF, NOTCH, PAX, and WNT signaling failed to indicate any of these genes as required for neural crest cell induction in the mouse, suggesting that the key regulator of this process involves one of the gene family members not examined or that the key regulator of this process is yet to be identified.

Germ cell nuclear factor is a Novel Regulator of Neural Crest Cell Formation

Germ cell nuclear factor (Gcnf) is an orphan nuclear receptor first identified in germ cells, where it has well characterized roles regulating gametogenesis (Chung

et al. 2001). Knockout analysis of *Gcnf* has revealed novel roles for this transcription factor in development; *Gcnf*$^{-/-}$ embryos are embryonic lethal due to chorioallantoic fusion defects. Additionally *Gcnf*$^{-/-}$ embryos fail to undergo axis rotation resulting in tailbud truncation defects (Chung et al. 2001) and halted somitogenesis (Chung et al. 2001). Anteriorly, *Gcnf* mutants exhibit neural tube closure and neural patterning defects (Chung et al. 2006), indicating the importance of this transcription factor during embryonic development. The defects observed in *Gcnf*$^{-/-}$ embryos are indicative of the dynamic expression of *Gcnf* during embryogenesis; *Gcnf* is present in the primitive streak at 7.5dpc. By 8.5dpc, *Gcnf* is upregulated in the neuroepithelium along the entire anterior-posterior axis, with heaviest expression along the dorsal neural folds (Fig. 21); at mid-gestation, *Gcnf* is subsequently downregulated until it is re-activated in adult germ cells (Chung et al. 2001).

We identified *Gcnf* from a microarray screen performed in the mouse model of Treacher Collins Syndrome (TCS) (Jones et al. 2008). TCS results from the haploinsufficiency of *TCOF1; mTcof1*$^{+/-}$ embryos decreased number of neural crest cells due to increased neuroepithelial apoptosis (Dixon et al. 2006). The downregulation of *Gcnf* in *Tcof1*$^{+/-}$ embryos indicates that *Gcnf* may be involved in the formation of neural crest cells (N. Jones and P. Trainor, unpublished data). Recently, *Gcnf* was identified in a microarray screen in avian embryos as a potential regulator of neural crest cell induction; *Gcnf* is expressed in migratory neural crest cells in the chick embryo, although functional analysis of *Gcnf* in neural crest cells was not addressed (Adams et al. 2008). Additionally, *Gcnf*$^{-/-}$ embryos have not been

examined for defects in neural crest cell formation. Collectively, the expression of *Gcnf* in the dorsal neural folds, the region from which neural crest cells arise, as well as the identification of *Gcnf* in microarray screens in neural crest cell populations, indicates this gene as a potential player in the induction of neural crest cells.

Analysis of neural crest cell formation in *Gcnf*$^{-/-}$ embryos revealed a lack of crest cell markers in general. In the majority of embryos analyzed, multiple neural crest cells markers were not expressed (Fig. 22), indicating that *Gcnf* is required for the generation of NCCs. Despite the absence of neural crest cell markers as a whole, an occasional *Gcnf*$^{-/-}$ embryo was processed that did exhibit minimal expression of neural crest cell markers; interestingly, the cells did not exhibit the normal expression pattern characterized for the respective gene in any of the embryos examined. For instance, *Sox9* was expressed in an occasional *Gcnf* mutant at the lateral edges of the neural folds but no migratory cells were present, indicating that if a neural crest cell was induced, they failed to migrate. This would be consistent with a role for *Gcnf* in the initiation of EMT and the onset of neural crest cell migration. Further, *Gcnf*$^{-/-}$ embryos may not activate the entire cascade of neural crest cell specific genes, indicating that if a *Sox9*$^{+}$ crest cell is induced, it may not express *Snail* and therefore would fail to migrate and remain in the neuroepithelium. In these circumstances, the definition of the neural crest cell come into question, is a cell a bona fide neural crest cell if it fails to migrate? Despite the occasional *Gcnf* mutant embryo with abnormal and diminished neural crest cell marker expression, as a whole, the majority of the

mutants analyzed failed to express any of the panel of crest cell specific genes, indicating that *Gcnf* is required for neural crest cell formation in the mouse.

Accompanying the defects in neural crest cell formation, *Gcnf*$^{-/-}$ embryos exhibit an enlarged neural plate, most likely the result of increased proliferation; indeed, the mitotic marker pH3 was dramatically increased in *Gcnf*$^{-/-}$ embryos (Fig. 24). *Gcnf* acts as a transcriptional repressor to downregulate the pluripotency genes *Oct4* (Fuhrmann et al. 2001; Gu et al. 2005) and *Nanog* (Gu et al. 2005) in the neuroepithelium; previous analysis of *Gcnf*$^{-/-}$ embryos revealed a dramatic upregulation of these genes (Fuhrmann et al. 2001; Gu et al. 2005), which in theory, would prevent the activation of differentiation paradigms within the neural plate and maintain the cells in a stem-cell like state. Indeed, overexpression of *Sox2* in the neural plate of avian embryos results in the downregulation of neural crest cell production as measured by inhibition of *Sox9* and *Sox10* (P. Trainor, unpublished). Analysis of SOX2 in *Gcnf*$^{-/-}$ embryos revealed an expansion in the domain of SOX2^{+} cells within the neural plate (Fig. 24) further supporting the hypothesis that *Gcnf* is required for downregulation of pluripotency within the neural plate, and that in its absence, the neural plate is maintained in a progenitor-like state. These data in conjunction with the increased numbers of mitotic cells indicate that the overproliferation of the neural plate due to maintenance of pluripotency gene expression prevents the activation of differentiation paradigms, such as the transition to a neural crest cell.

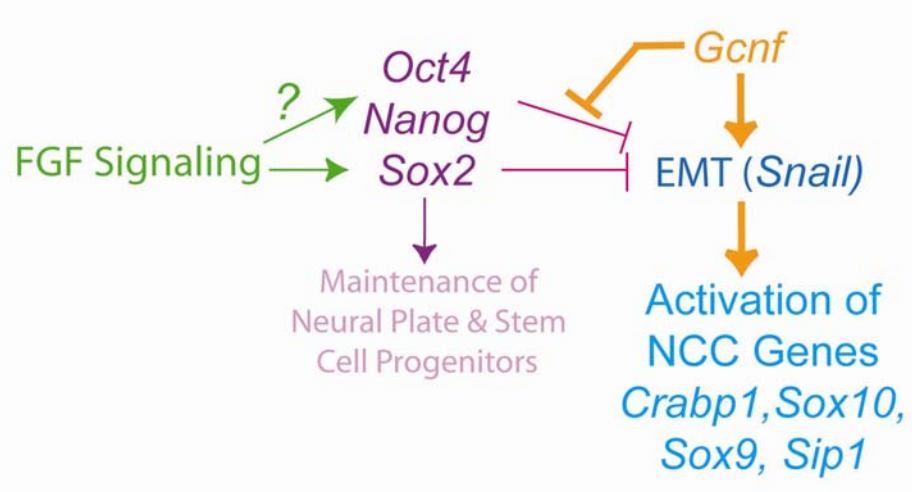

Figure Twenty-Six. Model for *Gcnf* in regulating Neural Crest Cell Formation and Differentiation. FGF signaling (green arrow) is required for the maintenance of *Sox2* (purple) but has not been directly shown as a regulator of *Oct4* and *Nanog*. *Sox2/Nanog/Oct4* (purple) within the neural plate is required for the maintenance of the neural plate and the stem cell progenitor pool. *Gcnf* (orange) in the neural plate is required to downregulate *Sox2/Nanog/Oct4,* allowing for the induction of cellular differentiation paradigms within the neuroepithelium. Binding of *Gcnf* to *Snail* (dark blue) activates the epithelial to mesenchymal transition (EMT) of neural crest cells, initiating their formation. Subsequent activation of neural crest cell specific genes (light blue), such as *Crabp1, Sip1, Sox10,* and *Sox9*, by *Gcnf* results in the onset of neural crest cell migration and differentiation paradigms.

Does Gcnf activate Neural Crest Cell Specific Genes?

Putative *Gcnf* binding sites were identified in *Snail1* and *Snail2, Sox9, Sox10, Sip1,* and *Crabp1* (Fig. 26). Currently, ChIP assays are being used to determine the binding of *Gcnf* to these genomic regions. Our analyses of *Gcnf*$^{-/-}$ embryos has indicated defects in neural crest cell formation and the transition of a neuroepithelial to neural crest cell; binding of *Gcnf* to the *Snail* promoters would demonstrate the requirement of *Gcnf* in the initiation of NCC formation through regulation of EMT. Further, binding of *Gcnf* to NCC specific genes, such as *Sox9, Sox10, Sip1,* and *Crabp1,* would result in the activation of neural crest cell specific gene paradigms (*Sox9, Sox10*) as well as the activation of genes required for proper crest cell migration (*Sip1* and *Crabp1*). Collectively, these data suggest that *Gcnf* may act as a bi-modal regulator of NCC formation (Fig. 26); first, *Gcnf* would regulate EMT through direct activation of *Snail1* and *Snail2*. Second, once EMT has commenced, *Gcnf* would subsequently activates NCC specific paradigms required for migration and differentiation.

E) Experimental Methods

Mouse lines and maintenance

CD1, Fgf8$^{+/\Delta 2,3}$*, Gcnf,* and *RBP-Jκ* mice were housed in the Laboratory Animal Services Facility at the Stowers Institute for Medical Research according to IACUC animal welfare guidelines. For embryo collection, dams were sacrificed by

cervical dislocation; day of plug was noted as 0 *days post coitum* (dpc). Embryos were removed from maternal tissue and fixed; yolk sacs collected for genotyping. Embryos were genotyped for the *Fgf8*$^{+/\Delta 2,3}$ (Meyers et al. 1998), *Gcnf* (Chung et al. 2001) and *RBP-Jκ* (de la Pompa et al. 1997) as previously reported. *Pax3;Pax7* embryos were kindly provided by S. Tajbakhsh (Pasteur Institute).

Cranial Explant Cultures

For 24-hour cranial explant cultures CD1 dams were sacrificed at 7.5dpc by cervical dislocation; embryos were removed from maternal tissue and dissected in Tyrode's solution (8.0g NaCl, 0.2g/L KCl, 0.2g $CaCl_2$, 0.21g/L $MgCl_2$, 0.057g NaH_2PO_4, 1.0g/L $NaHCO_3$, 1.0g/L Glucose in DEPC-H_2O). To harvest cranial explants, embryos were bisected into the cranial and posterior regions with insect pins, and the cranial regions collected; all three germ layers of the explants were kept intact. Cranial explants were attached to 0.4μM cell culture insert membranes (Millipore, Billerica, MA) in 3mL DMEM/F12-high glucose (control) (Invitrogen) or in DMEM/F12-high glucose with the antagonists DAPT (Sigma, St. Louis, MO), Frizzled-8/Fc (R & D Systems, Minneapolis, MN), Noggin/Fc (R & D Systems, Minneapolis, MN), or SU5402 (Calbiochem, San Diego, CA) in DMEM-F12 and cultured at 37°C with 5% CO_2; culture times are as indicated. Antagonist treatment was as follows: DAPT at 25, 50, 75, or 100μM and SU5402 at 12.5, 25, 37.5, and 50μM in DMSO; Frizzled-Fc and Noggin-Fc were used at 1, 5, 10, 20, 50, and 100μg/μL in sterile PBS. Explants were examined for viability as indicated by

beating heart tissue. After culturing, explants were fixed O/N in 4% PFA at 4°C; embryos were dehydrated in MeOH and processed for *in situ* hybridization.

For 8- and 12-hour SU5402 explant cultures, CD1 dams were sacrificed early on 8.0dpc by cervical dislocation; embryos were removed from maternal tissue and dissected in Tyrode's solution. For culture, two cuts were made in the yolk sac along the anterior-posterior axis, allowing for the planar attachment of the embryo to the cell culture insert membrane via the remaining extraembryonic membranes. Once attached with forceps, the developing amnion was removed from the neural plate region. Embryo explants were cultured in 37.5μM SU5402 for 8- or 12hrs; all cultures were viable as determined by the presence of beating heart tissue at the end of the culture period. Cultures were fixed in 4% PFA O/N at 4°C and processed for *in situ* hybridization.

In situ hybridization:

In situ hybridization was performed following the standard protocol described by Nagy et al. (2003). Briefly, embryos were fixed, dehydrated in methanol, and stored at -20°C until ready for use in the hybridization protocol. Anti-sense digoxigenin-labeled mRNA riboprobes were synthesized for *Crabp1* (S. Schneider-Maunoury), *Gcnf* (A. Cooney), *Pax3* (Takayoshi), *Snail* (A. Nieto), *Sox2* (P. Trainor), *Sox9* (R. Krumlauf), *Sox10* (M. Gassmann), and *Wnt1* (A. Gavalas).

Immunohistochemistry

For section immunohistochemistry, *Gcnf* litters were collected at 9.0dpc and fixed O/N in 1% PFA at 4°C. Embryos were processed through a sucrose gradient (15%, 30% in PBS), mounted in Tissue Tek O.C.T. (VWR, West Chester, PA) and sectioned at 10microns. Sections were rinsed 3X in PBT (PBS with 0.1% Triton X-100) for 5min and blocked in 10% normal goat serum (Invitrogen, Carlsbad, CA) in PBT for 1hr at RT. Slides were incubated in primary antibody diluted in 10% goat serum/PBT O/N at 4°C. The monoclonal antibodies to SOX2 (R & D Systems, Minneapolis, MN), anti-phospho Histone H3 (pH3; Upstate/Millipore, Billerica, MA), and anti-PAX3 were used at 1:500 (SOX2 and pH3) and 1:200 (PAX3) respectively. The antibody to PAX3 was obtained from the Developmental Studies Hybridoma Bank developed under the auspices of the NICHD and maintained by the University of Iowa, Department of Biological Sciences (Iowa City, IA 52242).

Slides were rinsed 3X 10min in PBT at RT on shaker and incubated in the appropriate Alexa 488 or 594 secondary antibody at 1:250 (Molecular probes/Invitrogen, Carlsbad, CA) for 2hrs at 4°C. Sections were counterstained with a 1/1000 dilution of 2mg/ml DAPI (Sigma, St. Louis, MO) in PBS for 5minutes, followed by rinses in PBS; slides were mounted with fluorescent mounting medium (DakoCytomation, Carpinteria, CA). All images were collected using a Ziess Axioplan microscope and processed using Photoshop CS2 (Adobe, San Jose, CA).

VII. Chapter Two: Conditional Inactivation of FGF8 Signaling in the Frontonasal Prominence using the *AP-2cre* Transgene does not result in Craniofacial Defects.

A) Abstract

The frontonasal prominence (FNP) develops as a midline tissue primordium populated by the cranial mesoderm and neural crest cells and forms mid-facial structures such as the forehead, nose, and the primary palate. Previous studies have indicated that the surface ectoderm overlying the FNP is required by cranial neural crest cells populating this region for patterning and outgrowth of the FNP (Hu et al. 2003; Marcucio et al. 2005), indicating that interactions between these two tissue layers are necessary for proper craniofacial development. *Fgf8*, expressed in the nasal ectoderm (Crossley and Martin 1995), has well characterized in regulating the outgrowth of the FNP (Hu et al. 2003). Hence, *Fgf8* is a good candidate for mediating interactions between the surface ectoderm and neural crest cells populating this region. To address the role of FGF8 signaling in the FNP of the mouse, we attempted to conditionally inactivate *Fgf8* in the surface ectoderm of the FNP using an *AP-2cre* driver. Analysis of *AP-2cre;Fgf8*$^{fx/fx}$ and *AP-2cre;Fgf8*$^{\Delta 2,3/fx}$ mutants revealed normal development of the cranial vault; cartilage and bone formation was identical between wildtype embryos and conditional mutants. *In situ* hybridization of conditional mutants at 10.5dpc revealed the maintenance of *Fgf8* in the nasal ectoderm of the FNP, indicating a lack of *Fgf8* excision by the *AP-2cre* driver in

mutant embryos. *AP-2cre* mice have been reported to express *AP-2cre* in the surface ectoderm of the FNP (Zhang and Williams 2003), but analyses of *AP-2cre;R26R*$^{+}$ embryos revealed *LacZ* expression in the mesenchyme but not the ectoderm of the FNP. Hence, the lack of overlap between *Fgf8* and *AP-2cre* in the FNP ectoderm results in the failure of *Fgf8* excision in conditional *AP-2cre;Fgf8*$^{fx/fx}$ and *AP-2cre;Fgf8*$^{\Delta 2,3/fx}$ mutants. Collectively, our analyses failed to address the specific role of *Fgf8* in the development of the FNP and indicate that use of the *AP-2cre* mice in FNP development is restricted to studies involving the FNP mesenchyme.

B) Introduction

Fgf8 and the Patterning of Craniofacial Tissues

Neural crest cells migrate into the developing facial region to form the craniofacial mesenchyme located between the surface ectoderm and the neuroepithelium. Interactions between neural crest cells and the surface ectoderm are essential in the patterning of the frontonasal prominence (FNP), the craniofacial primordium that gives rise to mid-facial structures. Indeed, the surface ectoderm of the FNP has been shown to be essential for the outgrowth, viability, and differentiation of cranial neural crest cells populating this region (Hu et al. 2003; Tapadia et al. 2005). Although many genes are known to be involved in the patterning of this region, *Fgf8* has been implicated in playing a critical role in influencing the growth and patterning of the face.

A specific region of the FNP, the frontonasal ectoderm zone (FEZ), is demarcated by a dorsal domain of *Fgf8* expression abutted to a ventral domain of *Sonic hedgehog* (*Shh*) expression (Hu et al. 2003). In chick embryos, this domain of *Fgf8/Shh* expression coincides directly with the tip of the upper beak; a derivative of the FNP (Hu et al. 2003). Experiments have demonstrated that the FEZ is responsible for establishing the dorsoventral axis of the upper beak; ectopic transplants of the FEZ to more dorsal regions of the FNP results in duplications of upper beak structures. In contrast, transplantation to more ventral regions resulted in duplication of lower beak structures (Hu et al. 2003). Collectively, these results indicate the FEZ as a critical regulator of outgrowth of the FNP and patterning of subsequent facial structures, and furthermore, it suggests that *Fgf8* may mediate this process.

A requirement for *Fgf8* in the patterning of the developing face is seen in experiments conditionally inactivating *Fgf8* in specific craniofacial tissues. Specific removal of FGF8 signaling in the olfactory epithelium and forebrain (Kawauchi et al. 2005) or the pharyngeal arch ectoderm (Trumpp et al. 1999; Macatee et al. 2003) results in severe craniofacial defects. Conditional excision of *Fgf8* from the *Foxg1-cre* domain of the forebrain results in a lack of the nasal cavity, forebrain, and eyelids; the snout is shortened and the lower jaw is reduced or absent (Kawauchi et al. 2005). When *Fgf8* is conditionally excised from the pharyngeal arch ectoderm, using *Nestin-cre* or *AP2-IREScre*, embryos lack first branchial arch derivatives, including the mandible and exhibit a reduced maxillary bone (Trumpp et al. 1999; Macatee et al. 2003). Although the conditional mutants do not exhibit defects in neural crest cell

formation, loss of FGF8 from the pharyngeal arch ectoderm results in increased neural crest cell death, indicating that FGF8 acts as a survival cue to cells populating the first branchial arch (Trumpp et al. 1999; Macatee et al. 2003).

Tcfap2a and the AP-2cre Transgene

AP-2 genes belong to a family of transcription factors critical for the development of both invertebrate and vertebrate species (Schorle et al. 1996; Zhang et al. 1996; Nottoli et al. 1998; Hilger-Eversheim et al. 2000; Donner and Williams 2006). To date, four members have been characterized in mouse and human, *AP-2α, AP-2β*, *AP-2γ,* and *AP-2ε* (Williams et al. 1988; Bosher et al. 1995; Moser et al. 1995; Oulad-Abdelghani et al. 1996; Zhao et al. 2001; Cheng et al. 2002), each sharing a conserved C-terminal basic-helix-span-helix DNA binding and dimerization domain (Williams and Tjian 1991b; Williams and Tjian 1991a; Garcia et al. 2000; Wankhade et al. 2000). The *AP-2* genes are expressed in somewhat overlapping domains of the extraembryonic tissues, central nervous system, neural crest, face, limb bud, kidney, eye, and skin (Hilger-Eversheim et al. 2000). Despite the similarities in their expression patterns, each individual *AP-2* gene is required for distinct aspects of embryonic development. *AP-2α* is important for formation and patterning of the eyes, heart, face, neural tube, limbs, and body wall (Schorle et al. 1996; Zhang et al. 1996; Nottoli et al. 1998; Brewer et al. 2002); *AP-2β* is crucial for kidney development (Moser et al. 1997). *AP-2γ* is required for development of the extraembryonic lineages that eventually give rise to the mature placenta, but it does

not appear to have a major role in development of the embryo proper (Auman et al. 2002). Finally, *AP-2ε* is required for establishing the neuronal network of the olfactory system (Feng and Williams 2003).

In the developing craniofacial region, *AP-2α* or *Tcfap2a* in mouse is expressed in the FNP, neural crest cells, branchial arches, and limbs (Mitchell et al. 1991). *Tcfap2a* is critically important for craniofacial development as *Tcfap2a*$^{-/-}$ embryos have severe craniofacial and body wall defects, including cranial clefting and outgrowth of the neural folds over the FNP, forcing midline structures to develop more laterally on the head (Schorle et al. 1996; Zhang et al. 1996). In addition, the maxilla and mandible fail to fuse medially and the embryos exhibit cranio-abdominoschisis, the failure of midline to close along the anterior-posterior body axis (Schorle et al. 1996; Zhang et al. 1996). Tissue-specific deletion of *AP-2α* in cranial neural crest cells using *Wnt1-cre* results in a range of craniofacial defects and perinatal lethality associated with neural tube closure defects and cleft secondary palate, delayed craniofacial growth, abnormal middle ear development, and defects in pigmentation (Brewer et al. 2004).

The *cis*-regulatory elements required for the tissue-specific domains of human *AP-2α* expression have been characterized (Zhang and Williams 2003). Major regulatory elements directing *AP-2α* expression to the developing facial prominences and limb buds were identified in the intronic sequence between exons 5 and 6 (Zhang and Williams 2003). Recently, transgenic *AP-2cre "Cre-face"* mice harboring this human FNP- and limb-specific enhancer element fused to Cre recombinase have been

characterized; *AP-2cre* mice are reported to have tissue specific expression of *Cre* in the developing ectoderm and mesenchyme of the FNP as well as in migratory neural crest cells and the distal limb bud (Nelson and Williams 2004). Tissue-specific deletion of *Tcfap2* in the *AP-2α* domain results in shortened snouts and hypertelorism (Nelson and Williams 2004). *AP-2cre* mice are particularly useful for tissue-specific gene inactivation as human *AP-2α* is expressed in both migratory neural crest cells as well as the ectoderm of the FNP (Nelson and Williams 2004), allowing for conditional studies of genes expressed in the FNP ectoderm. In contrast, while the mouse *Tcfap2* gene is expressed in migratory neural crest cells, it is not expressed in the ectoderm of the FNP (Mitchell et al. 1991). Overall, these studies highlight the important roles for *AP-2α* in craniofacial development and provide new avenues for addressing the roles of genes important during FNP development using the *AP-2cre* mice.

The Cre-loxP System

The *Cre-loxP* system is a method used for conditionally inactivating a gene of interest from a specific tissue or cell population (Nagy 2000; Kwan 2002); mating of two different strains of mice is required for the recombination event to take place. "*Floxed*" mice contain two Cre-recombinase recognition sites or "loxP" sites; loxP sites are composed of a 34 base pair consensus sequence consisting of two 13 base pair inverted repeats, flanking an eight base pair non-palindromic core that defines the orientation of the overall sequence of the recognition site (5'-

ATAACTTCGTATA-GCATACAT-TATACGAAGTTAT-3'). LoxP sites often flank one or more exons of the gene of interest and are called floxed alleles (flanked with loxP sites). Once the loxP sites are recognized by Cre recombinase the genomic sequence contained between the loxP sites is excised which can render the gene inactive (Nagy 2000; Kwan 2002). In addition, *floxed* mice may be intercrossed with a null allele of the gene of interest to obtain lines heterozygous for the floxed and null alleles. As only one *floxed* allele is present for the Cre-recombinase to recognize, the excision efficiency of the loxP sites is increased; the null allele remains resulting in no gene product being produced.

To produce conditional mutants, the "*Cre*" line, which contains *Cre-recombinase* fused to a tissue-specific promoter, is intercrossed with the *floxed* line. The "*Cre*" line directs *Cre* expression only to regions where the promoter is endogenously expressed. For example, using an enhancer of the human *AP-2α* transcription factor gene drives *Cre* expression specifically in the ectoderm and mesenchyme of the FNP (Nelson and Williams 2004). To obtain conditional mutants of the gene of interest, the *floxed* and *Cre* mouse strains are intercrossed to produce mice carrying both the *Cre* transgene and the *fx/fx* or *null/fx* alleles. In these embryos, the Cre-recominbase binds to the loxP sites, deleting any intervening sequence; excision can remove specific regulatory elements or exonic sequences, encoding for a tissue-specific null allele. Recombination is specific to the cells expressing the *Cre*-transgene; all remaining cells that do not express the promoter-*Cre* transgene do not undergo recombination and in theory, will show no defects.

Collectively, the *Cre-loxP* system allows for tissue-specific inactivation as the *Cre*-transgene is only located in a particular group of cells.

The *Cre-loxP* system is particularly useful for examining the roles of genes in a temporal manner (Nagy 2000), bypassing the limitations of complete knockouts of genes, such as when a gene of interest has multiple roles throughout development. This is particularly true for *Fgf8*, which in addition to its roles in craniofacial development, is also crucial in earlier developmental stages. *Fgf8* is expressed in the primitive streak and conventional knockouts of the gene result in embryonic lethality, as no mesoderm or endoderm develops (Sun et al. 1999). Conditional inactivation of the *Fgf8* gene, using the *Cre-loxP* system, is an advantageous approach for examining the specific role of *Fgf8* in craniofacial development without affecting other developmental roles of the gene (Meyers et al. 1998).

Fgf8, expressed in the facial ectoderm, and has been shown to play critical roles in the patterning of the developing face (Hu and Helms 1999; Tapadia et al. 2005). As cranial neural crest cells contribute to the majority of developing head and facial structures, a direct interaction between FGF8 signaling from the ectoderm and migrating neural crest cells during craniofacial development may have critical roles in the patterning of the face. In order to determine the role of FGF8 signaling from the surface ectoderm in the patterning of neural crest cells, the *Cre-loxP* system was used to conditionally inactivate *Fgf8*. The expression of a human *AP-2α* enhancer and *Fgf8* have similar domain of expression in the ectoderm of the FNP, hence removal of

the *Fgf8* domain from *AP-2α*-expressing cells in the ectoderm would be expected to result in craniofacial anomalies.

C) Results

Breeding of Fgf8 Conditional Mutants

To examine the craniofacial anomalies resulting from the removal of FGF8 signaling in the developing FNP, we employed the *Cre-loxP* system to create conditional mutants of FGF8 signaling using an *AP-2cre* driver; *AP-2cre* mice were intercrossed to generate conditional mutants using two mating schemes (Fig. 27). The first mating scheme intercrossed *AP-2cre* males with $Fgf8^{fx/fx}$ females to produce the *AP-2cre;*$Fgf8^{+/fx}$ heterozygous mice; *AP-2cre;*$Fgf8^{+/fx}$ females were backcrossed to $Fgf8^{fx/fx}$ males order to obtain *AP-2cre;*$Fgf8^{fx/fx}$ conditional mutants. The second mating scheme intercrossed the *AP-2cre* males with $Fgf8^{+/\Delta 2,3}$ females to obtain *AP-2cre;*$Fgf8^{+/\Delta 2,3}$ females, which were backcrossed to $Fgf8^{fx/fx}$ males to produce *AP-2cre;*$Fgf8^{\Delta 2,3/fx}$ conditional mutants. Using the mating schemes described above addressed any potential problems of the Cre recombinase excising the homozygous $Fgf8^{fx/fx}$ allele; when using the Cre-loxP system to generate conditional knockouts of a specific gene, it is common practice to examine the gene of interest using a $Fgf8^{fx/fx}$ and $Fgf8^{null/fx}$ approach as it results in a more efficient excision of the gene by the Cre recombinase as the enzyme is only required to excise one copy of the gene.

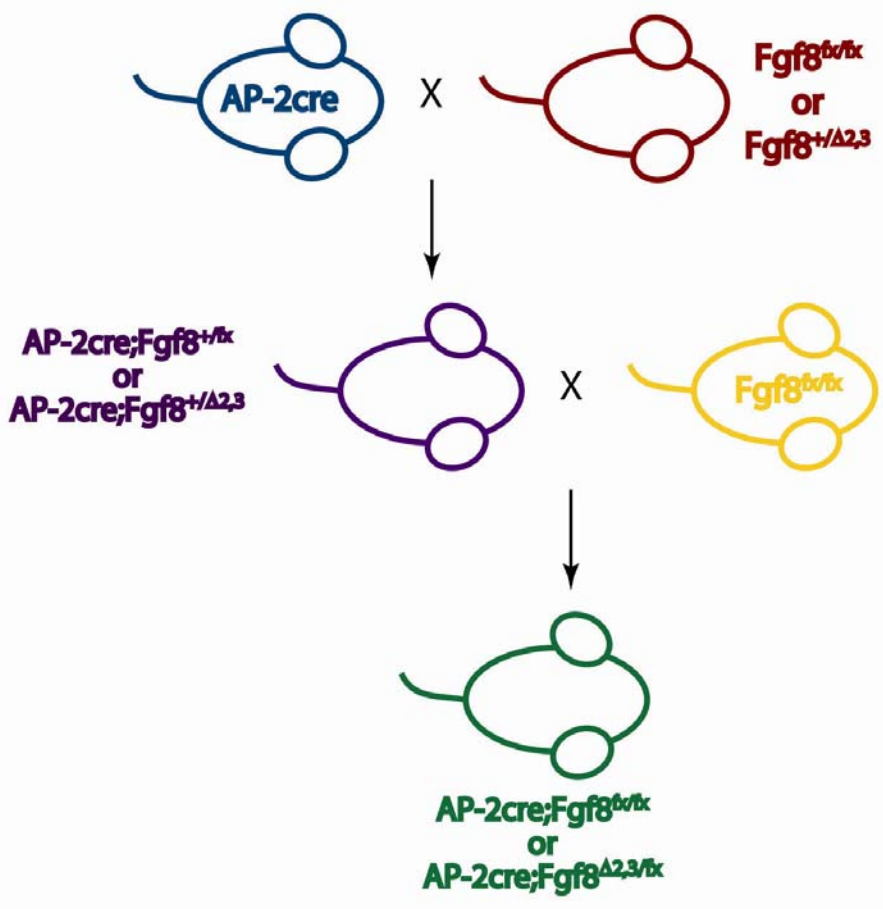

Figure Twenty-Seven. Breeding Scheme of *Fgf8* Conditional Mutants. *AP-2cre* males (blue) were outcrossed to homozygous $Fgf8^{fx/fx}$ females (red) to obtain *AP-2cre;*$Fgf8^{+/fx}$ (purple) females. *AP-2cre;*$Fgf8^{+/fx}$ females were then backcrossed to $Fgf8^{fx/fx}$ (yellow) males to obtain conditional *AP-2cre;* $Fgf8^{fx/fx}$ embryos (green). For *AP-2cre;* $Fgf8^{\Delta 2,3/fx}$ mutants, *AP-2cre* males (blue) were outcrossed to heterozygous $Fgf8^{+/delta2,3}$ females (red) to obtain *AP-2cre;*$Fgf8^{+/\Delta 2,3}$ (purple) females, which were backcrossed to $Fgf8^{fx/fx}$ (yellow) males to obtain conditional *AP-2cre;*$Fgf8^{\Delta/fx}$ embryos (green).

Examination of AP-2cre; Fgf8$^{fx/fx}$ Conditional Mutants

Fgf8 is expressed in the ectoderm of the nasal prominences at 10.5dpc and is subsequently downregulated by 11.5dpc (Crossley and Martin 1995). Therefore, we hypothesized that excision of *Fgf8* from the nasal ectoderm using the *AP-2cre* driver would result in late-staged bone and cartilage defects as indicated by previous reports of conditional *Fgf8* excision (Trumpp et al. 1999). To examine the craniofacial phenotypes resulting from *Fgf8* excision in the *AP-2cre* domain, we harvested *AP-2cre;Fgf8$^{fx/fx}$* litters at 17.5 and 14.5dpc and stained the embryos with Alcian Blue and Alizarin Red to stain cartilage and bone, respectively.

At 17.5dpc, *AP-2cre;Fgf8$^{fx/fx}$* conditional mutants exhibited normal cranial vault and vertebral column development in comparison to wild-type littermates (Fig. 28G, H). In all mutants examined, the exoccipital (EO), frontal (F), interparietal (IP), mandibular (Mn), maxillary (asterisks), premaxillary (Pmx), parietal (P), and supraoccipital (SO) bones were present, identical to the bones identified in wild-type littermates. Additionally, the bones of the limbs and vertebral column are unaffected in *AP-2cre;Fgf8$^{fx/fx}$* conditional mutants. Similar to conditional mutants harvested at 17.5pdc, *AP-2cre;Fgf8$^{fx/fx}$* mutants harvested at 14.5dpc were indistinguishable from their wild-type littermates (Fig. 29G, H). Analysis of mutant embryos revealed cartilage in the cranial vault, nasal region, limbs, and vertebral column; additionally, early ossification of the frontal (F), mandibular (Mn), maxillary (Mx), and premaxillary (PMx) bones was present. In posterior regions, *AP- 2cre;Fgf8$^{fx/fx}$*

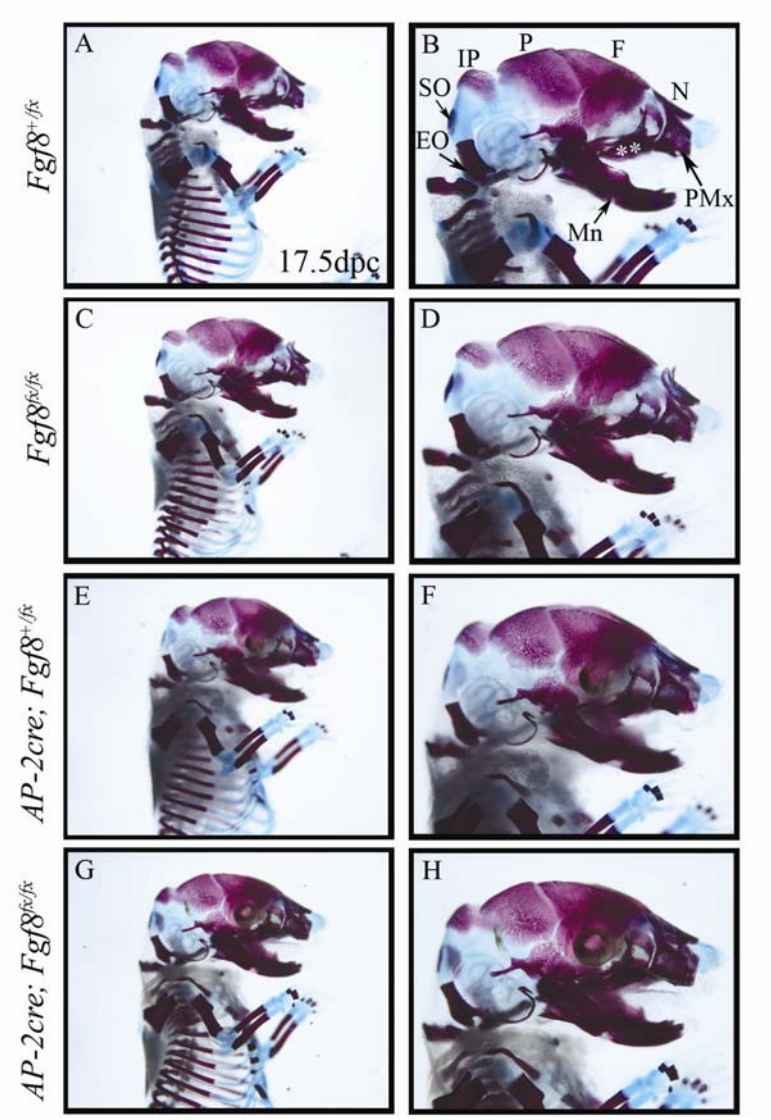

Figure Twenty-Eight. Skeletogenesis is unaffected in *AP-2cre; Fgf8$^{fx/fx}$* Mutants. Conditional *AP-2cre; Fgf8$^{fx/fx}$* mutants at 17.5dpc do not have defects in cranial vault bones due to a lack of *Fgf8* excision during early embryonic development. *AP-2cre; Fgf8$^{fx/fx}$* (G, H) are identical to wild-type (A-F) littermates. Frontal bone (F); exocipital bone (EO); interparietal bone (IP); mandible (Mn); maxilla (**); parietal bone (P); premaxillary bone (PMx); supraoccipital bone (SO).

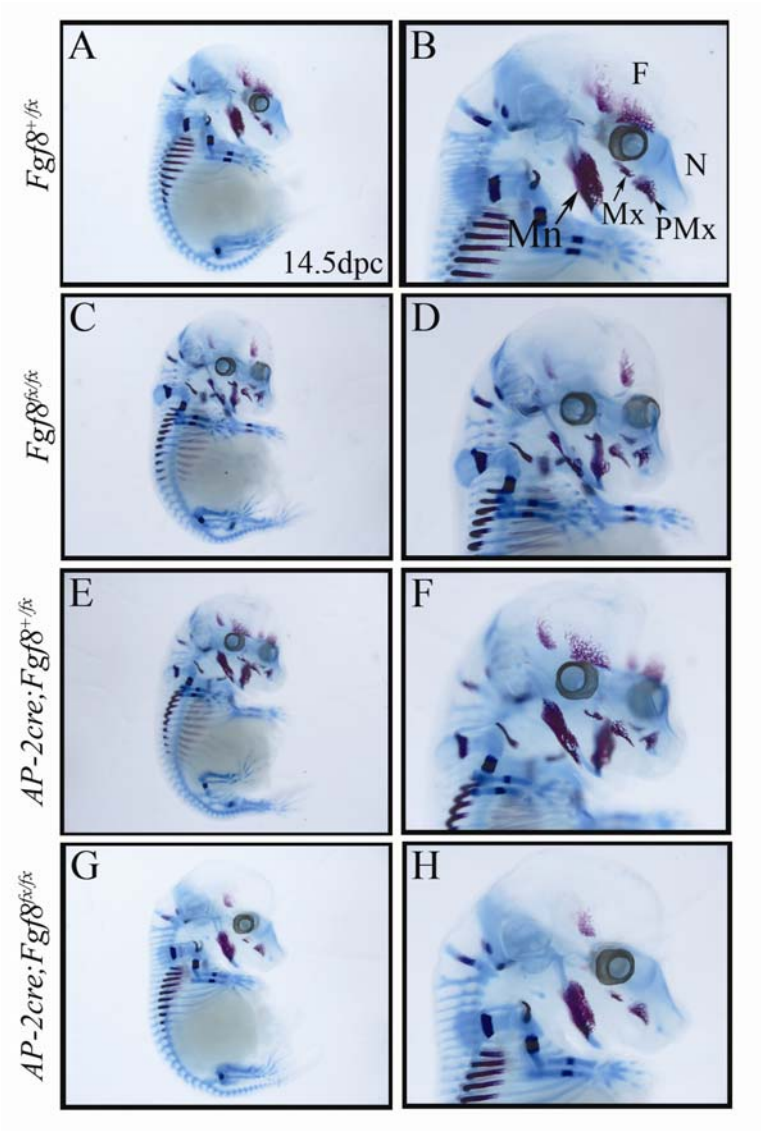

Figure Twenty-Nine. *AP-2cre; Fgf8$^{fx/fx}$* Mutants do not exhibit Defects in Chondrogenesis. Embryos were stained at 14.5dpc with Alcian blue and Alizarin red to stain cartilage and bone, respectively. G, H) Conditional *AP-2cre; Fgf8$^{fx/fx}$* mutants do not have obvious defects in cartilage or early bone formation in comparison to wild-type (A-F) littermates. The nasal cartilage (N) appears normal in conditional mutants, as do the early condensations of the frontal (F), maxilla (Mx), mandible (Mn) and premaxillary (PMx) bones.

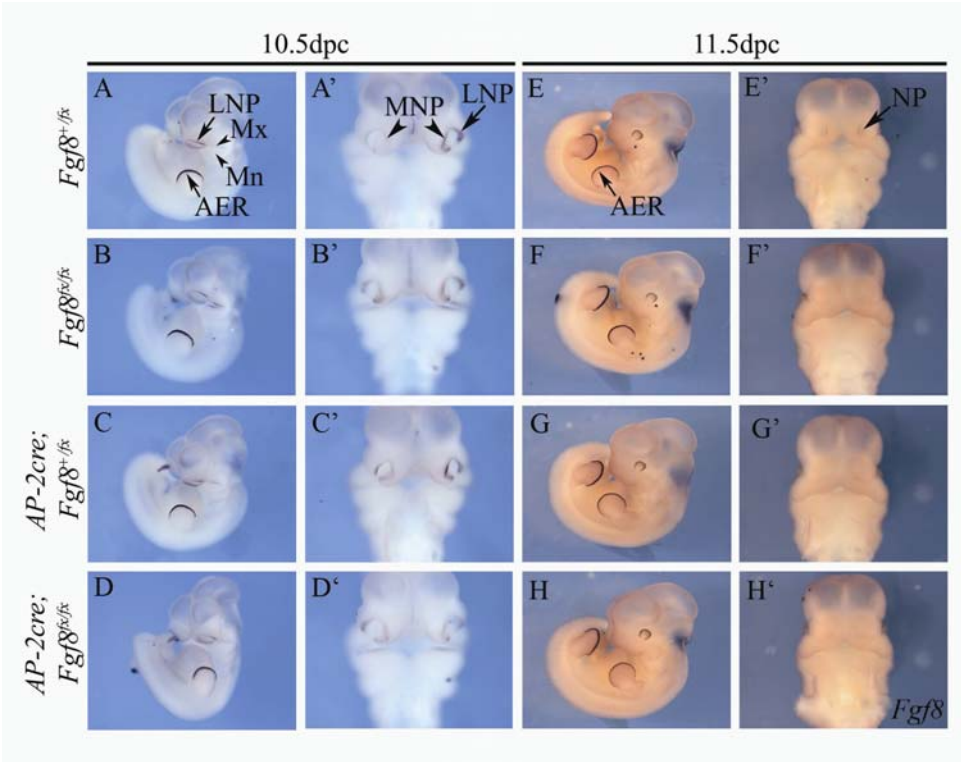

Figure Thirty. *Fgf8* Expression in *AP-2cre; Fgf8$^{fx/fx}$* Embryos. Embryos were harvested at 10.5 and 11.5dpc and processed for *Fgf8 in situ* hybridization. A-C) Wildtype embryos at 10.5dpc have *Fgf8* expression in the lateral nasal prominence (LNP, arrow), the proximal ectoderm of the maxillary (Mx) and mandibular (Mn) prominences (A, arrowheads), and in the limb in the apical ectodermal ridge (AER) (A, arrow). A') *Fgf8* is present in the medial (MNP, arrowhead) and lateral (LNP, arrow) nasal prominences. D, D') *Fgf8* expression in the conditional *AP-2cre; Fgf8$^{fx/fx}$* mutants at 10.5dpc is normal in comparison to wild-type (A-C) littermates. By 11.5dpc, *Fgf8* is downregulated in the ectoderm of the nasal pits (NP, arrow) in wildtype (E-G) and conditional *Fgf8* mutants (H). *Fgf8* remains in the AER (A, arrow) in all embryos examined (E-H).

mutants exhibited ossification sites in the developing limbs, shoulder girdle, and vertebral column. Collectively at both stages examined the conditional *AP-2cre;Fgf8*$^{fx/fx}$ mutants did not exhibit any developmental abnormalities.

The lack of skeletal phenotype in *AP-2cre;Fgf8*$^{fx/fx}$ mutants suggested a lack of function for FGF8 in the ectoderm of the FNP. However, as a control for proper excision of *Fgf8* from the nasal ectoderm (as this was an unexpected result) conditional mutants were harvested at 10.5 and 11.5dpc and processed for *Fgf8 in situ* hybridization. Conditional mutants at 10.5dpc exhibited a normal pattern of *Fgf8* expression in the ectoderm lining the nasal pits of the medial and lateral nasal prominences (Fig. 30D, D') as well as the apical ectodermal ridge (AER) of the developing limb. By 11.5dpc, *Fgf8* was downregulated in the nasal pits in all embryos examined, but remained in the AER (Fig. 30H, H'). Rather than an absence of a role for FGF8 these data indicate a failure of the *AP-2cre* driver to excise *Fgf8* from the ectoderm of the nasal prominences at early stages of development; collectively, the lack of *Fgf8* excision accounts for the presence of normal bone and cartilage development.

Examination of AP-2cre;Fgf8$^{\Delta 2,3/fx}$ *Conditional Mutants*

The lack of *Fgf8* excision in *AP-2cre;Fgf8*$^{fx/fx}$ conditional mutants had no impact on craniofacial development. One potential explanation for the lack of *Fgf8* excision is inefficient excision of the *Fgf8*$^{flox/flox}$ allele by the Cre recombinase. Therefore, we examined *AP-2cre;Fgf8*$^{\Delta 2,3/fx}$ conditional mutants for defects in craniofacial

development. *Fgf8*$^{\Delta 2,3}$, the null allele of *Fgf8*, was used to create conditional mutants resulting in more efficient excision of *Fgf8* due to the presence of only one floxed allele. *AP-2cre;Fgf8*$^{\Delta 2,3/fx}$ conditional mutants were harvested at 17.5 and 14.5dpc and processed for cartilage and bone staining. *AP-2cre;Fgf8*$^{\Delta 2,3/fx}$ conditional mutants at 17.5 (Fig. 31) and 14.5dpc (Fig. 32) were indistinguishable in comparison to their wild-type littermates. At 17.5dpc, *AP-2cre;Fgf8*$^{\Delta 2,3/fx}$ mutants exhibited normal development of cranial vault bones (Fig. 31G, H), including the exoccipital (EO), frontal (F), interparietal (IP), mandibular (Mn), maxillary (asterisks), premaxillary (Pmx), parietal (P), and supraocciptal (SO) bones. Analysis of 14.5dpc embryos revealed normal development of the nasal cartilage (N) and Meckel's (Mk) cartilage (Fig. 32G, H). Cartilage staining in the limbs and vertebral column of *AP-2cre;Fgf8*$^{\Delta 2,3/fx}$ mutants was identical to that in wild-type embryos.

To determine if *Fgf8* was excised in *AP-2cre;Fgf8*$^{\Delta 2,3/fx}$ mutants, embryos were harvested at 10.5 and 11.5dpc and processed for *Fgf8 in situ* hybridization; at 10.5dpc, *Fgf8* was located in the ectoderm lining the nasal pits (Fig. 33D, D') and the expression pattern was identical to that in wild-type littermates, indicating a lack of *Fgf8* excision using the *AP-2cre* driver. *Fgf8* expression at 11.5dpc was downregulated in the facial ectoderm in all embryos examined but was present in the AER of the limb bud (Fig. 33H, H').

In addition to examining *AP-2cre;Fgf8*$^{\Delta 2,3/fx}$ mutants to address the excision efficiency of the Cre recombinase, conditional *Fgf8* mutants harboring two copies of

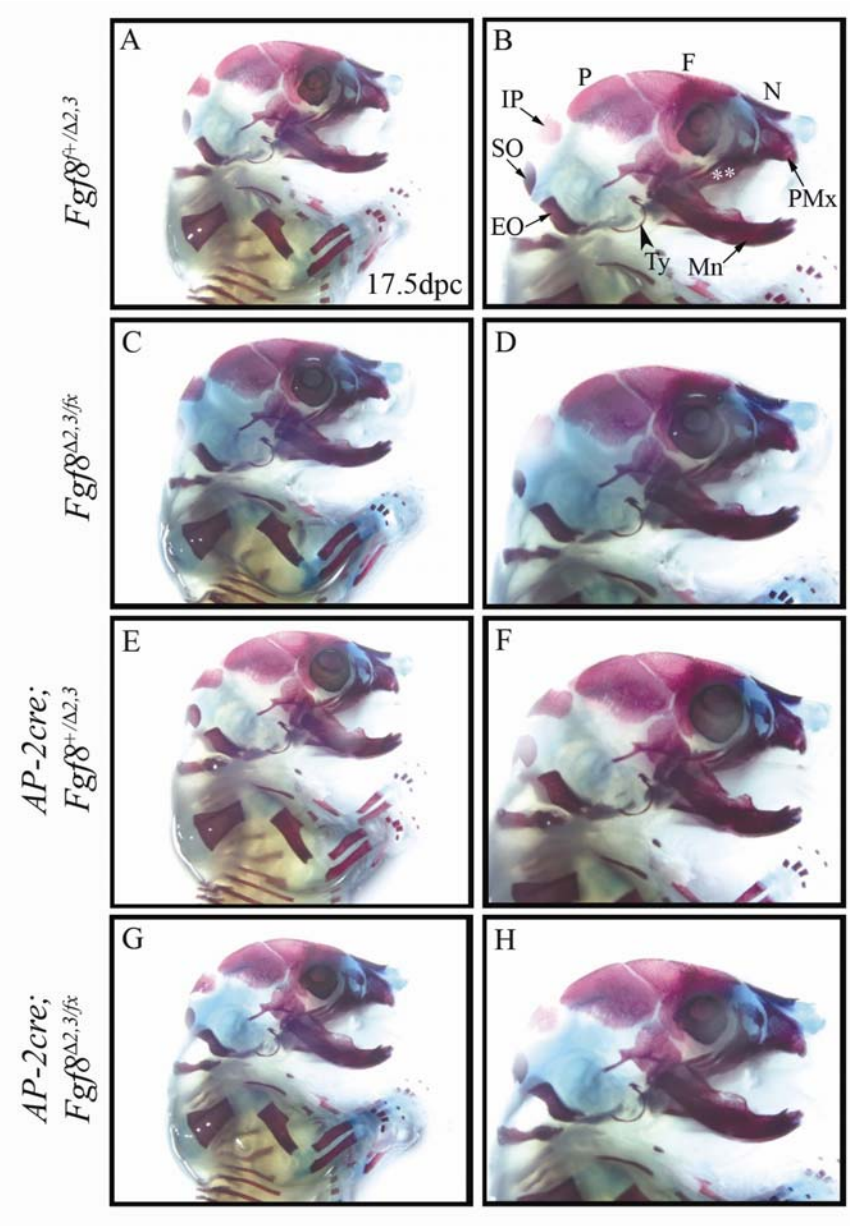

Figure Thirty-One. Conditional *AP-2cre;Fgf8$^{\Delta 2,3/fx}$* Mutants do not have Cranial Bone Defects. Embryos were collected and stained at 17.5dpc to examine cartilage and bone. Conditional *AP-2cre;Fgf8$^{\Delta 2,3/fx}$* mutants (G, H) have normal cranial bone formation in comparison to wild-type littermates (A-F). Exoccipital bone (EO); frontal bone (F); interparietal bone (IP); mandible (Mn); maxilla (asterisks); premaxillary bone (PMx); parietal bone (P); supraoccipital bone (SO); tympanic bone (Ty).

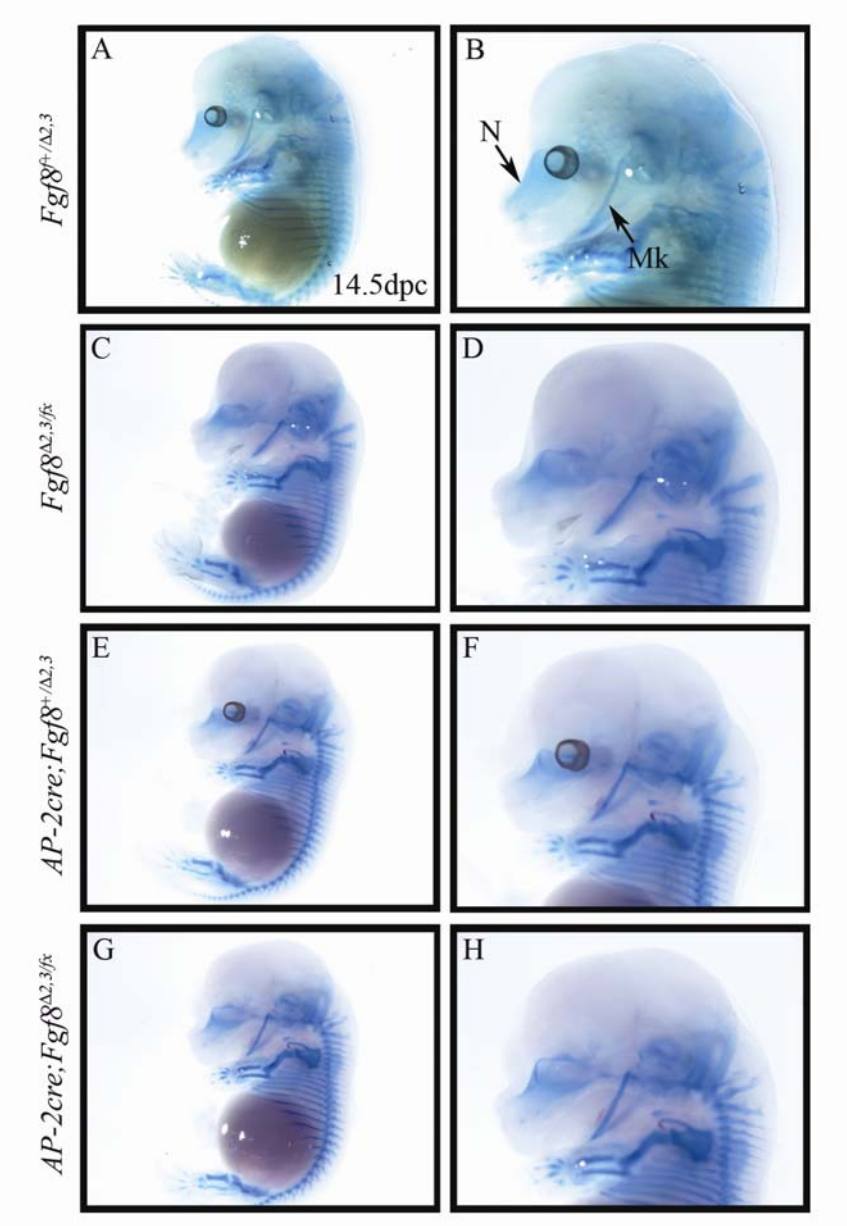

Figure Thirty-Two. Cartilage and Bone Staining of *AP-2cre;Fgf8$^{\Delta 2,3/fx}$* Embryos. Embryos were processed at 14.5dpc in Alcian blue and Alizarin red to stain carilage and bone, respectively. Conditional *AP-2cre;Fgf8$^{\Delta 2,3/fx}$* mutants (G, H) do not have obvious defects in cartilage and early bone formation in comparison to wild-type (A-F) littermates. The nasal cartilage (N) appears normal in conditional mutants, as does Meckel's cartilage (Mk).

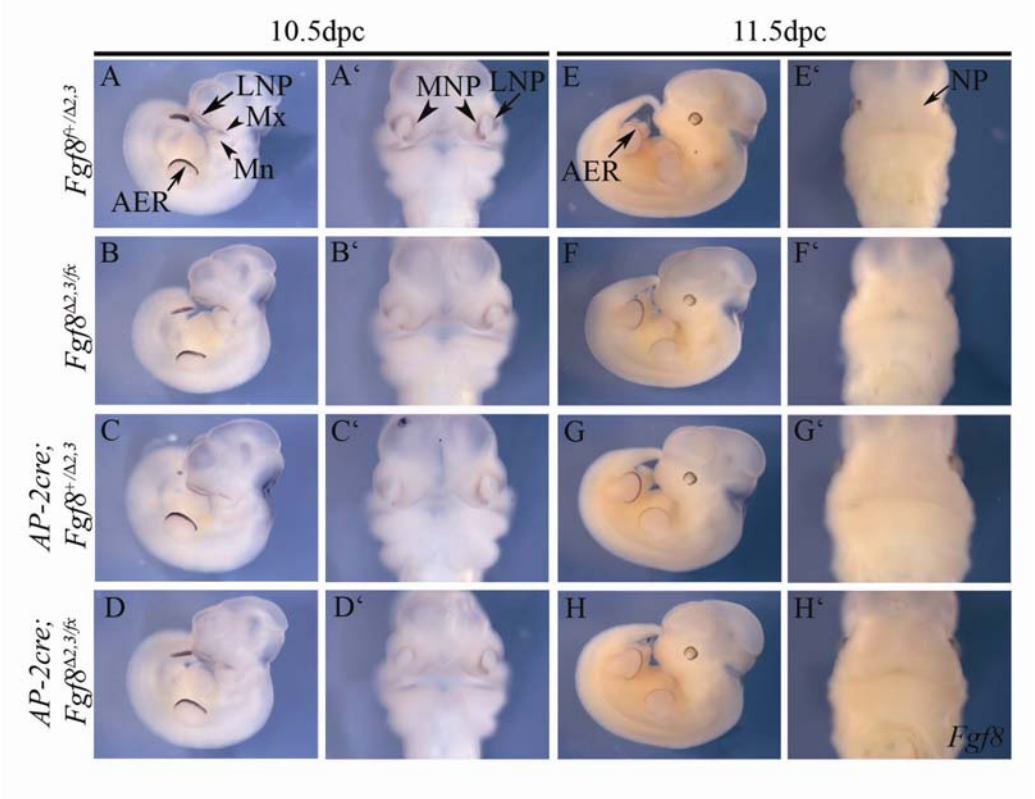

Figure Thirty-Three. *Fgf8* is Expressed in *AP-2cre;Fgf8$^{\Delta 2,3/fx}$* Embryos. Embryos were harvested at 10.5 and 11.5dpc and processed for *Fgf8 in situ* hybridization. D) *Fgf8* expression in the conditional *AP-2cre;Fgf8$^{\Delta 2,3/fx}$* mutants (D, D') is normal in comparison to wild-type littermates (A-C) and is present in the surface ectoderm of the maxillary (Mx) and mandibular (Mn) prominences (arrowheads) and the apical ectodermal ridge (AER, arrow) of the limb bud. D') *Fgf8* is present in the nasal ectoderm of the medial (MNP, arrowheads) and lateral (LNP, arrow) nasal prominences in a pattern identical to wildtype littermates at this stage (A-C). E-H) At 11.5dpc, *Fgf8* is downregulated in wildtype and mutant embryos in the nasal ectoderm (NP, arrowheads) but remains in the AER (A, arrow).

the *AP-2cre* transgene were examined. In theory, if the Cre recombinase is not sufficiently produced in the FNP, excision of *Fgf8* may be inefficient in the conditional mutants. Therefore, *AP-2cre*$^{T/T}$;*Fgf8*$^{\Delta 2,3/fx}$ mutants were created by mating *AP-2cre;Fgf8*$^{+/fx}$ mutants to *AP-2cre;Fgf8*$^{+/\Delta 2,3}$ mice to enhance the amount of Cre recombinase present in mutant embryos due to two copies of the *Cre-face* transgene; embryos were harvested at 14.5dpc to determine if any mutants embryos with craniofacial defects were present. Indeed, *AP-2cre*$^{T/T}$;*Fgf8*$^{\Delta 2,3/fx}$ mutants at 14.5dpc exhibited holoprosencephaly, a single nasal proboscis, reduced mandible, and often lacked external eyes (Fig. 34A, B); mutant embryos also had severe limb defects, vascular abnormalities, and edema.

To ensure that the phenotype identified in *AP-2cre*$^{T/T}$;*Fgf8*$^{\Delta 2,3/fx}$ mutants was due to conditional excision of *Fgf8*, control embryos from matings of *AP-2cre* mice were harvested at 14.5dpc. Surprisingly, *AP-2cre*$^{T/T}$ embryos at 14.5dpc were identical to *AP-2cre*$^{T/T}$;*Fgf8*$^{\Delta 2,3/fx}$ mutants at this stage (Fig. 34C, D), indicating that the defects identified in *AP-2cre*$^{T/T}$;*Fgf8*$^{\Delta 2,3/fx}$ mutants were not due to inactivation of FGF8 signaling, but rather homozygosity of the *Cre-face* transgene (characterization of the *Cre-face* mutants is described in Chapter Three). Collectively, these data demonstrate that the *AP-2cre* driver is not effective in excising *Fgf8* from the facial ectoderm in either *AP-2cre;Fgf8*$^{fx/fx}$ or *AP-2cre;Fgf8*$^{\Delta 2,3/fx}$ conditional mutants.

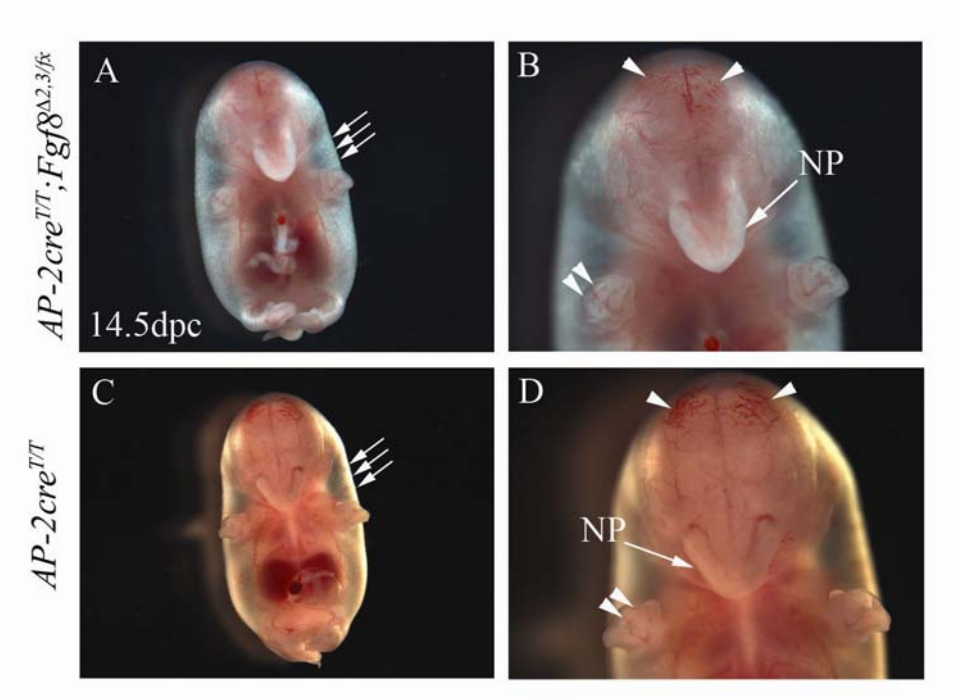

Figure Thirty-Four. Comparison of *AP-2cre$^{T/T}$;Fgf8$^{\Delta 2,3/fx}$* and *AP-2cre$^{T/T}$* Mutant Embryos at 14.5dpc. A-D) *AP-2cre$^{T/T}$;Fgf8$^{\Delta 2,3/fx}$* mutant embryos (A, B) harvested at 14.5dpc are identical to *AP-2cre$^{T/T}$* (C, D) embryos harvested from intercrossing *AP-2cre* mice, indicating that the craniofacial defects identified in *AP-2cre$^{T/T}$;Fgf8$^{\Delta 2,3/fx}$* embryos are not due to conditional excision of *Fgf8* but rather homozygosity of the *Cre-face* transgene. A, C) low magnification of mutant embryos reveals severe edema (arrows). B, D) At higher magnification, mutant embryos exhibit vascular defects (arrowheads), a single nasal proboscis (NP, arrow), and limb defects (double arrowheads).

Expression Pattern of the Cre-face Transgene

Characterization of *AP-2cre;Fgf8*$^{fx/fx}$ and *AP-2cre;Fgf8*$^{\Delta 2,3/fx}$ mutant embryos resulting from conditional inactivation of FGF8 signaling using a human *AP-2*α promoter revealed a lack of phenotype in the frontonasal prominence and head region. Previous studies have reported the expression pattern of the *AP-2cre "Cre-face"* transgene to be located in the surface ectoderm of the developing nasal prominences at 10.5dpc (Nelson and Williams 2004). One possible explanation for the failure of *Fgf8* excision in conditional *Fgf8* mutants could be a lack of overlapping expression between the *AP-2cre* transgene and *Fgf8* in the ectoderm of the nasal prominences. To address this as a possible cause for the failure of *Fgf8* excision in *AP-2cre;Fgf8*$^{fx/fx}$ and *AP-2cre;Fgf8*$^{\Delta 2,3/fx}$ mutant embryos, we determined the expression domain of the "*Cre-face*" transgene by mating *AP-2cre* mice to the *Rosa 26 reporter (R26R)* mice. *R26R* mice have a neo cassette and triple polyadenylation stop signal flanked between two loxP sites with the *lacZ* gene located 3' to the second loxP sequence (Soriano 1999). Once mated to the *AP-2cre* expressing line, a portion of the mice will not receive the *Cre* transgene and therefore will not undergo a recombination event, preventing the transcriptional read through of the *LacZ* gene. In contrast, embryos that are positive for the *Cre-face* transgene will undergo a recombination event and the neo cassette/stop signal is removed, resulting in the expression of the *LacZ* gene in the cells which express *Cre* (Soriano 1999) under the control of the *AP-2*α promoter (Zhang and Williams 2003).

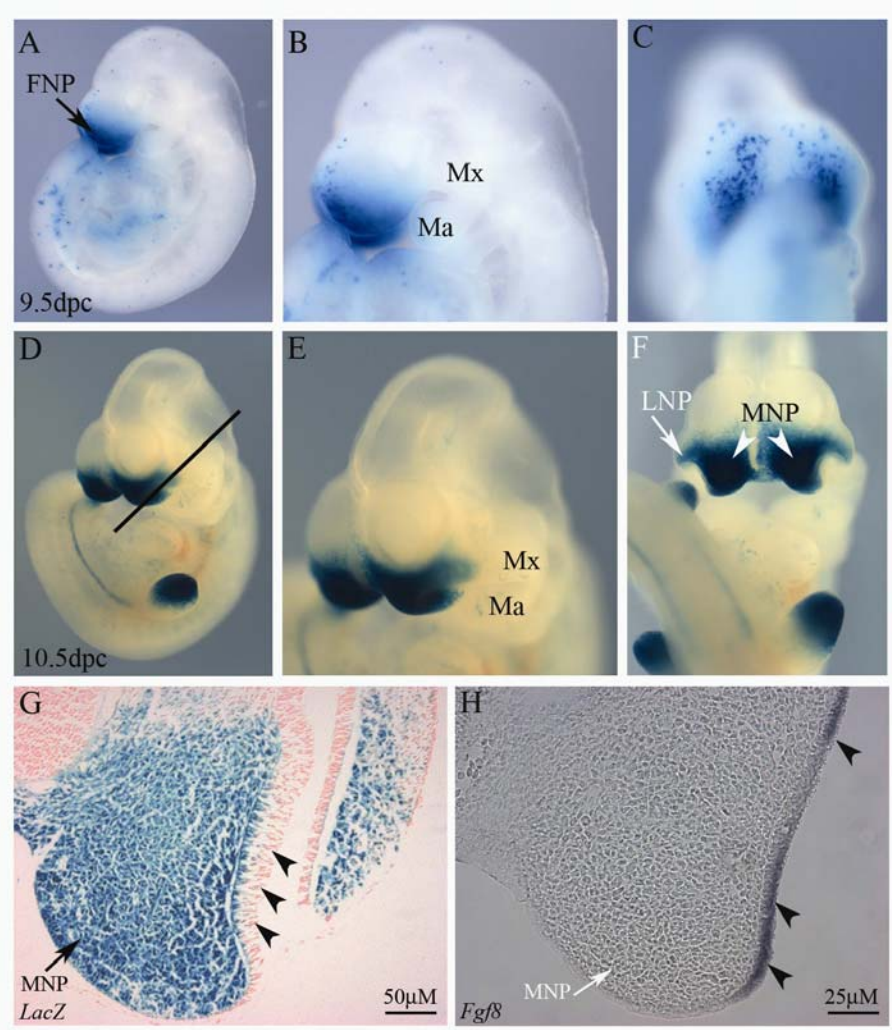

Figure Thirty-Five. Expression Pattern of the *AP-2cre* Transgene using the *Rosa 26 Reporter* Mice. Embryos were harvested at 9.5dpc (A-C) and 10.5dpc (D-F) and processed for β-galactosidase staining (blue). A-C) *AP-2cre* expression is seen in the mesenchyme of the FNP (arrow) but not in the maxillary (Mx) and mandibular (Mn) prominences of the first branchial arch. E, F) At 10.5dpc, *LacZ* expression is present in both the medial (MNP, arrowheads) and lateral (LNP, arrow) nasal prominences and in the developing limb bud. G) Sections of the embryo in panel D; level of section is indicated by the black line. β-gal staining is present in the mesenchyme of the right nasal prominence (arrow) but is absent from the nasal ectoderm (arrowheads). H) Sections of a 10.5dpc embryo processed for *Fgf8 in situ* hybridization; *Fgf8* is expressed in the nasal ectoderm of the right nasal prominence but not in the nasal mesenchyme.

Embryos were harvested at 9.5 and 10.5dpc and stained for β-galactosidase to confirm the expression pattern of the *Cre-face* transgene (Fig. 35). At 9.5dpc, *LacZ* expression was present in a patchy pattern in the FNP (Fig. 35A-C) and analysis of the nasal prominences at 10.5dpc revealed mesenchymal-specific expression of the *Cre-face* transgene (Fig. 35D-F); the ectoderm lining the nasal pit was devoid of any β-gal staining (Fig. 35G, arrowheads). In contrast, *Fgf8* expression is specific to the surface ectoderm of the nasal pits (Fig. 35H, arrowheads) (Crossley and Martin 1995). Expression of the *AP-2cre* transgene does not overlap with the known expression pattern of *Fgf8*, which prevents Fgf8 excision during embryogenesis. Therefore, this strain *AP-2cre* is not sufficient to examine the role of FGF8 signaling in the development of the FNP.

D) Discussion

Fgf8 is a key regulator of numerous developmental processes and has well characterized role in the patterning of the neuroepithelium (Delaune et al. 2004; Fletcher et al. 2006), limb bud (Lewandowski et al. 2000), and cardiovascular tissue (Abu-Issa et al. 2002). Additionally, *Fgf8* has been shown to be important for the patterning of the craniofacial region, including the frontonasal prominence (Hu and Helms 1999; Hu et al. 2003), mandible (Trumpp et al. 1999; Macatee et al. 2003), and neural crest cells (Trumpp et al. 1999; Hu et al. 2003; Macatee et al. 2003). The specific role of FGF8 signaling from the FEZ has well characterized roles in avian

embryos in the outgrowth of the upper beak and is required for the survival of neural crest cells populating this region (Hu et al. 2003; Marcucio et al. 2005).

The specific role of FGF8 signaling during mouse development has been more difficult to address due to the embryonic lethality of $Fgf8^{\Delta 2,3/\Delta 2,3}$ mutants. Indeed, $Fgf8^{\Delta 2,3/\Delta 2,3}$ embryos do not survive past 9.5dpc due to gastrulation defects (Meyers et al. 1998). Studies examining the role of FGF8 signaling in the craniofacial region have employed the Cre-loxP system to bypass the embryonic lethality at early developmental stages. Specific inactivation of *Fgf8* in the branchial arch ectoderm (Trumpp et al. 1999; Macatee et al. 2003) or the forebrain (Kawauchi et al. 2005) results in severe craniofacial defects, including a reduced mandible, increased cell death, and bone defects. We set out to address the role of FGF8 signaling from the ectoderm of the FNP in the patterning of neural crest cells that populate this developing primordium. Using the Cre-loxP system, we attempted to conditionally inactivate *Fgf8* using an *AP-2 cre* driver, which is expressed in the ectoderm and mesenchyme of the FNP.

Initial characterization of conditional *AP-2cre;*$Fgf8^{fx/fx}$ mutants revealed the lack of an obvious craniofacial phenotype, which is due to the lack of *Fgf8* excision at mid-gestational stages (Fig. 28-30). To determine if the failure of *Fgf8* excision was a result of reduced excision efficiency in the conditional mutants harboring two *Fgf8* floxed alleles by the *AP-2cre* driver, *AP-2cre;*$Fgf8^{\Delta 2,3/fx}$ were subsequently analyzed. *AP-2cre;*$Fgf8^{\Delta 2,3/fx}$ embryos harbor one floxed allele and a null allele, thereby potentially enhancing the excision efficiency of the Cre recombinase; interestingly,

conditional mutants harvested at 17.5 (Fig. 31) and 14.5dpc (Fig. 32) failed to exhibit craniofacial defects in comparison to wildtype littermates. Additionally, analysis of *Fgf8* expression at 10.5 and 11.5dpc revealed a lack of *Fgf8* excision (Fig. 33), indicating that the *AP-2cre* driver was not a useful tool for conditional excision of *Fgf8*.

Additional characterization of the *AP-2cre* transgene expression pattern revealed a lack of expression in the ectoderm of the FNP (Fig. 35). Using intercrosses of *AP-2cre* and *R26R* mice, embryos were processed for β-gal staining. At 10.5dpc, β-gal staining was present throughout the mesenchyme but not the surface ectoderm of the medial and lateral nasal prominences (Fig. 35G). In contrast, *Fgf8* is expressed in the ectoderm of the nasal prominence is a very thin layer of cells lining the nasal pits (Fig. 35H), revealing adjacent but non-overlapping expression domains of *AP-2cre* and *Fgf8*. Collectively, the lack of overlap between the *AP-2cre* transgene and *Fgf8* underlies the lack of craniofacial phenotype in conditional *AP-2cre;Fgf8*$^{fx/fx}$ and *AP-2cre;Fgf8*$^{\Delta 2,3/fx}$ embryos.

Interestingly, the pattern of expression characterized in *AP-2cre* mice differs from the previous characterization of these mice, where *Cre* is expressed in the nasal mesenchyme as well as the surface ectoderm (Nelson and Williams 2004). In contrast, the *AP-2cre* mice used in these series of experiments do not exhibit *Cre* expression in the ectoderm of the nasal pits where *Fgf8* is normally expressed. As the *Cre-face* transgene and *Fgf8* do not have overlapping domains of expression, resulting in the wild-type morphology of *AP-2cre;Fgf8*$^{fx/fx}$ and *AP-2cre;Fgf8*$^{\Delta 2,3/fx}$

embryos. The original *AP-2cre* mice characterized were maintained on a FVB background (Nelson and Williams 2004), while the *AP-2cre* mice housed in our animal colony were maintained on a CD1 background; this slight difference in background may result in the differences in the expression patterns between the two *AP-2cre* strains.

Although these analyses did not reveal the specific role of FGF8 signaling in the nasal ectoderm, the breeding of *AP-2cre* mice to homozygosity in the attempt to enhance Cre excision of *Fgf8*, lead to the identification of the "*Cre-face*" phenotype. *Cre-face* mice are a mouse model of holoprosencephaly, resulting from integration of two copies of the *Cre-face* transgene into a genomic locus required for proper craniofacial development; characterization of the *Cre-face* phenotype is addressed in following chapter.

E) Experimental Methods

Maintenance of Mouse Lines and Embryo Collection

Mice were housed in the Laboratory Animal Services Facility at the Stowers Institute for Medical Research according to IACUC animal welfare guidelines. *AP-2cre "Cre-face"* (Nelson and Williams 2004), $Fgf8^{fx/fx}$, (Meyers et al. 1998) $Fgf8^{\Delta 2,3}$ (Meyers et al. 1998), and *Rosa 26 reporter (R26R)* (Soriano 1999) mice were maintained and genotyped as previously described. Embryos were collected at 9.5, 10.5, 11.5, 14.5, and 17.5dpc; dams were sacrificed by cervical dislocation and day of plug was noted as 0 *days post coitum* (dpc).

β-Galactosidase Staining

To stain for β-galactosidase, *AP-2cre* mice were mated to *Rosa 26 reporter (R26R)* mice and embryos were collected at 9.5 and 10.5dpc as described above. Briefly, embryos were fixed on wet ice for 20-30min in the Tissue Fixative Solution, washed in Tissue Rinse Solution A for 30min and Tissue Rinse Solution B for 5min at RT. Embryos were incubated O/N at 37°C in Tissue Stain Solution with X-gal (40mg/mL in DMF) (Invitrogen, Carlsbad, CA). After incubation, embryos were washed PBS and re-fixed O/N in the Tissue Fixative Solution. Embryos were processed in paraffin, cut in 10micron sections, and counterstained in Nuclear Fast Red (Sigma, St. Louis, MO).

In situ hybridization

In situ hybridization for *Fgf8* was performed following the standard protocol described by Nagy et al. (2003). Briefly, embryos were fixed, dehydrated in methanol, and stored at -20°C until ready for use in the hybridization protocol. An anti-sense digoxigenin-labeled mRNA riboprobe was synthesized for *Fgf8* (I. Mason).

Cartilage & Bone Staining

Embryos were collected at 14.5 and 17.5dpc and fixed in 95% EtOH O/N. Embryos were washed in a stain solution containing 0.5% Alizarin red (Sigma, St. Louis, MO) and 0.4% Alcian blue 8X (Sigma, St. Louis, MO) in 60% EtOH O/N at RT. For 14.5dpc embryos, soft tissue was dissolved in 1% KOH for three hours and transferred to 0.25% for 30min. For 17.5dpc staining, the embryos were anesthetized in PBS for 1hr at 4°C, fixed O/N in 95% EtOH, skinned and eviscerated prior to staining; all remaining soft tissue was dissolved in 2% KOH for six hours and transferred to 0.25% KOH for 30min. Embryos were cleared in glycerol:KOH (20%:0.25%; 33%:0.25%; 50%:0.25%). Embryos were stored in 50% glycerol:0.25% KOH until photographed.

VIII. Chapter Three: Insertional Mutation of *Skinny Hedgehog (Skn/Hhat)* results in disrupted Hedgehog Signaling and Severe Craniofacial Defects.

Dennis, J.F., Williams, T., and Trainor, P.A.

A) Abstract

We have identified an embryonic mouse phenotype characterized by holoprosencephaly (HPE) with hypoplastic and fused maxillary and frontonasal prominences. Characterization of "*Cre-face*" mutant embryos revealed a disruption in *Sonic hedgehog (Shh)* as evidenced by its absence from the prechordal plate and SHH signaling is lost in the ventral telencephalon, pharyngeal endoderm, and floorplate. Furthermore, activation of *Patched1*, is significantly decreased, in these regions as well, indicating a global downregulation of Hedgehog (Hh) signaling. Coinciding with the loss of SHH in the pharyngeal endoderm, *Fgf8* and *Bmp4* are absent from the mandibular ectoderm, correlating with a role for SHH in branchial arch development and patterning of the jaw. Additionally, peripheral nervous system development are impaired; cranial nerve ganglia are reduced in size and exhibit fusion defects, which is not reflective of decreased contribution of neural crest or sensory placode cells. At later stages, $Hhat^{Cre\text{-}face}$ mutants exhibit tooth agenesis, delayed chondrogenesis, and an absence of cranial vault bones. Mapping of the "*Cre-face*" (Zhang and Williams 2003) transgene integration site revealed disruption of *Hedgehog acyltransferase* (*Hhat*), a gene responsible for palmitoylation of Hedgehog proteins; palmitolyation of SHH is required for the proper establishment

of the SHH signaling gradient (Chen et al. 2004). Our work therefore underscores the role of Hh signaling during craniofacial development.

B) Introduction

Holoprosencephaly (HPE) is a heterogeneous congenital malformation resulting from the failure of the forebrain to divide into the left and right hemispheres (Belloni et al. 1996a; Roessler et al. 1996). HPE occurs at the frequency of 1 in 10,000-20,000 live births, although embryonic cases are suggested to be as high as 1 in 250 pregnancies, making it the most common brain anomaly in humans (Muenke and Beachy 2000; Wallis and Muenke 2000). HPE manifests in a range of craniofacial anomalies in humans, including hypotelorism, microcephaly, cleft palate and/or a single incisor (Muenke et al. 1994; Roessler et al. 1996). In the most extreme cases of HPE, cyclopia and a nasal proboscis can occur (Muenke and Beachy 2000). Genetically, mutations in at least 12 different loci have been mapped to patients with HPE and include multiple signaling pathways, such as BMP, ZIC, SIX, and SHH (Wallis and Muenke 2000). Additionally, exposure to environmental teratogens such as alcohol (Cohen and Shiota 2002; Aoto et al. 2008) or retinoids (Cohen and Shiota 2002) can result in HPE phenotypes.

SHH, a member of the Hedgehog (Hh) family of secreted signaling molecules (Chiang et al. 1996), was the first loci mapped to human cases of HPE (Belloni et al. 1996a; Roessler et al. 1996). In the mouse, knockouts of *Shh* result in HPE and a complete absence of the craniofacial skeleton; $Shh^{-/-}$ embryos have a single optic

vesicle along the midline and a reduction in the overall size of the brain as well as dorsalization of the spinal cord (Chiang et al. 1996). At later developmental stages, a single nasal proboscis extends from the rostral midline and no external eye structures are present (Chiang et al. 1996), indicating the importance of this gene in embryonic development and the etiology of HPE. Additionally, knockouts of SHH signaling pathway members, such as *Patched (Ptc), Smoothened (Smo),* or *Glioma associated proteins (Gli)* (reviewed in (Wallis and Muenke 2000)) results in HPE phenotypes, further highlighting the importance of *Shh* in craniofacial development.

SHH is a secreted glycoprotein that undergoes post-translational modification into its active form via lipid modification. Autocatalytic cleavage of the carboxyl (C)-terminus results in the addition of a cholesterol moiety (Porter et al. 1996a; Porter et al. 1996b), which is required for determining the range of SHH diffusion to Hh-responsive targets; mutants that lack the C-terminal modification exhibit an extended range of SHH signaling (Porter et al. 1996a; Huang et al. 2007). Additionally, SHH undergoes an additional modification at its amino (N)-terminus via the addition of a palmitic acid moiety at an N-terminal cysteine residue (Pepinsky et al. 1998), which has been suggested to increase SHH potency (Taylor et al. 2001). In *Drosophila*, *skinny hedgehog* (*ski*) (Chamoun et al. 2001), *sightless* (*sit*) (Lee and Treisman 2001), *central missing (cmn)* (Amanai and Jiang 2001) and *rasp* (Micchelli et al. 2002) correspond to the same gene that encodes a Hedgehog acyltransferase responsible for the palmitoylation of Hh proteins.

More recently, *Skinny hedgehog* (*Skn*) or *Hedgehog acyltransferase* (*Hhat*), the murine homologue of *ski*, has been characterized. *Skn* mutants lack N-terminal modification of SHH, resulting in HPE as well as neural tube patterning defects (Chen et al. 2004). Classical knockouts of *Skn* indicate a direct role for palmitoylation in establishing the long-range SHH signaling gradient in the neural tube; lack of palmitoylation prevents the formation of SHH multimeric complexes, subsequently preventing establishment of the SHH gradient (Chen et al. 2004).

We have characterized the role of *Hhat* in an insertional mutant that carries the "*Cre-face*" transgene (Zhang and Williams 2003) in the *Hhat* locus. $Hhat^{Cre\text{-}face}$ mutants exhibit HPE and disrupted Hh signaling, which ultimately contributes to extensive craniofacial patterning defects. Indeed, $Hhat^{Cre\text{-}face}$ mutants have neural crest cell, branchial arch, and skeletal patterning defects, indicating the importance of Hh signaling in the proper development of the craniofacial complex and human syndromes such as HPE.

C) Results

Hedgehog acyltransferase (Hhat) is disrupted in Cre-face Mutants

"*Cre-face*" mutants are identifiable at early embryonic stages due to an abnormally shaped telencephalon and HPE, indicating disruptions in SHH signaling. Therefore, we intercrossed *Cre-face* mice to $Shh^{+/-}$ (Chiang et al. 1996), *Patched1-LacZ* (Goodrich et al. 1997), and $Gli3^{+/Xt}$ (Hui and Joyner 1993) mice, respectively, to directly test for genomic disruptions in *Shh* and *Shh* pathway components.

Intercrosses of *Cre-face* mice to *Shh* pathway mutants did not lead to a HPE phenotype; *Cre-face*$^{+/-}$*;Shh*$^{+/-}$*, Cre-face*$^{+/-}$*;Ptc-LacZ*$^{+/-}$*,* and *Cre-face*$^{+/-}$*;Gli3*$^{+/Xt}$ embryos harvested at 17.5dpc did not show any alterations in craniofacial development (data not shown), indicating that the HPE phenotype identified was not a direct result of integration of the *Cre-face* transgene into the *Shh, Ptc,* or *Gli3* genomic locus.. Therefore, we identified the transgene integration site using a Vectorette DNA library and sequenced clones; the *Cre-face* transgene integrated into Intron 9 of *Hedgehog acyltransferase* (*Hhat*) (Fig. 36A).

To verify *Hhat* as the gene disrupted in *Cre-face* mutants, genomic DNA from *Cre-face* embryos at 10.5dpc was genotyped using wild-type and transgene-specific reactions. Genotyping of the endogenous *Hhat* Intron 9 region produced a Wt band in both wild-type and heterozygous (*Cre-face*$^{+/-}$) DNA, but did not produce a band in mutant DNA as expected (Fig. 36B). In *Cre-face*$^{+/-}$ heterozygous and *Cre-face* mutant DNA, a *Cre-face:Hhat* specific product was amplified, indicating that these embryos have a *Cre*-specific sequence located within the *Hhat* intronic region (Fig. 36B). Integration of the *Cre-face* transgene most likely creates a physical disruption of Intron 9 of *Hhat,* rendering the gene non-functional; transgenes are well characterized as integrating into the host genome as concatemers and are therefore present in multiple copies (Costantini and Lacy 1981; Jaenisch 1988; Heaney and Bronson 2006). Indeed, cDNA created from *Cre-face* mutants failed to amplify *Hhat*

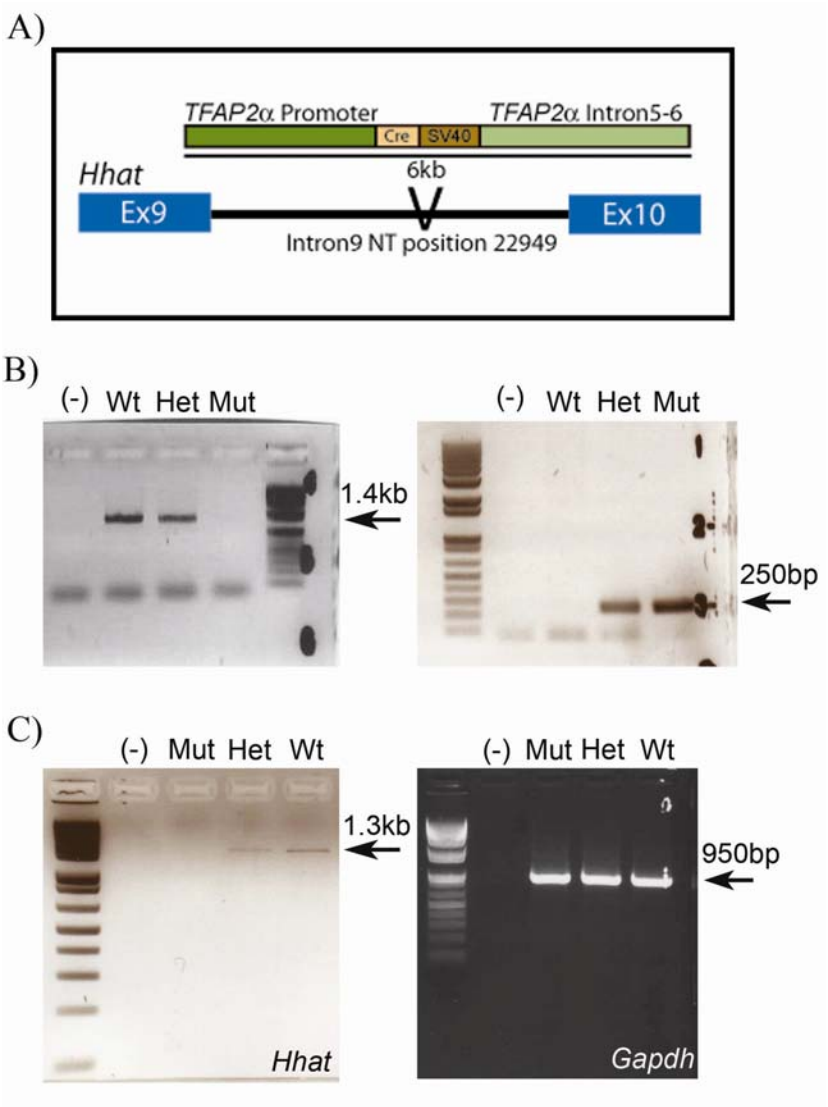

Figure Thirty-Six. *Hhat* is disrupted by the insertion of the *Cre-face* Transgene. A) Structure of the *Cre-face* transgene (Zhang and Williams 2003) and its position within Intron9 of *Hha*t. B) Genotyping of *Cre-face* genomic DNA at 10.5dpc using *Hhat* intronic primers amplifies a wild-type band of 1.4kb in wild-type (Wt) and heterozygous (Het) embryos but not in mutant embryos (Mut). A mutant band of 250bp using *Cre-face* and *Hhat*-specific primers was produced in Het and Mut embryos but not in Wt. Sequencing of these bands from genomic DNA identifies *Hhat* as the gene disrupted in mutant embryos. C) Amplification of *Hhat* mRNA in Wt, Het, and Mut embryos indicates that *Hhat* is not amplified as a result of transgene insertion in $Hhat^{Cre\text{-}face}$ mutants.

in comparison to wild-type and heterozygous cDNA (Fig. 36C), indicating that in *Cre-face* mutants *Hhat* is most likely degraded. These data verify that integration of the *Cre-face* into Intron 9 of *Hhat* results in the morphological defects characterized in *Cre-face* mutants and will herein be referred to $Hhat^{Cre\text{-}face}$.

Characterization of the $Hhat^{Cre\text{-}face}$ Phenotype

$Hhat^{Cre\text{-}face}$ mutants are readily identifiable at 9.5dpc due to an abnormally shaped telencephalon (Fig. 37A,A'); by 10.5dpc, mutant embryos were smaller in size and exhibited HPE, a hallmark of disrupted SHH signaling (Fig. 37B,B'). In mutant embryos, the medial and lateral nasal prominences were fused to the maxillary prominence; as a result, the FNP is hypoplastic and tube- or heart-shaped in appearance. The most proximal region of the maxillary prominence was identifiable but distal regions are not due to fusion with the FNP. The mandibular prominence was present but reduced in size, with an abnormal morphology at its most proximal regions. At 14.5dpc $Hhat^{Cre\text{-}face}$ embryos have a single tube-shaped nasal proboscis and a hypoplastic mandible. Moreover, mutant embryos exhibited micro- or anophthalmia and ear atresia. $Hhat^{Cre\text{-}face}$ embryos were edemic with the outer layer of skin significantly displaced from the body cavity most likely due to lymphatic defects; vascular defects were present with large blood pooling often seen in the anterior region of the embryos (Fig. 37C, C'). Additionally, organ development was impaired in the mutants, as the heart (Fig. 38B), liver (Fig. 38A), lungs (Fig. 38E), and stomach (Fig. 38D) were all reduced in size in comparison to heterozygotes.

Figure Thirty-Seven. *Hhat*$^{Cre\text{-}face}$ Mutants exhibit Holoprosencephaly and Craniofacial Defects. A, A') *Hhat*$^{Cre\text{-}face}$ mutants are identifiable at 9.5dpc with an abnormally shaped telencephalon; the optic cup is also positioned more ventrally in comparison to wild-type littermates. B, B') By 10.75dpc mutant embryos have a single nasal prominence that is fused with a hypoplastic maxillary prominence. The mandibular prominences also have an altered morphology at the midline, indicating an abnormal fusion. At late developmental stages, 14.5dpc (C, C') and 17.5dpc (D, D') mutants have a single nasal proboscis, microanopthalmia and/or ear atresia, and limb defects. Embryos are edemic with their epidermis significantly displaced from the body wall due to fluid build-up; blood pooling indicates vascular defects. All mutants were lethal by 18.5dpc

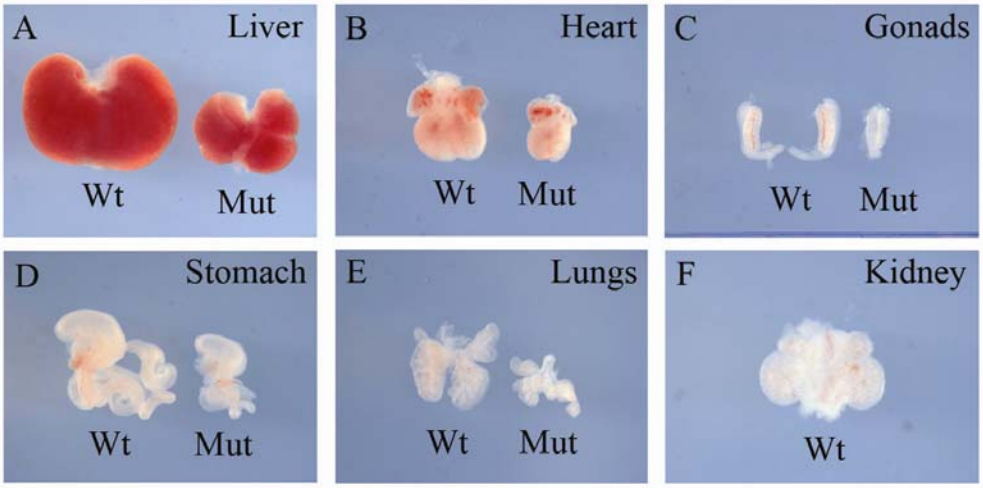

Figure Thirty-Eight. *Hhat*$^{Cre\text{-}face}$ Mutants have defects in Organogenesis at 14.5dpc. A) The liver in mutant embryos (Mut, right) is lobed but abnormally shaped and reduced in size in comparison to wildtype (Wt, left) embryo. B) The heart in *Hhat*$^{Cre\text{-}face}$ mutants is reduced in size but is multi-chambered although the right atrium and ventricle appear more reduced in size in comparison to the left atrium and ventricle. C) The gonads in the mutant embryo (right) are improperly formed; only one testes was present and it was reduced in size in comparison Wt littermates. D) The stomach was reduced overall in *Hhat*$^{Cre\text{-}face}$ embryos and the adjacent small intestine was not as elongated as in the Wt littermate. E) The lungs in *Hhat*$^{Cre\text{-}face}$ mutants were significantly reduced and the lobes were altered in appearance. F) No identifiable kidneys were present in the mutant embryos at this stage.

By 17.5dpc, the defects identified at 14.5dpc were much more pronounced (Fig. 37D, D'); all litters examined contained no live mutant embryos at 18.5dpc.

Histological examination of *Hhat*$^{Cre\text{-}face}$ mutants revealed a single–lobed neuroepithelium (NE) that was increased in size (Fig. 39F), perhaps due to the lack of cortical organization. The optic tissue (E), embedded in the telencephalic mesenchyme, was grossly disorganized (Fig. 39H). The single tubular nasal proboscis consisted of a ring of chondrocytes; mutants lacked the cartilage primordium of the nasal septum (NS) and had a large hole in this region (Fig. 39G, arrow). The palatal shelves (PS) (Fig. 39I) were also absent, indicating a defect in the vertical extension and medial protrusion of the palatal shelves toward the midline; in contrast, the vertical extension of the palatal shelves was readily identifiable in wild-type embryos (Fig. 39D, arrows). Additionally, *Hhat*$^{Cre\text{-}face}$ mutants exhibited disrupted tooth maintenance, early primordia of the lower and upper incisor and molar teeth were mis-shapen and had an altered morphology (Fig. 39I, arrowheads), whereas in wild-type littermates early primordia of the upper and lower molars and incisors were readily identifiable (Fig. 39D, arrowheads). By late developmental stages, mutants exhibited tooth agenesis, indicating a disruption in the maintenance of odontogenic precursors. In the trunk, *Hhat*$^{+/Cre\text{-}face}$ embryos had normal morphology of the spinal cord (Fig. 39E). In contrast, the spinal cord was grossly disorganized; no identifiable gray (G) or white (W) matter was present (Fig. 39J).

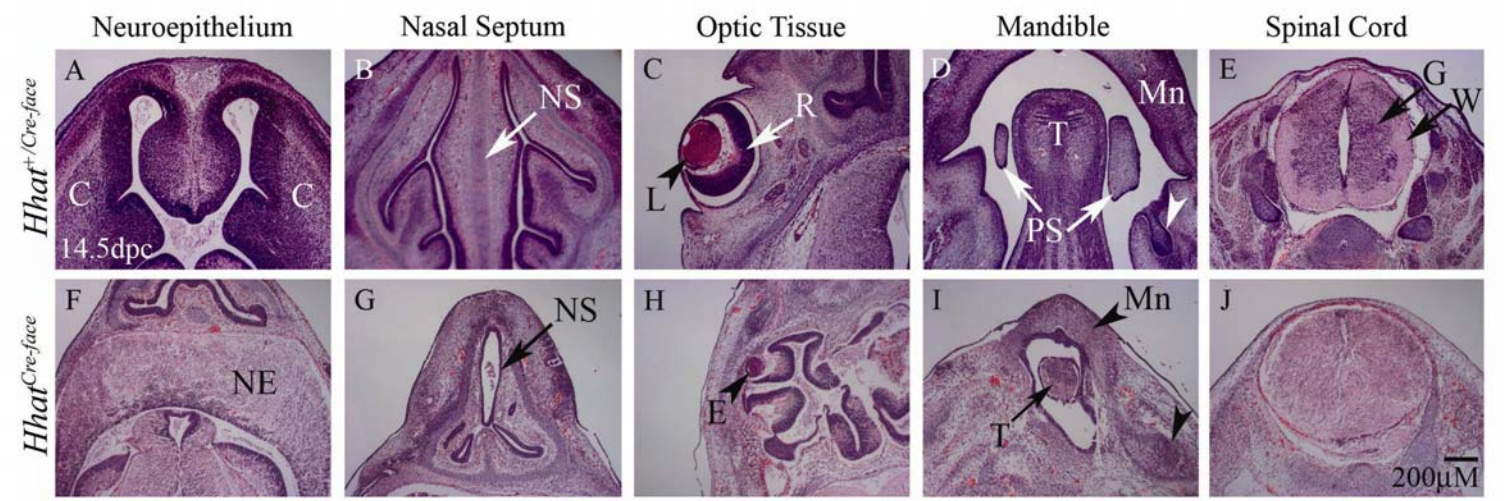

Figure Thirty-Nine. Section Histology of *Hhat*$^{Cre\text{-}face}$ Mutants at 14.5dpc. A) The neuroepithelium/cortex (C) is highly organized and has divided into bilateral hemispheres in *Hhat*$^{+/Cre\text{-}face}$ embryos, while in contrast, in mutants (F) the neuroepithelium (NE) is highly disorganized and lacks identifiable cortical layers. B) The cartilage of the nasal septum (NS, arrow) has formed in heterozygous embryos but has not fused in *Hhat*$^{Cre\text{-}face}$ mutants (G). The lack of fusion of the nasal septum has resulted in an open whole in this region (NS, arrow) of mutant embryos. C) The optic tissue is well developed in *Hhat*$^{+/Cre\text{-}face}$ embryos, with the multiple regions of the eye visible, including the retina (R, arrow) and lens (L, arrowhead). H) In contrast, the optic tissue (E, arrowhead) in mutant embryos is highly disorganized and remains embedded in the head mesenchyme; often mutants lack optic tissue completely. D, I) The mandible (Mn, arrowhead) in mutant embryos (I) is mis-shapen and has fused abnormally at its most distal point, while the mandible (Mn) of heterozygous embryos (D) is well formed and early teeth primordia (arrowhead) are present. E) The spinal cord has developed into identifiable grey (G, arrow) and white (W, arrow) matter in the *Hhat*$^{Cre\text{-}face}$ mutant, but is grossly disorganized in mutant littermates (J); no grey or white matter is discernible. C, cortex; E, eye; L, lens; Mn, mandible; NE, neuroepithelium; NS, nasal septum; PS, palatal shelves; R, retina; T, tongue. Scale bar, 200μM.

Loss of Hhat disrupts SHH Signaling

As HHAT is required for the palmitoylation of Hh proteins, we examined the expression of *Shh* in *Hhat*$^{Cre\text{-}face}$ mutants. *Shh* expression was absent from the prechordal plate (PCP, arrowhead) and downregulated in the notochord (NC, arrow) at 8.5 (Fig. 40C, D) and 9.5dpc (Fig. 40G, H) indicating a mis-regulation of *Shh* in *Hhat*$^{Cre\text{-}face}$ mutants. By 10.5dpc, *Shh* was absent from the branchial arch (BA) ectoderm (arrowheads) (Fig. 40K, L), this altered pattern of expression continued in mutant embryos up to 11.5dpc (Fig. 40O, P). The alterations in *Shh* expression and the HPE phenotype in *Hhat*$^{Cre\text{-}face}$ embryos suggested a specific disruption of the SHH pathway as *Hhat* is required for the proper establishment of the SHH signaling gradient (Chen et al. 2004), therefore we examined protein distribution at 9.5dpc to determine if the SHH gradient was established. SHH was absent from the ventral telencephalon (Fig. 41E, arrow), pharyngeal endoderm (Fig. 41G, arrowheads) and floorplate (Fig. 41H, arrow) in *Hhat*$^{Cre\text{-}face}$ mutants indicating disruptions in the SHH signaling gradient. Punctate labeling of SHH was present in random cells in the branchial arch (BA) ectoderm (Fig. 41F, arrowheads) and the notochord (Fig. 41H; NC, arrowhead) of *Hhat*$^{Cre\text{-}face}$ mutants indicating that localized signaling may occur in mutant embryos but that the SHH gradient is absent. Overall, the disruptions in SHH identified in *Hhat*$^{Cre\text{-}face}$ mutants indicate a direct requirement for *Hhat* in establishing the SHH signaling gradient.

Figure Fourty. *Shh* is downregulated in *Hhat*$^{Cre\text{-}face}$ Mutants throughout Development. A-F) In *Hhat*$^{+/Cre\text{-}face}$ embryos at 8.5 and 9.5dpc, *Shh* is expressed in the prechordal plate (PCP) (B, F, arrowheads) and notochord (NC) (A, E, arrows). D, H) *Hhat*$^{Cre\text{-}face}$ mutants at 8.5 and 9.5 dpc lack *Shh* expression in the PCP (D, H; arrowhead) and have decreased NC expression (C, G; arrow) in comparison to heterozygous littermates. I, J) At 10.5dpc, *Shh* is expressed in the ectoderm of the maxillary prominence (arrowhead) and in the zone of polarizing activity (ZPA, arrow) in the developing limb bud. K, L) In *Hhat*$^{Cre\text{-}face}$ mutants at 10.5dpc, *Shh* is absent from the maxillary ectoderm (L, arrowheads) but is still present in the ZPA (K, arrow). M, N) At 11.5dpc, *Shh* remains in the maxillary ectoderm (arrowheads) as well as in the ZPA. O, P) *Hhat*$^{Cre\text{-}face}$ embryos lack *Shh* expression at 11.5dpc in the ectoderm of the maxillary prominence (arrowheads) as well as the ZPA (O, arrow)..

Hhat+/Creface
Hhat Creface
A
B
C
D
NC
PCP
NC
PCP
8.5dpc
E
F
G
H
NC
PCP
NC
PCP
9.5dpc
I
J
K
L
ZPA
ZPA
10.5dpc
M
N
O
P
ZPA
ZPA
Shh
11.5dpc

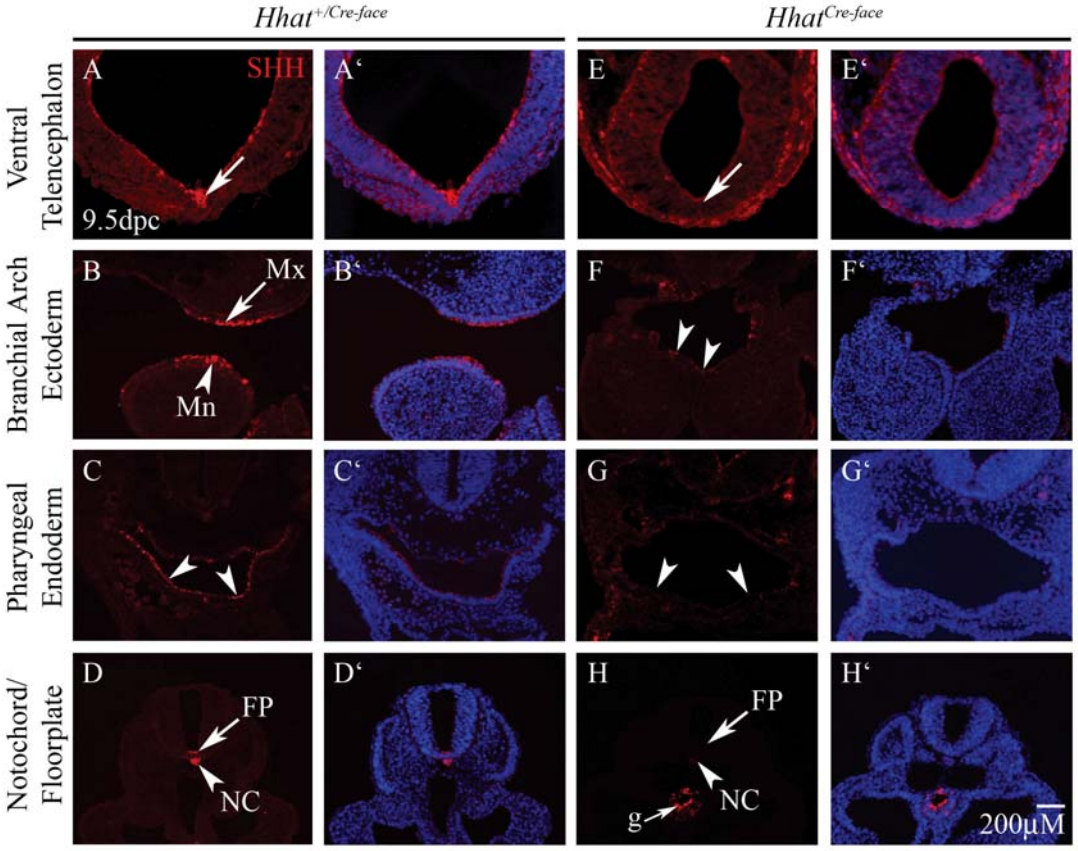

Figure Fourty-One. SHH Signaling is disrupted in *Hhat*$^{Cre\text{-}face}$ Mutants. A, A') SHH (red) is present in the ventral telencephalon (arrow) in *Hhat*$^{+/Cre\text{-}face}$ embryos while *Hhat*$^{Cre\text{-}face}$ mutants (E, E') lack SHH in this region. F, F') SHH is absent from the branchial arch (BA) ectoderm in *Hhat*$^{Cre\text{-}face}$ mutants, although a few random SHH^{+} cells are present (F, arrowheads). In contrast, SHH is present throughout the BA ectoderm of the maxillary (Mx, arrow) and mandibular (Mn, arrowhead) prominences in *Hhat*$^{+/Cre\text{-}face}$ (B, B') embryos. SHH is present in the pharyngeal endoderm (arrowheads) of *Hhat*$^{+/Cre\text{-}face}$ (C, C') embryos but *Hhat*$^{Cre\text{-}face}$ mutants (G, G') lack SHH in this region. *Hhat*$^{Cre\text{-}face}$ mutants (H, H') have reduced SHH signaling in the notochord (NC, arrowhead) and but lack SHH in the floorplate (FP, arrow); *Hhat*$^{+/Cre\text{-}face}$ (D, D') embryos have SHH present in both of these regions. g, gut. Red, SHH; Blue, DAPI; Scale bar for all images, 200μM.

$Hhat^{Cre\text{-}face}$ Mutants have decreased Activation of Patched

To further characterize the degree of altered Hh signaling in *$Hhat^{Cre\text{-}face}$* mutants, *$Hhat^{+/Cre\text{-}face}$* mice were outcrossed to *Patched1-LacZ* (*PtcLacZ*) mice (Goodrich et al. 1997) as a readout of *Ptc* activation. *$Hhat^{+/Cre\text{-}face}$;$PtcLacZ^{+}$* embryos from 9.5-11.5dpc exhibit intense *LacZ* expression in the ventral telencephalon (VT) (Fig. 42A, D, G), pharyngeal endoderm (PE) (Fig. 42B, E, H), notochord (NC, arrowhead) (Fig. C, F, I), and in the floorplate (FP, arrow) (Fig. 42C, F, I), reflecting Hh signaling in each of these regions. Additionally, a gradient of *Ptc* activation is present adjacent to these sites of synthesis (VT, PE, NC, FP), indicating the activation of *Ptc* through a gradient of Hh signaling.

The loss of SHH signaling in *$Hhat^{Cre\text{-}face}$* mutants should lead to decreased activation of *Ptc* and therefore decreased *LacZ* expression in *$Hhat^{Cre\text{-}face}$;$PtcLacZ^{+}$* embryos. Indeed, *$Hhat^{Cre\text{-}face}$;$PtcLacZ^{+}$* mutants lack *LacZ* expression in the VT (Fig. 42J, M, P), PE (arrowheads) (Fig. 42K, N, O), and FP (Fig. 42L, O, R) from 9.5 to 11.5dpc indicating a lack of Hh signaling in these regions in comparison to *$Hhat^{+/Cre\text{-}face}$;$PtcLacZ^{+}$* littermates. In the notochord (NC, arrowhead), decreased *LacZ* expression was present at all stages examined, but the gradient of *Ptc* activation is absent, indicating that localized Hh signaling may occur adjacent to the NC but that the gradient of Hh signaling is absent. Therefore, decreased Hh signaling, results in the defects characterized in *$Hhat^{Cre\text{-}face}$* mutants.

Figure Fourty-Two. *Patched (Ptc)* Activation is diminished in *Hhat*$^{Cre\text{-}face}$ Mutants. Embryos were harvested from 9.5 to 11.5dpc and processed for β-galactosidase (blue) staining as a readout of Hh signaling. A-I) *Hhat*$^{+/Cre\text{-}face}$*;PtcLacZ*$^{+}$ embryos exhibit intense *LacZ* expression at the sites of SHH synthesis, including the ventral telencephalon (A; VT), pharyngeal endoderm (B; arrowheads), notochord (C; NC, arrowhead), and the floorplate (C; FP, arrow). Adjacent to these regions a gradient of *Ptc* activation is present as indicated by the more diffuse *LacZ* expression. J-R) In *Hhat*$^{Cre\text{-}face}$*;PtcLacZ*$^{+}$ mutants, *LacZ* expression is absent from the VT (J, M, P), PE (K, N, Q), and FP (L, O, R) in all stages examined. Significantly decreased *Ptc* activation remains in the NC (L, O, Q, R) but the gradient of *Ptc* activation is absent, indicating localized Hh signaling through *Ptc* occurs in the notochord but that long-range signaling is inhibited. Double asterisks in (K) indicate localized Ptc activation around the NC. Scale bar for 9.5dpc panels is 50μM; for 10.5 and 11.5dpc 100μM.

Hhat+/cre-face;PtcLacZ+
Hhat Cre-face;PtcLacZ+
9.5dpc
10.5dpc
11.5dpc
9.5dpc
10.5dpc
11.5dpc
Ventral Telencephalon
Pharyngeal Endoderm
Spinal Cord
A
B
C
D
E
F
G
H
I
J
K
L
M
N
O
P
Q
R
VT
FP
NC
50μM
100μM
100μM

Hhat$^{Cre\text{-}face}$ *Mutants exhibit Increased Apoptosis*

The hypoplastic frontonasal and maxillary prominences were suggestive of alterations to cell survival either via apoptosis and/or proliferation. We examined *Hhat*$^{Cre\text{-}face}$ mutants for increased staining of the apoptotic marker cleaved Caspase-3, as SHH is required for the survival of neural crest cells (Ahlgren and Bronner-Fraser 1999; Ahlgren et al. 2002; Jeong et al. 2004). Loss of SHH signaling at early developmental stages in *Hhat*$^{Cre\text{-}face}$ mutants resulted in increased apoptosis in the frontonasal (Fig. 43E, E'; arrows), maxillary (Fig. 43F, F'; arrows), and mandibular prominences (Fig. 43G, G'; arrows). Additionally, increased apoptosis was present in the mesenchyme dorsal to the pharyngeal endoderm (Fig. 43H, H'). Interestingly, we did not see significant differences in the number of proliferative cells using the marker phospho Histone H3, a marker of cells in mitosis, or with Bromodeoxyuridine (BrdU), which marks cells in the synthesis phase (data not shown). The number of proliferative cells in the frontonasal prominence, mandible, and spinal cord of *Hhat*$^{Cre\text{-}face}$ mutants was comparable with heterozygous littermates and appeared only slightly decreased if at all (data not shown), indicating that disrupted SHH signaling results in increased apoptosis but does not drastically affect the cell cycle.

Hhat$^{Cre\text{-}face}$ *mutants have alterations in the Patterning of the Mandible*

We analyzed the expression of *Fgf8* and *Bmp4* in the mandible as these genes are known *Shh* targets; *Fgf8* is normally expressed in the proximal mandible (Fig. 44B, F; arrows) with an adjacent domain of *Bmp4* expression located in the distal

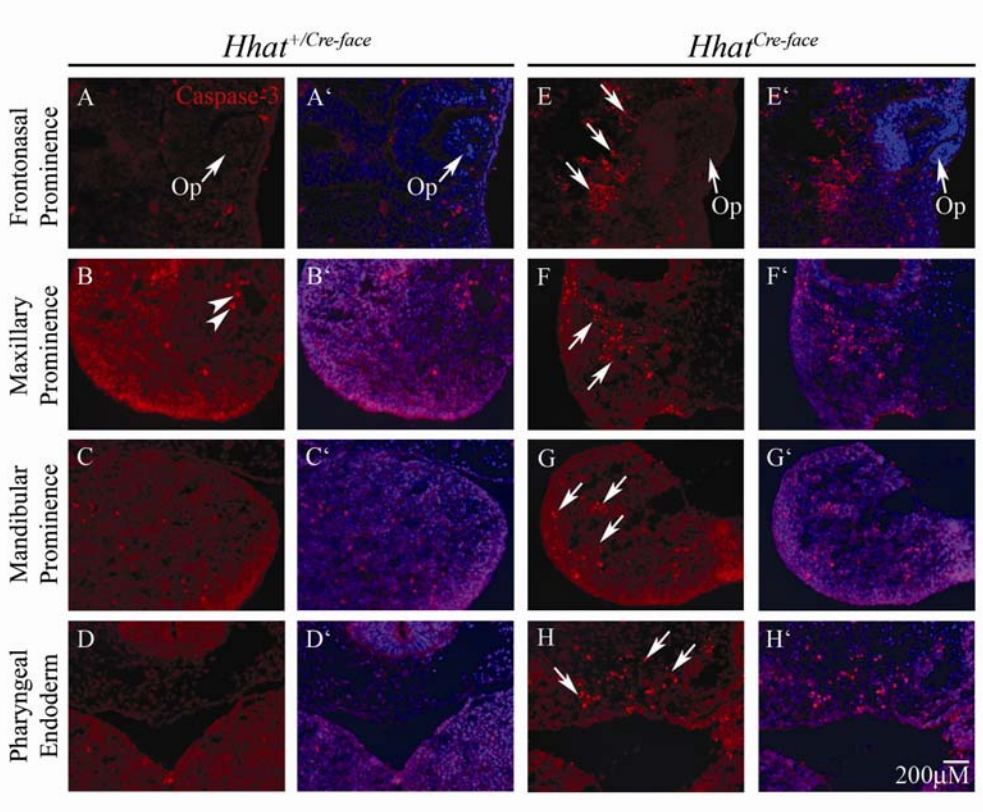

Figure Fourty-Three. *Hhat*$^{Cre\text{-}face}$ Mutants exhibit increased Apoptosis in the Developing Head. Embryos were harvested at 10.5dpc and processed for cleaved-Caspase 3 immunohistochemistry to mark apoptotic cells. A-D) *Hhat*$^{+/Cre\text{-}face}$ embryos have minimal Caspase-3 staining (red), indicating an overall lack of apoptosis in the frontonasal (A, A') and mandibular promiences (C, C'). A few Caspase-3^{+} cells (arrowheads) are present in the maxillary prominence (B, B'). The mesenchyme surrounding the pharyngeal endoderm (D, D') also lacks apoptotic cells. All other Caspase-3^{+} apparent cells are autofluorescent red blood cells. E-H) In contrast, *Hhat*$^{Cre\text{-}face}$ mutants have increased numbers of Caspase-3^{+} cells in the frontonasal (E, E'; arrows), maxillary (F, F'; arrows), and mandibular (G, G'; arrows) prominences as well as in the mesenchyme dorsal to the pharyngeal endoderm (H, H'; arrows). Red, cleaved-Caspase 3; blue, DAPI. Scale bar, 200μM

mandible (Fig. 44D, H; arrows). In *Hhat*$^{Cre\text{-}face}$ mutants, *Fgf8* (Fig. 44I, J; arrowheads) and *Bmp4* (Fig. 44K, L; arrowheads) were both absent from the mandibular ectoderm. Interestingly, both, *Fgf8* and *Bmp4*, were not affected in the nasal region (Fig. 44J, L), despite the single nasal prominence, indicating a region-specific role for SHH signaling in patterning the lower jaw. Collectively, the loss of SHH results in the downregulation of these genes, and in conjunction with the increased apoptosis in these regions, leads to the jaw patterning defects seen at late developmental stages.

Neural Crest Lineages are altered in Hhat$^{Cre\text{-}face}$ *Mutants*

Hhat$^{Cre\text{-}face}$ mutants have decreased SHH signaling in the ventral telencephalon beginning at 9.5dpc, coinciding with cranial neural crest cell migration into the adjacent frontonasal prominence and branchial arches. *Shh* is required for the proper migration and proliferation of cranial neural crest cells (Ahlgren and Bronner-Fraser 1999; Jeong et al. 2004; Moore-Scott and Manley 2005; Yamagishi et al. 2006), therefore, we examined *Hhat*$^{Cre\text{-}face}$ embryos for defects in neural crest cell formation using *in situ* hybridization and cell lineage tracing analysis. We examined the induction of neural crest cells using the markers *Crabp1, Snail, Sox9*, and *Sox10*; *Hhat*$^{Cre\text{-}face}$ mutants did not show specific defects in the initial induction of the neural crest cell population as indicated by *Crabp1* (Fig. 45C, D) and *Snail* (Fig. 45G, H). Expression of the lineage-specific neural crest cell markers *Sox9* (Fig. 45K, L) and *Sox10* (Fig. 45O, P) were slightly decreased in *Hhat*$^{Cre\text{-}face}$ mutants, particularly in the

Figure Fourty-Four. Branchial Arch Patterning is disrupted in *Hhat*$^{Cre\text{-}face}$ Mutants. *Hhat*$^{Cre\text{-}face}$ embryos have disruptions in the patterning of the mandibular prominence at 10.5dpc. (B, F) *Fgf8* is normally expressed in the surface ectoderm of the proximal branchial arch (BA) in wild-type (B, arrows) and heterozygous littermates (F, arrows). J) *Hhat*$^{Cre\text{-}face}$ mutants lack *Fgf8* in the BA ectoderm (arrowheads) in comparison to Wt and Het littermates. D, H) *Bmp4* is normally expressed in the surface ectoderm of the distal BA in wild-type (D, arrows) and heterozygous embryos (H, arrows). L) In *Hhat*$^{Cre\text{-}face}$ mutants, *Bmp4* is absent from the distal BA ectoderm (arrowheads) compared to Wt and Het littermates. Collectively, the lack of *Fgf8* and *Bmp4* expression in *Hhat*$^{Cre\text{-}face}$ mutants indicates a role for SHH in the patterning of the developing jaw.

Fgf8
Bmp4
A
B
C
D
E
F
G
H
I
J
K
L
10.5dpc
10.5dpc
Hhat+/+
Hhat+/Cre-face
HhatCre-face

anterior-most region of the head, suggesting that SHH may play a role in the maintenance of *Sox9* and *Sox10*$^{+}$ neural crest cells.

Additionally, we performed lineage tracing analysis in *Hhat*$^{Cre\text{-}face}$ mutants using *Wnt1-cre,* to permanently label neural crest cells. At 9.5dpc, *Wnt1-cre*$^{+}$*;R26R*$^{+}$ embryos (Fig. 46E) had *LacZ*$^{+}$ neural crest cells populating the developing frontonasal prominence (FNP, arrowhead); streams of migratory neural crest cells from rhombomeres2/3 (r2, arrow) and 3/4 (r4, arrow) were present populating BA1 and BA2, respectively. In *Hhat*$^{Cre\text{-}face}$;*Wnt1-cre*$^{+}$*;R26R*$^{+}$ embryos (Fig. 46G), neural crest cells were present in similar regions and were present in approximately equal numbers; cells had populated the FNP (arrowhead) and BA1/BA2 (arrows). At 10.5dpc, neural crest cells in *Wnt1-cre*$^{+}$*;R26R*$^{+}$ embryos (Fig. 46F) had populated the entire nasal region, as well as BA1/BA2. Additionally, cranial nerve ganglia (arrowheads) of the trigeminal (V), facial (VII), hypoglossal (IX) and vagus (X) nerves were identifiable. Although *Hhat*$^{Cre\text{-}face}$*;Wnt1-cre*$^{+}$*;R26R*$^{+}$ embryos (Fig. 46H) did not exhibit any obvious reductions in the pattern of *LacZ*$^{+}$ neural crest cells at 10.5dpc, mutant embryos at this stage did exhibit defects in the development of the cranial nerves (see *Hhat*$^{Cre\text{-}face}$ *Mutants exhibit Cranial Nerve Fusion Defects* below). Collectively, disruptions in the Hh signaling gradient due to loss of *Hhat* does not significantly impact neural crest cell formation.

Figure Fourty-Five. *Hhat*$^{Cre\text{-}face}$ Mutants have defects in Neural Crest Cell Lineage Segregation. The neural crest cell markers *Crabp1* (C, D) and *Snail* (G, H) were unaffected in *Hhat*$^{Cre\text{-}face}$ mutants in comparison to heterozygous littermates (A, B) and (E, F), indicating normal induction of neural crest cells. In contrast, *Sox9* (K, L) and *Sox10* (O, P) staining is slightly decreased in mutant embryos compared to heterozygous littermates (I, J and M, N) indicating alterations in the specification of these cell types.

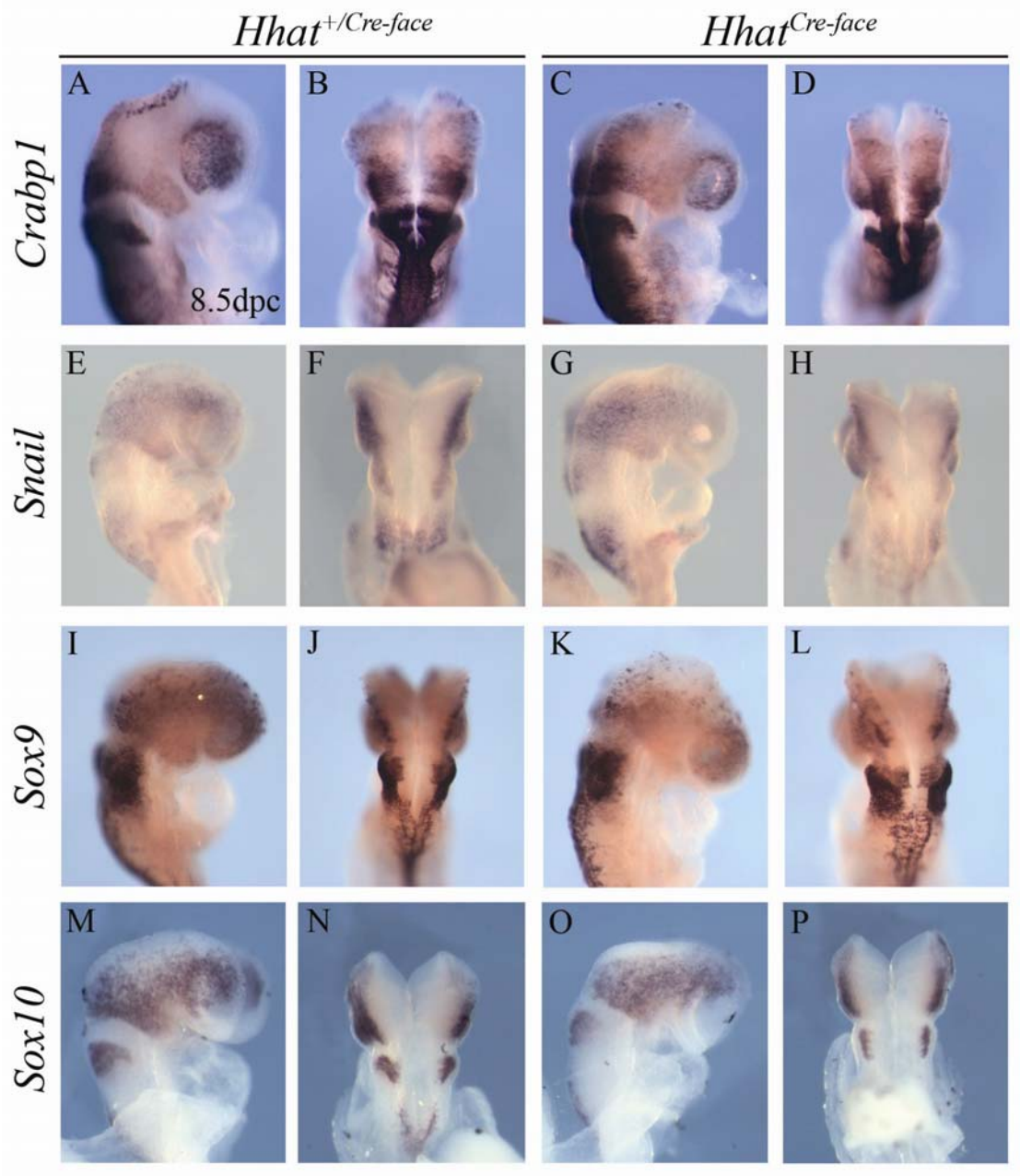
Hhat+/Cre-face
HhatCre-face
Crabp1
Snail
Sox9
Sox10
A
B
C
D
E
F
G
H
I
J
K
L
M
N
O
P
8.5dpc

Figure Fourty-Six. Lineage Tracing using *Wnt1-cre* in *Hhat*$^{Cre\text{-}face}$ Mutants does not reveal defects in Neural Crest Cell Formation. A-D) Expression pattern of the *AP-2cre* transgene at 9.5dpc (A, C) and 10.5dpc (B, D) in *Hhat*$^{+/Cre\text{-}face}$*;R26R*$^{+}$ (A, B) and *Hhat*$^{Cre\text{-}face}$*;R26R*$^{+}$ (C, D) embryos; *LacZ* expression is present in the frontonasal prominence (FNP, arrowhead). E-H) Expression pattern of the *Wnt1-cre* transgene in *Wnt1-cre*$^{+}$*;R26R*$^{+}$ (E, F) and *Hhat*$^{Cre\text{-}face}$*; Wnt1-cre*$^{+}$*;R26R*$^{+}$ (G, H) embryos. E, G) At 9.5dpc, *LacZ*$^{+}$ neural crest cells are present in the migratory streams from rhombomeres 2/3 (r2, arrow) and 3/4 (r4, arrow) as well as the FNP (arrowhead) in *Wnt1-cre*$^{+}$*;R26R*$^{+}$ (E) and *Hhat*$^{Cre\text{-}face}$*;Wnt1-cre*$^{+}$*;R26R*$^{+}$ (G) embryos. F, H) By 10.5dpc, cells have populated the entire FNP in *Wnt1-cre*$^{+}$*;R26R*$^{+}$ (F) and *Hhat*$^{Cre\text{-}face}$*;Wnt1-cre*$^{+}$*;R26R*$^{+}$ (H) embryos, although the mutant embryos (H) exhibit fusion defects of the hypoglossal (IX, arrowhead) and vagus (X, arrowhead) nerves. V, trigeminal ganglia; VII, facial ganglia.

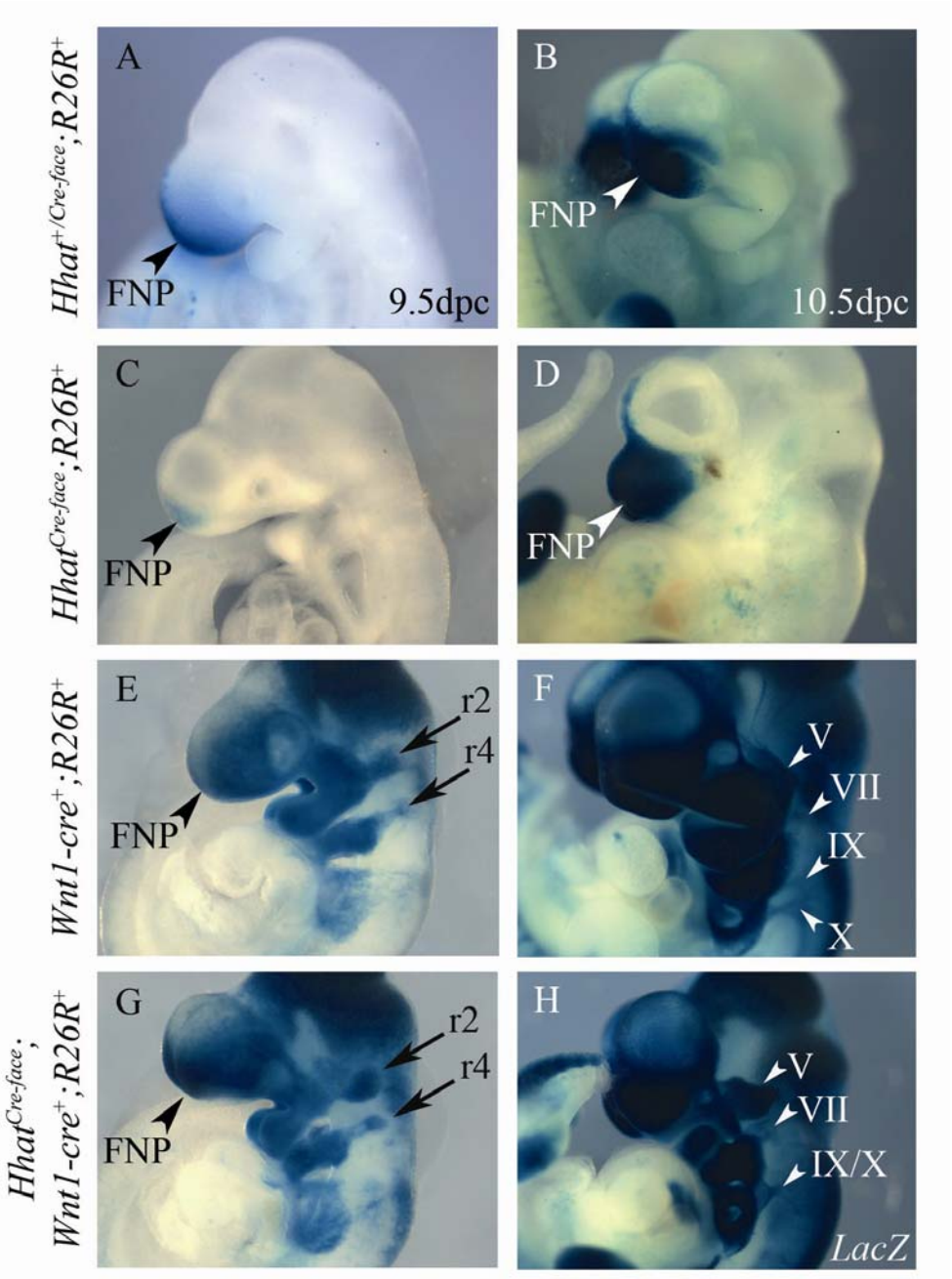
Hhat+/Cre-face·R26R+
A
FNP
9.5dpc
B
FNP
10.5dpc
HhatCre-face·R26R+
C
FNP
D
FNP
Wnt1-cre+;R26R+
E
r2
r4
FNP
F
V
VII
IX
X
HhatCre-face;
Wnt1-cre+;R26R+
G
r2
r4
FNP
H
V
VII
IX/X
LacZ

Hhat$^{Cre\text{-}face}$ *Mutants exhibit Cranial Nerve Fusion Defects*

The cranial nerves (CN) are a component of the peripheral nervous system that are derived from contributions of both neural crest cells and the sensory placodes (Larson 1993). Analysis of *Hhat*$^{Cre\text{-}face}$*;Wnt1-cre*$^{+}$*;R26R*$^{+}$ embryos did not indicate significant defects in neural crest cell formation, although mutant embryos exhibited defects in the development of the CN ganglia. *Hhat*$^{Cre\text{-}face}$*;Wnt1-cre*$^{+}$*;R26R*$^{+}$ embryos exhibited decreases in the overall size of the CN V and CN VII ganglia (Fig. compare 46F, H) and exhibited an obvious fusion defect of the CN IX and CN X (Fig. compare 46F, H), which were similarly reduced in size.

The defects in CN ganglia identified in *Hhat*$^{Cre\text{-}face}$*;Wnt1-cre*$^{+}$*;R26R*$^{+}$ embryos were consistent in *Hhat*$^{Cre\text{-}face}$ mutants stained with anti-neurofilament antibodies (Fig. 47A, D). In *Hhat*$^{+/Cre\text{-}face}$ (Fig. 47A) embryos the occulomotor (III) nerve and the CN V, VII, IX, and X were readily identifiable. In contrast, *Hhat*$^{Cre\text{-}face}$ embryos CN development is impaired; the CN III is completely absent, most likely due to the HPE phenotype (Fig. 47D). Additionally, CN V and VII were reduced in size overall and CN IX and X exhibited aberrant fusion defects (Fig. 47D).

As the CN ganglia are derived from neural crest cells and the sensory placodes, we subsequently examined each cell type to ascertain any abnormalities that would contribute to the overall reduction and/or fusion of the ganglia. *Hhat*$^{Cre\text{-}face}$ mutants were harvested at 10.5dpc and processed for *in situ* hybridization for *Eya2* and *Sox10*, to examine the sensory placodes and neural crest, respectively. Surprisingly, we did not find any significant reduction in either of the populations that

Figure Fourty-Seven. *Hhat*$^{Cre\text{-}face}$ Mutants exhibit Cranial Nerve (CN) Fusion Defects. *Hhat*$^{Cre\text{-}face}$ litters were harvested at 10.5dpc and processed for Neurofilament staining (A, D) and *Sox10* (B, E), and *Eya2* (C, F) *in situ* hybridization to examine the development cranial nerves. Neurofilament staining in the mutant embryos (D) revealed a reduced trigeminal (V) and facial (VII) ganglia and an abnormal fusion of the hypoglossal (IX) and vagal (X) nerves in comparison to heterozygous littermates (A). Additionally, *Hhat*$^{Cre\text{-}face}$ mutants lack the occulomotor (III) nerve. In *Hhat*$^{Cre\text{-}face}$ mutants both *Sox10* (E) and *Eya2* (F) show reduced expression in each of the ganglia (V, VII) and in CN IX and X. Interestingly, both populations of cells contributing to the CN show an abnormal fusion between CN IX and X, indicating a defect in the positioning of the nerves in *Hhat*$^{Cre\text{-}face}$ mutant embryos as opposed to a defect in the neural crest or placodal contribution to the CNs.

Neurofilament
Sox10
Eya2
Hhat+/Cre-face
HhatCre-face
A
B
C
D
E
F
III
V
VII
IX
X
IX/X
10.5dpc

would contribute to the overall defects identified. In both *Eya2* (Fig. 47C, F) and *Sox10* (Fig. 47B, E) stained embryos, the CN Vand VII were reduced in *Hhat*$^{Cre\text{-}face}$ mutants in comparison to wildtype littermates. The fusion defect affecting CN IX and X was also present in *Eya2* (Fig. 47F) and *Sox10* (Fig. 47E) stained *Hhat*$^{Cre\text{-}face}$ embryos, indicating that the fusion was present in both cell populations contributing to the ganglia. Collectively, these results indicate that disrupted Hh signaling is not directly required for the maintenance of the cell types contributing to the peripheral nervous system, but rather the positioning of the individual ganglia.

Skeletal development is disrupted in Hhat$^{Cre\text{-}face}$ *mutants*

Hedgehog signaling is required for cartilage and bone formation through the actions of both *Shh* (Chiang et al. 1996) and *Indian hedgehog (Ihh)* (St-Jacques et al. 1999). Because *Hhat* is required for the palmitoylation of Hh proteins, mutants lacking the palmitate moiety are likely to exhibit defects in the development of the cranial skeleton. To characterize any defects in chondro- and skeletogenesis in *Hhat*$^{Cre\text{-}face}$ mutants, we stained embryos at 15.5 and 17.5dpc (Fig. 48) with Alcian blue and Alizarin red to stain cartilage and bone, respectively. At 15.5dpc, wildtype littermates had cartilage present throughout the developing cranium (Fig. 48A, B); the nasal cartilage (NA, arrow) was clearly stained. Early ossification sites were present for multiple bones including the frontal (F) and parietal (P) bones (Fig. 48A, B). By 17.5dpc, these bones had completely mineralized, forming the

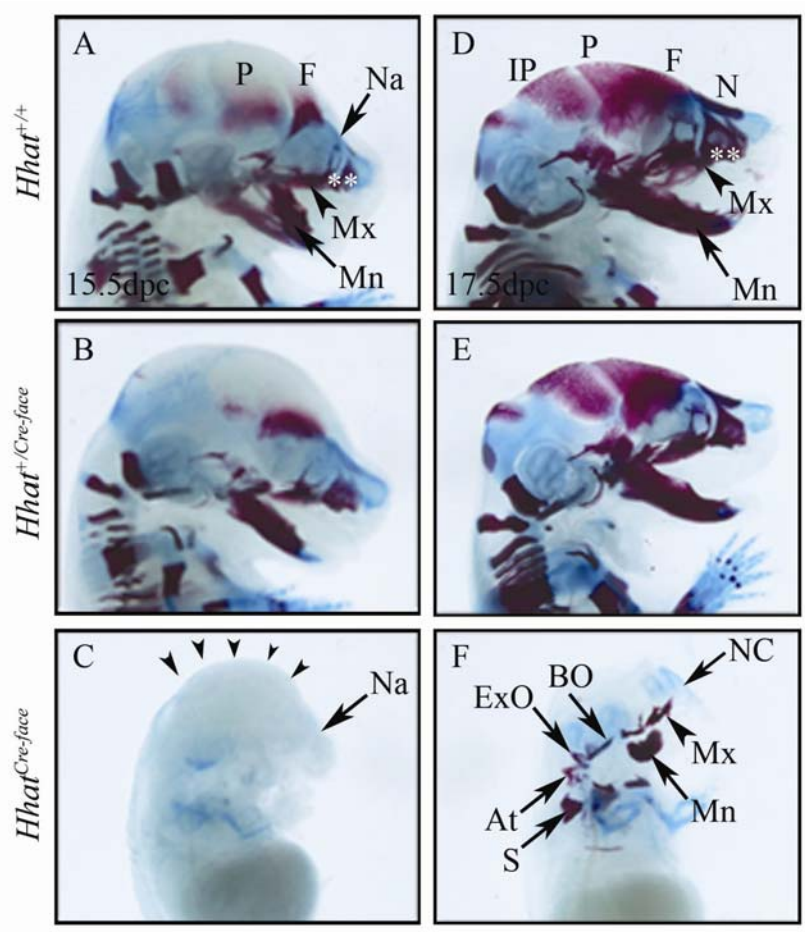

Figure Fourty-Eight. *Hhat*$^{Cre\text{-}face}$ Mutants have Cartilage and Bone Defects. *Hhat*$^{+/+}$ (A, D) and *Hhat*$^{+/Cre\text{-}face}$ (B, E) embryos at 15.5dpc (A, B) have ossification of the frontal (F), mandibular (Mn, arrow), maxilla (Mx, arrowhead), parietal (P), and premaxilla (double asterisks). The nasal (Na, arrow) cartilage is also identifiable. C) *Hhat*$^{Cre\text{-}face}$ mutants exhibit defects in cartilage formation and are lacking nasal (Na) cartilage; additionally, mutants are lacking any early ossification of the skull vault (arrowheads). At 17.5dpc, *Hhat*$^{Cre\text{-}face}$ mutants (F) have minimal cranial bone formation in comparison to wild-type (D) and heterozygous (E) littermates. Bones of the ventral face and skull are present, such as the exoccipital (EO) and basioccipital (BO) bones. Reduced jaw elements of the maxilla (Mx, arrowhead) and mandible (Mn, arrow) are present but abnormal. In *Hhat*$^{Cre\text{-}face}$ embryos (F), the interparietal (IP), parietal (P), frontal (F), nasal (N), and premaxilla (asterisks) bones are completely absent. (At) Atlas; (NC) nasal cartilage; (S) scapula.

skull vault (Fig. 48 D, E). Additionally, the nasal (N) bone (Fig. 48D, E) had ossified by this stage in comparison to the nasal cartilage identified at 15.5dpc. In both *Hhat*$^{+/+}$ and *Hhat*$^{+/Cre\text{-}face}$ embryos, skeletal components of the jaw, including the premaxilla (asterisks), maxilla (Mx, arrowhead), and mandible (Mn, arrow) were present at 15.5 and 17.5dpc (Fig. 48; A, D).

In contrast, *Hhat*$^{Cre\text{-}face}$ embryos at 15.5dpc had minimal cartilage development of the skull and the nasal cartilage was absent (Fig. 48C). By 17.dpc, these defects were much more pronounced, the frontal (F), interparietal (IP), parietal (P), and premaxillary bones were completely absent (Fig. 48F). Instead, a thin layer of cartilage appeared to be present surrounded the cranial vault. The nasal cartilage (NC, arrow) was present as a tube-shaped structure but no ossification had taken place (Fig. 48F). The ventral bones of the skull; the basioccipital (BO) and exoccipital (EO) bones were present, but reduced in size (Fig. 48F), which is consistent with skeletal preparations of late-staged 17.5dpc *Shh*$^{-/-}$ embryos (Chiang et al. 1996). *Hhat*$^{Cre\text{-}face}$ mutants have a rudimentary maxilla (Mx, arrowhead) and mandible (Mn, arrow), although it appears as though only the proximal regions of these jaw elements were present; no distal maxilla or mandible was present in any of the mutants examined at this stage (Fig. 48F). Finally, mutants at 17.5dpc have ossification in a portion of the bones that contribute to the shoulder girdle, as scapulae and what appears to be a clavicle was present (Fig. 49F).

The absence of cranial vault bones led us to examine histological sections of *Hhat*$^{+/Cre\text{-}face}$ and *Hhat*$^{Cre\text{-}face}$ embryos at 15.5dpc to identify any defects in

endochondral ossification as *Ihh* regulates this process (St-Jacques et al. 1999). During endochondral ossification proliferating chondrocytes at distal ends of a skeletal element undergo hypertrophy and dramatically increase in size; as development proceeds, hypertrophic chondrocytes undergo apoptosis and are replaced by invading osteoblasts (reviewed in (Kronenberg 2003)).

Sagittal sections of $Hhat^{+/Cre\text{-}face}$ through the ex- (Fig. 49A) and basioccipital (Fig. 49B) bones revealed normal cartilage development; early signs of osteoblast invasion are identifiable in each skeletal element. In each region, proliferating chondrocytes (PC) are located at the most distal end of the element (Fig. 49A, B), while prehypertrophic chondrocytes (PHC, arrow) are present more medially (Fig. 49A, B); hypertrophic chondrocytes (HC) have increased in size and are positioned more centrally within the element (Fig. 49A, B). In contrast, sections of $Hhat^{Cre\text{-}face}$ mutants (Fig. 49C, D) revealed a delay in chondrocyte development; the skeletal elements are reduced in size and proliferating chondrocytes (PC) and prehypertrophic chondrocytes (PHC) are absent from each of the bones. Indeed, each of the bones are almost entirely comprised of hypertrophic chondrocytes (Fig. 49C, D), indicating defects in the chondrocyte proliferation and apoptosis. Finally, osteoblasts were not present in either of the elements in all sections examined, indicating a delay in their initial invasion in comparison to heterozygous littermates or that the cells do not form.

Figure Fourty-Nine. *Hhat*$^{Cre\text{-}face}$ Mutants have defects in Endochondral Bone Formation resulting from defective Hh Signaling. A-D) Histological sections of *Hhat*$^{+/Cre\text{-}face}$ (A, B) and *Hhat*$^{Cre\text{-}face}$ (C, D) embryos at 15.5dpc. A, B) *Hhat*$^{+/Cre\text{-}face}$ embryos have normal development of the ex- (A) and basioccipital (B) bones. Proliferating chondrocytes (PC, arrowhead) are present at the distal ends of each skeletal element, while hypertrophic chondrocytes (HC, arrow) are more medially positioned. Prehypertrophic chondrocytes (PHC, arrow) are located between the PC and HC, and have condensed in size. C-D) In *Hhat*$^{Cre\text{-}face}$ embryos, both skull bones are reduced in size in comparison to littermates. C) HC are present throughout the exoccipital bone, although the PHC and PC are absent; HC are also identifiable in the basioccipital bone (D). E-H) *Hhat*$^{+/Cre\text{-}face}$*;PtcLacZ*$^{+}$ (E, F) and *Hhat*$^{+/Cre\text{-}face}$*;PtcLacZ*$^{+}$ (G, H) harvested at 15.5dpc and processed for β-gal staining. E, F) In *Hhat*$^{+/Cre\text{-}face}$*;PtcLacZ*$^{+}$ embryos, *Ptc* activation is present along the region that will give rise to the bone collar (arrowheads) in the ex- and basioccipital bones. G, H) In contrast, *Hhat*$^{Cre\text{-}face}$*;PtcLacZ*$^{+}$ mutants lack any *LacZ* expression in the exoccipital (G) bone and have significantly diminished *LacZ* expression in the basioccipital bone (H, arrowhead). Scale bars, 100μM.

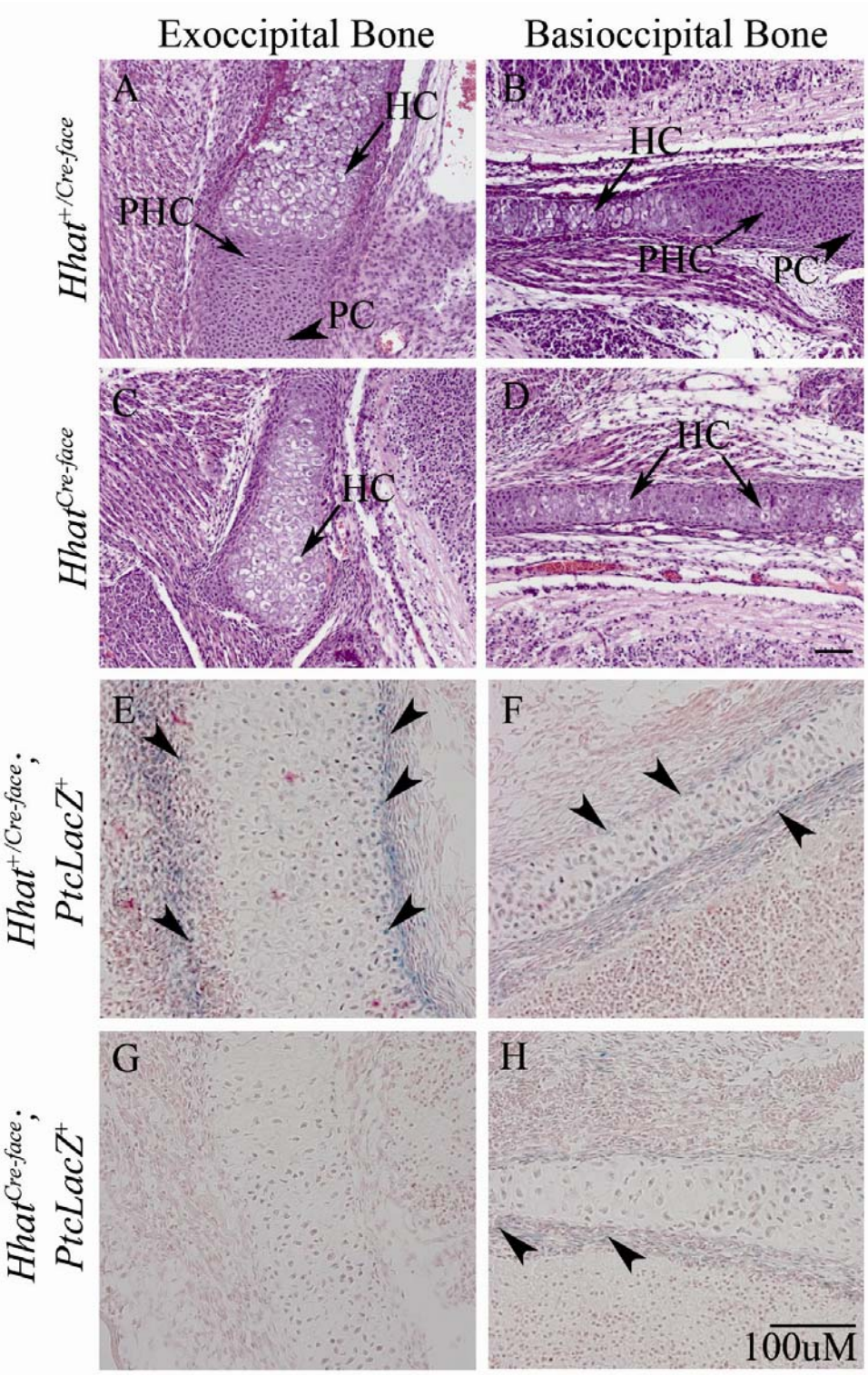
Exoccipital Bone
Basioccipital Bone
A
HC
PHC
PC
B
HC
PHC
PC
Hhat+/Cre-face
C
HC
D
HC
HhatCre-face
E
F
Hhat+/Cre-face;
PtcLacZ+
G
H
100uM
HhatCre-face;
PtcLacZ+

Additionally, we analyzed the activation of *Ptc* in the ex- and basioccipital bones, to determine if impaired Hh signaling was impaired and therefore contributing to the skull defects characterized in $Hhat^{Cre\text{-}face}$ mutants. $Hhat^{+/Cre\text{-}face};PtcLacZ^{+}$ and $Hhat^{Cre\text{-}face};PtcLacZ^{+}$ embryos were harvested at 15.5dpc and processed for β-gal staining to determine if *Ptc* activation was diminished in mutant embryos in comparison to heterozygous littermates. Indeed, *Ptc* activation was completely absent from the exoccipital bone in $Hhat^{Cre\text{-}face};PtcLacZ^{+}$ mutants (Fig. 49G), indicating that decreased Hh signaling, most likely IHH, contributes to the defects in bone development at 15.5 and 17.5dpc. $Hhat^{+/Cre\text{-}face};PtcLacZ^{+}$ embryos (Fig. 49E) have *LacZ* expression along the outer edges of the bone (arrowheads), a region that requires IHH signaling for ossification of the bone collar. Additionally, decreased *LacZ* expression was present in the basioccipital bone of $Hhat^{Cre\text{-}face};PtcLacZ^{+}$ embryos, a few random $LacZ^{+}$ cells (Fig. 49H, arrowheads) were present in this region but were far decreased in number in comparison to $Hhat^{+/Cre\text{-}face};PtcLacZ^{+}$ embryos (Fig. 49F; arrowheads). Overall, the bone defects characterized in $Hhat^{Cre\text{-}face}$ mutants clearly indicate a requirement of Hh signaling, most likely IHH, in regulating endochondral bone formation.

D) Discussion

We have identified a novel mouse model of holoprosencephaly (HPE) resulting from insertion of the *Cre-face* transgene into *Hedgehog acyltransferase (Hhat),* the gene responsible for palmitoylation of Hedgehog (Hh) proteins. *Hhat*

palmitoylates the N-terminal of SHH post-translationally, a reaction that is specific to Hh proteins (Buglino and Resh 2008). *Hhat*$^{Cre\text{-}face}$ embryos exhibit a complete absence of SHH signaling (Fig. 41) and downregulation of *Ptc* activation (Fig. 42) by 9.5dpc. Mutant embryos exhibit secondary defects including increased apoptosis in the developing head (Fig. 43) as well as neural crest cell and branchial arch patterning defects, which ultimately contributes to the extensive craniofacial defects at late developmental stages. At 17.5dpc *Hhat*$^{Cre\text{-}face}$ mutants have delayed chondrogenesis and lack the majority of the bones of the anterior skull (Fig. 48); only ventral bones, such as the basioccipital and exoccipital bones are present. Additionally, *Hhat*$^{Cre\text{-}face}$ mutants have defects in endochondral bone development resulting from impaired Hh signaling as indicated by histological sections through the skull and decreased *Ptc* activation (Fig. 49). Previous reports have indicated the importance of palmitoylation in Hh signaling; *in vitro*, palmitoylation increases the potency of SHH, although this has not been addressed *in vivo* (Taylor et al. 2001). *Drosophila* mutants lacking Hh palmitoylation exhibit patterning defects in Hh-responsive cells (Amanai and Jiang 2001; Chamoun et al. 2001; Lee and Treisman 2001; Micchelli et al. 2002) and the fatty acid modification is required for long-range SHH signaling in the mouse (Chen et al. 2004). Overall, these studies as well as data from *Hhat*$^{Cre\text{-}face}$ mutants highlight the requirement of palmitoylation in establishing the Hh signaling gradient.

Hhat$^{Cre\text{-}face}$ *Mutants have altered Hh Signaling*

The HPE phenotype identified in *Hhat*$^{Cre\text{-}face}$ mutants suggested disruptions in *Shh*. Indeed, *Shh* was absent from the ventral telencephalon (VT) and notochord as early as 8.5dpc (Fig. 40). By 9.5dpc *Shh* was downregulated in the floorplate (FP) and was absent from the branchial arch (BA) ectoderm by 10.5dpc (Fig. 40). Subsequent analysis of SHH in *Hhat*$^{Cre\text{-}face}$ mutants revealed an absence of SHH from the VT, pharyngeal endoderm (PE), BA ectoderm, and FP (Fig. 41), indicating a clear failure in the establishment of the SHH signaling gradient as has been reported in other *ski/Skn* mutants (Amanai and Jiang 2001; Chamoun et al. 2001; Lee and Treisman 2001; Micchelli et al. 2002; Chen et al. 2004). The loss of SHH at early developmental stages, in particular in the VT and PE, underlies the craniofacial patterning defects identified in *Hhat*$^{Cre\text{-}face}$ mutants; SHH signaling from the VT is required for the ventral patterning of tissues in the surrounding regions, for example the developing eye and nervous tissue (Macdonald et al. 1995; Dale et al. 1997), while SHH from the PE is required for patterning of the lower jaw components (Moore-Scott and Manley 2005; Brito et al. 2006). The lack of SHH signaling in the VT and PE in *Hhat*$^{Cre\text{-}face}$ mutants most likely underlies the apoptosis seen in the frontonasal, maxillary, and mandibular prominences (Fig. 43) as SHH is required for the proliferation and viability of neural crest cells contributing to this region (Ahlgren and Bronner-Fraser 1999).

Hh proteins are trafficked to the cell surface by the Dispatched receptor, diffuse to responding cells, and bind to the receptor, *Patched1 (Ptc)* (Ingham et al. 1991; Chen and Struhl 1996; Marigo et al. 1996). In the absence of Hh signaling, Ptc

inhibits the Hh co-receptor Smoothened (Smo) (Incardona et al. 2000; Martin et al. 2001), targeting it for degradation. Upon binding of Ptc, the complex is internalized and targeted for degradation causing the dis-inhibition of the receptor Smo, leading to its integration into the cell membrane (Alcedo et al. 2000; Denef et al. 2000; Ingham et al. 2000) and activation of Hh targets (Zhu et al. 2003). To determine the extent of Hh signaling present in *Hhat*$^{Cre\text{-}face}$ mutants, we analyzed the activation of *Patched (Ptc)* using the *PtcLacZ* reporter line. *Hhat*$^{+/Cre\text{-}face}$;*PtcLacZ*$^{+}$ embryos exhibit β-gal staining in the ventral telencephalon, pharyngeal endoderm, floorplate, and notochord; regions that require Hh signaling, in particular SHH, during development. In contrast, *Hhat*$^{Cre\text{-}face}$;*PtcLacZ*$^{+}$ mutants have an absence of *Ptc* activation, in the VT, PE, and FP (Fig. 42), indicating a disruption in Hh signaling in these regions; markedly reduced *LacZ* expression was present in the NC of *Hhat*$^{Cre\text{-}face}$;*PtcLacZ*$^{+}$ mutants. Although some *Ptc* activation was present in the *Hhat*$^{Cre\text{-}face}$ mutants, a gradient of *LacZ* expression was absent in every region analyzed, indicating Hh proteins were not secreted from their producing cells or that only localized Hh signaling is intact. Overall, these data indicate that the short- and long-range Hh signaling gradient fail to be established.

Interestingly, this suggests that in *Hhat*$^{Cre\text{-}face}$ mutants a cycling of Hh signaling occurs throughout embryonic development. At early developmental stages, Hh proteins are initially synthesized by Hh-producing cells and localized Hh signaling may occur in adjacent cells. In contrast, the Hh signaling gradient would not be established to the absence of palmitoylation of Hh proteins. As development

proceeds, reactivation of Hh signaling would occur at sites of synthesis, but only localized signaling could take place, if at all, which in theory would be perpetually repeated within each tissue that produces Hh proteins throughout development. In *Hhat*$^{Cre\text{-}face}$*;PtcLacZ*$^{+}$ mutants, the *LacZ* expression in the notochord indicate activation of *Ptc* has occurred, although the expression is restricted to cells adjacent to the NC. The induction of SHH in the floorplate by the NC fails to occur due to impaired SHH signaling from the lack of palmitoylation; therefore, the multiple defects in *Hhat*$^{Cre\text{-}face}$ mutants therefore reflect a defective Hh signaling gradient. The addition of the palmitic acid moiety is required for establishing the SHH signaling gradient (Chen et al. 2004), therefore, *Hhat*$^{Cre\text{-}face}$ mutants provide a model for examining the role of gradient signaling of all Hh proteins throughout development.

Shh is differentially expressed in Hhat$^{Cre\text{-}face}$ *and Skn*$^{-/-}$ *embryos*

Interestingly, *Skinny hedgehog (Skn)* mutants have defects in the palmitoylation of Hh proteins, but exhibit a normal pattern of *Shh* expression (Chen et al. 2004), indicating differences between our insertional mutant in comparison to the classic *Skn* knockout. Indeed, Shh transcript and protein are absent in *Hhat*$^{Cre\text{-}face}$ mutants at 9.5dpc, while only SHH protein is affected in *Skn*$^{-/-}$ embryos (Chen et al. 2004). Additionally, despite the altered SHH signaling in the neural tube of *Skn*$^{-/-}$ embryos, it was not reported to be disrupted in other tissues where SHH is secreted, such as the notochord and pharyngeal endoderm (Chen et al. 2004). This difference between *Hhat*$^{Cre\text{-}face}$ *and Skn* mutants has significant affects on the overall

morphology of the mutant embryos; *Skn*$^{-/-}$ embryos are postnatal lethal and exhibit dwarfism (Chen et al. 2004), defects less severe in comparison to *Hhat*$^{Cre\text{-}face}$ mutant embryos. In contrast, *Hhat*$^{Cre\text{-}face}$ mutants are embryonic lethal at 18.5dpc and exhibit extensive craniofacial and body wall defects.

The alterations in Shh transcripts and protein in *Hhat*$^{Cre\text{-}face}$ mutants are likely the result of regulatory feedback loops involving *Shh* and *Gli* family members. The *Gli* genes (*Gli1-3*) are the nuclear effectors of SHH signaling (Ruiz i Altaba 1999). *Gli1* and *Gli2* have well characterized roles as positive regulators of *Shh* targets and are directly activated by SHH (Ruiz i Altaba et al. 2003). In contrast, *Gli3* can act as a transcriptional activator or repressor, a function dependent upon C-terminal modification of *Gli3* into the repressor form, *Gli3*^{Rep} (Sasaki et al. 1999). *Gli3*^{Rep} is a potent repressor of SHH activity and is normally inhibited by the presence of SHH signaling (Litingtung and Chiang 2000); Indeed, *Gli3*^{Rep} is dramatically upregulated throughout the neural tube of *Shh*$^{-/-}$ embryos. Once activated, *Gli3*^{Rep} inhibits *Shh* transcription (Ruiz i Altaba et al. 2003).

In *Hhat*$^{Cre\text{-}face}$ mutants, *Shh* would initially be transcribed and translated at early developmental stages, but would not undergo the dual post-translational modification due to lack of *Hhat*. As evidenced by SHH immunohistochemistry at 9.5dpc, *Hhat*$^{Cre\text{-}face}$ mutants exhibit a global downregulation of SHH signaling thereby removing the inhibition of the *Gli3*^{Rep} and ultimately resulting in the downregulation of *Shh* at the transcriptional level as a secondary defect. In contrast, *Skn*$^{-/-}$ embryos lack SHH protein in the neural tube and exhibit a slight reduction of SHH in the

developing limb bud. If SHH signaling is maintained in other regions such as the pharyngeal endoderm and notochord, it would not result in a dramatic upregulation of *Gli3*^{Rep} in these regions and *Shh* transcripts would be normal. Indeed, *Shh* is seen in the pharyngeal region and notochord of *Skn*$^{-/-}$ mutants. Collectively, the lack of SHH signaling throughout *Hhat*$^{Cre\text{-}face}$ mutants directly contributes to the more severe phenotype.

The phenotype characterized in *Hhat*$^{Cre\text{-}face}$ mutants in comparison to *Skn*$^{-/-}$ embryos may also be indicative of strain background differences. Humans with defective SHH signaling exhibit a wide-range of craniofacial phenotypes, ranging from clinically normal to very severe, which are attributed to SHH modifiers and background differences reflecting the individual variation within the human population (Belloni et al. 1996b; Wallis and Muenke 2000). Background differences in mouse strains have been shown to contribute to different phenotypes in other craniofacial syndromes. Treacher Collins Syndrome (TCS) is an autosomal dominant disorder resulting from the haploinsufficiency of *TCOF1*. TCS is characterized by the hypoplasia of mid-facial structures (Dixon et al. 2006) and is highly penetrant in human populations but with varying severity (Dixon et al. 1997). *Tcof1*$^{+/-}$ embryos, the mouse model of TCS, exhibit varying degrees of severity depending on the background strain (Dixon and Dixon 2004). Considering the importance of background modifiers in the severity of TCS and the array of phenotypes associated with disrupted SHH signaling, it would not be surprising if background was contributing to the severity of defects identified in *Hhat*$^{Cre\text{-}face}$ mutants.

Branchial Arch Patterning is disrupted in Hhat$^{Cre\text{-}face}$ Mutants

During development, the mandible is patterned in a proximo-distal gradient dependent upon *Fgf8* and *Bmp4* expression, ultimately resulting in the specification of lower jaw derivatives, such as odontogenic and skeletogenic precursors (Tucker et al. 1999; Liu et al. 2005a). *Fgf8* and *Bmp4* are expressed in adjacent domains of the developing mandible (Bennett et al. 1995; Crossley and Martin 1995) and are regulated by SHH; *Shh*$^{-/-}$ embryos (Yamagishi et al. 2006; Haworth et al. 2007) show a specific absence of both *Fgf8* and *Bmp4*. Additionally, studies in which the pharyngeal endoderm, a source of SHH, was ablated in chick embryos resulted in the absence of *Fgf8* and *Bmp4* (Brito et al. 2006), indicating that SHH signaling from the pharyngeal endoderm is required for the maintenance these genes in the development of the lower jaw. Consistent with previous reports in *Shh*$^{-/-}$ embryos (Yamagishi et al. 2006; Haworth et al. 2007), retroviral experiments (Abzhanov and Tabin 2004), and chick ablation experiments (Moore-Scott and Manley 2005; Brito et al. 2006), analysis of *Hhat*$^{Cre\text{-}face}$ mutants revealed a complete absence of *Fgf8* and *Bmp4* in the proximal and distal branchial arch ectoderm (Fig. 44), respectively. Interestingly, both genes were expressed in the nasal region, despite the fusion of the medial and lateral nasal prominences into a single nasal prominence.

The specific loss of *Fgf8* and *Bmp4* in the mandible of mutant embryos underlies multiple defects in the development of the lower jaw. Indeed, *Fg8* is required for the development of molar teeth (Tucker and Sharpe 2004) and restricts

odontogenic precursors to the rostral half of the mandible (Tucker et al. 1999); conversely, development of the incisors is regulated by *Bmp4* in the distal mandible (Tucker and Sharpe 2004). At 14.5dpc, the early primordia of incisor and molar teeth were present in $Hhat^{Cre\text{-}face}$ mutants but cease development; by 17.5dpc, mutant embryos exhibit tooth agenesis. Overall, the lack of identifiable molar and incisor teeth in $Hhat^{Cre\text{-}face}$ embryos is consistent with the role of *Fgf8* and *Bmp4* in the maintenance of early tooth primordia.

Additionally, both *Fgf8* and *Bmp4* are positive regulators of cartilage outgrowth in the mandible. In the lower beak of chick embryos (Abzhanov and Tabin 2004), a derivative of the mandibular prominence, overexpression of *Fgf8* results in enhanced chondrogenesis *in vitro* and *in vivo* (Abzhanov and Tabin 2004). Conditional inactivation of *Bmp4* in the mandibular ectoderm results in a severely reduced and often absent mandible, indicating *Bmp4* in the maintenance of chondrogenic precursors in the developing jaw (Liu et al. 2005a). In $Hhat^{Cre\text{-}face}$ mutants, the mandible is reduced beginning at 10.5dpc and is abnormally fused by 14.5dpc. Additionally, small circular condensations of cartilage reminiscent of Meckel's cartilage were present within the developing mandible of mutant embryos but were significantly delayed in comparison to heterozygote littermates (data not shown). The specific loss of *Fgf8* and *Bmp4* in the mandible of $Hhat^{Cre\text{-}face}$ mutants at early developmental stages results in the lack of the distal mandibular bone by 17.5dpc (Fig. 48). Collectively, these data are consistent with previous findings demonstrating the requirement of *Fgf8* and *Bmp4* in the cartilage maintenance and

outgrowth. Collectively, the loss of SHH in *Hhat*$^{Cre\text{-}face}$ mutants results in the downregulation of *Fgf8* and *Bmp4* in the mandible and results in the lack of mandibular ossification seen at late developmental stages.

Neural Crest Cell & Cranial Nerve Defects are secondary to Disrupted Hh Signaling

Analysis of the neural crest cell induction using the general crest cell markers *Crabp1* and *Snail* revealed comparable numbers of neural crest cells in *Hhat*$^{Cre\text{-}face}$ mutants and *Hhat*$^{+/Cre\text{-}face}$ embryos (Fig. 45). Additionally, lineage tracing analysis examining the entire population of neural crest cells using *Wnt1-cre* did not reveal decreased neural crest cells in *Hhat*$^{Cre\text{-}face}$ embryos (Fig. 46); mutant embryos had *LacZ*$^{+}$ neural crest cells which had populated the FNP. Furthermore, cells were migrating in the r2/r4 migratory streams populating BA1/BA2. Although, general markers of the crest cell population were normal, *Hhat*$^{Cre\text{-}face}$ mutants exhibited decreased *Sox9*$^{+}$ and *Sox10*$^{+}$ neural crest cells, indicating lineage specific crest cell defects. The decreased number of cells may indicate a cell fate switch in the mutant embryos, or perhaps, delayed differentiation. Overexpression of *Sox10* using *in ovo* electroporation results in an increased number of migratory neural crest cells, although the cells fail to express any differentiation markers up to six days after electroporation, indicating that increased *Sox10* expression results in the maintenance of undifferentiated states (McKeown et al. 2003). Additionally, SHH is required by neural crest cell for the prevention of apoptosis (Ahlgren and Bronner-Fraser 1999), and the loss of SHH in *Hhat*$^{Cre\text{-}face}$ embryos may cause decreased *Sox9*$^{+}$ and *Sox10*$^{+}$

neural crest cells due to increased apoptosis as a secondary defect; this is supported by the increased Caspase-3 staining in the head mesenchyme and maxillary and mandibular prominences. Overall, Hh signaling is likely required for maintenance, specification, or survival of *Sox9* and *Sox10*$^{+}$ neural crest cells but, as a whole, is not required for the induction process.

Although *Hhat*$^{Cre\text{-}face}$ mutants do not exhibit neural crest cell induction defects, analysis of *Wnt1-cre* lineage tracing revealed abnormal development of the cranial nerves. In neurofilament stained embryos, the occulomotor nerve was absent (Fig. 47), which most likely results as a secondary defect due to the absence of SHH in the ventral neural tube and dorsalization of the CNS (Chiang et al. 1996; Ericson et al. 1996; Briscoe et al. 2001). Additionally, the remaining ganglia were reduced and CN IX and X were abnormally fused (Fig. 47). These defects were also present in mutants processed for additional CN markers, including *Eya2* and *Sox10*. The contribution of neural crest and sensory placodes appeared normal in *Hhat*$^{Cre\text{-}face}$ embryos, indicating that the fusion defect does not result from the abnormal development of either of these cell types, but rather from a requirement of Hh signaling in the positioning of the ganglia within the head mesenchyme.

Interestingly, conditional inactivation of Hh signaling in cranial neural crest cells in *Wnt1-cre;Smo*^{NC} embryos does not lead to decreased neural crest cells or defects in CN ganglia formation (Jeong et al. 2004). *Hhat*$^{Cre\text{-}face}$ mutants do not exhibit any defects in the initial induction of neural crest cells although *Hhat*$^{Cre\text{-}face}$ embryos have significant disruptions in CN ganglia. The differences between the CN

defects of *Hhat*$^{Cre\text{-}face}$ and *Wnt1-cre;Smo*^{NC} embryos are most likely due to the specific inactivation of Hh signaling in the cranial neural crest in *Wnt1-cre;Smo*^{NC} embryos, while *Hhat*$^{Cre\text{-}face}$ mutants have a global downregulation of Hh signaling. Therefore, defects in *Hhat*$^{Cre\text{-}face}$ mutants may reflect two different phenotypes of Hh signaling: first, the role for Hh proteins, particularly SHH, in the proliferation and survival of neural crest cells contributing to CN ganglia; *Hhat*$^{Cre\text{-}face}$ mutants exhibit increased apoptosis and slightly decreased *Sox9* and *Sox10*$^{+}$ cells. Second, Hh signaling may be required in placodal tissues that also contribute to CN ganglia. Indeed, previous reports have indicated a specific role for SHH signaling in the formation (McCabe et al. 2007), positioning (Fedtsova et al. 2003) and specification of the trigeminal ganglia (Ota and Ito 2003). Overall, the cranial nerve defects in *Hhat*$^{Cre\text{-}face}$ mutants are more severe than those identified in conditional SHH signaling mutants due to the global downregulation as opposed to specific inactivation of Hh proteins in neural crest cells.

Cranial Vault Defects may reflect Disrupted Shh and Ihh Signaling

SHH signaling is required for cranial vault formation; *Shh*$^{-/-}$ embryos at 17.5dpc lack the dorsal bones of the skull vault, including the frontal and parietal bones, while the ventral bones of the skull are present (Chiang et al. 1996). Moreover, conditional inactivation of Hh signaling in neural crest cells results in the specific disruption of neural crest derived bone (Jeong et al. 2004). In addition to the well characterized roles for *Shh* in cranial bone formation, *Indian hedgehog (Ihh)* is

required for this process. *Ihh*$^{-/-}$ embryos exhibit a marked dwarfism resulting from reduced chondrocyte proliferation and an absence of bone calcification (St-Jacques et al. 1999). Collectively, both *Shh* and *Ihh* are required the proper development of the cranial vault (St-Jacques et al. 1999; Jeong et al. 2004).

Similar to *Shh*$^{-/-}$ embryos, *Hhat*$^{Cre\text{-}face}$ mutants have extensive skeletal defects, lacking all but the ventral bones of the skull (Fig. 48). Mutant embryos appear to have the basioccipital and exoccipital bones, although the exact identification of the bones is somewhat difficult due to the severe morphology of the embryos. The severity of skeletal defects identified in *Hhat*$^{Cre\text{-}face}$ mutants are a clear result of defects in chondrogenesis at 15.5dpc (Fig. 48), where the skull vault lacks significant cartilage staining; only the nasal cartilage is present. The similar phenotypes in *Shh*$^{-/-}$ embryos and *Hhat*$^{Cre\text{-}face}$ mutants indicate the loss of SHH signaling in *Hhat*$^{Cre\text{-}face}$ mutants results in the extensive defects of the cranial vault. Histological analysis of *Hhat*$^{Cre\text{-}face}$ mutants at 15.5dpc revealed defects in endochondral ossification and decreased *Ptc* activation (Fig. 49), indicating that IHH is also disrupted in the mutant embryos; as *Hhat* is responsible for palmitoylation of IHH, these defects are not unexpected. Interestingly, both the ex- and basioccipital bones had hypertrophic chondrocytes throughout the skeletal element, but the absence of proliferating and prehypertrophic chondrocytes suggests defects in chondrocyte proliferation and apoptosis. Hypertrophic chondrocytes eventually undergo apoptosis once they are a far enough distance from the end of the skeletal element, a process regulated in part by IHH (Kronenberg 2003). As *Hhat*$^{Cre\text{-}face}$ mutants lack a Hh signaling gradient, this

would indicate that defective IHH signaling within each skeletal element would prevent the apoptosis of hypertrophic chondrocytes, allowing for osteoblast invasion. Additionally, IHH is required for the initiation of the bone collar, the first site of osteogenesis to occur in the developing endochondral bone. *Hhat*$^{Cre\text{-}face}$ embryos lack an identifiable bone collar and the lack of *Ptc* activation in mutant embryos indicates that the lack of IHH signaling underlies the lack of bone collar formation in the mutants. Collectively, these data support the well characterized role of IHH in endochondral bone development as well as indicate the cartilage and bone defects characterized in *Hhat*$^{Cre\text{-}face}$ embryos results from defective SHH and IHH signaling.

In contrast to the defects in chondro- and skeletogenesis in *Hhat*$^{Cre\text{-}face}$ mutants, *Skn*$^{-/-}$ embryos at 18.5dpc have skeletal abnormalities that are less severe. The skeletal defects in *Skn*$^{-/-}$ embryos more closely resemble the skeletal phenotypes present in *Ihh*$^{-/-}$ embryos, both mutants exhibit dwarfism in comparison to wild-type littermates (St-Jacques et al. 1999; Chen et al. 2004), whereas, the skeletal abnormalities in *Hhat*$^{Cre\text{-}face}$ embryos more closely mimic *Shh*$^{-/-}$ mutants (Chiang et al. 1996). The resulting differences in skeletal phenotypes characterized in *Hhat*$^{Cre\text{-}face}$ and *Skn* mutants most likely reflects the differences in SHH signaling, *Hhat*$^{Cre\text{-}face}$ mutants exhibit a global downregulation of SHH, while *Skn*$^{-/-}$ embryos lack SHH in the floorplate (Chen et al. 2004). The differences in the disruption of the SHH signaling gradient may be reflective of the severity of cranial bone phenotypes between the two mutants. The disruption in IHH signaling in *Hhat*$^{Cre\text{-}face}$ and *Skn* mutants requires additional examination to identify the differences, if any, exist

between the mutant embryos. As SHH exhibits varying degrees of disruption between the *Hhat/Skn* mutants, it would not be unexpected for IHH to be differentially disrupted as well. Finally, background strain differences may be contributing to the severity of phenotypes between the two mutants.

We have identified a novel phenotype of HPE resulting from the insertional disruption of *Hhat,* the gene required for palmitoylation of Hh proteins. *Hhat*$^{Cre\text{-}face}$ mutants lack Hh signaling throughout the developing embryo, ultimately resulting in increased apoptosis and extensive craniofacial defects. Mutant embryos have branchial arch patterning defects and lack *Fgf8* and *Bmp4* in the mandible, genes that are directly regulated by SHH signaling from the pharyngeal endoderm. Additionally, Hh signaling appears to be important for the positioning of CN IX and X as *Hhat*$^{Cre\text{-}face}$ mutants exhibit a novel fusion defect of the CN ganglia. Finally, *Hhat*$^{Cre\text{-}face}$ mutants have severe cartilage and bone defects at late developmental stages, most likely reflecting disrupted SHH and IHH signaling, as both of these genes are required for proper bone development. As *Hhat* is required for the palmitoylation of Hh proteins and the establishment of the Hh signaling gradient, the lack of Hh signaling in *Hhat*$^{Cre\text{-}face}$ mutants results in multiple craniofacial defects and highlights the importance of Hh signaling in craniofacial development and the etiology of HPE.

E) Experimental Methods

Mouse lines and maintenance

Mice were housed in the Laboratory Animal Services Facility at the Stowers Institute for Medical Research according to IACUC animal welfare guidelines. *Hhat*$^{+/Cre\text{-}face}$ mice were maintained on a CD1 background; genotyping as preformed as described below. The *Gli3*^{Xt} (Hui and Joyner 1993), *Patched1(Ptc)LacZ* (Goodrich et al. 1997), *Rosa 26 Reporter (R26R)* (Soriano 1999), *Shh* (Chiang et al. 1996), and *Wnt1-cre* (Chai et al. 2000; Jiang et al. 2000) mice were maintained as previously reported. For embryo collection, dams were sacrificed by cervical dislocation; day of plug was noted as 0 *days post coitum* (dpc). Embryos were removed from maternal tissue at the following stages: 8.5, 9.5, 10.5, 11.5, 14.5, 15.5, and 17.5dpc; embryos were fixed and yolk sacs collected for genotyping.

Identification of the Cre-face Transgene Insertion Site

The insertion location of the *Cre-face* transgene was identified using the Vectorette kit (Sigma, St. Louis, MO). A *Cre-face*;Vectorette DNA library was created using the EcoRI-Vectorette unit according to manufacturer's instructions. To amplify clone DNA containing the transgene and surrounding genomic region, the primer (5'-ACA TCT GGG GTG AAG GGA ATT AGG GAG TTG-3') was used in addition to the Vectorette-specific primer to amplify DNA bands containing the integration site. A step-down PCR was used according to manufacturer's instructions; a 5kb band, clone E1N3, was gel-purified (Gel Extraction Kit, Qiagen,

Valencia, CA) and sequenced using the Vectorette sequencing primer.

Verification of transgene insertion site was performed using PCR in wildtype, heterozygous, and mutant genomic DNA from embryos at 10.5dpc. Amplification of the region spanning the insertion site used the transgene-specific primer (5'-TGG TTA CCT TCC TCC AGA TAG TATG-3') and *Hhat*-specific primer (5'-CAC TTG CTA ACT AGA AGG AAC TTCC-3') produced a 250bp band; wildtype primers (5'-CCT GGG AAG GAA AAA CCA ATA TGTA-3') and (5'-GGT CCT ATC ATG CTA CCA AGA AA-3') amplified a 1.4kb band. Samples were denatured at 94°C for 30sec, annealed at 57°C for 30sec, and extended at 72°C for 30sec for 30 cycles for both reactions; PCR bands for the wildtype and mutant reactions were gel purified and sequenced, confirming *Hhat* as the gene disrupted by the *Cre-face* transgene.

To confirm the absence of *Hhat* mRNA in $Hhat^{Cre\text{-}face}$ mutants, RNA was isolated from $Hhat^{Cre\text{-}face}$ litters (RNeasy kit, Qiagen, Valencia, CA) and cDNA library was created using the Superscript first strand kit (Invitrogen, Carlsbad, CA). Primers (5'-AGG TTC TGG TGG GAC CCT GTGT-3') and (5'-AGA AAG CAG TGT CCC CAA CAGG-3') were used to amplify the full length *Hhat* mRNA in Wt, Het, and Mut embryos. Primers to glyceraldehyde 3-phosphate dehydrogenase *(Gapdh)* (5'-AGC CTC GTC CCG TAG ACA AAAT-3') and (5'-ACC AGG AAA TGA GCT TGA CAAA-3') were used as an internal positive control.

In situ hybridization

Embryos were collected as described above, fixed O/N in 4% paraformaldehyde (PFA) at 4°C, dehydrated in methanol (MeOH), and stored at -20°C until used in the staining protocol. *In situ* hybridizations were performed following the standard protocol described by Nagy et al. (2003). Anti-sense digoxigenin-labeled mRNA riboprobes were synthesized for *Bmp4* (R. Arkell), *Crabp1* (S. Schneider-Maunoury), *Eya2* (K. Melton), *Fgf8* (I. Mason), *Shh* (A. McMahon), *Snail* (A. Nieto), *Sox9* (R. Krumlauf), and *Sox10* (M. Gassmann).

β-galactosidase Staining

To stain for β-galactosidase, *AP-2cre* mice were mated to *Rosa 26 reporter (R26R)* mice and embryos were collected at 9.5 and 10.5dpc as described above. Briefly, embryos were fixed on wet ice for 20-30min in the Tissue Fixative Solution (Millipore, Billerica, MA), washed in Tissue Rinse Solution A for 30min and Tissue Rinse Solution B for 5min at RT. Embryos were incubated O/N at 37°C in Tissue Stain Solution with X-gal (40mg/mL in DMF) (Invitrogen, Carlsbad, CA). After incubation, embryos were washed PBS and re-fixed O/N in the Tissue Fixative Solution. Embryos were processed in paraffin, cut in 10micron sections, and counterstained in Nuclear Fast Red (Sigma, St. Louis, MO).

For β-gal staining on sections, 15.5dpc embryos were harvested and fixed in LacZ fixative (0.9% 25%glutaraldehyde, 10% 0.5M EGTA, and 10% 1M $MgCl_2$ in PBS) for 2.5hrs at 4°C. Embryos were processed through a sucrose gradient (15,

30% sucrose in PBS) and snap frozen in OCT. Eight micron sections were cut and re-fixed in LacZ fixative for 10min at RT; sections were washed in LacZ wash buffer (0.2% $MgCl_2$, 0.01% NaDOC, 0.02% NP40 in PBS) three times, 5min each. β-gal staining was developed using a LacZ stain solution (0.002% Potassium ferrocyanide, 0.01% Potassium ferricyanide, 0.04% X-gal (25mg/mL in DMF) in LacZ wash buffer) to the desired intensity and washed three times 5min after developing. Sections were counterstained in NFR and washed in distilled water for 1-2min; sections were mounted and photographed using a Ziess Axioplan microscope and processed using Photoshop CS2 (Adobe, San Jose, CA).

Immunohistochemistry

For whole-mount staining using a Neurofilament antibody, embryos were fixed in 4% PFA O/N at 4°C and dehydrated in a graded MeOH series; dehydrated embryos were bleached in methanol:DMSO:30% H_2O_2 (4:1:1) for 5hrs at RT and rehydrated in 50% methanol:PBS and 15% methanol:PBS, PBS for 30minutes each. For blocking, embryos were washed in PBSMT (2% milk powder, 0.1% Triton X-100 in PBS) twice for 1hour at RT. Embryos were incubated in primary antibody to Neurofilament (2H3) diluted at 1:250 O/N at 4°C in PBSMT. Embryos were rinsed in PBSMT and incubated in secondary antibody using a 1:200 dilution in PBSMT of HRP-coupled goat anti-rabbit IgG (Jackson Immunoresearch, West Grove, PA). For color development, embryos were rinsed in PBSMT and PBT (0.2% BSA, Sigma, 0.1% Triton X-100) three times, 20minutes each at RT and washed in 3,3-

Diaminobenzidine (0.3mg/mL) (Sigma, St. Louis, MO) in PBT for 20minutes; 0.03% H_2O_2 was added and color was developed to the desired intensity.

For section immunohistochemistry, litters were collected at 9.5 and/or 10.5dpc and fixed O/N in 1% PFA at 4°C. Embryos were processed through a sucrose gradient (15%, 30% sucrose in PBS), mounted in Tissue Tek O.C.T. (VWR, West Chester, PA) and sectioned at 10microns. Sections were rinsed 3X in PBT (PBS with 0.1% Triton X-100) for 5min and blocked in 10% normal goat serum (Invitrogen, Carlsbad, CA) in PBT for 1hr at RT. Slides were incubated in primary antibody diluted in 10% goat serum/PBT O/N at 4°C. The mouse monoclonal antibodies to cleaved Caspase-3 (Cell Signaling Technologies, Danvers, MA), anti-phospho Histone H3 (Upstate/Millipore, Billerica, MA), anti-BrdU (Abcam, Cambridge, MA), and to SHH (5e1) were used at 1:500 (Caspase-3, anti-pH3, anti-BrdU) and 1:25 (5e1), respectively. To stain for BrdU, slides were incubated in DNaseI at 1:300 (Invitrogen, Carlsbad, CA) in React3 buffer for 30min at 37°C to nick the DNA prior to blocking with 10% NGS.

Slides were rinsed 3X 10min in PBT at RT on shaker and incubated in the appropriate Alexa 488 or 594 secondary antibody at 1:250 (Molecular probes/Invitrogen, Carlsbad, CA) for 2hrs at 4°C. Sections were counterstained with a 1/1000 dilution of 2 mg/ml DAPI (Sigma, St. Louis, MO) in PBS for 5minutes, followed by rinses in PBS; slides were mounted with fluorescent mounting medium (DakoCytomation, Carpinteria, CA). All images were collected using a Ziess Axioplan microscope and processed using Photoshop CS2 (Adobe, San Jose, CA).

Antibodies to SHH (5e1) and Neurofilament (2H3) were obtained from the Developmental Studies Hybridoma Bank developed under the auspices of the NICHD and maintained by the University of Iowa, Department of Biological Sciences (Iowa City, IA 52242).

Hematoxylin and Eosin staining

Hhat$^{+/Cre\text{-}face}$ and *Hhat*$^{Cre\text{-}face}$ embryos were harvested at 14.5dpc and fixed O/N in 4% PFA at 4°C. Samples were dehydrated through a graded ethanol series, cleared in xylene, and embedded in liquid paraffin. Embryos were sectioned at 12microns and deparaffinized in xylene, and hydrated in graded alcohols to water. Sections were stained in Shandon hematoxylin for 1min and 30sec, differentiated in 1% aqueous acid alcohol for 10sec, blued in PBS for 30 seconds, and stained in eosin for 30sec. Sections were dehydrated in graded alcohols, cleared in xylene, and mounted in permanent mounting medium. All images were collected using a Ziess Axioplan microscope and processed using Photoshop CS2 (Adobe, San Jose, CA).

Cartilage & Bone Staining

Embryos were collected at 15.5 and 17.5dpc and fixed in 95% EtOH O/N. Embryos were washed in a stain solution containing 0.5% Alizarin red (Sigma, St. Louis, MO) and 0.4% Alcian blue 8X (Sigma, St. Louis, MO) in 60% EtOH O/N at RT. For 14.5dpc embryos, soft tissue was dissolved in 1% KOH for three hours and transferred to 0.25% for 30min. For 17.5dpc staining, the embryos were anesthetized in PBS for 1hr at 4°C, fixed O/N in 95% EtOH, skinned and eviscerated prior to

staining; all remaining soft tissue was dissolved in 2% KOH for six hours and transferred to 0.25% KOH for 30min. Embryos were cleared in glycerol:KOH (20%:0.25%; 33%:0.25%; 50%:0.25%). Embryos were stored in 50% glycerol:0.25% KOH until photographed.

IX. Chapter Four: Conclusions

Gcnf is required for Neural Crest Cell Induction

Neural crest cell induction is regulated by multiple signaling pathways in a species dependent manner and includes BMP, FGF, NOTCH, PAX, and WNT signaling pathways. Although these signaling cascades are involved in crest cell formation in multiple species, the key regulator of this process in mouse had not been extensively addressed. Therefore, we set out to determine which of these signaling pathways, if any, are required in the production of neural crest cells in the mouse using *in vivo* and *in vitro* approaches.

Our genetic analyses of *RBP-Jκ*$^{-/-}$ and *Fgf8*$^{\Delta 2,3/\Delta 2,3}$ mutants as well as *Pax3*$^{-/-}$;*Pax7*$^{-/-}$ double mutants clearly demonstrate that these genes are not required for neural crest cell formation in the mouse. Indeed, the neural crest cell markers *Crabp1, Snail*, *Sox9*, and *Sox10* were all present in the mutant embryos examined, with few exceptions. For example, *Sox9* and *Sox10* are both decreased in *RBP-Jk*$^{-/-}$ embryos, which most likely reflects roles for NOTCH signaling in neural crest cell lineage selection. Further, *Pax3*$^{-/-}$;*Pax7*$^{-/-}$ double mutants also exhibit decreased *Crabp1*$^{+}$ and *Sox10*$^{+}$ neural crest cells, although the decreased number of crest cells appears to be indicative of defects in the maintenance of the neuroepithelium; double mutant embryos have a significantly thinner neural plate in comparison to their littermates. Hence, *Pax3* and *Pax7* may be required for maintenance and proliferation of the neural plate rather than the induction of neural crest cells; additional analyses

of *Pax3*$^{-/-}$;*Pax7*$^{-/-}$ double mutants is necessary to determine the specific role of these *Pax* genes in neural plate maintenance.

Although these genes are not required for neural crest cell induction, each of these signaling pathways may be involved in later aspects of neural crest cell patterning and differentiation. Indeed, it would be interesting to examine the roles of each of these genes in neural crest cell development, perhaps using conditional mutants. Inactivation of NOTCH signaling specifically in neural crest cells may address lineage specific roles for *Sox9* and *Sox10* regulation. Although previous reports have removed NOTCH signaling in neural crest cells using *Wnt1-cre*, the authors focus their efforts on the role of *Notch* in gliogenesis of the central and peripheral nervous systems (Taylor et al. 2007). It would be useful to analyze these mutants at later developmental stages to determine if any alterations in cell fate are present in the developing frontonasal prominence or cranial nerve ganglia. Previous reports have indicated a role for NOTCH signaling in the specification of chondrocytes (Nakanishi et al. 2007), hence, mutant embryos may also exhibit defects in cartilage and bone formation.

In addition to our *in vivo* analyses of neural crest cell formation, our *in vitro* analyses did not indicate any of these pathways as required for crest cell induction. Treatment with BMP, NOTCH, and WNT signaling antagonists failed to inhibit the expression of *Sox10*. Treatment with SU5402, a FGFR signaling antagonist, did prevent the expression of *Sox10* in the explant cultures, but concomitantly resulted in decreased expression of the neural plate marker *Sox2*. Hence, the decreased

expression of *Sox10* may not reflect a direct role for FGF signaling in neural crest cell formation but may instead reflect decreased neuroepithelial progenitors. Varying the concentration and exposure to SU5402 in an attempt to circumvent these defects resulted in the continued decrease in both *Sox2* and *Sox10* expression, thereby preventing us from elucidating the exact role of FGF signaling in neural crest cell formation *in vitro*. Furthermore, analysis of *Fgf8* null embryos ($Fgf8^{\Delta 2,3/\Delta 2,3}$) did not result in neural crest cell formation defects, indicating that if FGF signaling does regulate crest cell induction, it does not elicit its affects via FGF8. At this point, it would be difficult to ascertain a direct role for FGF signaling in neural crest cell induction, *Fgf8* is the most likely family member to regulate this process as FGF8 is a key regulator of crest cell induction in *Xenopus* (Monsoro-Burq et al. 2003). As *Fgf8* is not required for crest cell formation or neural plate maintenance in the mouse, this leaves the potential for other *Fgf* family members to be involved. *Fgf4* has a similar domain of expression within the primitive streak (Niswander and Martin 1992) and plays similar roles in limb bud outgrowth as *Fgf8* (Niswander et al. 1993; Lewandoski et al. 2000; Sun et al. 2002), hence it is plausible that *Fgf4* could be involved in neural plate maintenance and/or neural crest cell formation. $Fgf4^{-/-}$ embryos are embryonic lethal (Feldman et al. 1995) at the early postimplantation stage and reports analyzing conditional mutants have largely been focused on the limb bud (reviewed in (Mariani and Martin 2003)). Hence to ascertain a role for *Fgf4*, if any, in neural crest cell induction, a conditional inactivation strategy must be used. Finally, analyses of *Fgf Receptor 1* (*FgfR1)* (Trokovic et al. 2003) and *2*

(*FgfR2)* (Xu et al. 1998) mutants still generate neural crest cells indicating that to determine the specific role of FGF signaling in neural crest cell induction analysis of compound conditional *FgfR* knockouts would be required.

Our previous analyses did not indicate any of the known signaling pathways as a requirement for murine neural crest cell induction to occur. In an attempt to identify novel regulators of neural crest cell induction, we identified *Germ cell nuclear factor (Gcnf)* from a microarray screen performed in *Tcof1*$^{+/-}$ embryos (Jones et al. 2008), the mouse model of Treacher Collins Syndrome (TCS); *Gcnf* was downregulated almost two-fold in *Tcof1*$^{+/-}$ compared to wildtype littermates (N. Jones and P. Trainor, unpublished). *Gcnf* is expressed during neural crest cell formation and is most intense in the dorsal neural folds, the area from which neural crest cells are induced; additionally, *Gcnf* is expressed in migratory neural crest cells.

The downregulation of *Gcnf* in *Tcof1*$^{+/-}$ embryos, which exhibit decreased neural crest cells, and the expression of *Gcnf* in migratory neural crest cells suggested that *Gcnf* may be a novel regulator of neural crest cell development. Analyses of neural crest cell makers in *Gcnf*$^{-/-}$ embryos revealed crest cell formation defects; *Snail, Crabp1*, and *Sox9* were all absent in *Gcnf* mutants and *Sox10* was abnormally expressed and cells significantly reduced in number. These defects were not a result from altered patterning of the neural plate as evidenced by the markers *Sox2, Wnt1*, and *Pax3*, indicating defects in the transition from a neuroepithelial to neural crest cell. Indeed, analyses of SOX2 and the mitotic marker phospho Histone H3 revealed prolonged maintenance of the neural plate and increased numbers of mitotic cells in

Gcnf$^{-/-}$ embryos. The enhanced expression of SOX2 in *Gcnf* mutants indicates prolonged maintenance of stem cell-like states within the neural plate, thereby preventing the transition of a neuroepithelial to neural crest cell. Additionally, the identification of putative *Gcnf* binding sites in neural crest cell specific genes such as *Snail1* and *Snail2, Sox9,* and *Sox10* indicate a direct role for *Gcnf* in the activation of neural crest cell formation and migration (via *Snail1* and *Snail2*) and differentiation paradigms (*Sox9, Sox10*). Current analyses are aimed at determining the extent of proliferation and apoptosis in *Gcnf* mutants which will further characterize the defects in neural plate maintenance as well as chromatin immunoprecipitation (ChIP) assays to determine the extent of *Gcnf* regulation in crest cell formation and differentiation.

Although *Gcnf*$^{-/-}$ embryos show a clear absence of neural crest cell formation, these defects are compounded by the embryonic lethality of the mutants; *Gcnf* mutants are lethal at 10.5dpc due to chorioallantoic fusion defects (Chung et al. 2001), thereby requiring the examination of conditional *Gcnf* mutants. *Gcnf* floxed mice have been generated (Lan et al. 2003) and, in conjunction with *Wnt1-cre*, would allow one to examine the specific neural crest cell defects present without any compounding abnormalities such as circulatory defects. In theory, *Wnt1-cre*$^{+}$*;Gcnf*$^{fx/fx}$ mutants would exhibit a lack of crest cell formation, potentially along the entire anterior-posterior axis, but would most likely die between 10.5-12.5dpc due to failure of cardiac neural crest cells to populate the heart. In these mutants, frontonasal prominence development would be altered; no neural crest cells would be present to give rise to the mesenchyme in this region. Additionally, early jaw

development would be impaired; neural crest cells would not migrate into the branchial arches, resulting in a lack of jaw cartilage primorida. Analyses of conditional *Gcnf* mutants would be a useful series of experiments to examine the specific neural crest cell defects resulting from the removal of *Gcnf*.

The results discussed herein provide clear evidence that *Gcnf* is a novel regulator of neural crest cell induction, hence, it is interesting to speculate whether *Gcnf* is playing a similar role in other species. One common theme in regards to crest cell formation has emerged, that the process has thus far been shown to be species dependent. When one considers how evolutionarily important neural crest cells are as well as the fact that crest cell patterning and differentiation is conserved at multiple stages of development, it is somewhat counterintuitive to think that neural crest cell induction would not be more highly conserved. Although, considering that *Gcnf* acts upstream of neural crest cell induction in the mouse and may be responsible for the activation of neural crest cells specific gene paradigms, it is very attractive to suggest that *Gcnf* could be playing similar roles in other model systems, thereby unveiling a conserved mechanism regulating crest cell induction across multiple species. All of the current models used for examining neural crest cell development, *Xenopus* (Joos et al. 1996), avian (Adams et al. 2008), and zebrafish (Braat et al. 1999; Bertrand et al. 2007) have *Gcnf* homologues. Furthermore, *Gcnf* is expressed in migratory neural crest cells in avian embryos (Adams et al. 2008) and the neuroepithelium and branchial arches in *Xenopus* (Joos et al. 1996). Zebrafish have two *Gcnf* paralogues, *Gcnfa* and *Gcnfb*, each of which are expressed in the cranial ganglia and neural tube;

*Gcnf*a is also appears to be expressed in migratory neural crest cells (Bertrand et al. 2007).

The pattern of *Gcnf* expression is conversed across multiple species, potentially indicating that *Gcnf* may be regulating neural crest cell induction in these species as well. Each of these species is amenable to functional assays, including overexpression using electroporation or mRNA injection as well as knockdown assays with morpholinos or dominant negative constructs. Hence, it would be very informative to determine if under these conditions, whether neural crest cells are induced or inhibited when *Gcnf* is overexpressed or knocked down. Functional analyses in each of these species would be required to determine the exact role of *Gcnf* in neural crest cell induction. Collectively, *Gcnf* is required for regulating the formation and migration of neural crest cells in murine embryos and verification of these roles in other model organisms would further define the role for *Gcnf* in regulating crest cell induction upstream of the known signaling pathways required for this process.

The Role of FGF Signaling in the Developing Frontonasal Prominence

The frontonasal prominence is a midline craniofacial primordia populated by neural crest cells that gives rise to mid-facial structures, including the forehead, middle of the nose, and philtrum of the upper lip. The outgrowth and patterning of the FNP is critically important for the formation of these tissues, and given that neural crest cells populate this region to give rise to FNP derivatives, it is likely that

interactions between neural crest cells and the surrounding tissue layers are critical for FNP development. *Fgf8* is expressed in frontonasal ectoderm zone (FEZ), a region of tissue that corresponds to the upper beak in avian embryos (Hu et al. 2003; Marcucio et al. 2005), and is required for the proper outgrowth of the FNP (Hu et al. 2003). Although numerous studies have determined the role of FGF8 signaling in FNP outgrowth, to date, no studies have examined this process in the mouse. To determine if FGF8 signaling was required by neural crest cells in the outgrowth of the FNP, we used the Cre-LoxP system to analyze conditional *Fgf8* mutants using the *AP-2cre* driver.

Our analyses failed to elucidate the specific role of extrinsic FGF8 signaling in the frontonasal prominence due to the lack of overlapping expression domains of the *AP2-cre "Cre-face"* transgene and *Fgf8* within the FNP ectoderm. Previous reports have characterized the expression pattern of the *Cre-face* transgene as present in the FNP mesenchyme as well as the overlying ectoderm (Nelson and Williams 2004), whereas our *Cre-face* mice only express *AP-2cre* in the mesenchyme. Ultimately, this difference in expression resulted in the failure of the Cre recombinase to excise *Fgf8* from the FNP ectoderm.

AP-2cre "Cre-face" mice were originally generated and maintained using a FVB background strain (Nelson and Williams 2004); our *Cre-face* mice are maintained on a CD1 background. Therefore, the difference in expression patterns between two *AP-2cre* strains is most likely due to background strain differences. Although *AP-2cre* CD1 mice are not useful in excising genes from the FNP ectoderm,

the restricted expression of the *Cre-face* transgene indicates this Cre driver would be useful for conditional excision from the FNP mesenchyme. Currently, we are in the process of generating *Cre-face* mice on a FVB background, as originally reported (Nelson and Williams 2004). Once these mice are available, it would be useful to determine whether the *Cre-face* transgene is expressed in the FNP ectoderm and mesenchyme as initially described. If so, intercrossing *AP-2cre* FVB mice with conditional $Fgf8^{fx/fx}$ mice would allow one to address the specific role of FGF8 signaling in the developing of the FNP. Conditional *Fgf8* mutants where *Fgf8* has been excised from the neuroepithelium (Kawauchi et al. 2005) or branchial arch ectoderm (Trumpp et al. 1999; Macatee et al. 2003) have thus far been characterized, the specific role of *Fgf8* in the FNP ectoderm has yet to be examined.

Hhat is required for establishing the Hedgehog Signaling Gradient

In our studies examining the role of FGF8 signaling in the developing FNP, we mated *AP-2cre* mice to homozygosity for the *Cre-face* transgene ($AP\text{-}cre^{T/T}$), and identified a novel phenotype of holoprosencephaly (HPE) in the resulting *Cre-face* mutants. HPE results from the failure of the forebrain to divide during embryogenesis, thus remaining as a single-lobed brain structure, and is accompanied by a range of craniofacial defects, such as a single incisor, hypertelorism, or a nasal proboscis (Belloni et al. 1996a; Roessler et al. 1996). HPE is one of the most common neurological malformations to occur in humans (Muenke and Beachy 2000;

Wallis and Muenke 2000), understanding the etiology of this syndrome extremely important.

Cre-face mutants present with HPE by 9.5dpc and by 10.5dpc exhibit a fusion between the frontonasal and maxillary prominences. Given the nature of the forebrain and craniofacial defects apparent in *Cre-face* embryos and the relevance of HPE to humans, we determined that the *Cre-face* transgene integrated into Intron 9 of *Hedgehog acyltransferase (Hhat)*, the gene required for palmitoylation of Hedgehog (Hh) proteins (Pepinsky et al. 1998; Buglino and Resh 2008). $Hhat^{Cre\text{-}face}$ mutants have a clear disruption in SHH signaling as evidenced by SHH immunostaining and decreased *Patched (Ptc)* activation. $Hhat^{Cre\text{-}face}$;$PtcLacZ^{+}$ embryos lack a gradient of *LacZ* expression that is present in heterozygous littermates, instead *Ptc* activation is only present in localized sources of SHH such as the notochord. In these regions, *LacZ* is restricted to the sites of synthesis indicating that the gradient of Hh signaling is disrupted, which is consistent with the role of *Hhat* in establishing the Hh signaling gradient.

The loss of SHH results in increased apoptosis and neural crest cell and branchial arch patterning defects. Overall, this indicates a role for long-range signaling in the maintenance of neural crest cell lineage selection, resulting in cranial nerve fusion defects. Additionally, *Bmp4* and *Fgf8* are absent in the developing mandible, resulting in the absence of odontogenic precursors and early jaw cartilages. Finally, the loss of long-range Hh signaling results in cartilage and bone defects, which is indicative of disrupted SHH and IHH signaling. Indeed, defects in

endochondral ossification are readily identifiable in *Hhat*$^{Cre\text{-}face}$ mutants, likely reflecting the loss of IHH signaling, although this needs further characterization to determine the extent of IHH disruption. Our data analyses of *Hhat*$^{Cre\text{-}face}$*;PtcLacZ*$^{+}$ embryos revealed significant decreases in *Ptc* activation in the ex- and basioccipital bones in comparison to wildtype littermates, indicating defective IHH signaling during cartilage and bone development, thereby contributing to the extensive bone defects at late developmental stages. Direct analysis of IHH protein distribution in *Hhat*$^{Cre\text{-}face}$ mutants, or the expected lack thereof, would further support the role of *Hhat* in the palmitoylation of Hh proteins, in general, and the requirement of palmitoylation in establishing the Hh signaling gradient.

Hhat$^{Cre\text{-}face}$ mice provide a useful mechanism for studying how modulation of Hh signaling affects development; it has been widely accepted that a gradient of Hh signaling is required for the specification of multiple tissues, in particular, neuronal identity in the spinal cord (Briscoe et al. 1999; Briscoe et al. 2000; Wijgerde et al. 2002) and digit identity and outgrowth in the limb (Zhu et al. 2008). Additionally, recent reports have indicated that a temporal and concentration gradient of SHH is required for the generation of specific domains of neurons in the spinal cord (Dessaud et al. 2007), indicating that a Hh signaling gradient, as well as its maintenance, is particularly important for neuronal specification. *Hhat*$^{Cre\text{-}face}$ mutants, in contrast to classic knockouts of *Shh* and *Ihh*, initiate Hh protein synthesis, although any Hh protein synthesized is restricted to localized regions, such as the notochord. Any initial SHH/IHH production may activate short-range Hh signaling cascades in

adjacent tissues. Temporally speaking, harvesting *Hhat*$^{Cre\text{-}face}$ embryos shortly after Hh synthesis in a particular region of interest would allow one to examine the requirement of long-range Hh signaling in a given tissue. Furthermore, it would simultaneously indicate any roles for short-range Hh signaling adjacent to its sites of synthesis.

As Hh signaling is critically important in multiple regions of the developing embryo for patterning and outgrowth, it is not surprising that the numerous Hh signaling components are also under great scrutiny in attempts to understand the role of Hh proteins during development. Hence, multiple knockouts of the genes involved in the Hh signaling cascade have been created, including *Patched1 (Ptc)* (Goodrich et al. 1996), *Glioma associated protein 3 (Gli3)* (Hui and Joyner 1993), and *Smoothened (Smo)* (Zhang et al. 2001). Each of these genes is differentially modulated within the Hh cascade, Hh proteins directly bind to *Ptc*, their receptor, and cause the disinihibition of *Smo*; in turn, *Smo* activates certain members of the *Gli* family in a mechanism that remains poorly understood. Hence, intercrossing *Hhat*$^{Cre\text{-}face}$ mice to various Hh pathway members could provide useful insight into the requirement of Hh proteins during development. For example, *Ptc* (in the absence of SHH) inhibits Smo, targeting it for degradation. By intercrossing *Hhat*$^{Cre\text{-}face}$ and *Ptc* knockout mice (*PtcLacZ*), one can examine how the Hh signaling is transduced or altered in the absence of long-range Hh proteins, but in an environment when Smo is constitutively disinhibited. *Hhat*$^{Cre\text{-}face}$;*PtcLacZ*$^{+/+}$ double mutants would lack long-range Hh proteins, but in the absence of *Ptc*, Smo would not be repressed, and in theory, may

activate Hh targets. Additionally, examination of *Shh*$^{-/-}$;*Gli3*$^{-/-}$ double mutants (Litingtung and Chiang 2000; Rallu et al. 2002) results in the rescue of neuronal subtypes lost in *Shh*$^{-/-}$ embryos, indicating a negative feedback loop between *Shh* and *Gli3*. In *Hhat*$^{Cre\text{-}face}$ mutants, the lack of SHH signaling in the floorplate results in the loss of ventral neuron specification (A. Iulianella, P. Trainor, unpublished), similar to the defects in *Shh*$^{-/-}$ embryos. Could these alterations in neuronal specification be rescued in *Hhat*$^{Cre\text{-}face}$;*Gli3*$^{-/-}$ double mutants? Furthermore, would the defects in *Hhat*$^{Cre\text{-}face}$;*Gli3*$^{-/-}$ mutants resemble those characterized in *Shh*$^{-/-}$;*Gli3*$^{-/-}$ embryos? If not, could the differences potentially be due to the presence of short-range Hh signaling? Or perhaps, the disruption of other Hh proteins, such as IHH or DHH in *Hhat*$^{Cre\text{-}face}$;*Gli3*$^{-/-}$ double mutants? As *Hhat*$^{Cre\text{-}face}$ mutants lack Hh signaling, they provide a useful model for teasing out the specific requirements of the signaling gradient during development.

Finally, *Hhat*$^{Cre\text{-}face}$ mice were identified by mating *AP-2cre* CD1 mice to homozygosity, resulting in the HPE phenotype characterized herein. As previously discussed, we are in the process of generating *AP-2cre* mice on a FVB background, as originally reported. In humans, HPE manifests in a wide range of neurological and craniofacial anomalies due to variations in the human population and background modifiers. Although the *Cre-face* transgene would be present in Intron 9 of *Hhat* on a FVB background, the surrounding modifiers may be different. Therefore, it would be interesting to determine if there any phenotypic differences were present in *Hhat*$^{Cre\text{-}face}$ mutants on a FVB versus a CD1 background.

The data presented herein addresses two broad areas of neural crest cell development: their initial induction and formation as well as the genes and signaling pathways required for their proper patterning and differentiation. As a whole, the identification of *Gcnf* as a novel regulator of neural crest cell formation introduces a gene required upstream of the known signaling pathways of neural crest cell induction. Subsequent analyses of *Gcnf* function in other model organisms will determine if this gene is conserved in this process. Additionally, the identification of a novel phenotype of holoprosencephaly resulting from the disruption of *Hhat* provides a useful for tool for examining how modulation of Hh signaling, a critically important pathway used during embryogenesis, results in a varying degree of craniofacial and body wall defects. Further analyses of *Hhat* mutants in conjunction with other Hh pathway mutants will highlight the requirement of this signaling cascade in various tissues, including the craniofacial complex, spinal cord, and limb. Collectively, these studies have provided new insight into the formation and patterning of neural crest cells at multiple stages of development.

X. Chapter Five: Materials & Methods

Mouse lines and maintenance

AP-2cre, AP-2cre;Fgf8$^{+/fx}$, AP-cre;Fgf8$^{+/\Delta 2,3}$, CD1, *Fgf8$^{+/\Delta 2,3}$, Fgf8$^{fx/fx}$, Gcnf, Gli3^{Xt}, Patched1(Ptc)LacZ , RBP-Jκ, Rosa 26 reporter (R26R)*, *Shh*, and *Wnt1-cre* mice were housed in the Laboratory Animal Services Facility at the Stowers Institute for Medical Research according to IACUC animal welfare guidelines. For embryo collection, dams were sacrificed by cervical dislocation; day of plug was noted as 0 *days post coitum* (dpc). Embryos were removed from maternal tissue and fixed; yolk sacs collected for genotyping. Embryos were genotyped for the *AP-2cre* (Nelson and Williams 2004), *Fgf8$^{+/\Delta 2,3}$* (Meyers et al. 1998), *Fgf8$^{fx/fx}$* (Meyers et al. 1998), *Gcnf* (Chung et al. 2001), *Gli3^{Xt}* (Hui and Joyner 1993), *PtcLacZ* (Goodrich et al. 1997), *RBP-Jk* (de la Pompa et al. 1997), *R26R* (Soriano 1999), *Shh* (Chiang et al. 1996), and *Wnt1-cre* (Chai et al. 2000; Jiang et al. 2000) alleles as previously reported. *Pax3;Pax7* embryos were kindly provided by S. Tajbakhsh (Pasteur Institute).

Cranial Explant Cultures

For 24-hour cranial explant cultures CD1 dams were sacrificed 7.5dpc by cervical dislocation; embryos were removed from maternal tissue and dissected in Tyrode's solution (8.0g NaCl, 0.2g/L KCl, 0.2g $CaCl_2$, 0.21g/L $MgCl_2$, 0.057g NaH_2PO_4, 1.0g/L $NaHCO_3$, 1.0g/L Glucose in DEPC-H_2O). To harvest cranial explants, embryos were bisected into the cranial and posterior regions with insect

pins, and the cranial regions collected; all three germ layers of the explants were kept intact. Cranial explants were attached to 0.4μM cell culture insert membranes (Millipore, Billerica, MA) in 3mL DMEM/F12-high glucose (control) (Invitrogen, Carlsbad, CA) or in DMEM/F12-high glucose with the antagonists DAPT (Sigma, St. Louis, MO), Frizzled-8/Fc (R & D Systems, Minneapolis, MN), Noggin/Fc (R & D Systems, Minneapolis, MN), or SU5402 (Calbiochem, San Diego, CA) in DMEM-F12 and cultured at 37°C with 5% CO_2; culture times are as indicated. Antagonist treatment was as follows: DAPT at 25, 50, 75, or 100μM and SU5402 at 12.5, 25, 37.5, and 50μM in DMSO; Frizzled-Fc and Noggin-Fc were used at 1, 5, 10, 20, 50, and 100μg/μL in sterile PBS. Explants were examined for viability as indicated by beating heart tissue. After culturing, explants were fixed O/N in 4% PFA at 4°C; embryos were dehydrated in MeOH and processed for *in situ* hybridization.

For 8- and 12-hour SU5402 explant cultures, CD1 dams were sacrificed early on 8.0dpc by cervical dislocation; embryos were removed from maternal tissue and dissected in Tyrode's solution. For culture, two cuts were made in the yolk sac along the anterior-posterior axis, allowing for the planar attachment of the embryo to the cell culture insert membrane via the remaining extraembryonic membranes. Once attached with forceps, the developing amnion was removed from the neural plate region. Embryo explants were cultured in 37.5μM SU5402 for 8- or 12hrs; all cultures were viable as determined by the presence of beating heart tissue at the end of the culture period. Cultures were fixed in 4% PFA O/N at 4°C and processed for *in situ* hybridization.

Identification of the Cre-face Transgene Insertion Site

The insertion location of the *Cre-face* transgene was identified using the Vectorette kit (Sigma, St. Louis, MO). A *Cre-face*;Vectorette DNA library was created using the EcoRI-Vectorette unit according to manufacturer's instructions. To amplify clone DNA containing the transgene and surrounding genomic region, the primer (5'-ACA TCT GGG GTG AAG GGA ATT AGG GAG TTG-3') was used in addition to the Vectorette-specific primer to amplify DNA bands containing the integration site. A step-down PCR was used according to manufacturer's instructions; a 5kb band, clone E1N3, was gel-purified (Gel Extraction Kit, Qiagen, Valencia, CA) and sequenced using the Vectorette sequencing primer.

Verification of transgene insertion site was performed using PCR in wildtype, heterozygous and mutant genomic DNA from embryos at 10.5dpc. Amplification of the region spanning the insertion site used the transgene-specific primer (5'-TGG TTA CCT TCC TCC AGA TAG TATG-3') and *Hhat*-specific primer (5'-CAC TTG CTA ACT AGA AGG AAC TTCC-3') produced a 250bp band; wildtype primers (5'-CCT GGG AAG GAA AAA CCA ATA TGTA-3') and (5'-GGT CCT ATC ATG CTA CCA AGA AA-3') amplified a 1.4kb band. Samples were denatured at 94°C for 30sec, annealed at 57°C for 30sec, and extended at 72°C for 30sec for 30 cycles for both reactions; PCR bands for the wildtype and mutant reactions were gel purified and sequenced, confirming *Hhat* as the gene disrupted by the *Cre-face* transgene.

To confirm the absence of *Hhat* mRNA in $Hhat^{Cre\text{-}face}$ mutants, RNA was isolated from $Hhat^{Cre\text{-}face}$ litters (RNeasy kit, Qiagen, Valencia, CA) and cDNA

library was created using the Superscript first strand kit (Invitrogen, Carlsbad, CA). Primers (5'-AGG TTC TGG TGG GAC CCT GTGT-3') and (5'-AGA AAG CAG TGT CCC CAA CAGG-3') were used to amplify the full length *Hhat* mRNA in Wt, Het, and Mut embryos. Primers to glyceraldehyde 3-phosphate dehydrogenase *(Gapdh)* (5'-AGC CTC GTC CCG TAG ACA AAAT-3') and (5'-ACC AGG AAA TGA GCT TGA CAAA-3') were used as an internal positive control.

In situ hybridization:

In situ hybridization was performed following the standard protocol described by Nagy et al. (2003). Briefly, embryos were fixed, dehydrated in a graded MeOH series, and stored at -20°C until ready for use in the hybridization protocol. Anti-sense digoxigenin-labeled mRNA riboprobes were synthesized for *Bmp4* (R. Arkell), *Crabp1* (S. Schneider-Maunoury), *Eya2* (K. Melton), *Fgf8* (I. Mason), *Gcnf* (A. Cooney), *Pax3* (Takayoshi), *Shh* (A. McMahon), *Snail* (A. Nieto), *Sox2* (P. Trainor), *Sox9* (R. Krumlauf), *Sox10* (M. Gassmann), and *Wnt1* (A. Gavalas).

Immunohistochemistry

For whole-mount staining using a Neurofilament antibody, embryos were fixed in 4% PFA O/N at 4°C and dehydrated in a graded MeOH series; dehydrated embryos were bleached in methanol:DMSO:30% H_2O_2 (4:1:1) for 5hrs at RT and rehydrated in 50% methanol:PBS and 15% methanol:PBS, PBS for 30minutes each. For blocking, embryos were washed in PBSMT (2% milk powder, 0.1% Triton X-100

in PBS) twice for 1hour at RT. Embryos were incubated in primary antibody to Neurofilament (2H3) diluted at 1:250 O/N at 4°C in PBSMT. Embryos were rinsed in PBSMT and incubated in secondary antibody using a 1:200 dilution in PBSMT of HRP-coupled goat anti-rabbit IgG (Jackson Immunoresearch, West Grove, PA). For color development, embryos were rinsed in PBSMT and PBT (0.2% BSA, Sigma, 0.1% Triton X-100) three times, 20minutes each at RT and washed in 3,3-Diaminobenzidine (0.3mg/mL) (Sigma, St. Louis, MO) in PBT for 20minutes; 0.03% H_2O_2 was added and color was developed to the desired intensity.

For section immunohistochemistry, litters were collected at the stages indicated and fixed O/N in 1% PFA at 4°C. Embryos were processed through a sucrose gradient (15%, 30% sucrose in PBS), mounted in Tissue Tek O.C.T. (VWR, West Chester, PA) and sectioned at 10microns. Sections were rinsed 3X in PBT (PBS with 0.1% Triton X-100) for 5min and blocked in 10% normal goat serum (Invitrogen, Carlsbad, CA) in PBT for 1hr at RT. Slides were incubated in primary antibody diluted in 10% goat serum/PBT O/N at 4°C. Antibodies to cleaved Caspase-3 (Cell Signaling Technologies, Danvers, MA), anti-phospho Histone H3 (Upstate/Millipore, Billerica, MA), anti-BrdU (Abcam, Cambridge, MA), anti-SOX2 (R & D Systems, Minneapolis, MN) and to SHH (5e1) were used at 1:500 (anti-Caspase-3, anti-pH3, anti-BrdU, anti-SOX2) and 1:25 (5e1), respectively. To stain for BrdU, slides were incubated in DNaseI at 1:300 (Invitrogen, Carlsbad, CA) in React3 buffer for 30min at 37°C to nick the DNA prior to blocking with 10% NGS.

Slides were rinsed 3X 10min in PBT at RT on shaker and incubated in the

appropriate Alexa 488 or 594 secondary antibody at 1:250 (Molecular probes/Invitrogen, Carlsbad, CA) for 2hrs at 4°C. Sections were counterstained with a 1/1000 dilution of 2mg/ml DAPI (Sigma, St. Louis, MO) in PBS for 5minutes, followed by rinses in PBS; slides were mounted with fluorescent mounting medium (DakoCytomation, Carpinteria, CA). Antibodies to SHH (5e1), Neurofilament (2H3), and PAX3 were obtained from the Developmental Studies Hybridoma Bank developed under the auspices of the NICHD and maintained by the University of Iowa, Department of Biological Sciences (Iowa City, IA 52242). All images were collected using a Ziess Axioplan microscope and processed using Photoshop CS2 (Adobe, San Jose, CA).

Hematoxylin and Eosin staining

Hhat$^{+/Cre\text{-}face}$ and *Hhat*$^{Cre\text{-}face}$ embryos were harvested at 14.5dpc and fixed O/N in 4% PFA at 4°C. Samples were dehydrated through a graded ethanol series, cleared in xylene, and embedded in liquid paraffin. Embryos were sectioned at 12microns and deparaffinized in xylene, and hydrated in graded alcohols to water. Sections were stained in Shandon hematoxylin for 1min and 30sec, differentiated in 1% aqueous acid alcohol for 10sec, blued in PBS for 30 seconds, and stained in eosin for 30sec. Sections were dehydrated in graded alcohols, cleared in xylene, and mounted in permanent mounting medium. All images were collected using a Ziess Axioplan microscope and processed using Photoshop CS2 (Adobe, San Jose, CA).

β-Galactosidase Staining

To stain for β-galactosidase (β-gal), embryos were collected at 9.5-11.5dpc as described above and stained with the β-gal stain solution kit (Chemicon/Millipore, Billerica, MA). Briefly, embryos were fixed on wet ice for 20min in the Tissue Fixative Solution, washed in Tissue Rinse Solution A for 30min and Tissue Rinse Solution B for 5min at RT. Embryos were incubated O/N at 37°C in Tissue Stain Solution with X-gal (40mg/mL in DMF) (Invitrogen, Carlsbad, CA). After incubation, embryos were washed PBS and re-fixed O/N in the Tissue Fixative Solution. Embryos were processed in paraffin, cut in 10micron sections, and counterstained in Nuclear Fast Red (Sigma, St. Louis, MO).

For β-gal staining on sections, 15.5dpc embryos were harvested and fixed in LacZ fixative (0.9% 25%glutaraldehyde, 10% 0.5M EGTA, and 10% 1M $MgCl_2$ in PBS) for 2.5hrs at 4°C. Embryos were processed through a sucrose gradient (15, 30% sucrose in PBS) and snap frozen in OCT. Eight micron sections were cut and re-fixed in LacZ fixative for 10min at RT; sections were washed in LacZ wash buffer (0.2% $MgCl_2$, 0.01% NaDOC, 0.02% NP40 in PBS) three times, 5min each. β-gal staining was developed using a LacZ stain solution (0.002% Potassium ferrocyanide, 0.01% Potassium ferricyanide, 0.04% X-gal (25mg/mL in DMF) in LacZ wash buffer) to the desired intensity and washed three times 5min after developing. Sections were counterstained in NFR and washed in distilled water for 1-2min; sections were mounted and photographed using a Ziess Axioplan microscope and processed using Photoshop CS2 (Adobe, San Jose, CA).

Bone & Cartilage Staining

Embryos were collected at 14.5, 15.5, and 17.5dpc and fixed in 95% EtOH O/N. Embryos were washed in a stain solution containing 0.5% Alizarin red (Sigma, St. Louis, MO) and 0.4% Alcian blue 8X (Sigma, St. Louis, MO) in 60% EtOH O/N at RT. For 14.5 and 15.5dpc embryos, soft tissue was dissolved in 1% KOH for three hours and transferred to 0.25% for 30min. For 17.5dpc staining, the embryos were anesthetized in PBS for 1hr at 4°C, fixed O/N in 95% EtOH, skinned and eviscerated prior to staining; all remaining soft tissue was dissolved in 2% KOH for six hours and transferred to 0.25% KOH for 30min. Embryos were cleared in glycerol:KOH (20%:0.25%; 33%:0.25%; 50%:0.25%). Embryos were stored in 50% glycerol:0.25% KOH until photographed.

XI. Chapter Six: References

Abu-Issa, R., Smyth, G., Smoak, I., Yamamura, K., and Meyers, E.N. 2002. Fgf8 is required for pharyngeal arch and cardiovascular development in the mouse. *Development (Cambridge, England)* **129:** 4613-4625.

Abzhanov, A., Protas, M., Grant, B.R., Grant, P.R., and Tabin, C.J. 2004. Bmp4 and morphological variation of beaks in Darwin's finches. *Science (New York, N.Y* **305:** 1462-1465.

Abzhanov, A. and Tabin, C.J. 2004. Shh and Fgf8 act synergistically to drive cartilage outgrowth during cranial development. *Developmental biology* **273:** 134-148.

Adams, M.S., Gammill, L.S., and Bronner-Fraser, M. 2008. Discovery of transcription factors and other candidate regulators of neural crest development. *Dev Dyn* **237:** 1021-1033.

Adams, S.L., Cohen, A.J., and Lassova, L. 2007. Integration of signaling pathways regulating chondrocyte differentiation during endochondral bone formation. *Journal of cellular physiology* **213:** 635-641.

Ahlgren, S.C. and Bronner-Fraser, M. 1999. Inhibition of sonic hedgehog signaling in vivo results in craniofacial neural crest cell death. *Curr Biol* **9:** 1304-1314.

Ahlgren, S.C., Thakur, V., and Bronner-Fraser, M. 2002. Sonic hedgehog rescues cranial neural crest from cell death induced by ethanol exposure. *Proc Natl Acad Sci U S A* **99:** 10476-10481.

Akam, M., Dawson, I., and Tear, G. 1988. Homeotic genes and the control of segment diversity. *Development (Cambridge, England)* **104:** 123-133.

Akiyama, H., Chaboissier, M.C., Martin, J.F., Schedl, A., and de Crombrugghe, B. 2002. The transcription factor Sox9 has essential roles in successive steps of the chondrocyte differentiation pathway and is required for expression of Sox5 and Sox6. *Genes & development* **16:** 2813-2828.

Alcedo, J., Zou, Y., and Noll, M. 2000. Posttranscriptional regulation of smoothened is part of a self-correcting mechanism in the Hedgehog signaling system. *Molecular cell* **6:** 457-465.

Amanai, K. and Jiang, J. 2001. Distinct roles of Central missing and Dispatched in sending the Hedgehog signal. *Development (Cambridge, England)* **128:** 5119-5127.

Aoto, K., Yayoi, S., Higashiyama, D., Shiota, K., and Motoyama, J. 2008. Fetal ethanol exposure activates protein kinase a and impairs Shh expression in prechordal mesendoderm cells in the pathogenesis of holoprosencephaly. *Birth defects research*.

Auman, H.J., Nottoli, T., Lakiza, O., Winger, Q., Donaldson, S., and Williams, T. 2002. Transcription factor AP-2gamma is essential in the extra-embryonic lineages for early postimplantation development. *Development (Cambridge, England)* **129:** 2733-2747.

Bang, A.G., Papalopulu, N., Kintner, C., and Goulding, M.D. 1997. Expression of Pax-3 is initiated in the early neural plate by posteriorizing signals produced by the organizer and by posterior non-axial mesoderm. *Development (Cambridge, England)* **124:** 2075-2085.

Barlow, A.J. and Francis-West, P.H. 1997. Ectopic application of recombinant BMP-2 and BMP-4 can change patterning of developing chick facial primordia. *Development (Cambridge, England)* **124:** 391-398.

Basch, M.L., Bronner-Fraser, M., and Garcia-Castro, M.I. 2006. Specification of the neural crest occurs during gastrulation and requires Pax7. *Nature* **441:** 218-222.

Basch, M.L., Garcia-Castro, M.I., and Bronner-Fraser, M. 2004. Molecular mechanisms of neural crest induction. *Birth Defects Res C Embryo Today* **72:** 109-123.

Baur, S.T., Mai, J.J., and Dymecki, S.M. 2000. Combinatorial signaling through BMP receptor IB and GDF5: shaping of the distal mouse limb and the genetics of distal limb diversity. *Development (Cambridge, England)* **127:** 605-619.

Becker, N., Seitanidou, T., Murphy, P., Mattei, M.-G., Topilko, P., Nieto, M.A., Wilkinson, D.G., Charnay, P., and Gilardi-Hebenstreit, P. 1994. Several receptor tyrosine kinase genes of the *Eph* family are segmentally expressed in the developing hindbrain. *Mech. Dev.* **47:** 3-18.

Bell, D.M., Leung, K.K., Wheatley, S.C., Ng, L.J., Zhou, S., Ling, K.W., Sham, M.H., Koopman, P., Tam, P.P., and Cheah, K.S. 1997. SOX9 directly regulates the type-II collagen gene. *Nature genetics* **16:** 174-178.

Belloni, E., Muenke, M., Roessler, E., Traverso, G., Siegel-Bartelt, J., Frumkin, A., Mitchell, H., Donis-Keller, H., Helms, C., Hing, A., Heng, H., Koop, B., Martindale, D., Rommens, J., Tsui, L., and Scherer, S. 1996a. Identification of *Sonic hedgehog* as a candidate gene responsible for holoprosencephaly. *Nature Genetics* **14:** 353-356.

Belloni, E., Muenke, M., Roessler, E., Traverso, G., Siegel-Bartelt, J., Frumkin, A., Mitchell, H.F., Donis-Keller, H., Helms, C., Hing, A.V., Heng, H.H., Koop, B., Martindale, D., Rommens, J.M., Tsui, L.C., and Scherer, S.W. 1996b. Identification of Sonic hedgehog as a candidate gene responsible for holoprosencephaly. *Nat Genet* **14:** 353-356.

Bennett, J.H., Hunt, P., and Thorogood, P. 1995. Bone morphogenetic protein-2 and -4 expression during murine orofacial development. *Archives of oral biology* **40:** 847-854.

Bertrand, S., Thisse, B., Tavares, R., Sachs, L., Chaumot, A., Bardet, P.L., Escriva, H., Duffraisse, M., Marchand, O., Safi, R., Thisse, C., and Laudet, V. 2007. Unexpected novel relational links uncovered by extensive developmental profiling of nuclear receptor expression. *PLoS genetics* **3:** e188.

Bi, W., Deng, J.M., Zhang, Z., Behringer, R.R., and de Crombrugghe, B. 1999. Sox9 is required for cartilage formation. *Nature genetics* **22:** 85-89.

Bi, W., Huang, W., Whitworth, D.J., Deng, J.M., Zhang, Z., Behringer, R.R., and de Crombrugghe, B. 2001. Haploinsufficiency of Sox9 results in defective

cartilage primordia and premature skeletal mineralization. *Proceedings of the National Academy of Sciences of the United States of America* **98:** 6698-6703.
Bitgood, M.J. and McMahon, A.P. 1995. Hedgehog and Bmp genes are coexpressed at many diverse sites of cell-cell interaction in the mouse embryo. *Developmental biology* **172:** 126-138.
Bitgood, M.J., Shen, L., and McMahon, A.P. 1996. Sertoli cell signaling by Desert hedgehog regulates the male germline. *Curr Biol* **6:** 298-304.
Bonstein, L., Elias, S., and Frank, D. 1998. Paraxial-fated mesoderm is required for neural crest induction in Xenopus embryos. *Developmental biology* **193:** 156-168.
Borycki, A.G., Li, J., Jin, F., Emerson, C.P., and Epstein, J.A. 1999. Pax3 functions in cell survival and in pax7 regulation. *Development (Cambridge, England)* **126:** 1665-1674.
Bosher, J.M., Williams, T., and Hurst, H.C. 1995. The developmentally regulated transcription factor AP-2 is involved in c-erbB-2 overexpression in human mammary carcinoma. *Proceedings of the National Academy of Sciences of the United States of America* **92:** 744-747.
Braat, A.K., Zandbergen, M.A., De Vries, E., Van Der Burg, B., Bogerd, J., and Goos, H.J. 1999. Cloning and expression of the zebrafish germ cell nuclear factor. *Molecular reproduction and development* **53:** 369-375.
Brault, V., Moore, R., Kutsch, S., Ishibashi, M., Rowitch, D.H., McMahon, A.P., Sommer, L., Boussadia, O., and Kemler, R. 2001. Inactivation of the beta-catenin gene by Wnt1-Cre-mediated deletion results in dramatic brain malformation and failure of craniofacial development. *Development (Cambridge, England)* **128:** 1253-1264.
Brewer, S., Feng, W., Huang, J., Sullivan, S., and Williams, T. 2004. Wnt1-Cre-mediated deletion of AP-2alpha causes multiple neural crest-related defects. *Developmental biology* **267:** 135-152.
Brewer, S., Jiang, X., Donaldson, S., Williams, T., and Sucov, H.M. 2002. Requirement for AP-2alpha in cardiac outflow tract morphogenesis. *Mechanisms of development* **110:** 139-149.
Briscoe, J., Chen, Y., Jessell, T.M., and Struhl, G. 2001. A hedgehog-insensitive form of patched provides evidence for direct long-range morphogen activity of sonic hedgehog in the neural tube. *Mol Cell* **7:** 1279-1291.
Briscoe, J., Pierani, A., Jessell, T.M., and Ericson, J. 2000. A homeodomain protein code specifies progenitor cell identity and neuronal fate in the ventral neural tube. *Cell* **101:** 435-445.
Briscoe, J., Sussel, L., Serup, P., Hartigan-O'Connor, D., Jessell, T.M., Rubenstein, J.L., and Ericson, J. 1999. Homeobox gene Nkx2.2 and specification of neuronal identity by graded Sonic hedgehog signalling. *Nature* **398:** 622-627.
Brito, J.M., Teillet, M.A., and Le Douarin, N.M. 2006. An early role for sonic hedgehog from foregut endoderm in jaw development: ensuring neural crest cell survival. *Proceedings of the National Academy of Sciences of the United States of America* **103:** 11607-11612.

Brito, J.M., Teillet, M.A., and Le Douarin, N.M. 2008. Induction of mirror-image supernumerary jaws in chicken mandibular mesenchyme by Sonic Hedgehog-producing cells. *Development (Cambridge, England)* **135:** 2311-2319.

Britsch, S., Goerich, D.E., Riethmacher, D., Peirano, R.I., Rossner, M., Nave, K.A., Birchmeier, C., and Wegner, M. 2001. The transcription factor Sox10 is a key regulator of peripheral glial development. *Genes & development* **15:** 66-78.

Bronner-Fraser, M. and Fraser, S. 1989. Developmental potential of avian trunk neural crest cells in situ. *Neuron* **3:** 755-766.

Brunet, L.J., McMahon, J.A., McMahon, A.P., and Harland, R.M. 1998. Noggin, cartilage morphogenesis, and joint formation in the mammalian skeleton. *Science (New York, N.Y* **280:** 1455-1457.

Buglino, J.A. and Resh, M.D. 2008. Hhat is a palmitoylacyl transferase with specificity for N-palmitoylation of sonic hedgehog. *The Journal of biological chemistry*.

Burns, A.J. and Douarin, N.M. 1998. The sacral neural crest contributes neurons and glia to the post-umbilical gut: spatiotemporal analysis of the development of the enteric nervous system. *Development (Cambridge, England)* **125:** 4335-4347.

Byrd, N., Becker, S., Maye, P., Narasimhaiah, R., St-Jacques, B., Zhang, X., McMahon, J., McMahon, A., and Grabel, L. 2002. Hedgehog is required for murine yolk sac angiogenesis. *Development (Cambridge, England)* **129:** 361-372.

Cano, A., Perez-Moreno, M.A., Rodrigo, I., Locascio, A., Blanco, M.J., del Barrio, M.G., Portillo, F., and Nieto, M.A. 2000. The transcription factor snail controls epithelial-mesenchymal transitions by repressing E-cadherin expression. *Nat Cell Biol* **2:** 76-83.

Carl, T.F., Dufton, C., Hanken, J., and Klymkowsky, M.W. 1999. Inhibition of neural crest migration in Xenopus using antisense slug RNA. *Developmental biology* **213:** 101-115.

Carney, T.J., Dutton, K.A., Greenhill, E., Delfino-Machin, M., Dufourcq, P., Blader, P., and Kelsh, R.N. 2006. A direct role for Sox10 in specification of neural crest-derived sensory neurons. *Development (Cambridge, England)* **133:** 4619-4630.

Chai, Y., Jiang, X., Ito, Y., Bringas, P., Jr., Han, J., Rowitch, D.H., Soriano, P., McMahon, A.P., and Sucov, H.M. 2000. Fate of the mammalian cranial neural crest during tooth and mandibular morphogenesis. *Development (Cambridge, England)* **127:** 1671-1679.

Chamberlain, C.E., Jeong, J., Guo, C., Allen, B.L., and McMahon, A.P. 2008. Notochord-derived Shh concentrates in close association with the apically positioned basal body in neural target cells and forms a dynamic gradient during neural patterning. *Development (Cambridge, England)* **135:** 1097-1106.

Chamoun, Z., Mann, R.K., Nellen, D., von Kessler, D.P., Bellotto, M., Beachy, P.A., and Basler, K. 2001. Skinny hedgehog, an acyltransferase required for

palmitoylation and activity of the hedgehog signal. *Science (New York, N.Y* **293:** 2080-2084.
Chang, C. and Hemmati-Brivanlou, A. 1998. Neural crest induction by Xwnt7B in Xenopus. *Developmental biology* **194:** 129-134.
Chang, D.T., Lopez, A., von Kessler, D.P., Chiang, C., Simandl, B.K., Zhao, R., Seldin, M.F., Fallon, J.F., and Beachy, P.A. 1994. Products, genetic linkage and limb patterning activity of a murine *hedgehog* gene. *Development (Cambridge, England)* **120:** 3339-3353.
Chen, M.H., Li, Y.J., Kawakami, T., Xu, S.M., and Chuang, P.T. 2004. Palmitoylation is required for the production of a soluble multimeric Hedgehog protein complex and long-range signaling in vertebrates. *Genes & development* **18:** 641-659.
Chen, Y. and Struhl, G. 1996. Dual roles for patched in sequestering and transducing Hedgehog. *Cell* **87:** 553-563.
Cheng, C., Ying, K., Xu, M., Zhao, W., Zhou, Z., Huang, Y., Wang, W., Xu, J., Zeng, L., Xie, Y., and Mao, Y. 2002. Cloning and characterization of a novel human transcription factor AP-2 beta like gene (TFAP2BL1). *The international journal of biochemistry & cell biology* **34:** 78-86.
Cheung, M. and Briscoe, J. 2003. Neural crest development is regulated by the transcription factor Sox9. *Development (Cambridge, England)* **130:** 5681-5693.
Chiang, C., Litingtung, Y., Lee, E., Young, K.E., Corden, J.L., Westphal, H., and Beachy, P.A. 1996. Cyclopia and defective axial patterning in mice lacking Sonic hedgehog gene function. *Nature* **383:** 407-413.
Christiansen, J.H., Coles, E.G., and Wilkinson, D.G. 2000. Molecular control of neural crest formation, migration and differentiation. *Curr Opin Cell Biol* **12:** 719-724.
Chung, A.C., Katz, D., Pereira, F.A., Jackson, K.J., DeMayo, F.J., Cooney, A.J., and O'Malley, B.W. 2001. Loss of orphan receptor germ cell nuclear factor function results in ectopic development of the tail bud and a novel posterior truncation. *Molecular and cellular biology* **21:** 663-677.
Chung, A.C., Xu, X., Niederreither, K.A., and Cooney, A.J. 2006. Loss of orphan nuclear receptor GCNF function disrupts forebrain development and the establishment of the isthmic organizer. *Developmental biology* **293:** 13-24.
Cobourne, M.T., Hardcastle, Z., and Sharpe, P.T. 2001. Sonic hedgehog regulates epithelial proliferation and cell survival in the developing tooth germ. *Journal of dental research* **80:** 1974-1979.
Cohen, M.M., Jr. and Shiota, K. 2002. Teratogenesis of holoprosencephaly. *Am J Med Genet* **109:** 1-15.
Cohen, S.M. 1990. Specification of limb development in the *Drosophila* embryo by positional cues from segmentation genes. *Nature* **343:** 173-177.
Colas, J.F. and Schoenwolf, G.C. 2001. Towards a cellular and molecular understanding of neurulation. *Dev Dyn* **221:** 117-145.

Colvin, J.S., Bohne, B.A., Harding, G.W., McEwen, D.G., and Ornitz, D.M. 1996. Skeletal overgrowth and deafness in mice lacking fibroblast growth factor receptor 3. *Nature genetics* **12:** 390-397.

Conway, S.J., Henderson, D.J., and Copp, A.J. 1997. Pax3 is required for cardiac neural crest migration in the mouse: evidence from the splotch (Sp2H) mutant. *Development (Cambridge, England)* **124:** 505-514.

Cordero, D., Marcucio, R., Hu, D., Gaffield, W., Tapadia, M., and Helms, J.A. 2004. Temporal perturbations in sonic hedgehog signaling elicit the spectrum of holoprosencephaly phenotypes. *The Journal of clinical investigation* **114:** 485-494.

Correia, A.C., Costa, M., Moraes, F., Bom, J., Novoa, A., and Mallo, M. 2007. Bmp2 is required for migration but not for induction of neural crest cells in the mouse. *Dev Dyn* **236:** 2493-2501.

Costantini, F. and Lacy, E. 1981. Introduction of a rabbit beta-globin gene into the mouse germ line. *Nature* **294:** 92-94.

Couly, G. and Le Douarin, N.M. 1990. Head morphogenesis in embryonic avian chimeras: evidence for a segmental pattern in the ectoderm corresponding to the neuromeres. *Development (Cambridge, England)* **108:** 543-558.

Couly, G.F., Coltey, P.M., and Le Douarin, N.M. 1992. The developmental fate of the cephalic mesoderm in quail-chick chimeras. *Development (Cambridge, England)* **114:** 1-15.

Couly, G.F., Coltey, P.M., and Le Douarin, N.M. 1993. The triple origin of skull in higher vertebrates: a study in quail-chick chimeras. *Development (Cambridge, England)* **117:** 409-429.

Crane, J. and Trainor, P. 2006. Neural Crest Stem and Progenitor Cells. *Annual Review of Cell and Developmental Biology* **(in press)**.

Crossley, P.H. and Martin, G.R. 1995. The mouse *FGF-8* gene encodes a family of polypeptides expressed in regions that direct outgrowth and patterning in the developing embryo. *Development (Cambridge, England)* **121:** 439-451.

Dale, J., Vesque, C., Lints, T., Sampath, K., Furley, A., Dodd, J., and Placzek, M. 1997. Cooperation of BMP7 and SHH in the induction of forebrain ventral midline cells by prechordal mesoderm. *Cell* **90:** 257-269.

Dassule, H.R., Lewis, P., Bei, M., Maas, R., and McMahon, A.P. 2000. Sonic hedgehog regulates growth and morphogenesis of the tooth. *Development (Cambridge, England)* **127:** 4775-4785.

De Calisto, J., Araya, C., Marchant, L., Riaz, C.F., and Mayor, R. 2005. Essential role of non-canonical Wnt signalling in neural crest migration. *Development (Cambridge, England)* **132:** 2587-2597.

de la Pompa, J.L., Wakeham, A., Correia, K.M., Samper, E., Brown, S., Aguilera, R.J., Nakano, T., Honjo, T., Mak, T.W., Rossant, J., and Conlon, R.A. 1997. Conservation of the Notch signalling pathway in mammalian neurogenesis. *Development (Cambridge, England)* **124:** 1139-1148.

del Barrio, M.G. and Nieto, M.A. 2002. Overexpression of Snail family members highlights their ability to promote chick neural crest formation. *Development (Cambridge, England)* **129:** 1583-1593.

Denef, N., Neubuser, D., Perez, L., and Cohen, S.M. 2000. Hedgehog induces opposite changes in turnover and subcellular localization of patched and smoothened. *Cell* **102:** 521-531.

Deng, C., Wynshaw-Boris, A., Zhou, F., Kuo, A., and Leder, P. 1996. Fibroblast growth factor receptor 3 is a negative regulator of bone growth. *Cell* **84:** 911-921.

Depew, M., Liu, J., Long, J., Prestley, R., Meneses, J., Pedersen, R., and Rubenstein, J. 1999. *Dlx5* regulates regional development of the branchial arches and sensory capsules. *Development (Cambridge, England)* **126:** 3831-3846.

Depew, M.J., Lufkin, T., and Rubenstein, J.L. 2002. Specification of jaw subdivisions by Dlx genes. *Science* **298:** 381-385.

Depew, M.J., Simpson, C.A., Morasso, M., and Rubenstein, J.L. 2005. Reassessing the Dlx code: the genetic regulation of branchial arch skeletal pattern and development. *Journal of anatomy* **207:** 501-561.

Dessaud, E., Yang, L.L., Hill, K., Cox, B., Ulloa, F., Ribeiro, A., Mynett, A., Novitch, B.G., and Briscoe, J. 2007. Interpretation of the sonic hedgehog morphogen gradient by a temporal adaptation mechanism. *Nature* **450:** 717-720.

Dixon, J. and Dixon, M.J. 2004. Genetic background has a major effect on the penetrance and severity of craniofacial defects in mice heterozygous for the gene encoding the nucleolar protein Treacle. *Dev Dyn* **229:** 907-914.

Dixon, J., Hovanes, K., Shiang, R., and Dixon, M.J. 1997. Sequence analysis, identification of evolutionary conserved motifs and expression analysis of murine tcof1 provide further evidence for a potential function for the gene and its human homologue, TCOF1. *Human Molecular Genetics* **6:** 727-737.

Dixon, J., Jones, N.C., Sandell, L.L., Jayasinghe, S.M., Crane, J., Rey, J.P., Dixon, M.J., and Trainor, P.A. 2006. Tcof1/Treacle is required for neural crest cell formation and proliferation deficiencies that cause craniofacial abnormalities. *Proc Natl Acad Sci U S A* **103:** 13403-13408.

Donner, A.L. and Williams, T. 2006. Frontal nasal prominence expression driven by Tcfap2a relies on a conserved binding site for STAT proteins. *Dev Dyn*.

Ducy, P., Starbuck, M., Priemel, M., Shen, J., Pinero, G., Geoffroy, V., Amling, M., and Karsenty, G. 1999. A Cbfa1-dependent genetic pathway controls bone formation beyond embryonic development. *Genes & development* **13:** 1025-1036.

Ducy, P., Zhang, R., Geoffroy, V., Ridall, A.L., and Karsenty, G. 1997. Osf2/Cbfa1: a transcriptional activator of osteoblast differentiation. *Cell* **89:** 747-754.

Dudley, A.T., Lyons, K.M., and Robertson, E.J. 1995. A requirement for bone morphogenetic protein-7 during development of the mammalian kidney and eye. *Genes & development* **9:** 2795-2807.

Dyer, M.A., Farrington, S.M., Mohn, D., Munday, J.R., and Baron, M.H. 2001. Indian hedgehog activates hematopoiesis and vasculogenesis and can respecify prospective neurectodermal cell fate in the mouse embryo. *Development (Cambridge, England)* **128:** 1717-1730.

Echelard, Y., Epstein, D., St-Jacques, B., Shen, L., Mohler, J., McMahon, J.A., and McMahon, A.P. 1993. *Sonic hedgehog*, a Member of a Family of Putative Signalling Molecules, Is implicated in the Regulation of CNS Polarity. *Cell* **75:** 1417-1430.

Ehlen, H.W., Buelens, L.A., and Vortkamp, A. 2006. Hedgehog signaling in skeletal development. *Birth Defects Res C Embryo Today* **78:** 267-279.

Endo, Y., Osumi, N., and Wakamatsu, Y. 2002. Bimodal functions of Notch-mediated signaling are involved in neural crest formation during avian ectoderm development. *Development (Cambridge, England)* **129:** 863-873.

Endo, Y., Osumi, N., and Wakamatsu, Y. 2003. Deltex/Dtx mediates NOTCH signaling in regulation of Bmp4 expression in cranial neural crest formation during avian development. *Development, growth & differentiation* **45:** 241-248.

Epstein, J.A., Li, J., Lang, D., Chen, F., Brown, C.B., Jin, F., Lu, M.M., Thomas, M., Liu, E., Wessels, A., and Lo, C.W. 2000. Migration of cardiac neural crest cells in Splotch embryos. *Development (Cambridge, England)* **127:** 1869-1878.

Ericson, J., Morton, S., Kawakami, A., Roelink, H., and Jessell, T.M. 1996. Two critical periods of Sonic Hedgehog signaling required for the specification of motor neuron identity. *Cell* **87:** 661-673.

Eswarakumar, V.P., Lax, I., and Schlessinger, J. 2005. Cellular signaling by fibroblast growth factor receptors. *Cytokine Growth Factor Rev* **16:** 139-149.

Evans, D.J. and Noden, D.M. 2006. Spatial relations between avian craniofacial neural crest and paraxial mesoderm cells. *Dev Dyn* **235:** 1310-1325.

Fallon, J.F., Lopez, A., Ros, M.A., Savage, M.P., Olwin, B.B., and Simandl, B.K. 1994. FGF-2: apical ectodermal ridge growth signal for chick limb development. *Science* **264:** 104-107.

Fedtsova, N., Perris, R., and Turner, E.E. 2003. Sonic hedgehog regulates the position of the trigeminal ganglia. *Developmental biology* **261:** 456-469.

Feldman, B., Poueymirou, W., Papaioannou, V.E., DeChiara, T.M., and Goldfarb, M. 1995. Requirement of FGF-4 for postimplantation mouse development. *Science (New York, N.Y* **267:** 246-249.

Feng, W. and Williams, T. 2003. Cloning and characterization of the mouse AP-2 epsilon gene: a novel family member expressed in the developing olfactory bulb. *Molecular and cellular neurosciences* **24:** 460-475.

Foster, J.W., Dominguez-Steglich, M.A., Guioli, S., Kowk, G., Weller, P.A., Stevanovic, M., Weissenbach, J., Mansour, S., Young, I.D., Goodfellow, P.N., and et al. 1994. Campomelic dysplasia and autosomal sex reversal caused by mutations in an SRY-related gene. *Nature* **372:** 525-530.

Franz-Odendaal, T.A., Hall, B.K., and Witten, P.E. 2006. Buried alive: how osteoblasts become osteocytes. *Dev Dyn* **235:** 176-190.

Fuhrmann, G., Chung, A.C., Jackson, K.J., Hummelke, G., Baniahmad, A., Sutter, J., Sylvester, I., Scholer, H.R., and Cooney, A.J. 2001. Mouse germline restriction of Oct4 expression by germ cell nuclear factor. *Dev Cell* **1:** 377-387.

Galli, L.M., Barnes, T.L., Secrest, S.S., Kadowaki, T., and Burrus, L.W. 2007. Porcupine-mediated lipid-modification regulates the activity and distribution of Wnt proteins in the chick neural tube. *Development (Cambridge, England)* **134:** 3339-3348.

Gammill, L.S., Gonzalez, C., Gu, C., and Bronner-Fraser, M. 2006. Guidance of trunk neural crest migration requires neuropilin 2/semaphorin 3F signaling. *Development (Cambridge, England)* **133:** 99-106.

Garcia-Castro, M.I., Marcelle, C., and Bronner-Fraser, M. 2002. Ectodermal Wnt function as a neural crest inducer. *Science* **297:** 848-851.

Garcia, M.A., Campillos, M., Ogueta, S., Valdivieso, F., and Vazquez, J. 2000. Identification of amino acid residues of transcription factor AP-2 involved in DNA binding. *Journal of molecular biology* **301:** 807-816.

Gendron-Maguire, M., Mallo, M., Zhang, M., and Gridley, T. 1993. Hoxa-2 mutant mice exhibit homeotic transformation of skeletal elements derived from cranial neural crest. *Cell* **75:** 1317-1331.

Glavic, A., Silva, F., Aybar, M.J., Bastidas, F., and Mayor, R. 2004. Interplay between Notch signaling and the homeoprotein Xiro1 is required for neural crest induction in Xenopus embryos. *Development (Cambridge, England)* **131:** 347-359.

Goddeeris, M.M., Schwartz, R., Klingensmith, J., and Meyers, E.N. 2007. Independent requirements for Hedgehog signaling by both the anterior heart field and neural crest cells for outflow tract development. *Development (Cambridge, England)* **134:** 1593-1604.

Goetz, J.A., Singh, S., Suber, L.M., Kull, F.J., and Robbins, D.J. 2006. A highly conserved amino-terminal region of sonic hedgehog is required for the formation of its freely diffusible multimeric form. *The Journal of biological chemistry* **281:** 4087-4093.

Goodrich, L.V., Johnson, R.L., Milenkovic, L., McMahon, J.A., and Scott, M.P. 1996. Conservation of the hedgehog/patched signaling pathway from flies to mice: induction of a mouse patched gene by Hedgehog. *Genes Dev* **10:** 301-312.

Goodrich, L.V., Milenkovic, L., Higgins, K.M., and Scott, M.P. 1997. Altered neural cell fates and medulloblastoma in mouse patched mutants. *Science (New York, N.Y* **277:** 1109-1113.

Grammatopoulos, G.A., Bell, E., Toole, L., Lumsden, A., and Tucker, A.S. 2000. Homeotic transformation of branchial arch identity after Hoxa2 overexpression. *Development (Cambridge, England)* **127:** 5355-5365.

Gu, P., LeMenuet, D., Chung, A.C., Mancini, M., Wheeler, D.A., and Cooney, A.J. 2005. Orphan nuclear receptor GCNF is required for the repression of pluripotency genes during retinoic acid-induced embryonic stem cell differentiation. *Molecular and cellular biology* **25:** 8507-8519.

Hardcastle, Z., Mo, R., Hui, C.C., and Sharpe, P.T. 1998. The Shh signalling pathway in tooth development: defects in Gli2 and Gli3 mutants. *Development (Cambridge, England)* **125:** 2803-2811.

Hari, L., Brault, V., Kleber, M., Lee, H.Y., Ille, F., Leimeroth, R., Paratore, C., Suter, U., Kemler, R., and Sommer, L. 2002. Lineage-specific requirements of beta-catenin in neural crest development. *The Journal of cell biology* **159:** 867-880.

Haworth, K.E., Wilson, J.M., Grevellec, A., Cobourne, M.T., Healy, C., Helms, J.A., Sharpe, P.T., and Tucker, A.S. 2007. Sonic hedgehog in the pharyngeal endoderm controls arch pattern via regulation of Fgf8 in head ectoderm. *Developmental biology* **303:** 244-258.

Heaney, J.D. and Bronson, S.K. 2006. Artificial chromosome-based transgenes in the study of genome function. *Mamm Genome* **17:** 791-807.

Helms, J.A., Cordero, D., and Tapadia, M.D. 2005. New insights into craniofacial morphogenesis. *Development (Cambridge, England)* **132:** 851-861.

Herbarth, B., Pingault, V., Bondurand, N., Kuhlbrodt, K., Hermans-Borgmeyer, I., Puliti, A., Lemort, N., Goossens, M., and Wegner, M. 1998. Mutation of the Sry-related Sox10 gene in Dominant megacolon, a mouse model for human Hirschsprung disease. *Proc Natl Acad Sci U S A* **95:** 5161-5165.

Hilger-Eversheim, K., Moser, M., Schorle, H., and Buettner, R. 2000. Regulatory roles of AP-2 transcription factors in vertebrate development, apoptosis and cell-cycle control. *Gene* **260:** 1-12.

Hoffman, K. 2000. A superfamily of membrane-bound O-acyl-transferases with implications for wnt signaling. *Trends in Biochemical Sciences* **25:** 111-112.

Hogan, B.L. 1996. Bone morphogenetic proteins: Multifunctional regulators of vertebrate development. *Genes and Development* **10:** 1580-1594.

Hong, C.S. and Saint-Jeannet, J.P. 2007. The activity of Pax3 and Zic1 regulates three distinct cell fates at the neural plate border. *Molecular biology of the cell* **18:** 2192-2202.

Hu, D. and Helms, J.A. 1999. The role of sonic hedgehog in normal and abnormal craniofacial morphogenesis. *Development (Cambridge, England)* **126:** 4873-4884.

Hu, D., Marcucio, R.S., and Helms, J.A. 2003. A zone of frontonasal ectoderm regulates patterning and growth in the face. *Development (Cambridge, England)* **130:** 1749-1758.

Huang, X., Litingtung, Y., and Chiang, C. 2007. Region-specific requirement for cholesterol modification of sonic hedgehog in patterning the telencephalon and spinal cord. *Development (Cambridge, England)* **134:** 2095-2105.

Huang, X. and Saint-Jeannet, J.P. 2004. Induction of the neural crest and the opportunities of life on the edge. *Developmental biology* **275:** 1-11.

Hui, C.-C. and Joyner, A. 1993. A mouse model of greig cephalopolysyndactyly syndrome: the *extra-toes*^{J} mutation contains an intragenic deletion of the *Gli3* gene. *Nature Genetics* **3:** 241-246.

Hunt, P., Gulisano, M., Cook, M., Sham, M., Faiella, A., Wilkinson, D., Boncinelli, E., and Krumlauf, R. 1991. A distinct *Hox* code for the branchial region of the head. *Nature* **353:** 861-864.

Hutson, M.R. and Kirby, M.L. 2007. Model systems for the study of heart development and disease. Cardiac neural crest and conotruncal malformations. *Seminars in cell & developmental biology* **18:** 101-110.

Ikeya, M., Lee, S.M., Johnson, J.E., McMahon, A.P., and Takada, S. 1997. Wnt signalling required for expansion of neural crest and CNS progenitors. *Nature* **389:** 966-970.

Incardona, J.P., Lee, J.H., Robertson, C.P., Enga, K., Kapur, R.P., and Roelink, H. 2000. Receptor-mediated endocytosis of soluble and membrane-tethered Sonic hedgehog by Patched-1. *Proceedings of the National Academy of Sciences of the United States of America* **97:** 12044-12049.

Ingham, P.W., Nystedt, S., Nakano, Y., Brown, W., Stark, D., van den Heuvel, M., and Taylor, A.M. 2000. Patched represses the Hedgehog signalling pathway by promoting modification of the Smoothened protein. *Curr Biol* **10:** 1315-1318.

Ingham, P.W., Taylor, A.M., and Nakano, Y. 1991. Role of the Drosophila patched gene in positional signalling. *Nature* **353:** 184-187.

Itoh, N. and Ornitz, D.M. 2008. Functional evolutionary history of the mouse Fgf gene family. *Dev Dyn* **237:** 18-27.

Jaenisch, R. 1988. Transgenic animals. *Science (New York, N.Y* **240:** 1468-1474.

Jeong, J., Mao, J., Tenzen, T., Kottmann, A.H., and McMahon, A.P. 2004. Hedgehog signaling in the neural crest cells regulates the patterning and growth of facial primordia. *Genes & development* **18:** 937-951.

Jiang, X., Iseki, S., Maxson, R.E., Sucov, H.M., and Morriss-Kay, G.M. 2002. Tissue origins and interactions in the mammalian skull vault. *Developmental biology* **241:** 106-116.

Jiang, X., Rowitch, D.H., Soriano, P., McMahon, A.P., and Sucov, H.M. 2000. Fate of the mammalian cardiac neural crest. *Development (Cambridge, England)* **127:** 1607-1616.

Jones, N.C., Lynn, M.L., Gaudenz, K., Sakai, D., Aoto, K., Rey, J.P., Glynn, E.F., Ellington, L., Du, C., Dixon, J., Dixon, M.J., and Trainor, P.A. 2008. Prevention of the neurocristopathy Treacher Collins syndrome through inhibition of p53 function. *Nat Med* **14:** 125-133.

Joos, T.O., David, R., and Dreyer, C. 1996. xGCNF, a nuclear orphan receptor is expressed during neurulation in Xenopus laevis. *Mechanisms of development* **60:** 45-57.

Kadowaki, T., Wilder, E., Klingensmith, J., Zachary, K., and Perrimon, N. 1996. The segment polarity gene porcupine encodes a putative multitransmembrane

protein involved in Wingless processing. *Genes & development* **10:** 3116-3128.

Kanzler, B., Foreman, R.K., Labosky, P.A., and Mallo, M. 2000. BMP signaling is essential for development of skeletogenic and neurogenic cranial neural crest. *Development (Cambridge, England)* **127:** 1095-1104.

Karaplis, A.C., Luz, A., Glowacki, J., Bronson, R.T., Tybulewicz, V.L., Kronenberg, H.M., and Mulligan, R.C. 1994. Lethal skeletal dysplasia from targeted disruption of the parathyroid hormone-related peptide gene. *Genes & development* **8:** 277-289.

Kato, H., Sakai, T., Tamura, K., Minoguchi, S., Shirayoshi, Y., Hamada, Y., Tsujimoto, Y., and Honjo, T. 1996. Functional conservation of mouse Notch receptor family members. *FEBS letters* **395:** 221-224.

Kawakami, Y., Ishikawa, T., Shimabara, M., Tanda, N., Enomoto-Iwamoto, M., Iwamoto, M., Kuwana, T., Ueki, A., Noji, S., and Nohno, T. 1996. BMP signaling during bone pattern determination in the developing limb. *Development (Cambridge, England)* **122:** 3557-3566.

Kawauchi, S., Shou, J., Santos, R., Hebert, J.M., McConnell, S.K., Mason, I., and Calof, A.L. 2005. Fgf8 expression defines a morphogenetic center required for olfactory neurogenesis and nasal cavity development in the mouse. *Development (Cambridge, England)* **132:** 5211-5223.

Kiecker, C. and Lumsden, A. 2005. Compartments and their boundaries in vertebrate brain development. *Nat Rev Neurosci* **6:** 553-564.

Kingsley, D.M., Bland, A.E., Grubber, J.M., Marker, P.C., Russell, L.B., Copeland, N.G., and Jenkins, N.A. 1992. The mouse short ear skeletal morphogenesis locus is associated with defects in a bone morphogenetic member of the TGF beta superfamily. *Cell* **71:** 399-410.

Kirby, M.L., Gale, T.F., and Stewart, D.E. 1983. Neural crest cells contribute to normal aorticopulmonary septation. *Science* **220:** 1059-1061.

Kirby, M.L. and Stewart, D.E. 1983. Neural crest origin of cardiac ganglion cells in the chick embryo: identification and extirpation. *Developmental biology* **97:** 433-443.

Kohtz, J.D., Lee, H.Y., Gaiano, N., Segal, J., Ng, E., Larson, T., Baker, D.P., Garber, E.A., Williams, K.P., and Fishell, G. 2001. N-terminal fatty-acylation of sonic hedgehog enhances the induction of rodent ventral forebrain neurons. *Development (Cambridge, England)* **128:** 2351-2363.

Komori, T., Yagi, H., Nomura, S., Yamaguchi, A., Sasaki, K., Deguchi, K., Shimizu, Y., Bronson, R.T., Gao, Y.H., Inada, M., Sato, M., Okamoto, R., Kitamura, Y., Yoshiki, S., and Kishimoto, T. 1997. Targeted disruption of Cbfa1 results in a complete lack of bone formation owing to maturational arrest of osteoblasts. *Cell* **89:** 755-764.

Kontges, G. and Lumsden, A. 1996. Rhombencephalic neural crest segmentation is preserved throughout craniofacial ontogeny. *Development (Cambridge, England)* **122:** 3229-3242.

Kronenberg, H.M. 2003. Developmental regulation of the growth plate. *Nature* **423:** 332-336.

Krull, C.E. 2001. Segmental organization of neural crest migration. *Mech Dev* **105:** 37-45.

Krull, C.E., Lansford, R., Gale, N.W., Marcelle, C., Collazo, A., Yancopoulos, G.D., Fraser, S.E., and Bronner-Fraser, M. 1997. Interactions of Eph-related receptors and ligands confer rostrocaudal pattern to trunk neural crest migration. *Curr. Biol.* **7:** 571-580.

Kulesa, P., Ellies, D.L., and Trainor, P.A. 2004. Comparative analysis of neural crest cell death, migration, and function during vertebrate embryogenesis. *Dev Dyn* **229:** 14-29.

Kwan, K.M. 2002. Conditional alleles in mice: practical considerations for tissue-specific knockouts. *Genesis* **32:** 49-62.

LaBonne, C. and Bronner-Fraser, M. 1998. Neural crest induction in *Xenopus*: evidence for a two-signal model. *Development (Cambridge, England)* **125:** 2403-2414.

LaBonne, C. and Bronner-Fraser, M. 1999. Molecular mechanisms of neural crest formation. *Annu Rev Cell Dev Biol* **15:** 81-112.

LaBonne, C. and Bronner-Fraser, M. 2000. Snail-related transcriptional repressors are required in Xenopus for both the induction of the neural crest and its subsequent migration. *Developmental biology* **221:** 195-205.

Lacosta, A.M., Canudas, J., Gonzalez, C., Muniesa, P., Sarasa, M., and Dominguez, L. 2007. Pax7 identifies neural crest, chromatophore lineages and pigment stem cells during zebrafish development. *Int J Dev Biol* **51:** 327-331.

Lan, Z.J., Xu, X., and Cooney, A.J. 2003. Generation of a germ cell nuclear factor conditional allele in mice. *Genesis* **37:** 172-179.

Lanske, B., Karaplis, A.C., Lee, K., Luz, A., Vortkamp, A., Pirro, A., Karperien, M., Defize, L.H., Ho, C., Mulligan, R.C., Abou-Samra, A.B., Juppner, H., Segre, G.V., and Kronenberg, H.M. 1996. PTH/PTHrP receptor in early development and Indian hedgehog-regulated bone growth. *Science (New York, N.Y* **273:** 663-666.

Larson, W.J. 1993. *Essentials of Human Embryology*. Churchill Livingstone Inc.

Le Douarin, N. and Kalcheim, C. 1999. *The Neural Crest*. Cambridge Univesity Press.

Le Douarin, N.M. 2004. The avian embryo as a model to study the development of the neural crest: a long and still ongoing story. *Mechanisms of development* **121:** 1089-1102.

Lee, H.Y., Kleber, M., Hari, L., Brault, V., Suter, U., Taketo, M.M., Kemler, R., and Sommer, L. 2004. Instructive role of Wnt/beta-catenin in sensory fate specification in neural crest stem cells. *Science (New York, N.Y* **303:** 1020-1023.

Lee, J.D. and Treisman, J.E. 2001. Sightless has homology to transmembrane acyltransferases and is required to generate active Hedgehog protein. *Curr Biol* **11:** 1147-1152.

Lee, K., Lanske, B., Karaplis, A.C., Deeds, J.D., Kohno, H., Nissenson, R.A., Kronenberg, H.M., and Segre, G.V. 1996. Parathyroid hormone-related peptide delays terminal differentiation of chondrocytes during endochondral bone development. *Endocrinology* **137:** 5109-5118.

Lefebvre, V., Huang, W., Harley, V.R., Goodfellow, P.N., and de Crombrugghe, B. 1997. SOX9 is a potent activator of the chondrocyte-specific enhancer of the pro alpha1(II) collagen gene. *Molecular and cellular biology* **17:** 2336-2346.

Lewandoski, M., Sun, X., and Martin, G.R. 2000. Fgf8 signalling from the AER is essential for normal limb development. *Nature genetics* **26:** 460-463.

Lewis, J.L., Bonner, J., Modrell, M., Ragland, J.W., Moon, R.T., Dorsky, R.I., and Raible, D.W. 2004. Reiterated Wnt signaling during zebrafish neural crest development. *Development (Cambridge, England)* **131:** 1299-1308.

Li, X. and Cao, X. 2006. BMP signaling and skeletogenesis. *Annals of the New York Academy of Sciences* **1068:** 26-40.

Liem, K.F., Jr., Tremml, G., Roelink, H., and Jessell, T.M. 1995. Dorsal differentiation of neural plate cells induced by BMP-mediated signals from epidermal ectoderm. *Cell* **82:** 969-979.

Litingtung, Y. and Chiang, C. 2000. Specification of ventral neuron types is mediated by an antagonistic interaction between Shh and Gli3. *Nat Neurosci* **3:** 979-985.

Liu, W., Selever, J., Murali, D., Sun, X., Brugger, S.M., Ma, L., Schwartz, R.J., Maxson, R., Furuta, Y., and Martin, J.F. 2005a. Threshold-specific requirements for Bmp4 in mandibular development. *Developmental biology* **283:** 282-293.

Liu, W., Sun, X., Braut, A., Mishina, Y., Behringer, R.R., Mina, M., and Martin, J.F. 2005b. Distinct functions for Bmp signaling in lip and palate fusion in mice. *Development (Cambridge, England)* **132:** 1453-1461.

Liu, Z., Xu, J., Colvin, J.S., and Ornitz, D.M. 2002. Coordination of chondrogenesis and osteogenesis by fibroblast growth factor 18. *Genes & development* **16:** 859-869.

Lumsden, A., Sprawson, N., and Graham, A. 1991. Segmental origin and migration of neural crest cells in the hindbrain region of the chick embryo. *Development (Cambridge, England)* **113:** 1281-1291.

Macatee, T.L., Hammond, B.P., Arenkiel, B.R., Francis, L., Frank, D.U., and Moon, A.M. 2003. Ablation of specific expression domains reveals discrete functions of ectoderm- and endoderm-derived FGF8 during cardiovascular and pharyngeal development. *Development (Cambridge, England)* **130:** 6361-6374.

Macdonald, R., Barth, K.A., Xu, Q., Holder, N., Mikkola, I., and Wilson, S.W. 1995. Midline signalling is required for Pax gene regulation and patterning of the eyes. *Development (Cambridge, England)* **121:** 3267-3278.

Mansouri, A., Stoykova, A., Torres, M., and Gruss, P. 1996. Dysgenesis of cephalic neural crest derivatives in Pax7-/- mutant mice. *Development (Cambridge, England)* **122:** 831-838.

Marchant, L., Linker, C., Ruiz, P., Guerrero, N., and Mayor, R. 1998. The inductive properties of mesoderm suggest that the neural crest cells are specified by a BMP gradient. *Developmental biology* **198:** 319-329.

Marcucio, R.S., Cordero, D.R., Hu, D., and Helms, J.A. 2005. Molecular interactions coordinating the development of the forebrain and face. *Developmental biology* **284:** 48-61.

Mariani, F.V. and Martin, G.R. 2003. Deciphering skeletal patterning: clues from the limb. *Nature* **423:** 319-325.

Marigo, V., Davey, R.A., Zuo, Y., Cunningham, J.M., and Tabin, C.J. 1996. Biochemical evidence that patched is the Hedgehog receptor. *Nature* **384:** 176-179.

Martin, V., Carrillo, G., Torroja, C., and Guerrero, I. 2001. The sterol-sensing domain of Patched protein seems to control Smoothened activity through Patched vesicular trafficking. *Curr Biol* **11:** 601-607.

Matthews, H.K., Marchant, L., Carmona-Fontaine, C., Kuriyama, S., Larrain, J., Holt, M.R., Parsons, M., and Mayor, R. 2008. Directional migration of neural crest cells in vivo is regulated by Syndecan-4/Rac1 and non-canonical Wnt signaling/RhoA. *Development (Cambridge, England)* **135:** 1771-1780.

Mayor, R., Guerrero, N., Young, R.M., Gomez-Skarmeta, J.L., and Cuellar, C. 2000. A novel function for the Xslug gene: control of dorsal mesendoderm development by repressing BMP-4. *Mechanisms of development* **97:** 47-56.

Mayor, R., Morgan, R., and Sargent, M.G. 1995. Induction of the prospective neural crest of Xenopus. *Development (Cambridge, England)* **121:** 767-777.

McBratney-Owen, B., Iseki, S., Bamforth, S.D., Olsen, B.R., and Morriss-Kay, G.M. 2008. Development and tissue origins of the mammalian cranial base. *Developmental biology*.

McCabe, K.L., Shiau, C.E., and Bronner-Fraser, M. 2007. Identification of candidate secreted factors involved in trigeminal placode induction. *Dev Dyn* **236:** 2925-2935.

McKeown, S.J., Newgreen, D.F., and Farlie, P.G. 2003. Temporal restriction of migratory and lineage potential in rhombomere 1 and 2 neural crest. *Developmental biology* **255:** 62-76.

Mellitzer, G., Xu, Q., and Wilkinson, D. 1999. Eph receptors and ephrins restrict cell intermingling and communication. *Nature* **400:** 77-81.

Meyers, E.N., Lewandoski, M., and Martin, G.R. 1998. An Fgf8 mutant allelic series generated by Cre- and Flp-mediated recombination. *Nat Genet* **18:** 136-141.

Micchelli, C.A., The, I., Selva, E., Mogila, V., and Perrimon, N. 2002. Rasp, a putative transmembrane acyltransferase, is required for Hedgehog signaling. *Development (Cambridge, England)* **129:** 843-851.

Minchin, J.E. and Hughes, S.M. 2008. Sequential actions of Pax3 and Pax7 drive xanthophore development in zebrafish neural crest. *Developmental biology* **317:** 508-522.

Minina, E., Kreschel, C., Naski, M.C., Ornitz, D.M., and Vortkamp, A. 2002. Interaction of FGF, Ihh/Pthlh, and BMP signaling integrates chondrocyte proliferation and hypertrophic differentiation. *Dev Cell* **3:** 439-449.

Minina, E., Wenzel, H.M., Kreschel, C., Karp, S., Gaffield, W., McMahon, A.P., and Vortkamp, A. 2001. BMP and Ihh/PTHrP signaling interact to coordinate chondrocyte proliferation and differentiation. *Development (Cambridge, England)* **128:** 4523-4534.

Mishina, Y., Suzuki, A., Ueno, N., and Behringer, R.R. 1995. Bmpr encodes a type I bone morphogenetic protein receptor that is essential for gastrulation during mouse embryogenesis. *Genes & development* **9:** 3027-3037.

Mitchell, P.J., Timmons, P.M., Hébert, J.M., Rigby, P.W.J., and Tjian, R. 1991. Transcription factor *AP-2* is expressed in neural crest cell lineages during mouse embryogenesis. *Genes and Development* **5:** 105-119.

Miura, G.I., Buglino, J., Alvarado, D., Lemmon, M.A., Resh, M.D., and Treisman, J.E. 2006. Palmitoylation of the EGFR ligand Spitz by Rasp increases Spitz activity by restricting its diffusion. *Dev Cell* **10:** 167-176.

Mohler, J. and Vani, K. 1992. Molecular organization and embryonic expression of the hedgehog gene involved in cell-cell communication in segmental patterning of Drosophila. *Development (Cambridge, England)* **115:** 957-971.

Monsoro-Burq, A.H., Fletcher, R.B., and Harland, R.M. 2003. Neural crest induction by paraxial mesoderm in Xenopus embryos requires FGF signals. *Development (Cambridge, England)* **130:** 3111-3124.

Monsoro-Burq, A.H., Wang, E., and Harland, R. 2005. Msx1 and Pax3 cooperate to mediate FGF8 and WNT signals during Xenopus neural crest induction. *Dev Cell* **8:** 167-178.

Moon, A.M. and Capecchi, M.R. 2000. Fgf8 is required for outgrowth and patterning of the limbs. *Nature genetics* **26:** 455-459.

Moore-Scott, B.A. and Manley, N.R. 2005. Differential expression of Sonic hedgehog along the anterior-posterior axis regulates patterning of pharyngeal pouch endoderm and pharyngeal endoderm-derived organs. *Developmental biology* **278:** 323-335.

Morgan, R. and Sargent, M.G. 1997. The role in neural patterning of translation initiation factor eIF4AII; induction of neural fold genes. *Development (Cambridge, England)* **124:** 2751-2760.

Moser, M., Imhof, A., Pscherer, A., Bauer, R., Amselgruber, W., Sinowatz, F., Hofstadter, F., Schule, R., and Buettner, R. 1995. Cloning and characterization of a second AP-2 transcription factor: AP-2 beta. *Development (Cambridge, England)* **121:** 2779-2788.

Moser, M., Pscherer, A., Roth, C., Becker, J., Mücher, G., Zerres, K., Dixkens, C., Weis, J., Guay-Woodford, L., Buettner, R., and Fässler, R. 1997. Enhanced apoptotic cell death of renal epithelial cells in mice lacking transcription factor AP-2ß. *Genes and Development* **11:** 1938-1948.

Moury, J.D. and Jacobson, A.G. 1990. The origins of neural crest cells in the axolotl. *Developmental biology* **141:** 243-253.

Muenke, M. and Beachy, P.A. 2000. Genetics of ventral forebrain development and holoprosencephaly. *Curr Opin Genet Dev* **10:** 262-269.

Muenke, M., Gurrieri, F., Bay, C., Yi, D.H., Collins, A.L., Johnson, V.P., Hennekam, R.C., Schaefer, G.B., Weik, L., Lubinsky, M.S., and et al. 1994. Linkage of a human brain malformation, familial holoprosencephaly, to chromosome 7 and evidence for genetic heterogeneity. *Proceedings of the National Academy of Sciences of the United States of America* **91:** 8102-8106.

Mundlos, S., Otto, F., Mundlos, C., Mulliken, J.B., Aylsworth, A.S., Albright, S., Lindhout, D., Cole, W.G., Henn, W., Knoll, J.H., Owen, M.J., Mertelsmann, R., Zabel, B.U., and Olsen, B.R. 1997. Mutations involving the transcription factor CBFA1 cause cleidocranial dysplasia. *Cell* **89:** 773-779.

Murray, S.A. and Gridley, T. 2006. Snail family genes are required for left-right asymmetry determination, but not neural crest formation, in mice. *Proceedings of the National Academy of Sciences of the United States of America* **103:** 10300-10304.

Nagy, A. 2000. Cre recombinase: the universal reagent for genome tailoring. *Genesis* **26:** 99-109.

Nakanishi, K., Chan, Y.S., and Ito, K. 2007. Notch signaling is required for the chondrogenic specification of mouse mesencephalic neural crest cells. *Mechanisms of development* **124:** 190-203.

Naski, M.C., Colvin, J.S., Coffin, J.D., and Ornitz, D.M. 1998. Repression of hedgehog signaling and BMP4 expression in growth plate cartilage by fibroblast growth factor receptor 3. *Development (Cambridge, England)* **125:** 4977-4988.

Nelson, D.K. and Williams, T. 2004. Frontonasal process-specific disruption of AP-2alpha results in postnatal midfacial hypoplasia, vascular anomalies, and nasal cavity defects. *Developmental biology* **267:** 72-92.

Nichols, D.H. 1986. Formation and distribution of neural crest mesenchyme to the first pharyngeal arch region of the mouse embryo. *Am J Anat* **176:** 221-231.

Nieto, M.A., Sargent, M.G., Wilkinson, D.G., and Cooke, J. 1994. Control of cell behavior during vertebrate development by *slug*, a zinc finger gene. *Science* **264:** 835-839.

Niswander, L. and Martin, G.R. 1992. *Fgf-4* expression during gastrulation, myogenesis, limb and tooth development in the mouse. *Development (Cambridge, England)* **114:** 755-768.

Niswander, L., Tickle, C., Vogel, A., Booth, I., and Martin, G.R. 1993. FGF-4 replaces the apical ectodermal ridge and directs outgrowth and patterning of the limb. *Cell* **75:** 579-587.

Noden, D. 1978a. The control of avian cephalic neural crest cytodifferentiation I. skeletal and connective tissues. *Devl Biol.* **67:** 296-312.

Noden, D. 1988. Interactions and fates of avian craniofacial mesenchyme. *Development (Cambridge, England)* **103:** 121-140.

Noden, D.M. 1978b. The control of avian cephalic neural crest cytodifferentiation. I. Skeletal and connective tissues. *Developmental biology* **67:** 296-312.

Nottoli, T., Hagopian-Donaldson, S., Zhang, J., Perkins, A., and Williams, T. 1998. AP-2-null cells disrupt morphogenesis of the eye, face, and limbs in chimeric mice. *Proceedings of the National Academy of Sciences of the United States of America* **95:** 13714-13719.

Oka, C., Nakano, T., Wakeham, A., de la Pompa, J.L., Mori, C., Sakai, T., Okazaki, S., Kawaichi, M., Shiota, K., Mak, T.W., and Honjo, T. 1995. Disruption of the mouse RBP-J kappa gene results in early embryonic death. *Development (Cambridge, England)* **121:** 3291-3301.

Okamura, Y. and Saga, Y. 2008. Notch signaling is required for the maintenance of enteric neural crest progenitors. *Development (Cambridge, England)*.

Olsen, B.R., Reginato, A.M., and Wang, W. 2000. Bone development. *Annual review of cell and developmental biology* **16:** 191-220.

Opperman, L.A. 2000. Cranial sutures as intramembranous bone growth sites. *Dev Dyn* **219:** 472-485.

Ornitz, D.M. and Itoh, N. 2001. Fibroblast growth factors. *Genome Biol* **2:** REVIEWS3005.

Ornitz, D.M. and Marie, P.J. 2002. FGF signaling pathways in endochondral and intramembranous bone development and human genetic disease. *Genes & development* **16:** 1446-1465.

Osumi-Yamashita, N., Ninomiya, Y., Doi, H., and Eto, K. 1994. The contribution of both forebrain and midbrain crest cells to the mesenchyme in the frontonasal mass of mouse embryos. *Developmental biology* **164:** 409-419.

Osumi-Yamashita, N., Ninomiya, Y., Doi, H., and Eto, K. 1996. Rhombomere formation and hind-brain crest cell migration from prorhombomeric origins in mouse embryos. *Develop Growth Differ* **38:** 107-118.

Ota, M. and Ito, K. 2003. Induction of neurogenin-1 expression by sonic hedgehog: Its role in development of trigeminal sensory neurons. *Dev Dyn* **227:** 544-551.

Otto, F., Thornell, A.P., Crompton, T., Denzel, A., Gilmour, K.C., Rosewell, I.R., Stamp, G.W., Beddington, R.S., Mundlos, S., Olsen, B.R., Selby, P.B., and Owen, M.J. 1997. Cbfa1, a candidate gene for cleidocranial dysplasia syndrome, is essential for osteoblast differentiation and bone development. *Cell* **89:** 765-771.

Oulad-Abdelghani, M., Bouillet, P., Chazaud, C., Dolle, P., and Chambon, P. 1996. AP-2.2: a novel AP-2-related transcription factor induced by retinoic acid during differentiation of P19 embryonal carcinoma cells. *Experimental cell research* **225:** 338-347.

Panganiban, G. and Rubenstein, J.L. 2002. Developmental functions of the Distal-less/Dlx homeobox genes. *Development (Cambridge, England)* **129:** 4371-4386.

Parmantier, E., Lynn, B., Lawson, D., Turmaine, M., Namini, S.S., Chakrabarti, L., McMahon, A.P., Jessen, K.R., and Mirsky, R. 1999. Schwann cell-derived Desert hedgehog controls the development of peripheral nerve sheaths. *Neuron* **23:** 713-724.

Pasqualetti, M., Ori, M., Nardi, I., and Rijli, F.M. 2000. Ectopic Hoxa2 induction after neural crest migration results in homeosis of jaw elements in Xenopus. *Development (Cambridge, England)* **127:** 5367-5378.

Pepinsky, R.B., Zeng, C., Wen, D., Rayhorn, P., Baker, D., Williams, K.P., Bixler, S.A., Ambrose, C.M., Garber, E.A., Miatkowski, K., Taylor, F.R., Wang, E.A., and Galdes, A. 1998. Identification of a palmitic acid-modified form of human Sonic hedgehog. *Journal of Biological Chemistry* **273:** 14037-14045.

Pevny, L.H. and Lovell-Badge, R. 1997. Sox genes find their feet. *Curr Opin Genet Dev* **7:** 338-344.

Pizette, S. and Niswander, L. 2000. BMPs are required at two steps of limb chondrogenesis: formation of prechondrogenic condensations and their differentiation into chondrocytes. *Developmental biology* **219:** 237-249.

Porter, J.A., Ekker, S.C., Park, W.J., von Kessler, D.P., Young, K.E., Chen, C.H., Ma, Y., Woods, A.S., Cotter, R.J., Koonin, E.V., and Beachy, P.A. 1996a. Hedgehog patterning activity: role of a lipophilic modification mediated by the carboxy-terminal autoprocessing domain. *Cell* **86:** 21-34.

Porter, J.A., Young, K.E., and Beachy, P.A. 1996b. Cholesterol modification of hedgehog signaling proteins in animal development. *Science (New York, N.Y* **274:** 255-259.

Qiu, M., Bulfone, A., Ghattas, I., Meneses, J.J., Christensen, L., Sharpe, P.T., Presley, R., Pedersen, R.A., and Rubenstein, J.L. 1997. Role of the Dlx homeobox genes in proximodistal patterning of the branchial arches: mutations of Dlx-1, Dlx-2, and Dlx-1 and -2 alter morphogenesis of proximal skeletal and soft tissue structures derived from the first and second arches. *Developmental biology* **185:** 165-184.

Qiu, M., Bulfone, A., Martinez, S., Meneses, J.J., Shimamura, K., Pedersen, R.A., and Rubenstein, J.L. 1995. Null mutation of Dlx-2 results in abnormal morphogenesis of proximal first and second branchial arch derivatives and abnormal differentiation in the forebrain. *Genes Dev* **9:** 2523-2538.

Rallu, M., Machold, R., Gaiano, N., Corbin, J.G., McMahon, A.P., and Fishell, G. 2002. Dorsoventral patterning is established in the telencephalon of mutants lacking both Gli3 and Hedgehog signaling. *Development (Cambridge, England)* **129:** 4963-4974.

Riddle, R.D., Johnson, R.L., Laufer, E., and Tabin, C. 1993. *Sonic hedgehog* mediates the polarizing activity of the ZPA. *Cell* **75:** 1401-1416.

Rijli, F.M., Mark, M., Lakkaraju, S., Dierich, A., Dolle, P., and Chambon, P. 1993. A homeotic transformation is generated in the rostral branchial region of the head by disruption of Hoxa-2, which acts as a selector gene. *Cell* **75:** 1333-1349.

Roessler, E., Belloni, E., Gaudenz, K., Jay, P., Berta, P., Scherer, S.W., Tsui, L.C., and Muenke, M. 1996. Mutations in the human Sonic Hedgehog gene cause holoprosencephaly. *Nat Genet* **14:** 357-360.

Rogers, C.D., Archer, T.C., Cunningham, D.D., Grammer, T.C., and Casey, E.M. 2008. Sox3 expression is maintained by FGF signaling and restricted to the

neural plate by Vent proteins in the Xenopus embryo. *Developmental biology* **313:** 307-319.
Rollhauser-ter Horst, J. 1977. Artificial neural induction in amphibia. I. Sandwich explants. *Anat Embryol (Berl)* **151:** 309-316.
Rosen, V. 2006. BMP and BMP inhibitors in bone. *Annals of the New York Academy of Sciences* **1068:** 19-25.
Ruiz i Altaba, A. 1999. Gli proteins and Hedgehog signaling: development and cancer. *Trends Genet* **15:** 418-425.
Ruiz i Altaba, A., Nguyen, V., and Palma, V. 2003. The emergent design of the neural tube: prepattern, SHH morphogen and GLI code. *Curr Opin Genet Dev* **13:** 513-521.
Saint-Jeannet, J.P., He, X., Varmus, H.E., and Dawid, I.B. 1997. Regulation of dorsal fate in the neuraxis by Wnt-1 and Wnt-3a. *Proc Natl Acad Sci U S A* **94:** 13713-13718.
Santagati, F. and Rijli, F.M. 2003. Cranial neural crest and the building of the vertebrate head. *Nat Rev Neurosci* **4:** 806-818.
Sarkar, L., Cobourne, M., Naylor, S., Smalley, M., Dale, T., and Sharpe, P.T. 2000. Wnt/Shh interactions regulate ectodermal boundary formation during mammalian tooth development. *Proceedings of the National Academy of Sciences of the United States of America* **97:** 4520-4524.
Sasaki, H., Nishizaki, Y., Hui, C., Nakafuku, M., and Kondoh, H. 1999. Regulation of Gli2 and Gli3 activities by an amino-terminal repression domain: implication of Gli2 and Gli3 as primary mediators of Shh signaling. *Development (Cambridge, England)* **126:** 3915-3924.
Sato, T., Sasai, N., and Sasai, Y. 2005. Neural crest determination by co-activation of Pax3 and Zic1 genes in Xenopus ectoderm. *Development (Cambridge, England)* **132:** 2355-2363.
Schipani, E., Lanske, B., Hunzelman, J., Luz, A., Kovacs, C.S., Lee, K., Pirro, A., Kronenberg, H.M., and Juppner, H. 1997. Targeted expression of constitutively active receptors for parathyroid hormone and parathyroid hormone-related peptide delays endochondral bone formation and rescues mice that lack parathyroid hormone-related peptide. *Proceedings of the National Academy of Sciences of the United States of America* **94:** 13689-13694.
Schorle, H., Meier, P., Buchert, M., Jaenisch, R., and Mitchell, P.J. 1996. Transcription factor AP-2 is essential for cranial closure and craniofacial development. *Nature* **381:** 235-238.
Sechrist, J., Scherson, T., and Bronner-Fraser, M. 1994. Rhombomere rotation reveals that multiple mechanisms contribute to segmental pattern of hindbrain neural crest migration. *Development (Cambridge, England)* **120:** 1777-1790.
Sechrist, J., Serbedzija, G.N., Scherson, T., Fraser, S.E., and Bronner-Fraser, M. 1993. Segmental migration of the hindbrain neural crest does not arise from its segmental generation. *Development (Cambridge, England)* **118(3):** 691-703.

Selkoe, D. and Kopan, R. 2003. Notch and Presenilin: regulated intramembrane proteolysis links development and degeneration. *Annual review of neuroscience* **26:** 565-597.

Selleck, M.A. and Bronner-Fraser, M. 1995. Origins of the avian neural crest: the role of neural plate-epidermal interactions. *Development (Cambridge, England)* **121:** 525-538.

Selleck, M.A., Garcia-Castro, M.I., Artinger, K.B., and Bronner-Fraser, M. 1998. Effects of Shh and Noggin on neural crest formation demonstrate that BMP is required in the neural tube but not ectoderm. *Development (Cambridge, England)* **125:** 4919-4930.

Serbedzija, G., Fraser, S., and Bronner-Fraser, M. 1992. Vital dye analysis of cranial neural crest cell migration in the mouse embryo. *Development (Cambridge, England)* **116:** 297-307.

Serbedzija, G.N. and McMahon, A.P. 1997. Analysis of neural crest cell migration in Splotch mice using a neural crest-specific LacZ reporter. *Developmental biology* **185:** 139-147.

Smits, P., Li, P., Mandel, J., Zhang, Z., Deng, J.M., Behringer, R.R., de Crombrugghe, B., and Lefebvre, V. 2001. The transcription factors L-Sox5 and Sox6 are essential for cartilage formation. *Dev Cell* **1:** 277-290.

Solloway, M.J. and Robertson, E.J. 1999. Early embryonic lethality in Bmp5;Bmp7 double mutant mice suggests functional redundancy within the 60A subgroup. *Development (Cambridge, England)* **126:** 1753-1768.

Soriano, P. 1999. Generalized lacZ expression with the ROSA26 Cre reporter strain. *Nature genetics* **21:** 70-71.

Southard-Smith, E.M., Kos, L., and Pavan, W.J. 1998. Sox10 mutation disrupts neural crest development in Dom Hirschsprung mouse model. *Nature genetics* **18:** 60-64.

St-Jacques, B., Hammerschmidt, M., and McMahon, A.P. 1999. Indian hedgehog signaling regulates proliferation and differentiation of chondrocytes and is essential for bone formation. *Genes & development* **13:** 2072-2086.

Stavridis, M.P., Lunn, J.S., Collins, B.J., and Storey, K.G. 2007. A discrete period of FGF-induced Erk1/2 signalling is required for vertebrate neural specification. *Development (Cambridge, England)* **134:** 2889-2894.

Stottmann, R.W., Choi, M., Mishina, Y., Meyers, E.N., and Klingensmith, J. 2004. BMP receptor IA is required in mammalian neural crest cells for development of the cardiac outflow tract and ventricular myocardium. *Development (Cambridge, England)* **131:** 2205-2218.

Sun, X., Mariani, F.V., and Martin, G.R. 2002. Functions of FGF signalling from the apical ectodermal ridge in limb development. *Nature* **418:** 501-508.

Sun, X., Meyers, E.N., Lewandoski, M., and Martin, G.R. 1999. Targeted disruption of Fgf8 causes failure of cell migration in the gastrulating mouse embryo. *Genes & development* **13:** 1834-1846.

Szabo-Rogers, H.L., Geetha-Loganathan, P., Nimmagadda, S., Fu, K.K., and Richman, J.M. 2008. FGF signals from the nasal pit are necessary for normal facial morphogenesis. *Developmental biology* **318:** 289-302.

Takemoto, T., Uchikawa, M., Kamachi, Y., and Kondoh, H. 2006. Convergence of Wnt and FGF signals in the genesis of posterior neural plate through activation of the Sox2 enhancer N-1. *Development (Cambridge, England)* **133:** 297-306.

Tanaka, K., Kitagawa, Y., and Kadowaki, T. 2002. Drosophila segment polarity gene product porcupine stimulates the posttranslational N-glycosylation of wingless in the endoplasmic reticulum. *The Journal of biological chemistry* **277:** 12816-12823.

Tapadia, M.D., Cordero, D.R., and Helms, J.A. 2005. It's all in your head: new insights into craniofacial development and deformation. *Journal of anatomy* **207:** 461-477.

Taylor, F.R., Wen, D., Garber, E.A., Carmillo, A.N., Baker, D.P., Arduini, R.M., Williams, K.P., Weinreb, P.H., Rayhorn, P., Hronowski, X., Whitty, A., Day, E.S., Boriack-Sjodin, A., Shapiro, R.I., Galdes, A., and Pepinsky, R.B. 2001. Enhanced potency of human Sonic hedgehog by hydrophobic modification. *Biochemistry* **40:** 4359-4371.

Taylor, M.K., Yeager, K., and Morrison, S.J. 2007. Physiological Notch signaling promotes gliogenesis in the developing peripheral and central nervous systems. *Development (Cambridge, England)* **134:** 2435-2447.

Trainor, P. and Krumlauf, R. 2000a. Patterning the cranial neural crest: Hindbrain segmentation and *Hox* gene plasticity. *Nature Reviews Neuroscience* **1:** 116-124.

Trainor, P. and Krumlauf, R. 2000b. Plasticity in mouse neural crest cells reveals a new patterning role for cranial mesoderm. *Nature Cell Biology* **2:** 96-102.

Trainor, P.A. 2005. Specification of neural crest cell formation and migration in mouse embryos. *Semin Cell Dev Biol*.

Trainor, P.A., Melton, K.R., and Manzanares, M. 2003. Origins and plasticity of neural crest cells and their roles in jaw and craniofacial evolution. *Int J Dev Biol* **47:** 541-553.

Trainor, P.A. and Tam, P.P.L. 1995. Cranial paraxial mesoderm and neural crest of the mouse embryo-codistribution in the craniofacial mesenchyme but distinct segregation in the branchial arches. *Development (Cambridge, England)* **121:** 2569-2582.

Trokovic, N., Trokovic, R., Mai, P., and Partanen, J. 2003. Fgfr1 regulates patterning of the pharyngeal region. *Genes Dev* **17:** 141-153.

Trumpp, A., Depew, M.J., Rubenstein, J.L., Bishop, J.M., and Martin, G.R. 1999. Cre-mediated gene inactivation demonstrates that FGF8 is required for cell survival and patterning of the first branchial arch. *Genes Dev* **13:** 3136-3148.

Tucker, A. and Sharpe, P. 2004. The cutting-edge of mammalian development; how the embryo makes teeth. *Nat Rev Genet* **5:** 499-508.

Tucker, A.S., Matthews, K.L., and Sharpe, P.T. 1998. Transformation of tooth type induced by inhibition of BMP signaling. *Science (New York, N.Y* **282:** 1136-1138.

Tucker, A.S. and Sharpe, P.T. 1999. Molecular genetics of tooth morphogenesis and patterning: the right shape in the right place. *J Dent Res* **78:** 826-834.

Tucker, A.S., Yamada, G., Grigoriou, M., Pachnis, V., and Sharpe, P.T. 1999. Fgf-8 determines rostral-caudal polarity in the first branchial arch. *Development (Cambridge, England)* **126:** 51-61.

Ueta, C., Iwamoto, M., Kanatani, N., Yoshida, C., Liu, Y., Enomoto-Iwamoto, M., Ohmori, T., Enomoto, H., Nakata, K., Takada, K., Kurisu, K., and Komori, T. 2001. Skeletal malformations caused by overexpression of Cbfa1 or its dominant negative form in chondrocytes. *The Journal of cell biology* **153:** 87-100.

Vallin, J., Thuret, R., Giacomello, E., Faraldo, M.M., Thiery, J.P., and Broders, F. 2001. Cloning and characterization of three Xenopus slug promoters reveal direct regulation by Lef/beta-catenin signaling. *J Biol Chem* **276:** 30350-30358.

Vortkamp, A., Lee, K., Lanske, B., Segre, G.V., Kronenberg, H.M., and Tabin, C.J. 1996. Regulation of rate of cartilage differentiation by Indian hedgehog and PTH-related protein. *Science (New York, N.Y* **273:** 613-622.

Wagner, T., Wirth, J., Meyer, J., Zabel, B., Held, M., Zimmer, J., Pasantes, J., Bricarelli, F.D., Keutel, J., Hustert, E., and et al. 1994. Autosomal sex reversal and campomelic dysplasia are caused by mutations in and around the SRY-related gene SOX9. *Cell* **79:** 1111-1120.

Wallis, D. and Muenke, M. 2000. Mutations in holoprosencephaly. *Human mutation* **16:** 99-108.

Wankhade, S., Yu, Y., Weinberg, J., Tainsky, M.A., and Kannan, P. 2000. Characterization of the activation domains of AP-2 family transcription factors. *The Journal of biological chemistry* **275:** 29701-29708.

Washington Smoak, I., Byrd, N.A., Abu-Issa, R., Goddeeris, M.M., Anderson, R., Morris, J., Yamamura, K., Klingensmith, J., and Meyers, E.N. 2005. Sonic hedgehog is required for cardiac outflow tract and neural crest cell development. *Developmental biology* **283:** 357-372.

Wijgerde, M., McMahon, J.A., Rule, M., and McMahon, A.P. 2002. A direct requirement for Hedgehog signaling for normal specification of all ventral progenitor domains in the presumptive mammalian spinal cord. *Genes Dev* **16:** 2849-2864.

Williams, T., Admon, A., Luscher, B., and Tjian, R. 1988. Cloning and expression of AP-2, a cell-type-specific transcription factor that activates inducible enhancer elements. *Genes & development* **2:** 1557-1569.

Williams, T. and Tjian, R. 1991a. Analysis of the DNA-binding and activation properties of the human transcription factor AP-2. *Genes & development* **5:** 670-682.

Williams, T. and Tjian, R. 1991b. Characterization of a dimerization motif in AP-2 and its function in heterologous DNA-binding proteins. *Science (New York, N.Y* **251:** 1067-1071.

Wilson, J. and Tucker, A.S. 2004. Fgf and Bmp signals repress the expression of Bapx1 in the mandibular mesenchyme and control the position of the developing jaw joint. *Developmental biology* **266:** 138-150.

Wilson, P.A. and Hemmati-Brivanlou, A. 1995. Induction of epidermis and inhibition of neural fate by Bmp-4. *Nature* **376:** 331-333.

Winnier, G., Blessing, M., Labosky, P.A., and Hogan, B.L. 1995. Bone morphogenetic protein-4 is required for mesoderm formation and patterning in the mouse. *Genes & development* **9:** 2105-2116.

Wright, E., Hargrave, M.R., Christiansen, J., Cooper, L., Kun, J., Evans, T., Gangadharan, U., Greenfield, A., and Koopman, P. 1995. The Sry-related gene Sox9 is expressed during chondrogenesis in mouse embryos. *Nature genetics* **9:** 15-20.

Wu, J., Yang, J., and Klein, P.S. 2005. Neural crest induction by the canonical Wnt pathway can be dissociated from anterior-posterior neural patterning in Xenopus. *Developmental biology* **279:** 220-232.

Xu, Q., Mellitzer, G., Robinson, V., and Wilkinson, D. 1999. *In vivo* cell sorting in complementary segmental domains mediated by *Eph* receptors and *ephrins*. *Nature* **399:** 267-271.

Xu, X., Weinstein, M., Li, C., Naski, M., Cohen, R.I., Ornitz, D.M., Leder, P., and Deng, C. 1998. Fibroblast growth factor receptor 2 (FGFR2)-mediated reciprocal regulation loop between FGF8 and FGF10 is essential for limb induction. *Development (Cambridge, England)* **125:** 753-765.

Yamagishi, C., Yamagishi, H., Maeda, J., Tsuchihashi, T., Ivey, K., Hu, T., and Srivastava, D. 2006. Sonic hedgehog is essential for first pharyngeal arch development. *Pediatr Res* **59:** 349-354.

Yanfeng, W., Saint-Jeannet, J.P., and Klein, P.S. 2003. Wnt-frizzled signaling in the induction and differentiation of the neural crest. *Bioessays* **25:** 317-325.

Yi, S.E., Daluiski, A., Pederson, R., Rosen, V., and Lyons, K.M. 2000. The type I BMP receptor BMPRIB is required for chondrogenesis in the mouse limb. *Development (Cambridge, England)* **127:** 621-630.

Yoshida, T., Vivatbutsiri, P., Morriss-Kay, G., Saga, Y., and Iseki, S. 2008. Cell lineage in mammalian craniofacial mesenchyme. *Mechanisms of development* **125:** 797-808.

Zhang, H. and Bradley, A. 1996. Mice deficient for BMP2 are nonviable and have defects in amnion/chorion and cardiac development. *Development (Cambridge, England)* **122:** 2977-2986.

Zhang, J., Hagopian-Donaldson, S., Serbedzija, G., Elsemore, J., Plehn-Dujowich, D., McMahon, A.P., Flavell, R.A., and Williams, T. 1996. Neural tube, skeletal and body wall defects in mice lacking transcription factor AP-2. *Nature* **381:** 238-241.

Zhang, J. and Williams, T. 2003. Identification and regulation of tissue-specific cis-acting elements associated with the human AP-2alpha gene. *Dev Dyn* **228:** 194-207.

Zhang, X.M., Ramalho-Santos, M., and McMahon, A.P. 2001. Smoothened mutants reveal redundant roles for Shh and Ihh signaling including regulation of L/R symmetry by the mouse node. *Cell* **106:** 781-792.

Zhang, Y.W., Bae, S.C., Takahashi, E., and Ito, Y. 1997. The cDNA cloning of the transcripts of human PEBP2alphaA/CBFA1 mapped to 6p12.3-p21.1, the locus for cleidocranial dysplasia. *Oncogene* **15:** 367-371.

Zhao, F., Satoda, M., Licht, J.D., Hayashizaki, Y., and Gelb, B.D. 2001. Cloning and characterization of a novel mouse AP-2 transcription factor, AP-2delta, with unique DNA binding and transactivation properties. *The Journal of biological chemistry* **276:** 40755-40760.

Zhou, G., Lefebvre, V., Zhang, Z., Eberspaecher, H., and de Crombrugghe, B. 1998. Three high mobility group-like sequences within a 48-base pair enhancer of the Col2a1 gene are required for cartilage-specific expression in vivo. *The Journal of biological chemistry* **273:** 14989-14997.

Zhu, A.J., Zheng, L., Suyama, K., and Scott, M.P. 2003. Altered localization of Drosophila Smoothened protein activates Hedgehog signal transduction. *Genes & development* **17:** 1240-1252.

Zhu, J., Nakamura, E., Nguyen, M.T., Bao, X., Akiyama, H., and Mackem, S. 2008. Uncoupling Sonic hedgehog control of pattern and expansion of the developing limb bud. *Dev Cell* **14:** 624-632.

Zou, H., Wieser, R., Massague, J., and Niswander, L. 1997. Distinct roles of type I bone morphogenetic protein receptors in the formation and differentiation of cartilage. *Genes & development* **11:** 2191-2203.